THE FORMULATION OF SUBSTITUTE MATERIALS WITH PREDETERMINED CHARACTERISTICS OF RADIATION ABSORPTION AND SCATTERING

D.R. WHITE

A THESIS SUBMITTED TO THE UNIVERSITY OF LONDON

FOR THE DEGREE OF DOCTOR OF PHILOSOPHY

1974

ABSTRACT

A comprehensive study of the substitute materials used in clinical radiation dosimetry has shown that many of the existing products give poor simulation for both photon and electron interactions. Those materials with known composition were classified according to the errors in their attenuation and energy absorption coefficients, stopping and angular scattering powers compared to those for the material being simulated. Large discrepancies were found at low photon energies, with lung and bone substitutes giving poor results.

The existing selection procedures were evaluated and two new techniques were evolved, namely, the BASIC DATA METHOD and the EXTENDED $\overline{Y}(x)$ METHOD. The first procedure was based on the attenuation and absorption quantities, while the second method used an extension of the popular, but misused, concept of effective atomic number.

A thorough analysis of the dependence of photon and electron interactions on atomic number was made so that the effective atomic number data could be manipulated more accurately.

Computer programs based on the new procedures were written and, using a library of some 1040 materials, produced 77 new formulations including muscle, fat, lung, bone, skin, breast, liver, thyroid and air substitutes.

Techniques were developed for the manufacture and quality testing

of 35 of these new materials.

The results of a series of 'narrow-beam' photon attenuation measurements, nominally from 10 keV to 1 MeV, verified the high precision of the selection procedures and provided useful data on the contaminants present in some of the base materials.

Finally, the applications of the new substitutes in practical dosimetry were investigated.

ACKNOWLEDGEMENTS

I would like to express my gratitude to Professor J. Rotblat for acting as my supervisor during this study, for his continued support and for his comments on this thesis. The advice given by Professor R.E. Ellis, during the first three years of the study, is gratefully appreciated.

My employers, St. Bartholomew's Hospital, are acknowledged for permitting me to perform this research on a part-time basis. The help and encouragement of numerous colleagues at the hospital is appreciated. Special thanks are due to Dr C.A. Greatorex for his interest in the project; to Dr N.F. Kember and Dr W.E. Liversage for their comments on the thesis; and to Mr A. Rickwood and Mr R. Darlison for technical assistance in the manufacturing of the new substitutes.

I would like to thank Mr L.H.J. Peaple (A.E.R.E., Harwell), for permitting me to use his low energy photon attenuation apparatus and Mr I.M.G. Thompson for permission to use the radiation facilities at Berkeley Nuclear Laboratories. Messrs R.J. Martin (CIBA-GEIGY LTD), M. Cass (I.C.I. Ltd), J.A. Brydson, D.E.A. Jones and A.J. Stacey and Professor F.W. Spiers are gratefully acknowledged for their advice and helpful discussions.

Finally, I would like to thank my family for their continued encouragement during the five years of this study. In particular, without the unfailing support and practical assistance of my wife, this work would never have been completed.

D.R. WHITE

Physics Department
St. Bartholomew's Hospital

CONTENTS

CHAPTER 1

AN INTRODUCTION TO THE THESIS

For many years experiments concerned with the dosimetric effects within and around irradiated human tissues have used so-called 'TISSUE EQUIVALENT MATERIALS'. These materials must absorb and scatter radiation in exactly the same manner as the tissues being simulated. Formulations have been produced which are said to simulate tissues such as muscle, bone, lung and fat.

An important example of another type of material which has been considered in this context is air. Air substitutes are used in the manufacture of thimble ionization chambers which are employed extensively in dosimetric investigations.

This thesis deals with the general problem of simulation for both photon and electron radiation. Existing materials are evaluated theoretically and experimentally and two new simulation procedures are developed and used to formulate a family of new materials with radiation characteristics superior to those of the existing systems.

1.1 THEORETICAL ASPECTS

It was decided at an early stage in this study that, as the available data on published formulations were incomplete and often non-existent, means of accurately calculating the important physical properties had to be established. A comprehensive suite of

computer programs was subsequently written for this purpose and is tabulated in APPENDIX 4. The large complex of computers at the University of London Computer Centre (CDC 6600 and CDC 6400) was utilized when large amounts of data were being handled, and the computers in St. Bartholomew's Hospital (Honeywell DDP 516) and Medical College (PDP 8(S)) when smaller quantities of data were involved.

Published data on photon attenuation and energy absorption cross sections for the 70 elements shown in APPENDIX 2, were compiled and stored on magnetic tape (HUBBELL, 1969; STORM & ISREAL, 1970). Thirty-three energy points were selected in the range 10 keV-100 MeV and the corresponding partial cross sections [coherent, incoherent (Compton), pair production and photoelectric interactions] were extracted from the tabulated data.

Electron stopping power data (collision and radiation) for the first 25 elements were similarly compiled from published reports (BERGER & SELTZER, 1964; PAGES et al, 1970) and stored on magnetic tape.

Accuracy and consistency of both sets of data were checked by manually plotting the stored data on large scale graph paper.

Elemental angular scattering powers were not stored on magnetic tape, but generated when required using the formulae quoted by ICRU, 1972 (Figure 1.1). (For simplicity, the meaning of all the

MASS ANGULAR SCATTERING POWERS

(a) ELEMENTS

IF.... $\left(\frac{280}{A^{1/3}} \cdot \frac{m_e c^2}{p_e c}\right) < 1$,

$$\frac{\overline{\Theta}^2}{\rho \ell} = 16\pi N_A \cdot \frac{Z^2}{A} \cdot r_e^2 \left(\frac{m_e c^2}{\beta p_e c}\right)^2 \ln\left[196\, Z^{-1/3} \left(\frac{Z}{A}\right)^{1/6}\right] \quad \cdots\cdots (1.1)$$

IF.... $\left(\frac{280}{A^{1/3}} \frac{m_e c^2}{p_e c}\right) > 1$,

$$\frac{\overline{\Theta}^2}{\rho \ell} = 16\pi N_A \cdot \frac{Z^2}{A} \cdot r_e^2 \left(\frac{m_e c^2}{\beta p_e c}\right)^2 \ln\left[\frac{137 p_e c}{Z^{1/3} m_e c^2}\right]^{1/2} \quad \cdots\cdots (1.2)$$

(b) COMPOUNDS

$$\frac{\overline{\Theta}^2}{\rho \ell} = \sum_i \omega_i \left(\frac{\Theta^2}{\rho \ell}\right)_i \quad \cdots\cdots (1.3)$$

FIGURE 1.1 PRINCIPAL FORMULAE USED FOR ELECTRON MASS ANGULAR SCATTERING POWERS (SYMBOLS DEFINED IN APPENDIX 1).

symbols used in Figure 1.1 and subsequent equations are given in APPENDIX 1).

The calculation of mass attenuation and energy absorption coefficients for compounds was performed with the well-known 'ADDITION FORMULA'. In a general form the coefficient (C) for a compound may be expressed as,

$$C = \sum_i \omega_i C_i$$

{ where ω_i is the proportion by weight of

the i^{th} constituent having a coefficient denoted by C_i.

This method is known to be accurate for photon interactions to a few percent for energies above 10 keV, except in the fine structure regions just above absorption edges (HUBBELL, 1969; DESLATTES, 1969).

Two methods were used to calculate mass electron stopping powers for compounds. The first method involved the use of the addition formula and the elemental stopping powers stored on magnetic tape. This technique is claimed to produce results within a few percent of the true values (BISCHEL, 1968). The second method utilised the conventional stopping power formulae derived from first principles (Figure 1.2). The evaluation of the density correction, δ, was not included in this analysis and was given a zero value in equation 1.4. The values of the mean excitation energy (I) and the ratio of atomic number to atomic weight for compounds were calculated by addition formulae (equations 1.8 and 1.7).

MASS STOPPING POWERS

(a) ELEMENTS

$$\left(\frac{S}{\rho}\right)_{col} = \frac{2\pi N_A r_e^2 m_e c^2}{\beta^2}\frac{Z}{A}\left[\ln\left\{\frac{\tau^2(\tau+2)}{2(I/m_e c^2)}\right\} + F^-(\tau) - \delta\right] \quad \text{(1.4)}$$

$$F^-(\tau) = 1 - \beta^2 + \left[\frac{\tau^2}{8} - (2\tau+1)\ln 2\right](\tau+1)^{-2}$$

$$\beta = \left[\tau(\tau+2)\right]^{1/2}(\tau+1)^{-1} = \frac{v}{c}$$

$$I = Z(9{\cdot}76 + 58{\cdot}8\,Z^{-1{\cdot}19}) \quad \text{eV}$$

$$\left(\frac{S}{\rho}\right)_{rad} = \frac{E(Z+1.2)}{700}\left(\frac{S}{\rho}\right)_{col} \quad \text{(1.5)}$$

$$\left(\frac{S}{\rho}\right)_{total} = \left(\frac{S}{\rho}\right)_{col} + \left(\frac{S}{\rho}\right)_{rad} \quad \text{(1.6)}$$

(b) COMPOUNDS (First Principles)

Formulae in addition to (a) above

$$\left\langle\frac{Z}{A}\right\rangle = \sum_i \omega_i \left(\frac{Z}{A}\right)_i \quad \text{(1.7)}$$

$$\ln\langle I\rangle = \left(\left\langle\frac{Z}{A}\right\rangle\right)^{-1}\sum_i \omega_i \left(\frac{Z}{A}\right)_i \ln I_i \quad \text{(1.8)}$$

(c) COMPOUNDS (Addition Formula)

$$\frac{S}{\rho} = \sum_i \omega_i \left(\frac{S}{\rho}\right)_i \quad \text{(1.9)}$$

FIGURE 1.2 PRINCIPAL FORMULAE USED FOR ELECTRON MASS STOPPING POWERS (SYMBOLS DEFINED IN APPENDIX 1).

The agreement between electron stopping powers for muscle calculated by these two methods with the data given in the comprehensive reviews of BERGER & SELTZER, 1964 and PAGES et al., 1970, is shown in Figure 1.3. The data are normalized to the values given by BERGER & SELTZER. Curve A depicts the values quoted by PAGES et al., and curves B & C the calculated values by the addition formula and first principles respectively. It can be seen that up to 1-2 MeV, the agreement between the different sets of data is excellent. At higher energies the calculated powers show maximum variations ranging from 13% for curve B and 35% for curve C. The data of PAGES et al., shows maximum differences of ~3% over the complete energy range.

These results indicate that if reliable absolute stopping powers are required above 2 MeV, then an evaluation of the density correction should be made. This effect is probably affecting both calculation techniques. The first principle method (curve C) is also liable to be in error at high energies due to the approximate equation used to derive the radiation energy loss $\left(\frac{S}{\rho}\right)_{rad}$ (EQUATION 1.5).

Fortunately in this study absolute values of stopping powers were not required. For comparisons over the complete energy range 10 keV-100 MeV, relative stopping powers were specified. The differences in these sets of data when stopping power ratios are considered are shown in Figure 1.4.

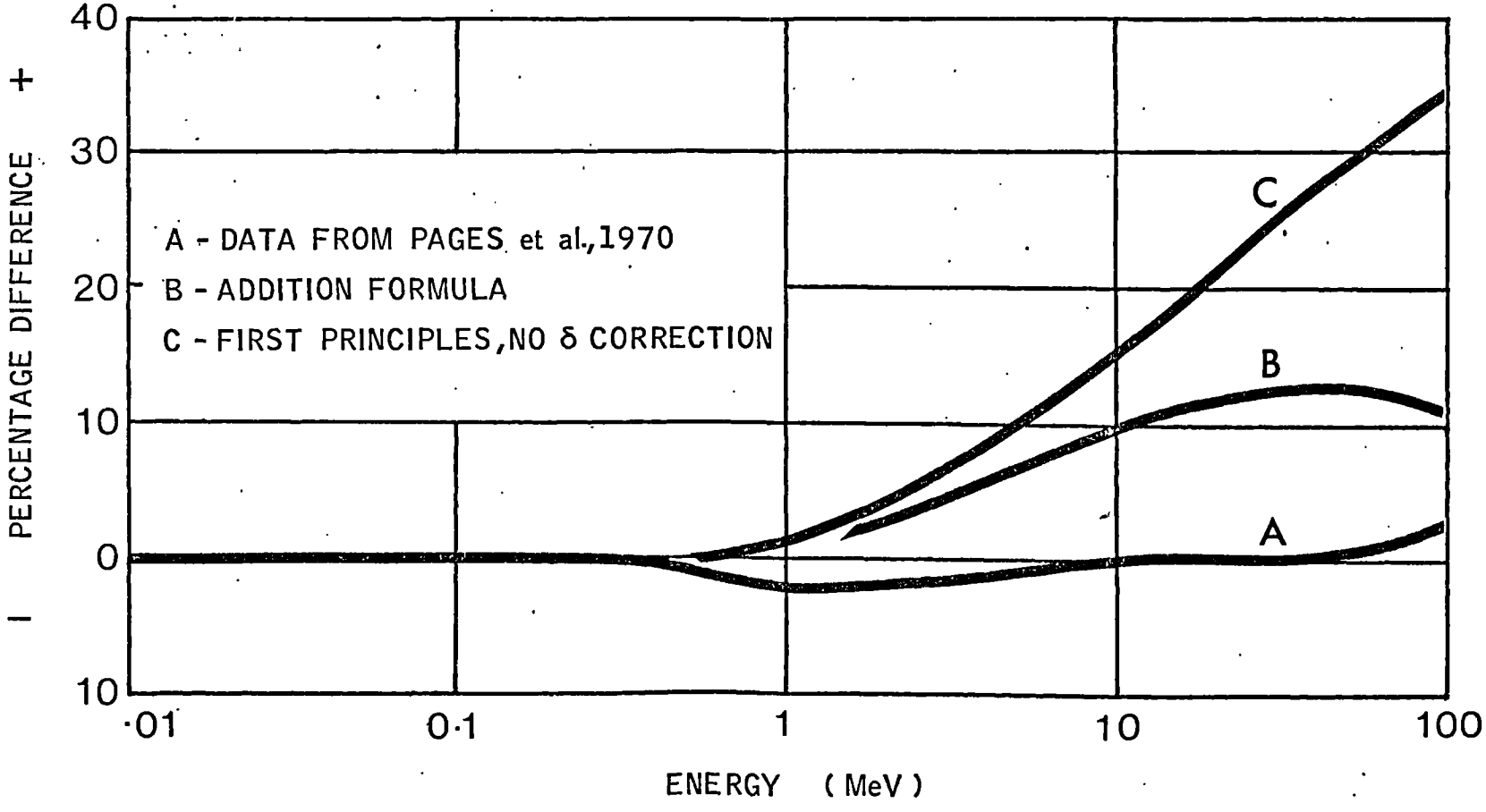

FIGURE 1.3 A COMPARISON OF ELECTRON MASS STOPPING POWERS FOR MUSCLE WITH THE DATA OF BERGER & SELTZER, 1964.

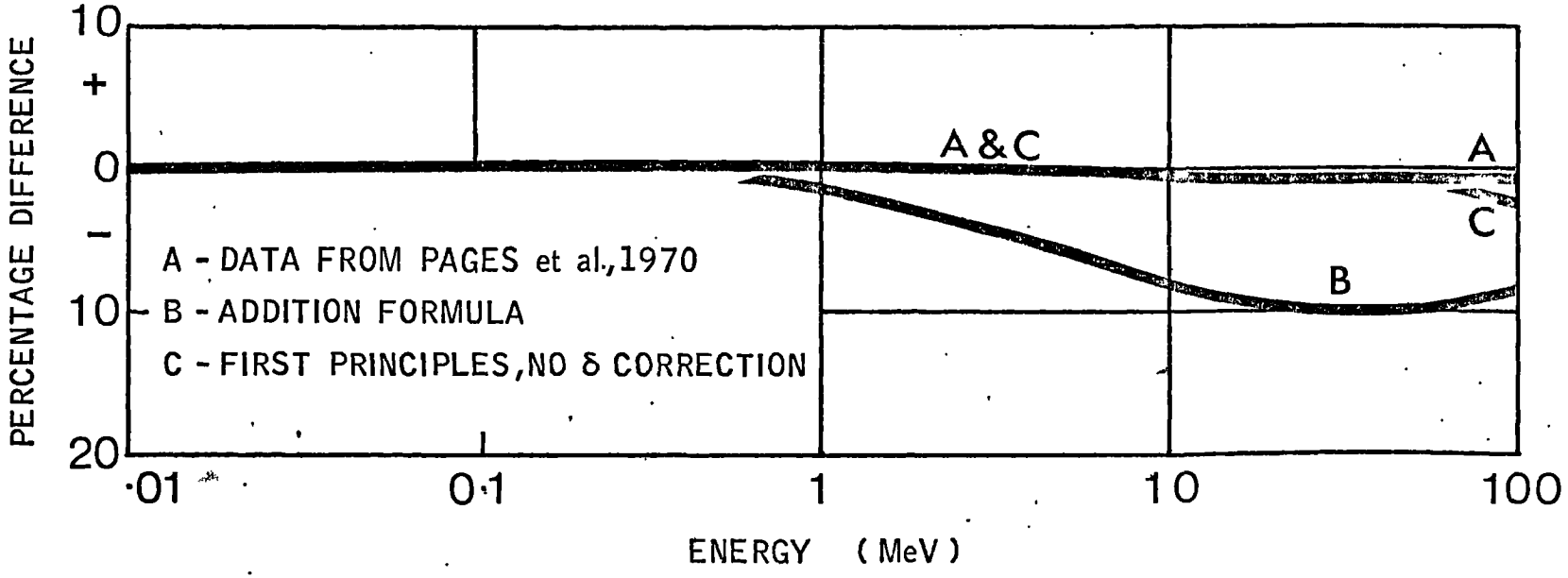

FIGURE 1.4 A COMPARISON OF ELECTRON MASS STOPPING POWER RATIOS FOR POLYSTYRENE/MUSCLE WITH THE DATA OF BERGER & SELTZER, 1964.

In this figure, the ratios for polystyrene/muscle have been calculated using the data of PAGES et al., (curve A), addition formula, (curve B), and first principles, (curve C), all normalized to the data of BERGER & SELTZER. The muscle formulation was as quoted by ICRU in the National Bureau of Standards (1964) Handbook 85. Divergencies are considerably reduced, curve C showing a maximum difference of only 2% at 100 MeV. The negative differences shown in curves B & C are due to the calculated stopping powers of polystyrene having marginally smaller differences from BERGER & SELTZER data than the values for muscle.

The reason for the improved agreement is the small variation in the ratios of calculated (first principle) data to BERGER & SELTZER data for different materials. At 100 MeV, this ratio is within a few percent of 1.30 for the majority of materials considered in this survey.

Subsequently stopping power ratios were calculated from the first principle method and, when required, low energy absolute stopping powers were derived from the addition formula.

Electron mass angular scattering powers for compounds were calculated by the addition formula in accordance with the suggestions made by ICRU, 1972.

The computer programs that were written for all of these calculations are tabulated in Appendix 4.

1.2 PRACTICAL ASPECTS

At the beginning of this study it was decided that a comprehensive experimental evaluation of existing substitutes and any new formulations produced during the study was extremely desirable. This would have two important roles. Firstly, the results would establish the validity of any theoretical analysis. Secondly, it would be essential if the chemical composition of the components within a formulation were not precisely known. This latter point applies to commercial substitutes, complex resins and polymers with imprecise formulae.

The most effective method of evaluating photon characteristics is the measurement of narrow beam attenuation coefficients at low energies (10 keV - 60 keV). As the predominant interaction in this range is photoelectric absorption which is strongly dependent upon the atomic number, Z, of the constituents, formulation errors are readily detected. This is especially true as compounds containing elements of high-Z (called 'fillers') are frequently employed to correct the attenuation characteristics in a low-Z base material (for example, paraffin wax). A reliable simulation procedure must be able to select the correct amounts of base material and filler to give acceptable results at these energies so that confidence in the data is essential.

Photon attenuation measurements were made on some 40 materials using the characteristic X-radiation from germanium

and molybdenum targets. These targets gave monoenergetic beams with the following X-ray energies (Handbook of Physics & Chemistry, 1971-72):-

GERMANIUM:

- 9.8864 keV
- 9.8553 "
- 10.9821 "
- 11.1008 "

MOLYBDENUM:

- 17.4793 keV
- 17.3743 "
- 19.6083 "
- 19.9652 "

In addition to these energies, the γ-rays from an Americium-241 source were employed, which gave results at 59.57 keV.

At photon energies around 1 MeV, the predominant interaction is incoherent (Compton) scattering, which depends upon the electron density of the absorbing material. Measurements in this region were made with γ-rays from a cobalt-60 source (1.1732 and 1.3325 MeV).

It was thought that these photon energies would adequately evaluate the simulation procedures and the manufactured materials and also provide valuable data for medical radiation studies.

The attenuation measurements involving characteristic radiation were performed at the Berkeley Nuclear Laboratories using equipment provided by the Environmental & Medical Sciences Division of A.E.R.E., Harwell. The measurements with Americium & Cobalt were performed at the Physics Department, St Bartholomew's Hospital.

In chapter 8 the uses of the old and new materials in radiation dosimetry are explored. Experiments are presented on such topics as thermoluminescent dosimetry, skin doses in mammography procedures and organ doses with radionuclides. It is hoped that these experiments will illustrate the many possible applications of the new simulation procedures and the flexibility of the new materials.

1.3 TERMINOLOGY

The symbols and nomenclature referred to in this thesis are summarised in APPENDIX 1.

Chemical formulae are either quoted in the form of elemental atomic proportions (e.g. H_2O) or as proportions by weight [H (11.19); O (88.81)]

The term 'SUBSTITUTE' will be applied in a general sense to describe any material which has been, or could be used experimentally to simulate a tissue or other medium. An 'EQUIVALENT' material was arbitrarily taken to mean any substitute having radiation characteristics (that is, photon attenuation coefficients, stopping powers, etc) within 1% of the material being simulated over a given energy range.

As the terms 'attenuation coefficient' and 'energy absorption coefficient' are frequently discussed, the contraction 'COEFFICIENTS' will be used in a general sense to describe both total and partial interactions. Similarly the term 'POWER' will be taken to generally mean collision and radiation stopping powers and angular scattering powers.

CHAPTER 2

A CRITICAL EVALUATION OF EXISTING SUBSTITUTES

2.1 THE MEANING OF 'EQUIVALENCE'

Of the many terms used in radiation dosimetry, 'TISSUE EQUIVALENCE' is probably the one which has been misused more consistently than any other. Materials which have acceptable mass densities but of unknown composition are frequently referred to as 'TISSUE EQUIVALENT'. Unsubstantiated statements such as 'TISSUE EQUIVALENT WAX' or 'AN EQUIVALENT MATERIAL' are found in papers spanning 60 years of radiation measurements.

There have, of course, been some excellent studies on this subject (SPIERS, 1943 and 1946; MARKUS, 1956; ROSSI and FAILLA, 1956; SHONKA et al, 1956; FRIGERIO & SAMPSON, 1969) but all too often the advice given by the authors has not been heeded. A typical example is the use of pressdwood. From 1940 - 1943 two independent reports were published each showing that pressdwood had variable photon attenuation properties depending upon the wood-pulp and bonding resins used during the manufacturing process. Despite these warnings, reports of measurements based on pressdwood phantoms continue to be published, even to the present day.

For two materials to absorb and scatter photons and electrons in exactly the same way, five physical quantities must be identical, namely,

(i) MASS ATTENUATION COEFFICIENTS (μ/ρ)

(ii) MASS ENERGY ABSORPTION COEFFICIENTS (μ_{en}/ρ)

(iii) ELECTRON MASS STOPPING POWERS (S/ρ)

(iv) ELECTRON MASS ANGULAR SCATTERING POWERS ($\bar{\Theta}^2/\rho\ell$)

(v) MASS DENSITY (ρ) (or specific gravity)

(The symbols have conventional meanings and are stated in APPENDIX 1).

Quantities (i) and (ii) describe photon absorption and scattering interactions while (iii) and (iv) describe similar processes for electrons. Strictly, partial coefficients or powers must be identical and not simply the total effects. If, at a certain energy, two effects are equally important (for example incoherent scattering and photoelectric absorption), then a positive error in one could be counteracted by a negative error in the other making the total apparently correct. For these reasons, the partial contributions - coherent & incoherent scattering, photoelectric absorption, pair production, electron collision and radiation interactions - must be considered in any serious study of equivalence.

If the two materials are to have the same physical dimensions then the mass densities, or specific gravities, must be the same.

Nearly 80 different formulations have been published which are claimed to simulate tissues (muscle, fat, lung, bone), air and one polymer. Less than one-tenth of these have the five quantities mentioned above with a few percent of those for the material being simulated over the energy range 10 keV-100 MeV. All too frequently

the maximum errors are in the energy ranges for which the materials are designed. The best materials have been based upon mass attenuation coefficients and specific gravities, whilst the least acceptable are based on specific gravity only. Apparently no material has been produced which takes into account the five quantities.

The applications of the material will often decide which quantities have to be analysed. For example, if a material is to be used for low energy photon scattering experiments, then perhaps mass attenuation coefficients and specific gravities need only be considered. In electron scattering studies, angular scattering powers may be of prime importance. Conversely if absorbed dose studies are being planned, then the five quantities must be considered, because the attenuation and absorption coefficients will decide the types and magnitudes of the photon interactions while the stopping and scattering powers will influence the energy deposition of the secondary electrons created by the photons.

When it has been established which effects have to be investigated, the degree of simulation has to be selected. Again this will be dependent upon the particular experimental arrangement and the dosimetric equipment being employed. Differences of 1 - 2% may easily be detected in the photon attenuation and absorption coefficients for materials by simple photographic techniques (JONES & RAINE, 1949; STACEY, 1973). Similarly differences

of a few percent in stopping and angular scattering powers may be detected with suitable sensitive measuring equipment.

In this study the computation techniques permit the selection of any 'FITTING RATIO', which is defined as the ratio of the coefficients or powers at a given energy for a substitute and the 'real' material. In most cases a fitting ratio of 1.01 (1% simulation) was chosen because it was thought that as the accuracies of dosimetric procedures are continually improving, the closest simulation was desirable.

A problem which should be mentioned at this stage is the imprecise formulae of the materials being simulated, in particular biological tissues. The uncertainties and apparent lack of knowledge in the composition of many tissues (TIPTON, 1973) makes the task of simulation more difficult. It can be argued that it is futile to simulate to 1% a tissue whose published composition varies considerably. It is thought that until there is more precise data on tissue composition, substitutes should be available which represent the most reliable published data. If the composition is known to vary over a given range, then a family of substitutes should be formulated which adequately cover this range. Means of formulating materials having coefficients and powers within narrow limits is obviously required if such substitutes are to be successfully manufactured.

2.2 AN HISTORICAL SURVEY

The development of equivalent materials falls naturally into two phases (Tables 2.1 and 2.2). In the first phase a general awareness of the problems involved appears to develop with most experimental studies using either water or wax. At the end of this period a more analytical approach evolved and the concept of adding compounds to wax in order to improve its attenuation properties was introduced.

During the second phase, which continues to the present day, many mixtures of solids and liquids are derived as substitutes for biological tissues and other media. This phase is characterised by the gradual improvement in the manufactured materials and the use of effective atomic numbers which most authors employ in their formulation procedures.

As in most prolonged developments, the transition from one phase to another is blurred and not precise. In this survey 1940 was chosen as the 'mid-point' year.

1906	KIENBÖCK states that water and muscle have similar X-ray absorption properties.
1913	CHRISTÉN used bakelite to simulate water.
1920	JÜNGLING used talc as bolus in radiotherapy treatments.
1922	BAUMEISTER introduced wax as 'tissue' substitute.
1924	A body phantom was constructed by WESTMAN for gynaecological radiation measurements.
1925	The concept of 'effective atomic number' was discussed by FRICKE & GLASSER in connection with 'air-walled' ionization chambers.
1933	Rice used by PETTIT & LANDAUER for depth dose studies and by HOLFELDER as a bolus material in radiotherapy treatments.
1937	TRÜBESTEIN used triolein as fat substitute. FAILLA introduced pressdwood as a muscle substitute. SIEMENS' WAX, a mixture of paraffin wax and magnesium oxide, was described by OTT. MAYNEORD re-introduced and extended the concept of effective atomic number.

TABLE 2.1 THE DEVELOPMENT OF EQUIVALENT MATERIALS

CHRONOLOGY - 1906-1939

1940	BRAESTRUP and BLATZ reported on the attenuation properties of pressdwood.
1943	SPIERS published comprehensive paper entitled 'materials for depth dose measurements' and introduced a rice/sodium bicarbonate mixture.
1944	A cellular lung substitute introduced by EDLING.
1946	SPIERS discussed effective atomic numbers with reference to tissues and used plaster of Paris as a bone substitute.
1949	JONES and RAINE introduced Mix D. SPIERS used glass as a bone substitute.
1953	'LINCOLNSHIRE' bolus produced by LINDSAY & STERN.
1956	Improved wax based mixtures introduced by MARKUS and HARRIS et al. ROSSI & FAILLA discussed liquid and gel systems.
1958	A family of conducting plastics produced (SHONKA et al).
1961	'TEMEX' body phantom introduced (STACEY et al).
1962	'RANDO' body phantom introduced (ALDERSON et al).
1969	WEBER & van den BERGE presented a new analysis of effective atomic numbers. Complex liquid systems introduced (FRIGERIO & SAMPSON).
1972	The formulation of 'TEMEX' lungs reported by STACEY.

TABLE 2.2 THE DEVELOPMENT OF EQUIVALENT MATERIALS

CHRONOLOGY - 1940-PRESENT DAY

2.2(i) PRE-1940

The study of equivalent materials started in the early part of this century, when the newly discovered X-rays were being intensively investigated both in Europe and the U.S.A. The June edition of the 'Archives of the Roentgen Ray' for 1906 contains a report by a Viennese radiologist, Professor KIENBÖCK, on a new dosemeter, called a 'quantimeter'. (Figure 2.1). Towards the end of the contribution Kienböck reasons that 'an aluminium foil 1 millimetre thick is equivalent in absorption power to a layer of water or muscle, 1 centimetre thick'. The study of equivalent materials had begun.

Unfortunately the implications of these results were not formalised until 1913. During the intervening years a number of important investigations were made on the attenuation properties of biological tissues. In 1907 BORDIER measured X-ray absorption in adipose, mammary and muscular tissues using 'pastille' dosimetry. Two years later WILLIAMS compared lung tissue and water, and GUILLEMINOT compared fat, liver, lung and spleen tissues. In 1912, at meetings of the Roentgen Society and the Royal Society, RUSS reported on tissue absorption but added data on scattered radiation from water, blood, spleen, liver and kidney samples. (RUSS, 1912 (a) & (b)).

The ideas inherent in these results were crystallised in 1913 by a Swiss radiologist, mathematician and politician, FRANZ THEOPHIL CHRISTÉN. In his book 'Messung und Dosierung

Annual Subscription,
16 - net ($4), in advance.

No. 71.

Price 1 6 net (with postage 1 8).
„ 36 cents (with postage 40 cents).

ARCHIVES
— OF —
THE ROENTGEN RAY
AND ALLIED PHENOMENA
(*Formerly* ARCHIVES OF SKIAGRAPHY).

AN INTERNATIONAL MONTHLY REVIEW
OF
THE PRACTICE OF PHYSICAL THERAPEUTICS.

Edited by CLARENCE A. WRIGHT, F.R.C.S. Edin., F.F.P.S.G., and W. DEANE BUTCHER, M.R.C.S.

IN COLLABORATION WITH
ROBERT ABBE, M.D., (*New York*); T. P. BEDDOES, F.R.C.S., (*Lock Hospital, London*); J. BELOT, M.D., (*Paris*); H. BORDIER, M.D., (*Lyons*); R. HIGHAM COOPER, L.S.A., (*Tottenham Hospital, London*); EDRED M. CORNER, M.A., B.Sc., F.R.C.S., (*London*); H. EVELYN CROOK, M.D., (*Twickenham*); R. W. FELKIN, M.D., F.R.S.E., (*London*); J. HALL-EDWARDS, L.R.C.P., F.R.P.S., (*General and Royal Orthopædic Hospitals, Birmingham*); MILTON FRANKLIN, M.D., (*New York*); LEOPOLD FREUND, M.D., (*Vienna*); H. E. GAMLEN, M.D., (*West Hartlepool*); A STANLEY GREEN, M.D., (*Lincoln, Eng.*); C. THURSTAN HOLLAND, M.R.C.S., (*Royal Infirmary, Liverpool*); GUIDO HOLZKNECHT, M.D., (*Vienna*); HENRY LEWIS JONES, M.D., (*St. Bartholomew's Hospital, London*); ARCH. JUBB, M.D., (*Royal Infirmary, Glasgow*); STEPHANE LEDUC, M.D., (*Nantes*); JOHN MACINTYRE, M.D., (*Glasgow*); HORACE MANDERS, M.D., F.R.C.S., (*London*); DAVID MORGAN, M.B., (*Liverpool*); E. REGINALD MORTON, M.D., C.M., F.R.C.S. Edin., (*London Hospital, London*); HENRY G. PIFFARD, M.D., (*New York*); GUSTAV REUS, Ph.D., M.D., (*Chemnitz*); Prof. WERTHEIM SALOMONSON, (*Amsterdam*); EDWARD W. SHENTON, M.R.C.S., (*Guy's Hospital, London*); SAMUEL SLOAN, M.D., (*Glasgow*); W. F. SOMERVILLE, M.D., F.F.P.S.G., (*Glasgow*); DAWSON TURNER, M.D., (*Royal Infirmary, Edinburgh*); HUGH WALSHAM, M.D., (*St. Bartholomew's Hospital, London.*); SYDNEY WHITAKER, M.D., (*Liverpool*); WALTER KENNETH WILLS, M.A., M.S., B.C. Camb.; (*General Hosp., Bristol*).

VOL. XI. RADIOTHERAPY — No. 1. RADIOTHERAPY — ELECTROTHERAPY — JUNE. — 1906.

CONTENTS.

LONDON
REBMAN LIMITED
129 Shaftesbury Avenue, W.C.

NEW YORK
REBMAN COMPANY
1123 Broadway

FIGURE 2.1 AN EARLY JOURNAL CONTAINING KIENBÖCK'S ORIGINAL CONCEPT OF 'TISSUE EQUIVALENCE'

der Roentgenstrahlen', Christén stated that X-ray beam quality should be specified in terms of water attenuation, as water gave similar results to soft tissue. He also introduced a solid water substitute in the form of bakelite, which was said to have 'exactly the same roentgen opacity as water'.

The claims on the attenuation properties of water were substantiated during 1914 in a paper by SZILARD and independently by SALMOND, while addressing the Electro-Therapeutic section of the Royal Society of Medicine.

During 1922, in a lecture before members of the Swedish Society for Medical Radiology, BAUMEISTER stated that wax had the same absorption and scattering properties as 'tissue' (BAUMEISTER, 1923).

The profound effect that the statements of Kienböck, Christén & Baumeister had on future radiation measurements is evident from the considerable quantities of data produced using water and wax. Radium & radon isodose curves in water (FRIEDRICH & GLASSER, 1922; SCHMITZ & HUTH, 1922) and wax, (QUIMBY, 1928; HOED & STOEL, 1929) together with X-ray measurements (DESSAUER & VIERHELLER, 1921; WEATHERWAX & WIDMANN, 1929; MAYNEORD, 1929(a))are reported in numerous papers in the journals of that time. It was not until much later that it was realized that wax was not ideal, especially at low photon energies (MAYNEORD, 1933; QUIMBY & ARNESON, 1937).

It is frequently thought that tissue substitutes moulded into the shape of a human body, or, so-called 'body phantoms', are a relatively modern innovation; but in 1924 WESTMAN used a 'pelvic phantom' made of wax and bolus alba for gynaecological measurements.

[BOLUS ALBA is a mixture of 2 parts flour and 1 part china clay, by weight (STENSTRÖM, 1926)] Although a few attempts at more realistic phantom shapes were reported during this period, (FAILLA, 1925; MAY, 1934; GRIMMETT, 1939) the majority of experiments were performed with tanks of water or blocks of wax.

The type of wax used is not always clear from the early papers. Paraffin wax and beeswax were popular in the early work and 'unit density wax' was frequently quoted towards the end of the period. A mixture known as 'Columbia wax' was sometimes used, which consisted of paraffin wax, beeswax and sawdust (JONES, 1969; CLARKSON, 1973).

The use of bolus materials during radiotherapy treatments, to fill interstices over the patient's skin commenced in 1920 (JÜNGLING, 1920). Talc was one of the first materials to be employed, but bolus alba, rice, dough & water-bags are reported by many authors (WESTMAN, 1924; FAILLA, 1925; PETTIT & LANDAUER, 1933; HOLFELDER, 1933).

Rice was also used for dosimetric studies in some countries.

In America PETTIT & LANDAUER (1933) used rice for depth dose studies & were followed in France by BELOT & DAUVILLIER (1939) and, perhaps inevitably, by WILLIAMS (1936) at the Department of Radiology of the PEIPING Union Medical College, China.

It must be stressed that many dosimetric studies were made that did not revolve around tissue substitutes. Work was progressing on the attenuation properties of real tissues (FAILLA, 1920; GLASSER, 1932; WILSON & MYERS, 1936). Cadavers were also used for dosimetric measurements (QUIMBY et al., 1934); but as WEATHERWAX stated a few years earlier, 'in a cadaver, we have not reproduced the living' (WEATHERWAX & ROBB, 1930).

The only reported simulation of other media appears to be attempts to find air equivalent materials (FRICKE & GLASSER, 1925; GLOCKER & KAUPP, 1927; GLASSER et al., 1928; MAYNEORD & ROBERTS, 1937; SIEVERT, 1937) and TRÜBESTEIN'S use of triolein as a fat substitute in 1937. The effects of air cavities in wax phantoms were investigated by LEDDY & WITTING in 1930, but a lung substitute does not appear to have been devised until much later.

Pressdwood, a compressed cellulose material, was introduced in 1937 by FAILLA and enjoyed a long period of use, especially in the U.S.A. (QUIMBY et al., 1938; AEBERSOLD & CHAFFEE, 1939).

This phase ends with the introduction of SIEMENS' WAX , a

mixture of paraffin wax (100) and magnesium oxide (21) which had improved attenuation properties compared to wax alone. (OTT, 1937). In the same year MAYNEORD re-examined the concept of effective atomic number that he had considered in 1929 (MAYNEORD, 1929(b)) and that was discussed in 1925 by FRICKE & GLASSER. Mayneord calculated the effective atomic numbers for photoelectric processes for a range of carbohydrates, proteins, etc and applied the results to energy absorption in tissues, which became the basis of future simulation studies.

In summary, during this period both water and wax had universal acceptance as soft tissue substitutes, with the limitations of wax being gradually realized. Other materials introduced included rice, grain, flour, etc, and were utilized both in dosimetric measurements and as bolus materials in radiotherapy treatments. The period ends with the first attempt at modifying wax and a theoretical study of energy absorption in biological tissues. Many changes were to take place during the next few years, but these will be described in the next section.

2.2(ii) 1940-PRESENT DAY

The general mood of intense scientific investigation and innovation which started in the late 1930's continued into this period with two notable papers by SPIERS. In 1943 SPIERS published a paper entitled 'Materials for depth dose measurements', in which he investigated the photon attenuation properties of many materials, including water, wax, rice, sugar and borax. Significantly he measured the properties of a number of woods & pressdwoods, and in support of an earlier communication by BRAESTRUP and BLATZ (1940), concluded that pressdwood had variable characteristics and was not suitable when low energies were employed. Spiers also substantiated earlier claims that wax was not suitable as a muscle substitute at low photon energies, and some mixtures of rice and sodium bicarbonate were developed, claimed to have acceptable properties at these energies. Another paper by this author in 1946 extended the concept of effective atomic numbers and energy absorption in biological tissues. The absorption characteristics of muscle, fat, skin and bone samples were analysed both experimentally and theoretically.

Attention was now being given to other tissue substitutes. In 1944 EDLING introduced a cellular lung substitute called 'ZELLSTOFF', while plaster of Paris and glass were used to simulate bone (SPIERS, 1946 and 1949). Bolus materials were also dramatically changed when in 1953, LINDSAY & STERN introduced, at the Lincolnshire Radiotherapy Centre, a particulate system consisting of sucrose (87) and magnesium carbonate levis (13), to be known

later as 'LINCOLNSHIRE BOLUS'. Within a few years most hospitals throughout Britain were using this material in preference to the rice, flour, etc which had been extensively employed in the past.

The way in which the substitutes were applied to dosimetric problems shifted in emphasis during this period from the techniques based on solid blocks of material or tanks of liquids, to those based upon body phantoms. Numerous reports of 'home-made' body phantoms are to be found in the literature. A selection of these phantoms, described in TABLE 2.3, should illustrate the diversity of approach.

From 1949-1962 a number of substitutes were introduced which, as water and wax did much earlier, strongly influenced experimental dosimetry. In 1949 JONES & RAINE produced a water substitute called 'MIX D'. This was a mixture of paraffin wax (60.8), polyethylene (30.4), magnesium oxide (6.4) and titanium dioxide (2.4) that could be cast into sheets or more complex body sections. [NIKL (1965) has discussed an interesting and apparently fragrant variation of MIX D which he calls the 'Japanese version', composed of paraffin wax (61), polyethylene (25), pine resin (16.2), magnesium oxide (6.4) and titanium dioxide (2.4)]

In 1956, ROSSI and FAILLA introduced some liquid & gel systems based on an approximate formula for soft tissue, $C_5 H_{40} O_{18} N$.

REFERENCE	DESCRIPTION OF BODY PHANTOM
JENSEN, 1945	Female pelvis, partially dissected, filled with bags of talc and '...gathered in a canvas corset and wrapped in a sheet...'
OSBORN et al., 1945	Model of child's head '...made of wax containing a small proportion of starch to correct its density...'
NAHON & HAWKES, 1954	Plywood thorax phantom
WHEATLEY & LISTER, 1957	Human skeleton immersed in mix D (described later), packed with Lincolnshire bolus. Sawdust lungs.
LINCOLN & GUPTON, 1958	Adult female paper-mâché display manikin, covered with thin layer of plaster and filled with wax. Two empty polyethylene bottles inserted to simulate lungs.
JACOBS & PAPE, 1961	Fibreglass shell manikin (female) filled with rice.
TROUT & KELLEY, 1972	'...Masonite sheets in the shape of a torso...'

TABLE 2.3 SOME PUBLISHED BODY PHANTOMS

These systems, in particular the liquid mixture consisting of water (56.9), glycerol (28.4), urea (7.6) and sucrose (7.1), have been used repeatedly over the years, both in the original form and also with small variations in composition (AGAGI & LEHMAN, 1963; FAIRCHILD, 1965; FIELD & PARNELL, 1965; GOODMAN, 1969; OSHINO, 1973).

A family of electrically conducting plastics simulating muscle, bone, air and polystyrene were manufactured in 1958 (SHONKA et al., 1958). The materials were compounded from a number of polymers and inert fillers. For example, the muscle substitute was blended from carbon (13.5), polyethylene (52.1), nylon (28.2), silica (2.2) and calcium fluoride (4.0). Due to their conducting properties these plastics, with some minor modifications (SPOKAS, 1973) have been used extensively in the construction of ionization chambers.

Two other important systems simulating soft tissues were produced in the early 1960's. In 1961 a material to be known subsequently as 'TEMEX' was devised at the Royal Marsden Hospital in London (STACEY, et al., 1961). This was basically a depolymerised natural rubber with the addition of carbon and titanium dioxide (STACEY, 1972). In 1962, the 'RANDO' system was introduced in the U.S.A. (ALDERSON et al., 1962). The material used was a synthetic isocyanate rubber, but no indication was given in the original paper of the fillers employed. Some more

information may be gleaned from the Complete British Patent specification published in 1966 (ALDERSON, 1966), which states that phenolic microballoons & antimony trioxide were added to the isocyanate. 'Temex' and 'Rando' are both produced in sheet form and moulded around human skeletons as sliced body phantoms. Lung substitutes are also available, 'Temex' using a formulation based on latex, while 'Rando' is based on an epoxy resin (STACEY, 1972; ALDERSON, 1966).

So, during the period 1949-1962, five major systems were developed, namely mix D, Rossi-Failla liquids & gels, the Shonka plastics, 'Temex" & 'Rando'. Of course there were other formulations, often having superior properties to these five systems, but the uses were frequently localised at the centre or country of origin and have not enjoyed world-wide acceptance. In this context the wax formulations of MARKUS (1956) (called 'M3') and HARRIS et al., (1956) have useful attenuation properties but have not been widely applied.

Most substitutes have been designed for photon interactions, and materials specifically for electron & beta dosimetry are not to be found in the literature. Electron studies using 'conventional' materials, including perspex , polyethylene and polystyrene, are reported by many authors (LAUGHLIN, et al., 1953 and 1965; HAYBITTLE, 1960; MARKUS, 1960 and 1961; ALMOND et al., 1967).

Unfortunately a large number of inferior products have found applications during the past 20 years. It has already been stated that pressdwood, although known to be variable in composition and poor at low photon energies, continues to be popular, presumably because of its cheapness and availability. Lung substitutes have suffered most from the continued use of materials of unknown and variable composition. Sawdust, cork, sponge, oatmeal and even breakfast cereals have been employed and, in fact, are still being reported simply because their mass densities are of the correct order of magnitude.

The study of air substitutes for ionization chambers has not progressed as rapidly as might be expected. Formulations have been communicated by BERNSTEDT (1940), ALY and WILSON (1949), and OTLET & GEORGE (1960). A spokesman for a major U.K. nucleonic organisation has reported that nylon, graphite coated perspex and P.T.F.C.E. have been considered to give simulation over restricted energy ranges (WRIGHT, 1973).

During the past fiveyyears two important contributions to the study of equivalent materials have appeared. In 1969 a new analysis of effective atomic numbers was published (WEBER & van den BERGE, 1969) which has thrown some light on the poor performances of earlier formulations based upon this quantity. In the same year some liquid systems were developed which simulated 'standard man' & muscle tissue (FRIGERIO & SAMPSON, 1969). These were complex aqueous mixtures containing many

additives and designed to give a direct simulation of elemental composition.

The modern radiation physicist has a large number of substitutes available for dosimetric studies. All too often the choice is dictated by finance and the materials used by former colleagues. The choice is made even more difficult by the sparse and far from complete data given by authors on their products. A typical report on a formulation might have only one effective atomic number, the mass density and, perhaps, the electron density quoted. In the next section a comprehensive analysis of the physical properties of all the important substitutes will be discussed.

2.3 THE CHARACTERISTICS OF PUBLISHED SUBSTITUTES

In the previous section it was stated that the available data on existing substitutes were incomplete and frequently non-existent, The only adequate method of analysing the usefulness of a formulation over a wide range of energies, is to consider the five physical quantities discussed at the beginning of the chapter (namely mass attenuation & energy absorption coefficients, mass stopping & angular scattering powers, and specific gravities).

Calculations of coefficients and powers at 33 energy points in the range 10 keV - 100 MeV have been made on as many substitutes of known compositions as could be found in a thorough search of the literature. Some 77 materials were analysed in 8 categories, as outlined below,

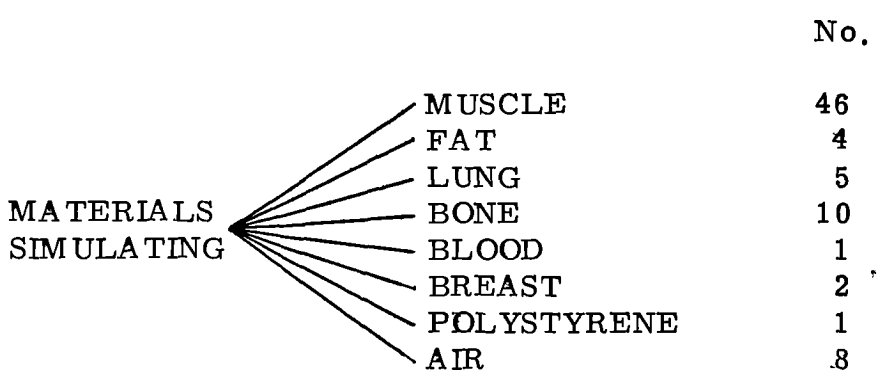

Each of these categories will now be considered in detail.

2.3(i) MUSCLE

The elemental compositions of 46 muscle substitutes were calculated and their coefficients & powers derived for the energy range 10 keV - 100 MeV. These values were compared with the

coefficients and powers for the composition of striated muscle given by the ICRU (National Bureau of Standards, 1964) [H(10.2); C(12.3); N(3.5); O(72.893); Na(0.08); Mg(0.02); P(0.2); S(0.5); K(0.3); Ca(0.007)] The specific gravity of muscle was taken to be in the range 1.00-1.06.

A selection of the important muscle substitutes, with brief descriptions of compositions, is given in TABLE 2.4 (for solids) and TABLE 2.5 (for liquids, powders and gels).

The substitutes may be conveniently split into three classifications according to the magnitudes of the maximum errors in their coefficients and powers compared to ICRU muscle. Classes A, B and C refer to errors $<5\%$, 5-20% and $>20\%$ respectively.

For low energy photons the energy range 10-150 keV was considered, being the predominant photoelectric region. (At 150 keV the photoelectric contribution to the TOTAL mass attenuation coefficient is $\sim 1\%$ for muscle). This energy range is also the one for which most substitutes are designed. The classifications are given below and were based on a comparison of mass attenuation and energy absorption coefficients.

CLASS A (Errors $<5\%$):

Liquid systems	(FRIGERIO & SAMPSON, 1969)
M3	(MARKUS, 1956)
Powder systems	(SPIERS, 1943)
Water	

TYPE/NAME	COMPOSITION	REFERENCE
SIEMENS' WAX	PARAFFIN WAX + MgO	OTT, 1937
PRESSDWOOD	?	FAILLA, 1937
MIX D	PARAFFIN WAX + POLYETHYLENE + MgO + TiO_2	JONES and RAINE, 1949
WAX BASED	PARAFFIN WAX + SiO_2	HARRIS, et al, 1956
M 3	PARAFFIN WAX + MgO + $CaCO_3$	MARKUS, 1956
CONDUCTING PLASTICS	POLYETHYLENE + NYLON - 6 + C + SiO_2 + CaF_2	SHONKA, et al, 1958
"	TEFLON + CARBON	SHONKA, et al, 1958
PHILITE	ARTIFICIAL RESIN	OOSTERKAMP and PROPER, 1959
BIO - PLASTIC	THERMO - POLYESTER	RODERICK, 1959
'TEMEX'	NATURAL RUBBER + FILLERS	STACEY, et al, 1961
'RANDO'	ISOCYANATE RUBBER + FILLERS	ALDERSON, et al, 1962

TABLE 2.4 SOME PUBLISHED MUSCLE SUBSTITUTES - SOLIDS

TYPE/NAME	COMPOSITION	REFERENCE
LIQUID	WATER	KIENBÖCK, 1906
"	WATER + GLYCEROL + UREA + SUCROSE	ROSSI and FAILLA, 1956
"	WATER + GLYCEROL + UREA	GOODMAN, 1969
"	WATER + MISC. COMPONENTS	FRIGERIO & SAMPSON, 1969
POWDERS	RICE + SODIUM BICARBONATE	SPIERS, 1943
LINCOLNSHIRE BOLUS	SUCROSE + MAGNESIUM CARBONATE	LINDSAY and STERN, 1953
PASTE	PARAFFIN + MgO + $CaCO_3$	MARKUS, 1956
POWDER	PARAFFIN + B_2O_3 + $MgCO_3$	WEBER & van den BERGE, 1969
GEL	WATER + GELATIN + GLYCEROL + SUCROSE	ROSSI and FAILLA, 1956
"	WATER + AGAR + MISC COMPONENTS	FRIGERIO, 1962

TABLE 2.5 SOME PUBLISHED MUSCLE SUBSTITUTES - LIQUIDS, POWDERS, GELS

CLASS B (Errors 5-20%):

Lincolnshire bolus	(LINDSAY & STERN, 1953)
Lithium fluoride	
Mix D	(JONES & RAINE, 1949)
Shonka plastics	(SHONKA et al., 1958)
Siemens' wax	(OTT, 1937)
Gel system	(ROSSI & FAILLA, 1956)
Liquid systems	(ROSSI & FAILLA, 1956)
(& derivatives)	(GOODMAN, 1969)
Powder system	(WEBER & van den BERGE, 1969)
TLD lithium borate	(JAYACHANDRAN, 1968)
Wax system	(HARRIS et al., 1956)

CLASS C (Errors >20%)

A-150	(SHONKA PLASTIC DERIVATIVES)
Bakelite	
Beryllium oxide	
Bio-plastic	(RODERICK, 1959)
Cellophane	
'Markite'	(ROSSI & FAILLA, 1956)
Paraffin wax	
Perspex	
Polystyrene	
Rice	
Silicon encapsulant DP2628	
'Temex'	(STACEY et al., 1961)

At medium photon energies (~1 MeV) when the response is not dependent upon the atomic numbers of the constituents but upon the electron density and hence the hydrogen content, the errors are reduced significantly. Discrepancies often start to increase as the photon energy approaches 100 MeV.

Similar classifications may be made for electron interactions. Considering the complete energy range, 10 keV-100 MeV, the majority of the materials quoted are CLASS B, with only 9 materials split between the other two classes. Water, the gel and liquid of ROSSI & FAILLA (with derivatives), FRIGERIO and GOODMAN'S

liquids are CLASS A materials. Paraffin wax, the silicon encapsulant DP2628, talc & lithium fluoride are CLASS C materials.

The specific gravities generally fall within the range 0.92-1.20. The wax compounds are at the lower end of the scale and the polymers at the upper end.

FIGURES 2.2-2.5 show how a selection of these systems respond over the complete energy range. The curves depict the calculated ratios of the mass attenuation & energy absorption coefficients (A and B), mass stopping & angular scattering powers (C and D) for the materials compared to muscle. Data for WATER, PARAFFIN WAX, MIX D and 'TEMEX' are presented. The curves illustrate an earlier comment that errors are frequently greatest at the extremes of the energy ranges.

The main conclusions from these calculations are that the existing substitutes, with the exception of a minority such as water, some wax & powder systems and the complex FRIGERIO liquids, may introduce large errors in most dosimetric studies. Even water has errors approaching 5% for low energy photon absorption processes. Errors in excess of 20% cannot be tolerated and equally divergencies of 5% appear excessive by today's standards.

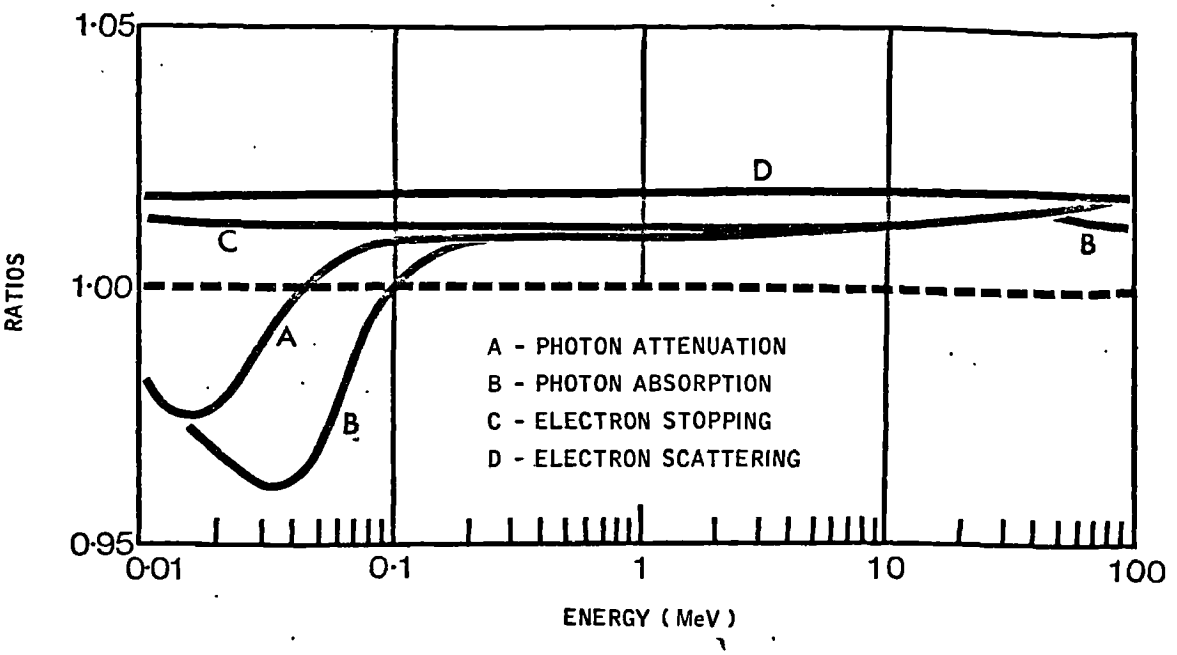

FIGURE 2.2 COEFFICIENT & POWER RATIOS - WATER/MUSCLE

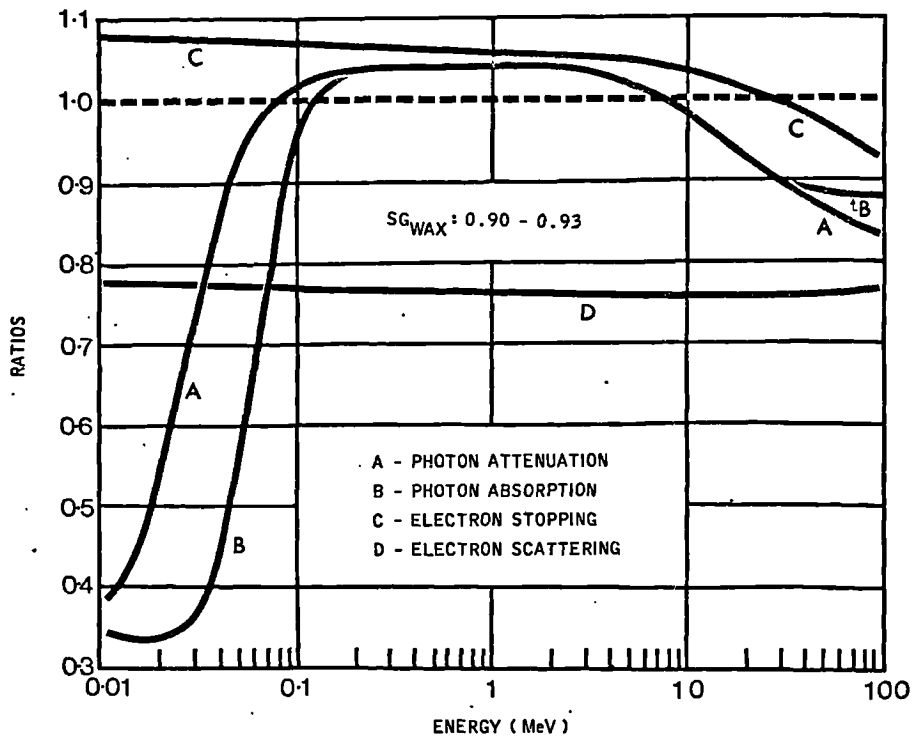

FIGURE 2.3 COEFFICIENT & POWER RATIOS - PARAFFIN WAX/MUSCLE

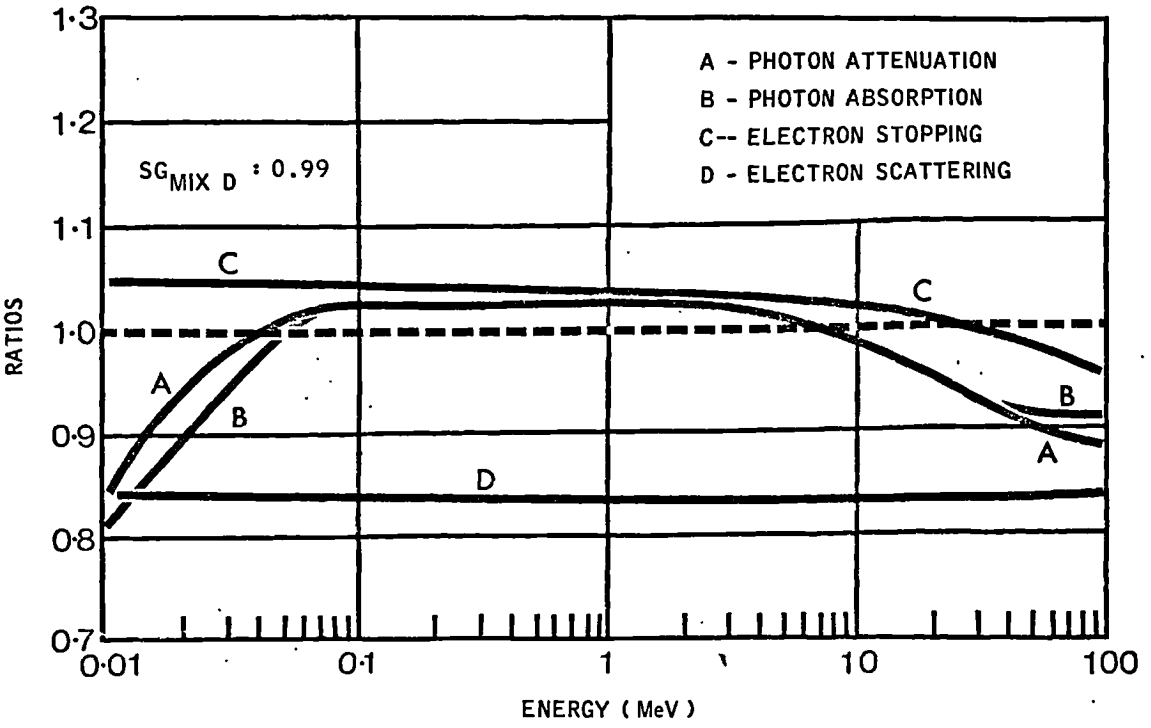

FIGURE 2.4 COEFFICIENT & POWER RATIOS - MIX D/MUSCLE

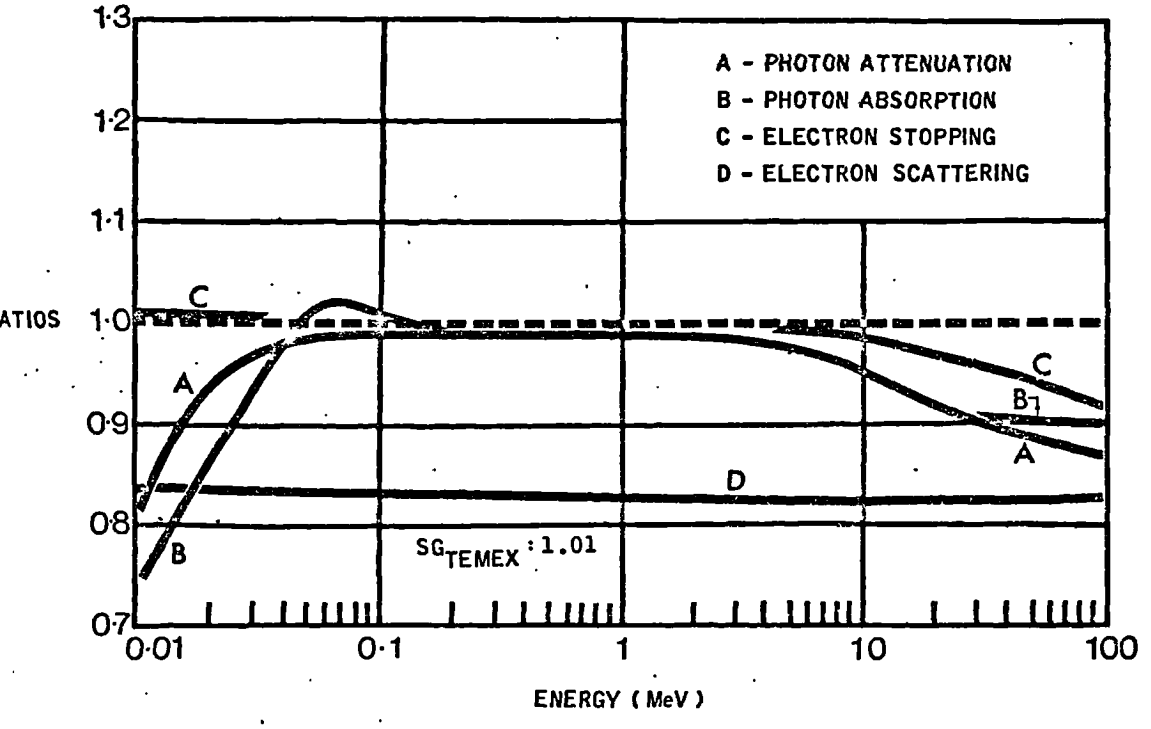

FIGURE 2.5 COEFFICIENT & POWER RATIOS - 'TEMEX'/MUSCLE

2.3(ii) FAT

The only fat substitutes that are published are:

POLYETHYLENE
POLYETHYLENE/CARBON SYSTEM (FOWLER, 1957)
POLYSTYRENE
TRIOLEIN

In addition to these four a commercial product is available from ALDERSON RESEARCH LABORATORIES, U.S.A. The composition of this material is not published.

As a published formula for fat was not available when this study began, the composition was derived from the biochemistry texts of HILDITCH, 1956; WEST et al., 1966 and WHITE et al., 1968. This gave a formula of ....

C (76.05); H (12.21); O (11.74)

The composition was later confirmed in a preprint of an ICRP publication on Reference Man (TIPTON, 1970) which gave a formula for 'body fat' as ....

C (74.1); H (11.9); O (11.1)

Triolein has a formula extremely close to those given above and its coefficients & powers are within 1% of those calculated for fat.

The polyethylene/carbon system used by FOWLER has maximum coefficient errors ~13% and power errors ~7% (CLASS B).

In the energy range 10-100 keV (that is, photoelectric contribution down to below 1% for fat), polyethylene has maximum

coefficient errors ~20%, while polystyrene has errors ~15%. For electrons, both materials have power errors ~5% over the complete energy range.

2.3(iii) LUNG

Only five lung substitutes could be analysed due to the variable and often unknown composition of many of the materials used (for example, cork, sawdust, sponge, etc) (SPIERS, 1943; STONE, 1973) (TABLE 2.6).

COMPOSITION	REFERENCE
CELLULAR MATERIAL 'ZELLSTOFF'	EDLING,1944
PARAFFIN WAX + SAWDUST	KORNELSEN,1954
PLYWOOD	NAHON & HAWKES,1954
CORK + FILLER	COHEN,1955
SPONGE + WATER	LOCHMAN,1955
GELATIN CAPSULES	HARRIS,et al.,1956
FOAM RUBBER	KOREN & MAUDAL,1957
SPONGE + 'CASCO' GLUE	SPLETTSTOSSER & SEEMANN,1955
POLYSTYRENE FOAM	ANDERSON,et al.,1969
ADIPRENE + FILLERS	ROGERS,1970
PERFORATED POLYSTYRENE	NORDBERG,1972
LATEX + FILLERS	STACEY,1972
GRANULATED SHONKA DERIVATIVE (A150)	McGINLEY,1973

TABLE 2.6 SOME PUBLISHED LUNG SUBSTITUTES

Comparisons were made with the ICRU muscle formula, considering lung as an expanded muscle-type tissue. The specific gravity ranges from 0.26 when the lung is inflated, to 1.05 when deflated (TIPTON, 1970).

The classifications for low energy photons in the range 10-150 keV are shown below.

CLASS A (Errors < 5%):	NONE
CLASS B (Errors 5-20%):	NONE
CLASS C (Errors > 20%):	Adiprene (ROGERS, 1970) Gelatin capsules Granulated A-150 Latex (STACEY, 1972) Polystyrene (foam & sheets)

For electron interactions (10 keV - 100 MeV), the above materials are CLASS B.

The specific gravities for all of these materials were of the correct order of magnitude.

The coefficient and power ratios over the complete energy range for STACEY's latex lung substitute are illustrated in FIGURE 2.6. Errors in excess of 20% at low energies occur for mass energy absorption coefficient ratios.

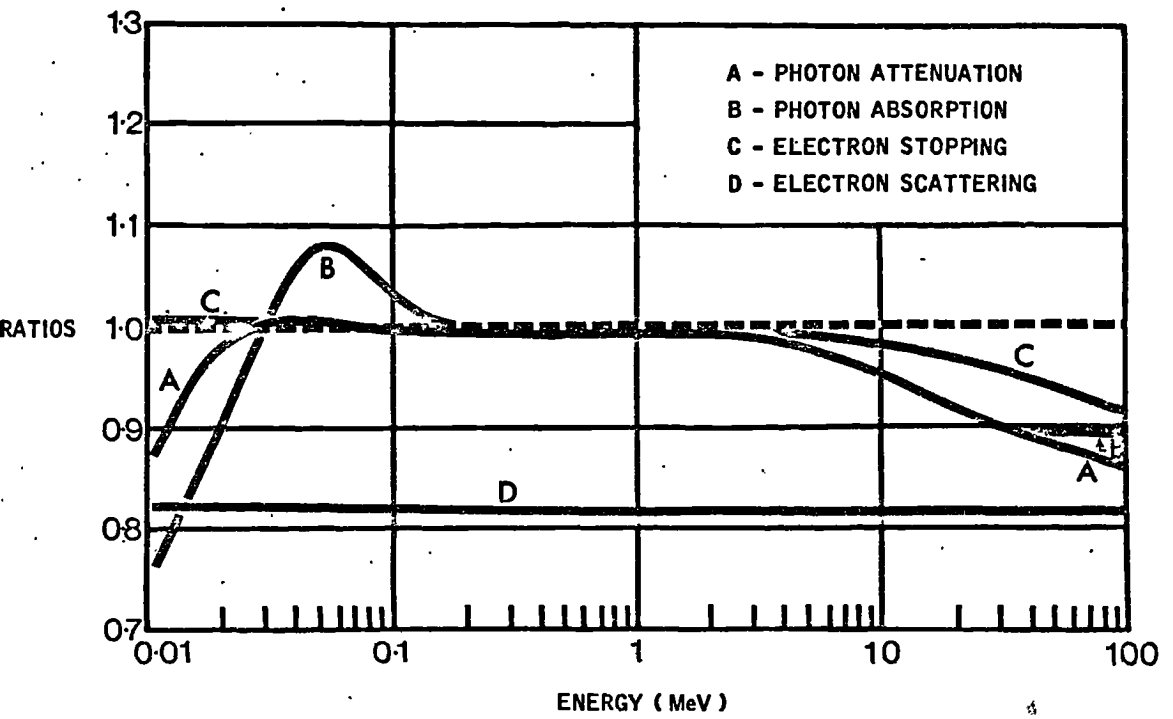

FIGURE 2.6 COEFFICIENT AND POWER RATIOS FOR - STACEY'S LATEX/LUNG

It is concluded that these materials have errors which are unacceptably high for most dosimetric purposes, and that new CLASS A lung substitutes are urgently required.

2.3(iv) BONE

Ten bone substitutes are summarised below in TABLE 2.7.

COMPOSITION	REFERENCE
PLASTER OF PARIS	SPIERS,1946
GLASS	SPIERS,1949
POLYETHYLENE + NYLON-6 + C + CaF_2	SHONKA et al.,1958
ALUMINIUM	GOODWIN,1960
SULPHUR	MARKUS,1960
WATER + $CaBr_2$	SPIERS & CHESTERS,1962
MAGNESIUM	LAUGHLIN et al.,1965
WATER + $CaCl_2$	FACEY,1968
EPOXY RESIN + FILLER	POLL,1972
CARBON TETRACHLORIDE + ETHYL ALCOHOL	VAKHLAKOVA & SKOROPAD,1972

TABLE 2.7 SOME PUBLISHED BONE SUBSTITUTES

Again the coefficients and powers for photon and electron interactions have been calculated over the energy range 10 keV - 100 MeV. The data were compared with a formulation of hard bone given by WOODARD (1962), which is said to be superior to the recommendations given by the ICRU in the National Bureau of Standards' Handbook 85 of 1964 (SPIERS, 1971). The Woodard formulation may be represented as C(15.5); H(3.39); N(3.97); O(44.1); Na(0.06); Mg(0.21); P(10.2); S(0.31); Ca(22.2). The specific gravity was taken to be 1.85 (SPIERS, 1971).

For low energy photons in the energy range 10-300 keV (representing the predominant photoelectric region) the ten

substitutes may be classified as follows:-

CLASS A (Errors < 5%):	NONE
CLASS B (Errors 5-20%):	Aluminium Resin (POLL, 1972)
CLASS C (Errors > 20%):	Liquid Bone (VAKHLAKOVA & SKOROPAD, 1972) Magnesium Plaster of Paris Pyrex Shonka plastic bone Sulphur

Specific gravities vary from approximately 1.7 to 2.7.

In fairness it must be noted that the ICRU formula for bone has been used in the derivation of some substitutes, for example Shonka plastic bone. If comparisons with this composition are made, much better agreement is found.

FIGURES 2.7 and 2.8 show the complete variation in the coefficients and powers for PLASTER OF PARIS and PYREX compared to Woodard bone. Pyrex gives large coefficient errors at low photon energies.

For electrons, most of the substitutes were CLASS B materials. Exceptions were the resin system of POLL (CLASS A), sulphur (CLASS C) and the liquid of VAKHLAKOVA & SKOROPAD (CLASS C). The last two materials gave particularly high angular scattering errors.

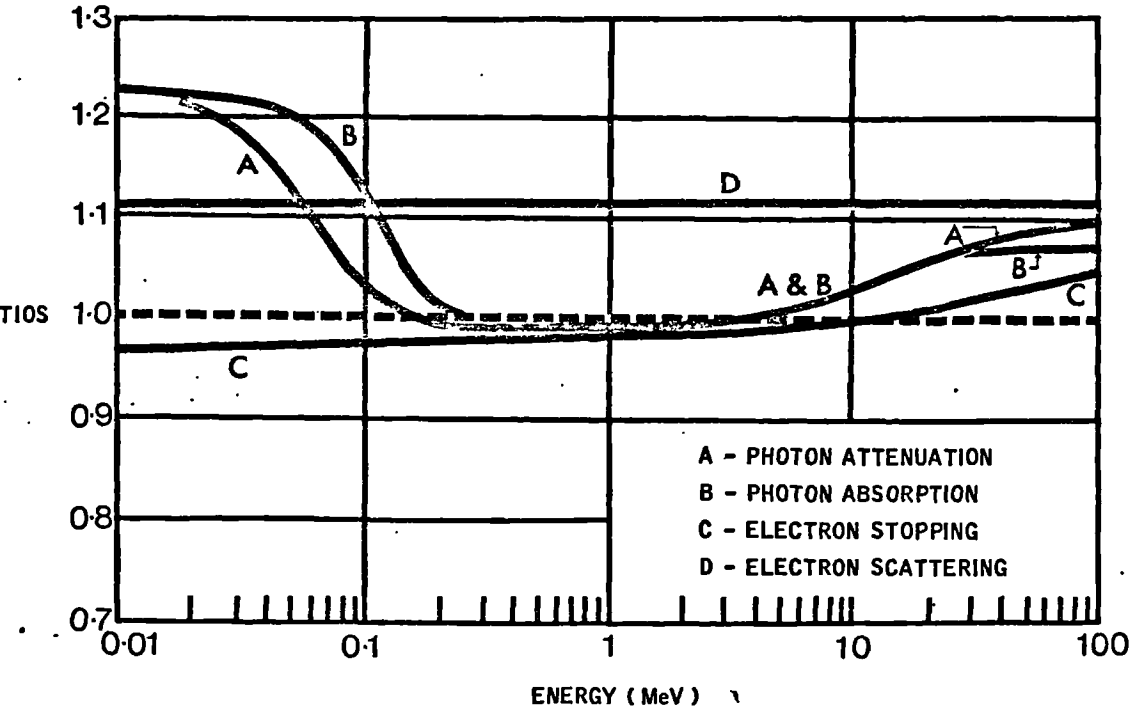

FIGURE 2.7 COEFFICIENT & POWER RATIOS - PLASTER OF PARIS/BONE

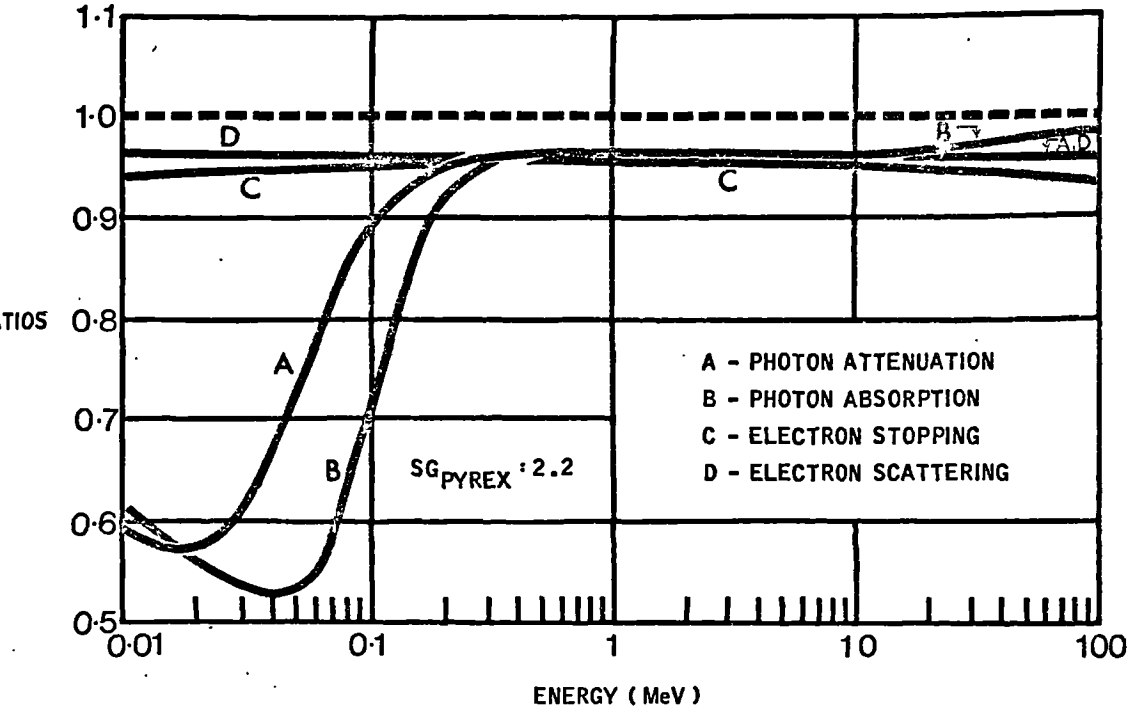

FIGURE 2.8 COEFFICIENT & POWER RATIOS - PYREX/BONE

2.3(v) MISCELLANEOUS MATERIALS

In this section, the remaining categories of blood, breast, polystyrene and air substitutes are considered.

Only one blood substitute could be found (HARRIS et al., 1956), compounded from methyl methacrylate (95) & silica (5). The final product has a specific gravity of 1.19 [the specific gravity of blood is given as 1.06 (TIPTON, 1970)]. For low energy photons the material may be classified as CLASS C, and for electrons CLASS B.

The coefficient and power ratios for the breast tissue substitutes could not be calculated as a reliable formula of 'average' breast tissue was not available.

The single polystyrene substitute (SHONKA et al., 1958) is an electrically conducting mixture of polystyrene (72); polyethylene (15.1); carbon (12.9). As this mixture resolves into a chemical composition almost identical with that of polystyrene, agreement from 10 keV - 100 MeV for both photon and electron processes is excellent.

Some of the important air substitutes are shown in TABLE 2.8.

COMPOSITION	REFERENCE
BAKELITE + C + Si	GLOCKER & KAUPP,1927
BAKELITE	BEHNKEN & JAEGER,1928
CELLULOID	BERNSTEDT,1940
BAKELITE + C + VO	ALY & WILSON,1949
NYLON-6 + C + SiO_2	SHONKA et al.,1958
BAKELITE + C + TiO_2	OTLET & GEORGE,1960
LITHIUM BORATE + Mn	JAYACHANDRAN,1968

TABLE 2.8 SOME PUBLISHED AIR SUBSTITUTES

Calculations were performed on eight formulations, comparing coefficients & powers with similar data derived from the composition of air given by ICRU, (National Bureau of Standards, 1964). For low energy photons (10-200 keV) most of the materials gave maximum errors in the range 5-20% (CLASS B). There were three exceptions; Shonka plastic had errors $< 5\%$ (CLASS A) while the bakelite based substitute of GLOCKER & KAUPP (1927) and also pure bakelite had errors in excess of 20% (CLASS C). For electron interactions (10 keV - 100 MeV) all the materials gave maximum errors in the range 5-20% (CLASS B).

From the data presented in these five sections it can be seen that many of the existing materials purporting to be 'equivalent' to biological tissues and other media are inadequate, especially at low photon energies. This is particularly evident for the lung, bone and many of the popular muscle substitutes. The reasons for these discrepancies will be considered in the next chapter when more reliable selection procedures will be proposed.

CHAPTER 3

THE FORMULATION OF MATERIALS EXHIBITING PREDETERMINED RADIATION CHARACTERISTICS

3.1 EXISTING SELECTION PROCEDURES

Two principal techniques have been applied to the problem of formulating substitution materials. These may be described as (i) the ELEMENTAL EQUIVALENCE METHOD and (ii) the EFFECTIVE ATOMIC NUMBER, $\overline{Z}(x)$, METHOD.

In the first method the substitute is formulated such that it has the same elemental composition as the material being simulated. This method was originated by ROSSI & FAILLA (1956) when they introduced their liquid & gel systems. Mixtures of water, urea, sucrose, etc were made in an attempt to reproduce an approximate formula for soft tissue ($C_5H_{40}O_{18}N$) The liquid system, which with minor variations is still popular in neutron dosimetry, had the formula, $C_5H_{37.5}O_{18}N_{0.97}$.

The methods of arriving at these formulae are frequently omitted and the impression is given that 'trial-and-error' is employed. There are, of course, exceptions to this, a notable one being the method discussed by FRIGERIO and SAMPSON (1969).

Frigerio uses a simplified version of Gibbs' Method of Canonical Components. In the case of the formula $C_5H_{40}O_{18}N$, the canonically required component H_2O is transferred to yield $C_5H_4N(H_2O)_{18}$ Urea, with the formula CH_4N_2O, is next transferred to satisfy

the nitrogen requirement. By writing urea in canonical form, $CH_2N_2(H_2O)$, it is evident that 0.5 moles are required, which gives $C_{4.5}H_3 + 0{\cdot}5(CH_2N_2(H_2O)) + 17{\cdot}5H_2O$. Glycerol, with a formula $C_3H_2(H_2O)_3$, is finally transferred (1.5 moles) to give:- $1{\cdot}5(C_3H_2(H_2O)_3) + 0{\cdot}5(CH_2N_2(H_2O)) + 13H_2O$, which exactly resolved into $C_5H_{40}O_{18}N$.

This method becomes more involved as the reliable tissue formulae, such as ICRU muscle, are used and leads to complex systems having 10-13 components.

Another interesting variation of the Elemental Equivalence Method was devised by SHONKA et al.(1958), to produce a series of electrically conducting plastics. The composition of a muscle substitute was decided from the solution of a set of simultaneous equations derived to satisfy (a) the nitrogen content, (b) the hydrogen content, (c) the electrical conductivity (13% free carbon), (d) Compton interactions and (e) photoelectric interactions.

It appears from the literature that the methods of SHONKA & FRIGERIO are the only ones based on any logical procedures.

The Elemental Equivalence Method accounts for less than 10% of all the published substitutes. The second method, involving so-called EFFECTIVE ATOMIC NUMBERS, is the technique most frequently used for substitutes developed for dosimetric studies with photon beams. In this method a single number is calculated or measured, which is said to characterise the magnitude of the

photon interaction likely to occur. Generally the effective atomic number for photoelectric processes is considered as, historically, low energy X-rays predominated for many years in Medical Establishments. The fact that this energy range is frequently the one in which the largest errors are found, means a thorough investigation of this procedure is imperative if improved simulation techniques are to be developed. In the next section the effective atomic number method will be discussed in detail and its limitations and anomalies probed.

3.2 THE EFFECTIVE ATOMIC NUMBER METHOD

When an element is placed in a beam of photons, the interactions that occur will depend upon the photon energy (E) and the elemental atomic number (Z). It has been shown that the cross section per atom for an interaction (photoelectric absorption, coherent scattering, incoherent scattering or pair production) is directly proportional to the atomic number raised to some numerical power. (BRAGG & PEIRCE, 1914; RICHTMYER & WARBURTON, 1923). For convenience this power will be represented by 'x + 1', so that,

$$\text{ELEMENTAL CROSS SECTION } (\sigma) \propto Z^{x+1} \quad \text{(PER ATOM)}$$

(when compounds are considered, the adoption of the 'x + 1' convention results in formulae which are less tedious to manipulate).

The value of the power 'x + 1' is dependent upon the type of process analysed and is reported to vary from 1 to 5 (HUBBELL, 1969).

A compound may be regarded as a single element with an effective atomic number, $\bar{Z}(x)$, given by

$$\bar{Z}(x) = \left(\sum_i a_i Z_i^x \right)^{1/x}$$

The derivation of this concept is illustrated in FIGURE 3.1. In general, the sum of the constituent elemental atomic numbers, Z_i, raised to the power 'x' and weighted according to their fractional electron content, a_i, within the compound gives the quantity $[\bar{Z}(x)]^x$ from which $\bar{Z}(x)$ may be calculated.

EFFECTIVE ATOMIC NUMBERS

(photon interactions)

(1) ELEMENTS :

CROSS SECTION (σ) $\propto Z^{x+1}$
(per atom)

(2) COMPOUNDS :

By ADDITION FORMULA , the mass attenuation coefficient (μ/ρ) is given by ,

$$\frac{\mu}{\rho} = \sum_i \omega_i \left(\frac{\mu}{\rho}\right)_i$$

But $\sigma_i = k.Z_i^{x+1}$ and $\left(\frac{\mu}{\rho}\right)_i = \frac{N_A}{A_i}.k.Z_i^{x+1}$

So, $$\frac{\mu}{\rho} = \sum_i \omega_i . \frac{N_A}{A_i}.k.Z_i^{x+1}$$

IF n_o = electron density of compound $= N_A \sum_i \omega_i \frac{Z_i}{A_i}$

and α_i = fractional electron content $= N_A \omega_i Z_i / A_i n_o$

Then, $$\frac{\mu}{\rho} = k.n_o.\left(\sum_i \alpha_i Z_i^x\right)$$

Compound may be regarded as a SINGLE element , with EFFECTIVE ATOMIC NUMBER, $\bar{Z}(x)$ where ,

$$\bar{Z}(x) = \left(\sum_i \alpha_i Z_i^x\right)^{1/x}$$

FIGURE 3.1 THE DERIVATION OF EFFECTIVE ATOMIC NUMBERS (DESCRIPTIONS OF THE SYMBOLS USED ARE GIVEN IN APPENDIX 1)

This method of defining effective atomic number is the one normally favoured in simulation studies (FRICKE & GLASSER, 1925; MAYNEORD, 1937; SPIERS, 1946). The technique of weighting according to the relative masses of the constituents has been discussed, but is not widely used (HINE, 1952; HENRIKSEN & BAARLI, 1957; MURTY, 1965).

The mass attenuation coefficient, μ/ρ, for a compound is directly proportional to the product of the electron density, n_o, and the effective atomic number raised to the power, x, or,

$$\mu/\rho \propto n_o [\bar{Z}(x)]^x \quad \text{.....} (3.1)$$

The values of the exponent, x, which have been applied to the study of tissue substitutes are shown in TABLE 3.1. The exponent for photoelectric interactions has varied from 2.94 to 3.4, with the majority of formulations based on the former value. An exponent of 1.7 for coherent scattering processes was introduced by WEBER & van den BERGE (1969). The pair production exponent is always taken to be unity.

The large errors in the properties of the substitutes based on this concept are due mainly to the manipulation of the above relationship (3.1). Usually the simulation procedure is to adjust the composition of the substitute so that the value of $\bar{Z}(x)$ is as close as possible to that of the material being simulated. This is normally performed for only one photon interaction, namely photoelectric absorption. But the coefficients depend upon the

values of $[\bar{Z}(x)]^x$ to be called '$\bar{Z}$-Powers' in this study. A small difference in the values of $\bar{Z}(x)$ will produce a significantly larger difference in coefficients. This is especially true for photoelectric processes when x is generally taken ~3. The electron density is frequently only referred to when incoherent (Compton) scattering is analysed. For this interaction (per electron) x is zero, so the coefficients are directly proportional to the electron density. If the values of the $\bar{Z}$-Powers are exactly equal, any differences in the electron densities will result in differences in the coefficients, even for the photoelectric interactions. The two materials must therefore have identical $\bar{Z}$-Powers and electron densities if good simulation is required.

COHERENT	PHOTO	PAIR	REFERENCE
-	2.94	-	WALTER, 1926 (MAYNEORD, 1937) (SPIERS, 1946)
-	3.1	1.0	HINE, 1952
1.7	3.4	-	WEBER and vanden BERGE, 1969

TABLE 3.1 $\bar{Z}$-EXPONENTS USED IN THE STUDY TISSUE SUBSTITUTES (FOR MASS ATTENUATION COEFFICIENT DATA)

The effects of using the product $n_o[\bar{Z}(x)]^x$ for simulation are illustrated in TABLE 3.2. In the tabulation the notation 'Z(3.0)', refers to the value of $\bar{Z}(x)$ obtained by making $x \approx 3.0$. For simplicity

the product $n_o[\bar{Z}(x)]^X$ will be called '$\bar{Y}(x)$'. Hence '$\bar{Y}(3.0)$' is equivalent to $n_o[\bar{Z}(3.0)]^{3.0}$.

(a)

MATERIAL	$\bar{Z}(3.0)$	$\bar{Y}(3.0)$	$\bar{Y}(3.5)$	$\bar{Y}(4.0)$
MUSCLE	7.483	1388×10^{23}	4077×10^{23}	1223×10^{24}
WAX	5.436	5541×10^{22}	1356×10^{23}	3320×10^{23}
MIX D	7.031	1182×10^{23}	4066×10^{23}	1517×10^{24}
BONE	13.25	7219×10^{23}	3025×10^{24}	1290×10^{25}
PYREX	11.20	4201×10^{23}	1492×10^{24}	5364×10^{24}
PLASTER OF PARIS	14.17	8749×10^{23}	3663×10^{24}	1535×10^{25}

(b)

DATA	RATIOS FOR ----			
	WAX/ MUSCLE	MIX D/ MUSCLE	PYREX/ BONE	PLASTER/ BONE
$\bar{Z}(3.0)$	0.73	0.94	0.85	1.07
$\bar{Y}(3.0)$	0.40	0.85	0.58	1.21
$\bar{Y}(3.5)$	0.33	1.00	0.49	1.21
$\bar{Y}(4.0)$	0.27	1.24	0.42	1.21

(c)

PHOTOELECTRIC MASS ATTEN. COEFF. RATIO	0.34-0.30	0.83-1.03	0.58-0.46	1.22-1.21

TABLE 3.2 EFFECTIVE ATOMIC NUMBER DATA FOR SOME MUSCLE AND BONE SUBSTITUTES

TABLE 3.2 is split into three parts (a), (b) and (c). The tabulation in (a) shows the values of $\bar{Z}(3.0)$, $\bar{Y}(3.0)$, $\bar{Y}(3.5)$ and $\bar{Y}(4.0)$ for two muscle substitutes, WAX and MIX D, and two bone substitutes PYREX and PLASTER OF PARIS. Similar values for muscle and bone are also included. The tabulation (b) shows the ratios of the four quantities for the substitutes and the tissue being simulated. The final tabulation (c) gives the range of values for the ratios of the mass attenuation coefficients for the substitute and tissue, in the photoelectric region. The ratios are quoted for 10 keV - 150 keV for the muscle substitutes and 10 keV - 300 keV for the bone substitutes. In each case the ratio for the lowest energy is given first. These coefficient ratios indicate that the substitutes have either increasing, decreasing or constant errors.

It can be seen from the data that if the data for $\bar{Z}(3.0)$ is used to characterise the photoelectric effect, then large discrepancies will occur. For example, with wax the $\bar{Z}(3.0)$ ratios appear to indicate a coefficient ratio of 0.73, but ratios from 0.34-0.30 actually occur.

The magnitude of these errors is evident from an inspection of the relationship 3.1. If the ratio of $\bar{Z}(x)$ for a substitute$(\bar{Z}_S(x))$ and a tissue $(\bar{Z}_T(x))$ equals 'ε' then the coefficient ratio given by $\frac{(n_o)_S[\bar{Z}_S(x)]^X}{(n_o)_T[\bar{Z}_T(x)]^X}$, resolves into $\frac{(n_o)_S}{(n_o)_T} \cdot \varepsilon^X$. So, if a substitute has the same electron density as the tissue but a $\bar{Z}(x)$ ratio of, say, 1.05. then for x = 3.0 a coefficient ratio of $(1.05)^{3.0}$ or 1.16 would be expected.

For larger exponents, larger differences occur.

The data of TABLE 3.2 also indicate that a single exponent will not in general give adequate agreement over the complete energy range that photoelectric absorption is significant. As the energy increases larger exponents are required. A single exponent will only characterise within certain limits the interactions at a particular energy.

It is instructive to apply some of these ideas to the formulation of MIX D. The method employed by the authors was as follows:-

(a) The proportions of paraffin wax/polyethylene/MgO were adjusted to give the same electron density as water.

(b) The amount of TiO_2 to give the same value of $\overline{Z}(x)$ as water was calculated ($x = 2.94$).

If these calculations are repeated, but in (b) the quantity $\overline{Y}(x)$ is matched and not $\overline{Z}(x)$, the formulae given in TABLE 3.3 are produced ('MIX E' and 'MIX F').

The ratios of the photoelectric mass attenuation coefficients for the three mixes to those of water are shown in TABLE 3.4. It can be seen that the 15% errors found with MIX D are immediately reduced to 6% when the modified 'MIX F' is considered.

	PERCENTAGE WEIGHTS				FORMULA BASED UPON...
	PARAFFIN WAX	POLYETHYLENE	MgO	TiO_2	
MIX D	60.8	30.4	6.4	2.4	$\overline{Z}(2.94)$
'MIX E'	52.44	26.22	20.33	1.01	$\overline{Y}(3.00)$
'MIX F'	52.80	26.40	20.47	0.33	$\overline{Y}(3.5)$

TABLE 3.3 THE COMPOSITION OF MIX D AND THE MODIFIED VERSIONS, 'MIX E' AND 'MIX F'

	PHOTOELECTRIC MASS ATTENUATION COEFFICIENT RATIOS					
	10 keV	20	40	80	100	150 keV
MIX D	0.85	0.97	1.03	1.08	1,09	1.11
'MIX E'	1.03	1.13	1.16	1.19	1.21	1.22
'MIX F'	0.94	1.01	1.02	1.04	1.05	1.05

TABLE 3.4 THE PHOTOELECTRIC MASS ATTENUATION COEFFICIENTS FOR MIX D, 'MIX E' AND 'MIX F' COMPARED TO THOSE FOR WATER

In the formulation of substitutes, effective atomic numbers have only once been applied to another photon interaction. WEBER & van den BERGE (1969) considered both photoelectric and coherent processes, using $\overline{Z}(x)$ with values of x of 3.4 and 1.7 respectively. The powder produced in their survey was given a CLASS B (5-20% errors) identification for low energy photons (CHAPTER 2).

The relative importance of other photon interactions are illustrated in FIGURE 3.2, which depicts the calculated ratios of the partial attenuation coefficients (photoelectric, coherent, incoherent & pair production) to the total coefficients from 10 keV - 100 MeV for MUSCLE. Coherent interactions are seen to account for a maximum of ~10% at 30 keV, while above 3 MeV pair production predominates. From 200 keV - 2 MeV incoherent processes are responsible for 99% of all the effects.

It is clear from the data given in this section that effective atomic numbers, together with electron densities, can indicate formulations having useful photon attenuation properties if the basic formulae are manipulated correctly. For this method to produce systems acceptable over a large energy range, the concept must be extended to include all of the partial attenuation data and not restricted to photoelectric processes as it has been, almost exclusively, in the past. If agreement for other effects are required, then the possibility of using analagous effective atomic numbers for energy absorption coefficients & electron stopping and angular scattering powers must be investigated.

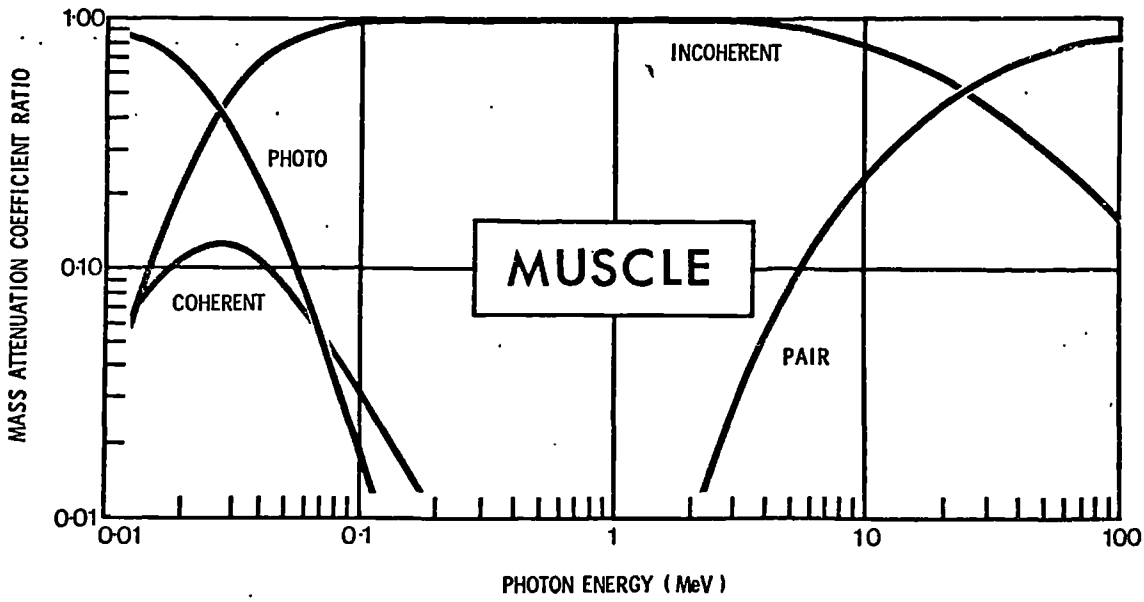

FIGURE 3.2 MASS ATTENUATION COEFFICIENT RATIOS, COMPARING PARTIAL TO TOTAL EFFECTS FOR MUSCLE

3.3 NEW SELECTION PROCEDURES

(i) SOME GENERAL PRINCIPLES

In this section an account will be given of two new selection procedures developed, and subsequently tested practically, for simulating materials with predetermined characteristics for photon and electron interactions. Both methods were based on the three following general principles:-

(a) The procedure must precisely establish the relative weights of the components of a substitute having partial attenuation & absorption coefficients, electron collision and radiation stopping powers, angular scattering powers and specific gravities within pre-defined limits.

(b) The procedure must effectively select from a library of compounds those which are suitable for addition to a specified base material so that an acceptable substitute is formed.

(c) If feasible two-component substitutes (that is, base material and added 'correcting' compound) should be formulated.

The first principle, (a), may in practice be relaxed in certain circumstances when the application of the substitute requires only a fraction of the photon and electron interactions to be within

selected limits.

The second principle, (b), was designed to establish criteria for selecting suitable components for a substitute. Frequently, the choice of the base material is restricted by its subsequent application; for example, paraffin wax may be chosen for its moulding or casting characteristics. The choice of compounds added to 'improve' the base material is, in general, completely arbitrary and without any sound quantitative reason. It may be shown that some added compounds result in acceptable products, while others produce inferior substitutes. A typical example is found with muscle substitutes based on wax when the addition of magnesium oxide yields a product with better attenuation properties than the addition of silicon dioxide. The reason for this is extremely important if precise procedures are to be formulated.

The final principle, (c), was made so that the manufacture of the resulting substitutes would be relatively straightforward. If two-component substitutes can be produced with radiation characteristics within the defined limits, then it appears pointless to consider more complex systems. It will be shown in a later chapter that this principle was in general adhered to but had to be modified in the case of epoxy resin based muscle, lung and fat substitutes. In this instance an extra low mass density compound (phenolic microspheres) had to be added to reduce the final specific gravity to acceptable limits. The two-component procedure was

still applied as the resin plus the fixed percentage of microspheres was considered to be the base material.

The two selection procedures based on these three principles may be described as ....

THE BASIC DATA METHOD

THE EXTENDED $\overline{Y}(x)$ METHOD

Each method will now be described in detail.

3.3(ii) THE BASIC DATA METHOD

Together with the elemental equivalence technique, this method, which uses coefficients and powers for compounds, is the most precise for substitute formulation. The basic concept is very simple. If a substitute, S, is composed of two components A and B and precisely simulates a material, X, at one energy and for one interaction, the coefficients (or powers) being respectively C_S, C_A, C_B, C_X, then if the Addition Formula is obeyed,

$$C_S = C_X = \omega_A . C_A + \omega_B . C_B \qquad \left\{ \begin{array}{l} \omega_A, \omega_B \text{ are} \\ \text{proportions by} \\ \text{weight} \end{array} \right.$$

But $\omega_A + \omega_B = 1$,

So,
$$\omega_A = \frac{C_S - C_B}{C_A - C_B} \qquad \ldots\ldots\ldots\ldots\ldots\ldots (3.2)$$

For the proportions given by equation 3.2, the coefficient at the appropriate energy for the substitute is exactly the same as that for the material being simulated. The agreement for other energies and other partial interactions will depend upon the choice of materials.

If a procedure could be devised so that the two selected components gave acceptable coefficients (or powers) over an extended energy range, then this single estimation of weight proportion would be adequate for <u>one</u> effect. The method of compound selection to facilitate these aims was based on the slopes of the coefficients (or powers) versus energy curves.

To simplify matters, only photoelectric attenuation coefficients will be considered at this stage in the analysis. These coefficients

(or cross-sections for elements) on a log-log plot against photon energy form linear graphs over certain energy ranges (FIGURE 3.3). The slope of this photoelectric curve (to be called 'PHOTO-SLOPE') for a compound will depend upon the slopes of the photoelectric curves of the elements that make up the compound. This is because the photo-slopes for the elements vary as the atomic numbers change.

The variation in the photo-slopes for the first 25 elements is shown in FIGURE 3.4. The data for this graph were calculated from elemental cross sections, in the energy interval 10-150 keV. The absolute slopes are seen to decrease from 3.434 to 2.968 as the atomic numbers increase from 1 to 25. The small graph in the top right-hand corner of Figure 3.4 illustrates the change (exaggerated) in the slopes for three elements of atomic numbers Z_1, Z_2 and Z_3

Compounds will each have a photo-slope depending upon the elemental composition. Typical examples are fat and bone. In this same energy interval, 10-150 keV, the numerical value of the photo-slope for fat is 3.249 and that for bone is 3.071. As expected, fat has the larger value due to its larger hydrogen content.

The same reasoning applies, of course, to a substitute made up of <u>two</u> compounds. The final slope will depend upon the compounds and their percentage weights.

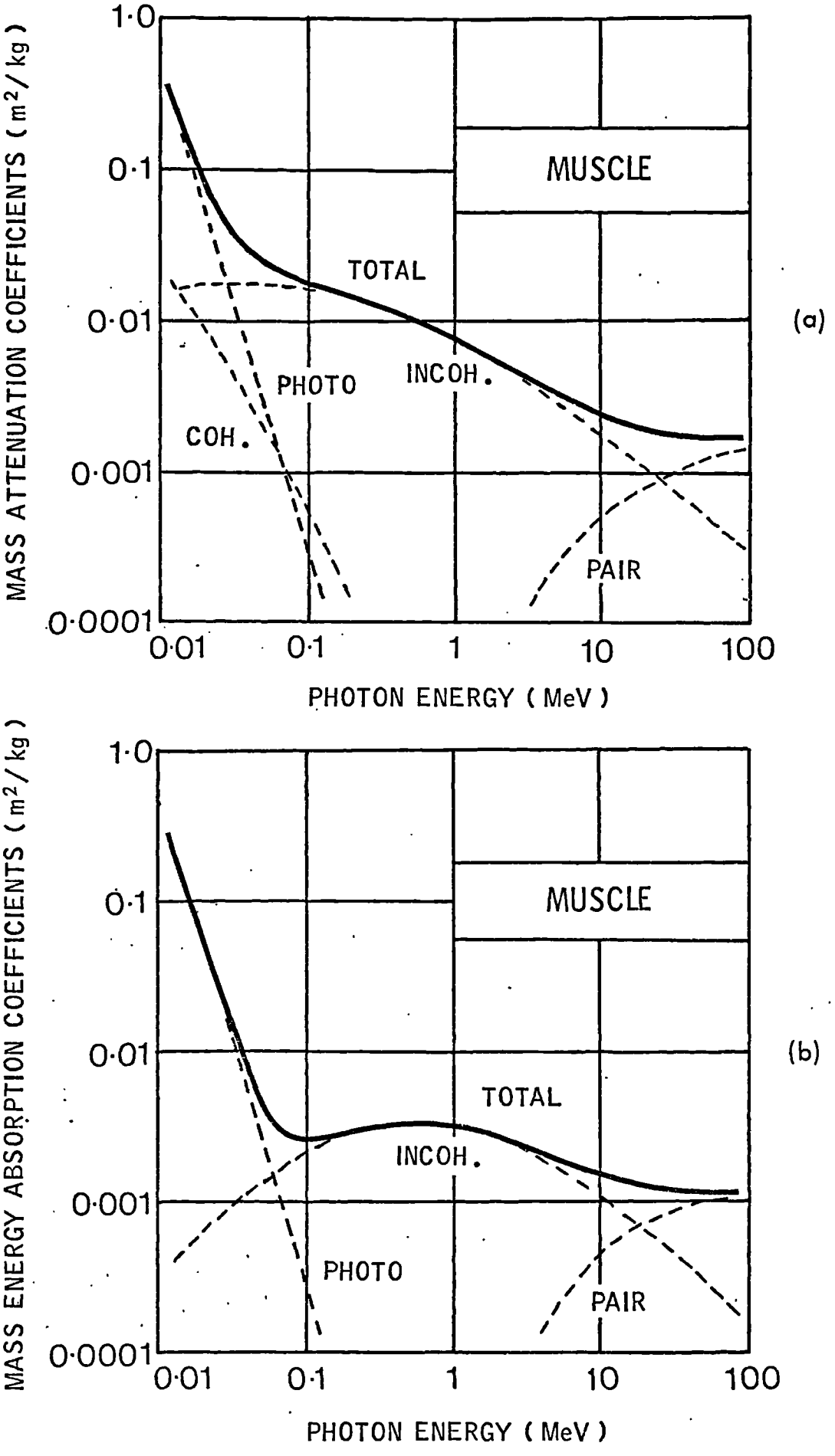

FIGURE 3.3 THE (a) MASS ATTENUATION COEFFICIENTS AND (b) MASS ENERGY ABSORPTION COEFFICIENTS FOR MUSCLE

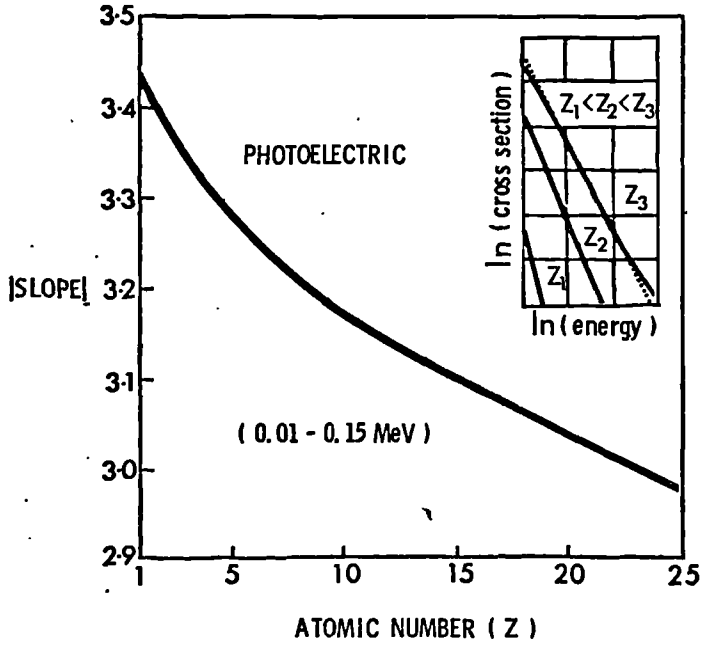

FIGURE 3.4 THE VARIATION IN SLOPE OF ln (CROSS SECTION)vs ln (ENERGY) FOR DIFFERENT ATOMIC NUMBERS (ATTENUATION DATA)

The permissible variation in the slope of the final material may be calculated as shown in FIGURE 3.5. In the figure the substitute material (S) and the material being simulated (X), have exactly the same photoelectric attenuation coefficients (C'_X) at some mid-point energy, E_m. The photo-slope for the substitute, m_S, resolves into the ratio $\ln\left(\frac{C_S}{C'_X}\right) \Big/ \ln\left(\frac{Em}{Eo}\right)$. [$C_S$ and C_X are the coefficients for the substitute and the 'real' material at the minimum energy, E_o]. A similar expression may be derived for the photo-slope, m_X. If the ratio C_S / C_X is called the FITTING RATIO, f, then the differences in the slopes m_S and m_X may be

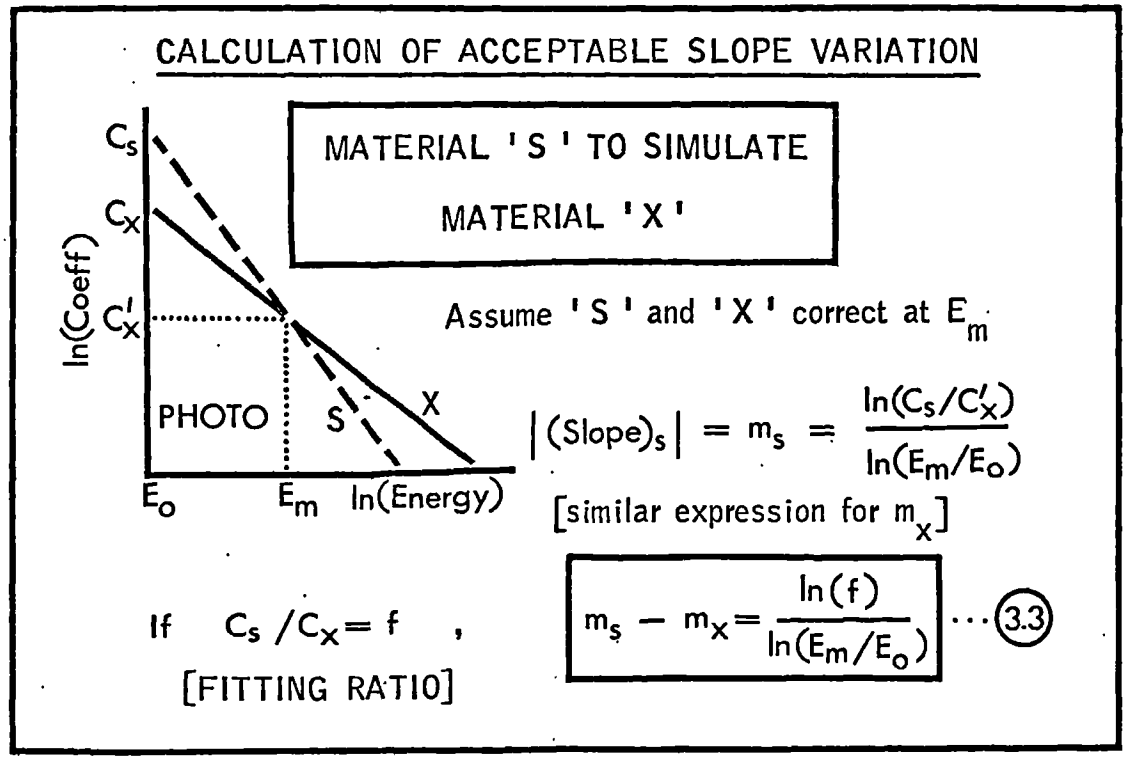

FIGURE 3.5 THE CALCULATION OF THE PERMISSIBLE VARIATION IN PHOTO-SLOPES FOR A SUBSTITUTE, 'S', SIMULATING A MATERIAL, 'X'

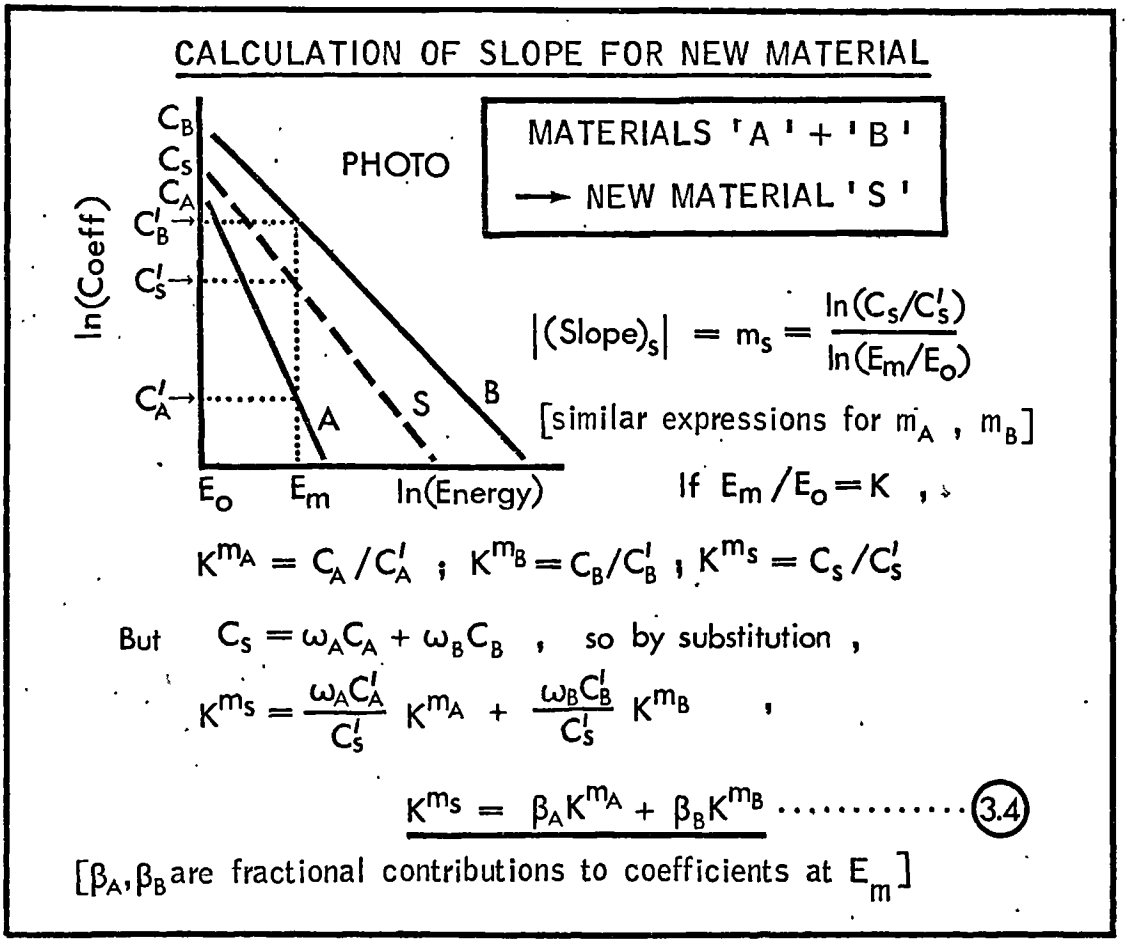

FIGURE 3.6 THE CALCULATION OF THE PHOTO-SLOPE OF A TWO-COMPONENT SUBSTITUTE

expressed in terms of the ratio $\ln(f)/\ln\left[\frac{E_m}{E_o}\right]$. Once the variation in the coefficients at energy E_o has been set, then the permitted variation between the photo-slopes of the substitute and the material being simulated may be calculated (Equation 3.3).

If the substitute, S, is a mixture of two compounds A & B, where A is the base material and B an unknown compound which will be added to improve the radiation characteristics, then equation 3.4, derived in FIGURE 3.6, relates the photo-slopes for the three materials, S, A and B. Here, an addition formula relating the quantity K^{m_S} (with K being the energy ratio E_m/E_o) to the same expressions for A and B (K^{m_A} and K^{m_B}) has been produced.

The final step in the analysis is the specification of the photo-slope of the added compound, B (m_B). If the 'real' material, X, and the base material, A, are fixed and compound B is added to the base so that the coefficients (C'_X and C'_S) agree exactly at energy E_m, then m_B is given by Equation 3.5 (FIGURE 3.7). This slope is derived from an expression which includes m_S, m_A, K, ω_A, and also the coefficients at E_m, namely C'_A and C'_X. The inclusion of the fractional weight, ω_A, shows predictably that the acceptable photo-slope of B depends upon the relative amounts of A and B that are to be added together. If the variation of m_S is set by means of the Fitting Ratio, C_S/C_X, then the permitted spread in m_B may be calculated.

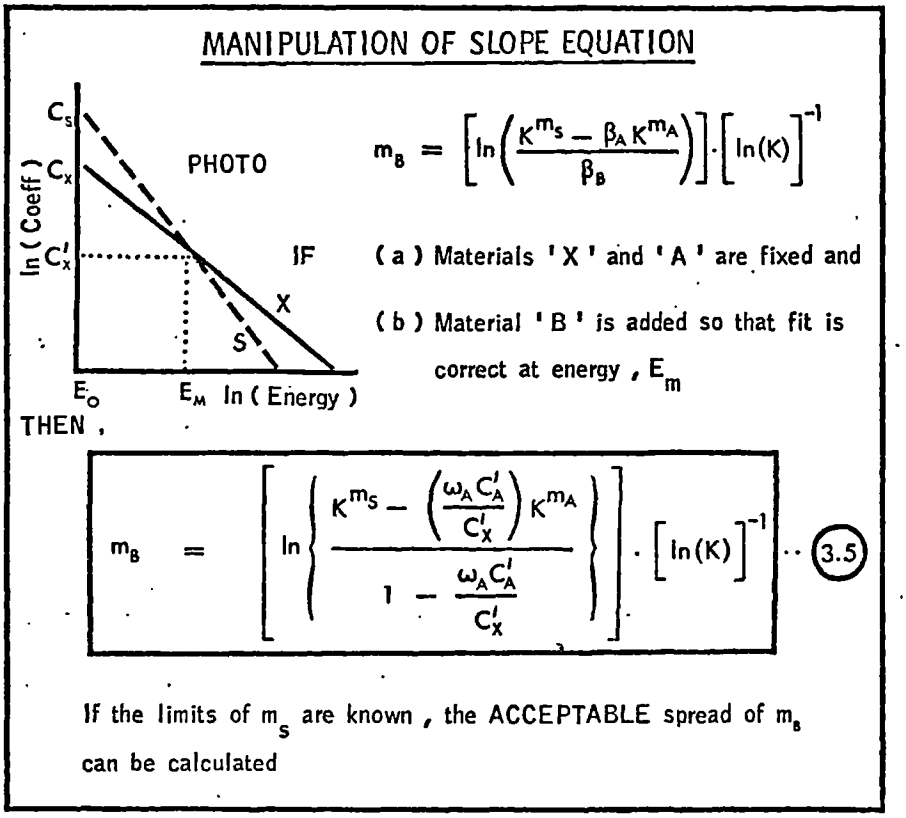

FIGURE 3.7 THE CALCULATION OF THE PHOTO-SLOPE OF THE ADDED COMPOUND IN A TWO-COMPONENT SUBSTITUTE

It is now feasible to select and formulate two-component substitutes having photoelectric coefficients within specified limits, The material to be simulated and the base material are selected and the permitted variation in the photo-slope of the substitute is calculated. A material has then to be found which, when added to the base in the correct mass ratio, gives a mixture with exactly the same photoelectric coefficients, at a mid-point energy, as the 'real' material. In addition the photo-slope of the added compound must fall within certain limits, which may be calculated once the mass ratios are known. If the photo-slope of the proposed additional compound falls within these limits, the resulting

photoelectric coefficients for the substitute will be acceptable over the extended energy range.

For this method to be completely adequate, it must be possible to apply the technique to interactions other than solely photoelectric absorption. The restrictions on its application are (a) the Addition Formula must be obeyed and (b) the relationship between the coefficients (or powers) and energy must be expressed in a form which is, for closely approximates to, a linear function,

It was stated in the first chapter that the Addition Rule was obeyed, within a few percent, for photons over the energy range 10 keV - 100 MeV. For electrons it is apparently held for angular scattering powers over this same energy range and for stopping powers from 10 keV - 2 MeV. Above 2 MeV the Addition Formula gives divergencies from the values calculated theoretically.

The linearity of coefficient and power data versus energy is evident from FIGURES 3.3 and 3.8. For photon attenuation processes, photoelectric and coherent interactions produce near-linear curves when plotted against energy on a log-log scale. Pair production effects may be approximated to straight lines over restricted energy ranges. Similar comments also apply to photoelectric and pair production in energy absorption interactions. In both photon attenuation and absorption, the incoherent curves were considered to be unchanging in slope (or shape) and varying only in amplitude. Incoherent data were consequently only

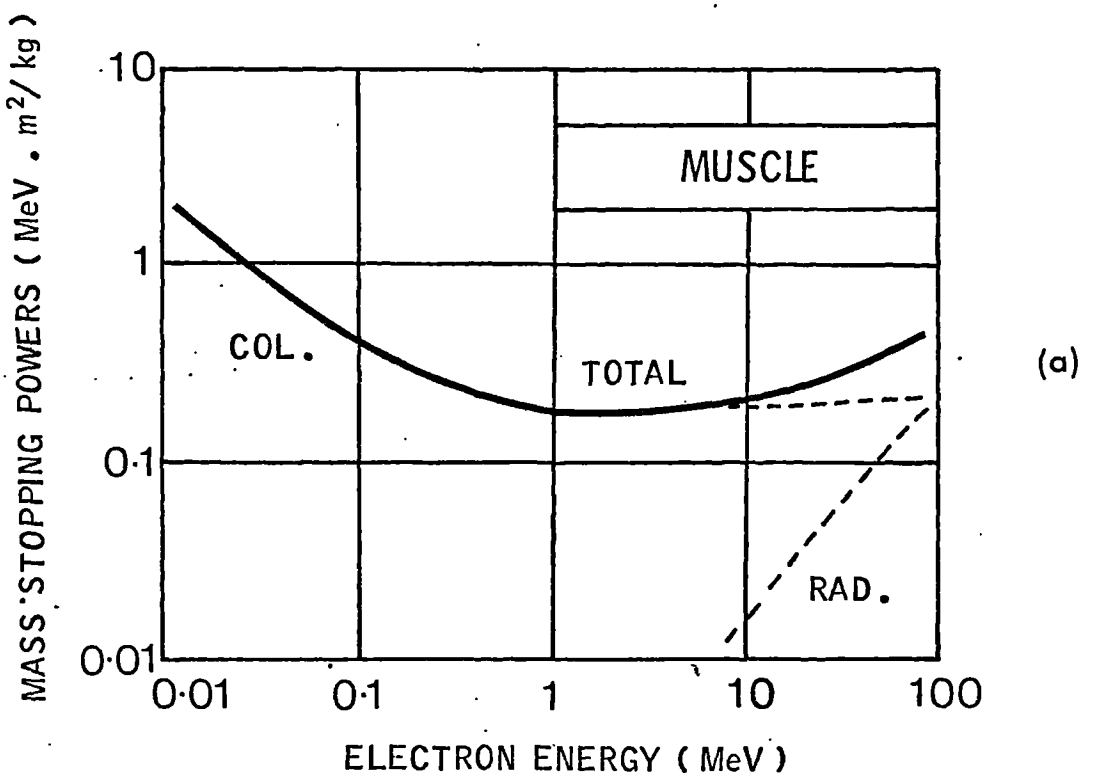

(a)

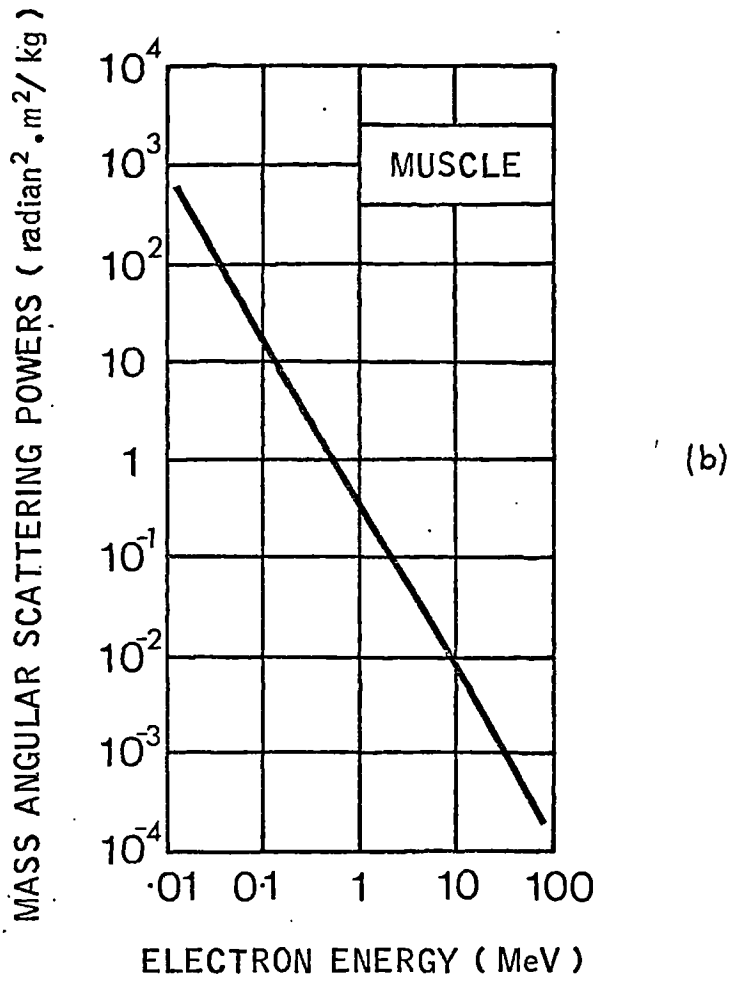

(b)

FIGURE 3.8 THE (a) ELECTRON MASS STOPPING POWERS AND (b) MASS ANGULAR SCATTERING POWERS FOR MUSCLE

evaluated at a single energy point, namely 1 MeV. This approximation proved to be completely acceptable in practice.

For electrons, collision and radiation stopping power curves may be approximated to straight lines over limited energy ranges, while angular scattering powers are predominantly linear over extended ranges.

A few numerical examples should illustrate the degree of linearity that exists. In the energy intèrval 10-150 keV the coefficient & power slopes, together with standard deviations, were calculated for CARBON. The slopes, assuming a log-log relationship between coefficients (or powers) and energy, were as follows:-

PHOTOELECTRIC ATTENUATION..... -3.263 ± 0.005
PHOTOELECTRIC ABSORPTION..... -3.303 ± 0.007
COHERENT ATTENUATION ..... -1.702 ± 0.042
ANGULAR SCATTERING POWER..... -1.768 ± 0.007

The way in which this method was applied in practice will be described in the next chapter.

3.3(iii) EXTENDED $\overline{Y}(x)$ METHOD

It was apparent from the analysis of effective atomic number given in section 3.2 that this quantity, together with electron density, could produce useful formulations. In the past their application has been limited almost completely to photoelectric interactions when a single $\overline{Z}$-exponent is used to characterise the effect. For a more rigorous treatment, effective atomic numbers must be applied to the other important interactions, namely coherent, incoherent & pair production processes, collision and radiation stopping powers and angular scattering powers. These numbers, or derivations from them, should also indicate the suitability of added compounds for two-component formulations, in an analagous way to the manipulation of photo-slopes developed in the Basic Data Method. With these aims in mind, the Extended $\overline{Y}(x)$ Method has been produced.

Using the same criteria as discussed earlier, the method should effectively....

(a) Establish precisely the relative masses of the components of substitutes which have coefficients and powers within specified limits.

(b) Screen an array of compounds and locate the best components for a defined substitute,

(c) Formulate two-component substitutes.

Similarly as in the previous method, the simulation for photoelectric interactions will be discussed initially, followed by the application to other effects.

To establish the relative masses of a two-component material (A + B) which yields a specific photoelectric coefficient at a given energy, the $\overline{Y}(x)$ value must be considered. The magnitude of the effect for the substitute (S) is proportional to the product of the electron density, $(n_o)_S$, and the $\overline{Z}$-Power, $[\overline{Z}_S(x)]^X$, which in this study is termed $\overline{Y}_S(x)$. If this quantity equals $\overline{Y}_X(x)$ for the 'real' material, the photoelectric processes, at this particular energy, will be the same in the two materials.

The relationship which relates the $\overline{Y}$-values in a two-component substitute is developed in FIGURES 3.9 and 3.10. The development is in three parts.

In FIGURE 3.9(a) equation 3.6 is produced, relating the $\overline{Z}$-Powers for compounds S, A and B. The general form of this equation is, $[\overline{Z}_S(x)]^X = \sum_i a_i [\overline{Z}_i(x)]^X$, where a_i is the fractional electron contribution of the i^{th} compound of $\overline{Z}$-Power, $[\overline{Z}_i(x)]^X$.

A similar equation (3.7) is then developed for electron densities, n_o, in FIGURE 3.9(b) . The general form of this equation is, $1/(n_o)_S = \sum_i a_i/(n_o)_i$, where $(n_o)_i$ is the electron density of the i^{th} compound.

TWO-COMPONENT SUBSTITUTES

(a) EFFECTIVE ATOMIC NUMBER, $\bar{Z}(x)$

$$[\bar{Z}(x)]^x = \sum_i a_i Z_i^x$$

$\left\{ \begin{array}{l} a_i = \text{Electron fraction} \\ Z_i = \text{Atomic No. } i^{th} \text{ element} \end{array} \right.$

If the substitute is made up of compounds A & B in molecular proportions p , q , or... $(A)_p + (B)_q \rightarrow S$, then ,

$$[\bar{Z}_s(x)]^x = \frac{p\left(\sum_i n_i Z_i^x\right)_A + q\left(\sum_i n_i Z_i^x\right)_B}{p(N)_A + q(N)_B}$$

$\left\{ \begin{array}{l} n_i = \text{No. electrons from } i^{th} \text{ el.} \\ (N)_A = \text{Total no. electrons in A} \\ (N)_B = \text{Total no. electrons in B} \end{array} \right.$

But, $\left(\sum_i n_i Z_i^x\right)_A = (N)_A [\bar{Z}_A(x)]^x$, etc

So, $$[\bar{Z}_s(x)]^x = \frac{p(N)_A[\bar{Z}_A(x)]^x + q(N)_B[\bar{Z}_B(x)]^x}{p(N)_A + q(N)_B}$$

or, $$\underline{[\bar{Z}_s(x)]^x = a_A[\bar{Z}_A(x)]^x + a_B[\bar{Z}_B(x)]^x} \quad \cdots\cdots\cdots\cdots\cdots (3.6)$$

(b) ELECTRON DENSITY , n_o

$$(n_o)_A = N_A \frac{(N)_A}{M_A} \; ; \; (n_o)_B = N_A \frac{(N)_B}{M_B}$$

$\left\{ \begin{array}{l} N_A = \text{Avogadro's Number} \\ M_A \, , \, M_B = \text{Mol. Wts} \end{array} \right.$

If substitute is made as before... $(A)_p + (B)_q \rightarrow S$

Then, $$(n_o)_s = \frac{N_A[p(N)_A + q(N)_B]}{pM_A + qM_B}$$

But, $$M_A = \frac{N_A(N)_A}{(n_o)_A} \quad , \text{ etc}$$

So, $$(n_o)_s = \frac{N_A[p(N)_A + q(N)_B]}{p.\frac{N_A(N)_A}{(n_o)_A} + q.\frac{N_A(N)_B}{(n_o)_B}}$$

or, $$\underline{1/(n_o)_s = a_A/(n_o)_A + a_B/(n_o)_B} \quad \cdots\cdots\cdots\cdots\cdots (3.7)$$

FIGURE 3.9 THE CALCULATION OF EFFECTIVE ATOMIC NUMBER AND ELECTRON DENSITY FOR TWO-COMPONENT SUBSTITUTES

$\bar{Y}(x)$ FOR TWO-COMPONENT SUBSTITUTES

MATERIALS 'A' + 'B' ⟶ NEW MATERIAL 'S'

$$[\bar{Z}_S(x)]^x = \alpha_A.[\bar{Z}_A(x)]^x + \alpha_B.[\bar{Z}_B(x)]^x$$

and $\quad 1/(n_o)_s = \alpha_A/(n_o)_A + \alpha_B/(n_o)_B \quad$ or $\quad (n_o)_s = (n_o)_A (n_o)_B / [\alpha_A (n_o)_B + \alpha_B (n_o)_A]$

Now, $\quad \bar{Y}_S(x) = (n_o)_S [\bar{Z}_S(x)]^x$

By Substitution, $\quad \underline{\bar{Y}_S(x) = \phi_A \bar{Y}_A(x) + \phi_B \bar{Y}_B(x)} \cdots\cdots\cdots\cdots\cdots\cdots\cdots\cdots (3.8)$

where $\begin{cases} \phi_A = \alpha_A (n_o)_B / [\alpha_A (n_o)_B + \alpha_B (n_o)_A] \\ \phi_A + \phi_B = 1 \end{cases}$

FIGURE 3.10 THE CALCULATION OF $\bar{Y}(x)$ VALUES IN TWO-COMPONENT SUBSTITUTES

The product of these two relationships results in equation 3.8 (FIGURE 3.10), which relates the $\overline{Y}$-values for S, A and B. The fractional quantities ϕ_A, ϕ_B, are functions of the electron fractions and electron densities of A and B.

If the $\overline{Z}$-exponent, x, has been correctly chosen, equation 3.8 should effectively dictate the electron fractions that will give a perfect simulation at the one energy point. For the agreement to be within specified limits at other energies, the photo-slopes have to be analysed.

FIGURE 3.11 illustrates the application of $\overline{Z}$-Powers to the specification of photo-slopes. Again, the new material, S, is made up of compounds A and B. If the coefficients at two photon energies are considered, each will be characterised by the product $n_o[\overline{Z}(x)]^x$, or $\overline{Y}(x)$, with the value of x being dependent upon the energies chosen. For energies E_o and E_m, the values of x are denoted by x_o and x_m. Using this approach an equation similar to 3.4 (FIGURE 3.6) is developed, which relates the photo-slopes of A and B to that of S in terms of E_m/E_o, or K, the electron fractions and the $\overline{Z}$-Powers at the mid-point energy, E_m (Equation 3.9). This reasoning leads to Equation 3.10, giving the relationship of the $\overline{Z}$-Power Ratios, $\frac{[\overline{Z}(x_o)]^{x_o}}{[\overline{Z}(x_m)]^{x_m}}$, for the three materials in an analagous equation to the one which related the photo-slopes. Hence, the $\overline{Z}$-Power Ratio, R, which is the ratio of the $\overline{Z}$-Powers at two energies, may be used to test whether the added compound,

PHOTO SLOPES AND $\bar{Z}$ - POWER RATIOS

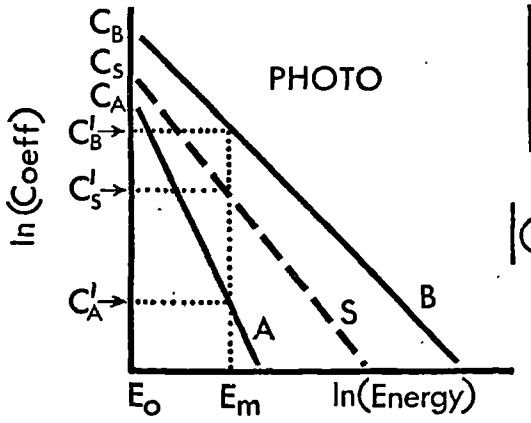

MATERIALS 'A' + 'B'
→ NEW MATERIAL 'S'

$$\left|(\text{Slope})_S\right| = m_S = \frac{\ln(C_S/C'_S)}{\ln(E_m/E_o)}$$

If $E_m / E_o = K$, then ,

$$K^{m_S} = C_S / C'_S$$

[similarly for m_A and m_B]

If $\bar{Z}$ - exponent , x , has values x_o and x_m at energies E_o and E_m ;

$$C_S = (n_o)_S \left[\bar{Z}_S(x_o)\right]^{x_o}.k_o \quad \text{and} \quad C'_S = (n_o)_S \left[\bar{Z}_S(x_m)\right]^{x_m}.k_m$$

(k_o , k_m are constants)

$$\text{So,} \quad K^{m_S} = \frac{k_o\left[\bar{Z}_S(x_o)\right]^{x_o}}{k_m\left[\bar{Z}_S(x_m)\right]^{x_m}} = \frac{k_o\left(a_A\left[\bar{Z}_A(x_o)\right]^{x_o} + a_B\left[\bar{Z}_B(x_o)\right]^{x_o}\right)}{k_m\left(a_A\left[\bar{Z}_A(x_m)\right]^{x_m} + a_B\left[\bar{Z}_B(x_m)\right]^{x_m}\right)}$$

$$\text{or,} \quad K^{m_S} = \psi_A K^{m_A} + \psi_B K^{m_B} \quad \cdots\cdots\cdots\cdots\cdots\cdots \quad (3.9)$$

$$\text{where,} \quad \psi_A = \frac{a_A\left[\bar{Z}_A(x_m)\right]^{x_m}}{a_A\left[\bar{Z}_A(x_m)\right]^{x_m} + a_B\left[\bar{Z}_B(x_m)\right]^{x_m}} \quad \text{and} \quad \psi_A + \psi_B = 1$$

[ψ_A, ψ_B-fractional components of $\left[\bar{Z}_S(x_m)\right]^{x_m}$]

If the $\bar{Z}$-Power Ratios are denoted by 'R',

$$\text{then,} \quad R_S = \frac{\left[\bar{Z}_S(x_o)\right]^{x_o}}{\left[\bar{Z}_S(x_m)\right]^{x_m}} \quad \text{and similarly for } R_A , R_B$$

$$\text{So,} \quad K^{m_S} = \frac{k_o}{k_m} R_S \text{ , etc}$$

$$\text{By Substitution,} \quad R_S = \psi_A R_A + \psi_B R_B \quad \cdots\cdots\cdots\cdots\cdots\cdots \quad (3.10)$$

FIGURE 3.11 THE RELATIONSHIPS BETWEEN PHOTO-SLOPES AND $\bar{Z}$-POWER RATIOS

B, is acceptable.

The Fitting Ratio, f, the permitted ratio of the coefficients at the extremes of the energy range, established the relationship between the $\overline{Z}$-Power Ratios for the substitute and the material being simulated (Equation 3.11 - FIGURE 3.12). Once the permitted variation in the $\overline{Z}$-Power Ratio for the substitute, R_S, has been calculated and knowing the electron fractions of A and B which give a perfect fit at the mid-point energy (from the $\overline{Y}$-values), the permitted variation of the $\overline{Z}$-Power ratio for the added compound, B, may be computed (Equation 3.12 - FIGURE 3.13). If the value of R_B lies within the permitted limits, then an acceptable substitute should follow for the particular effect.

This method, to be of general use, must be applicable to the other photon and electron interactions. As the basic definition of effective atomic number (section 3.2) assumes that the Addition Rule is obeyed, the comments regarding this Rule recorded in the last section (3.3(ii)) are applicable. With the exception of electron stopping powers above 2 MeV, all other photon and electron interactions appear to obey the Rule.

When this method is applied to electron interactions it is more convenient to redefine effective atomic number in terms of fractional weights (ω_i), instead of the definition based on electron fractions (α_i). The electron fraction terms were introduced

CALCULATION OF ACCEPTABLE $\bar{Z}$ - POWER RATIO (R) VARIATION

From BASIC DATA METHOD :

$$m_s - m_x = \frac{\ln(f)}{\ln(E_m/E_o)}$$

or, $K^{m_s - m_x} = f$ (FITTING RATIO) , where $K = E_m/E_o$

But $K^{m_s} \propto R_s$ and $K^{m_x} \propto R_x$

So, $K^{m_s} / K^{m_x} = R_s/R_x$, or ,

$$R_s/R_x = f \qquad \text{.....} \quad (3.11)$$

FIGURE 3.12 THE RELATIONSHIP BETWEEN R-VALUES AND FITTING RATIO FOR MATERIALS 'S' AND 'X'

MANIPULATION OF $\bar{Z}$ - POWER RATIO

$$R_B = \frac{R_S - \psi_A R_A}{\psi_B}$$

IF (a) Materials 'X' and 'A' are fixed and

(b) Material 'B' is added so that the value of $\bar{Y}(x)$ for the mixture A + B is the same as that for S .

THEN ,

$$R_B = \frac{R_S - \dfrac{a_A[\bar{Z}_A(x_m)]^{x_m}}{[\bar{Z}_S(x_m)]^{x_m}} \cdot R_A}{1 - \dfrac{a_A[\bar{Z}_A(x_m)]^{x_m}}{[\bar{Z}_S(x_m)]^{x_m}}} \qquad \text{.....} \quad (3.12)$$

If the limits of R_S are known , the ACCEPTABLE spread of R_B may be calculated

FIGURE 3.13 THE CALCULATION OF THE $\bar{Z}$-POWER RATIO OF THE ADDED COMPOUND IN A TWO-COMPONENT SUBSTITUTE

historically in the evaluation of photon attenuation processes and although completely adequate for photons, are difficult to apply to electron interactions. The difficulties are easily resolved by saying that, for a compound, the interaction is proportional to $\sum_i \omega_i Z_i^X$, which, in this study, is made equal to a term designated by $[\bar{Z}(x)]_W^X$. The only modifications which have to be made to the derived formulae involve Equations 3.6 (FIGURE 3.9(a)), 3.7 (FIGURE 3.9(b)) and 3.8 (FIGURE 3.10).

In Equation 3.6, the electron fractions are replaced by fractional weights, or,

$$[\bar{Z}_S(x)]_W^X = \omega_A [\bar{Z}_A(x)]_W^X + \omega_B [\bar{Z}_B(x)]_W^X$$

Equations 3.7 and 3.8, which involve electron densities, are no longer required in this approach. The relative masses of the components are calculated by comparing the new $\bar{Z}$-Power data and not $\bar{Y}$-values. The equation (3.10) for $\bar{Z}$-Power Ratios has a similar structure, but the fractions ψ_A, ψ_B, contain fractional weights instead of electron fractions.

The extension of the concept of effective atomic numbers in this manner is strongly dependent upon the accuracy of the $\bar{Z}$-Power law for the different interactions. If the dependence is imprecise, then the resultant simulation procedure will be ineffectual. The next, and last, section in this chapter deals with an intensive analysis of Z-dependence which has been made for photon and electron interactions.

3.4 AN ANALYSIS OF Z-DEPENDENCE

The investigation of Z-dependence was performed in two phases. In the first phase photon attenuation interactions were analysed and three computational procedures developed and assessed. In the second phase photon absorption and electron processes were investigated using the procedure which was considered to be most appropriate.

The three procedures assessed during the first phase may be classified as ....

(a) Unweighted elemental analysis
(b) Weighted elemental analysis
(c) Compound analysis

These methods will now be described with reference to photon attenuation data.

(a) The variation of elemental photon cross section per atom, σ, with atomic number (Z) was analysed using the relationship,

$$\sigma = k Z^{x+1}$$

or, $$\ln(\sigma) = \ln(k) + (x + 1) \ln(Z)$$

Unweighted linear regression of $\ln(\sigma)$ against $\ln(Z)$ was performed for different energies and different groups of elements. Each regression produced a specific value for the Z-exponent, '$x + 1$'.

The procedure was completed for photoelectric, coherent, incoherent, pair production and total cross sections, in the energy

ranges where the interactions were important.

Three groups of elements were chosen. As most biological tissues have 'effective atomic numbers' for all photon processes between 5 and 15, these Z-limits were selected in the first group (that is, boron through to phosphorus). The second group hydrogen (Z = 1) through to manganese (Z = 25), represented the extremes of the atomic numbers to be employed in new formulations. As hydrogen is present in all tissues, the third group was similar to the first but included hydrogen (that is, hydrogen, boron through to phosphorus).

The calculations were performed on the elemental cross sections stored on magnetic tape (Program : DATAPE), using the computer program DATFIT (Appendix 4).

FIGURE 3.14 shows the values of (x + 1), from these calculations, for the photoelectric process. Values are plotted, together with the magnitudes of the standard deviations, over the energy range 10 keV to 10 MeV. It can be seen that the Z-exponent depends strongly upon the photon energy and also the elemental grouping. A minimum exponent value of 4.39 occurs at 10 keV with the Z-grouping of 5 to 15, and a maximum in excess of 5 at energies above 150 keV for the Z-grouping 1, 5 to 15. The effect of hydrogen is very prominent. The only difference in the upper (TRIANGLES) and lower (SQUARES) curves is the addition of data for hydrogen to the regression calculation.

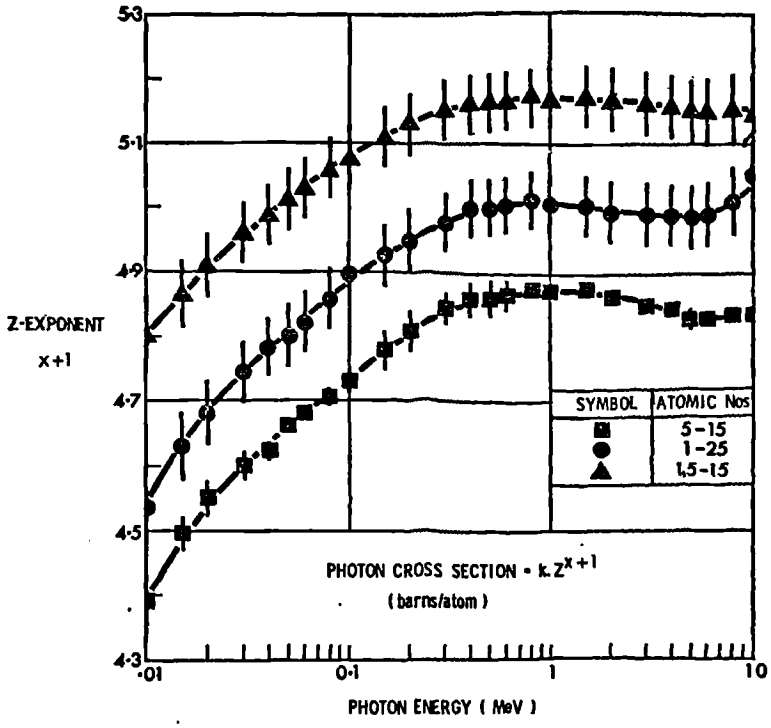

FIGURE 3.14 Z-EXPONENTS FOR PHOTOELECTRIC ATTENUATION PROCESS (UNWEIGHTED REGRESSION)

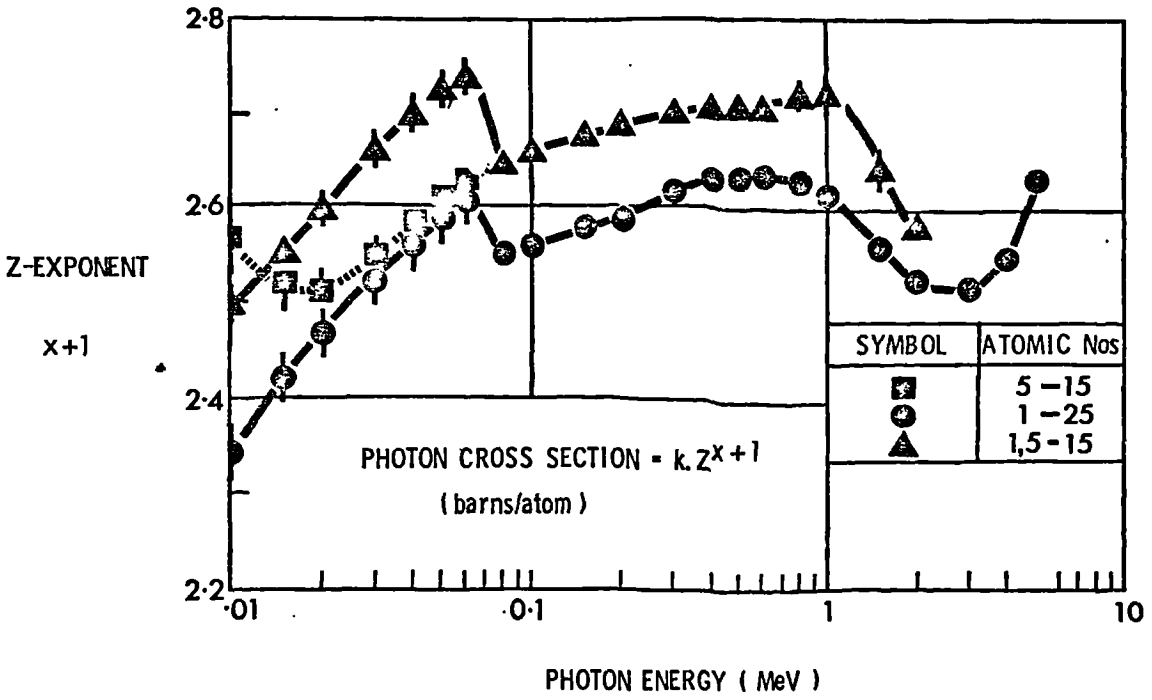

FIGURE 3.15 Z-EXPONENTS FOR COHERENT ATTENUATION PROCESS (UNWEIGHTED REGRESSION)

The use of effective atomic numbers for photoelectric interactions appears very tenuous from these results. Not only will different exponents have to be considered at different energies, but exponents will change at constant energy as the elemental composition changes. The total variation in the exponents may be reduced if the energy range 10-150 keV is regarded as most important, being the range in which photoelectric interactions make up more than 1% of the total interactions for most tissues. This restriction gives an exponent variation of 4.39-4.80 at 10 keV to 4.78-5.11 at 150 keV.

Similar analyses have been made for coherent, pair production and incoherent cross sections and are illustrated in FIGURES 3.15, 3.16 and 3.17.

From 10-150 keV, the exponents for coherent processes vary from 2.34 to 2.74.

Pair production interactions gave exponents of 1.91-1.96 at 5 MeV to 1.81-1.91 at 20 MeV. Exponents as low as 1.76 were recorded at 100 MeV.

Incoherent processes gave exponents of unity from approximately 500 keV to 100 MeV. At lower energies, exponents down to 0.73 were obtained.

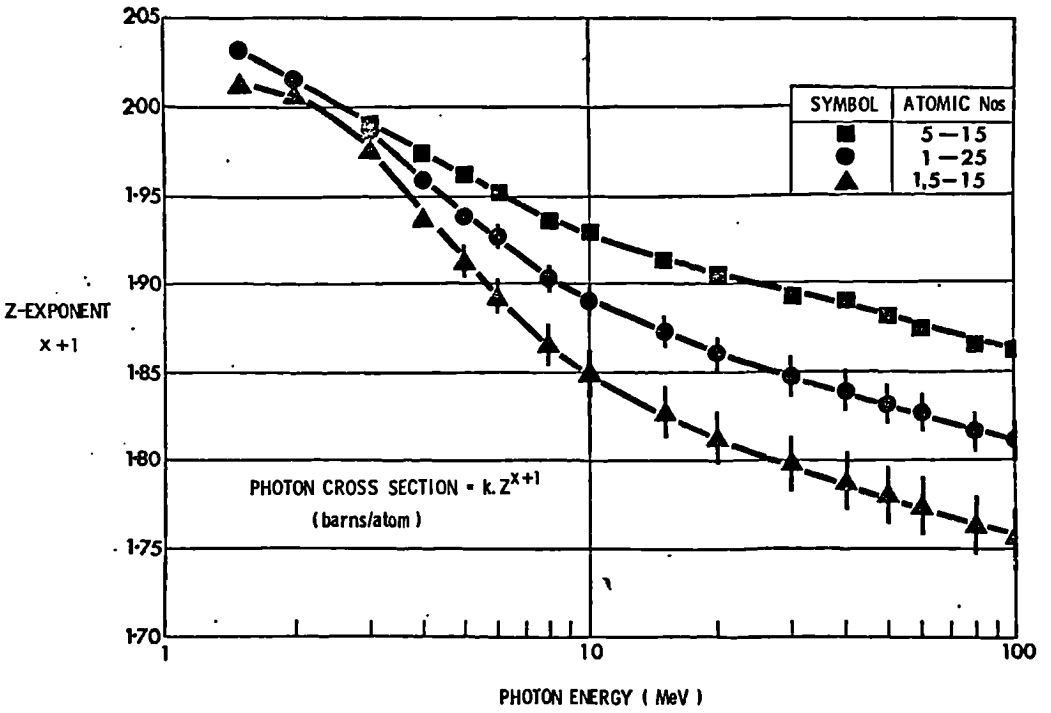

FIGURE 3.16 Z-EXPONENTS FOR PAIR PRODUCTION ATTENUATION PROCESS (UNWEIGHTED REGRESSION).

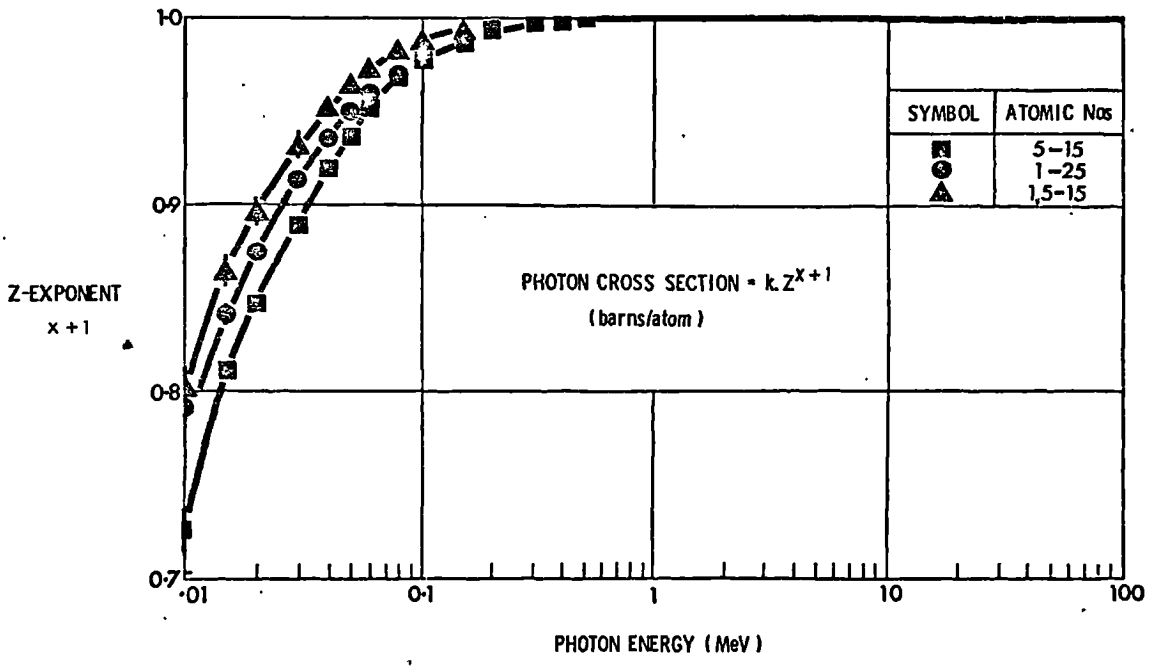

FIGURE 3.17 Z-EXPONENTS FOR INCOHERENT ATTENUATION PROCESS (UNWEIGHTED REGRESSION)

(b) The second analytical procedure was a linear regression of the form given in (a), but based on three new elemental groupings. These groups were the elements found in FAT (C, H, O), MUSCLE (C, H, N, O, Na, Mg, P, S, K, Ca) and BONE (C, H, N, O, Na, Mg, P, S, Ca). With each of the three groups a linear regression calculation was made, [ln(σ) against ln(Energy)] weighted according to the relative elemental masses found in the tissues.

The results for photoelectric interactions are shown in FIGURE 3.18. As with the previous graphs, the values of Z-exponents (x + 1) are plotted against energy (10 keV-10 MeV).

The effect of hydrogen is evident from the curves. The highest exponents correspond to the tissue with the largest hydrogen content, namely, FAT. Bone, which has the smallest hydrogen content has the lowest Z-exponents.

Similar data were obtained for the other photon attenuation interactions.

(c) The third analysis involved data generated for a library of compounds compiled for the simulation programs (chapter 4). At the time this analysis was made, 1041 compounds were assessed.

The mass attenuation coefficient for a compound, μ/ρ, was assumed to be $k.(\overline{Y}(x))^m$, where $\overline{Y}(x)$ was as defined previously. So, as $\ln\left[\frac{\mu}{\rho}\right] = \ln(k) + m.\ln(\overline{Y}(x))$, a plot of $\ln\left[\frac{\mu}{\rho}\right]$ versus $\ln(\overline{Y}(x))$ should

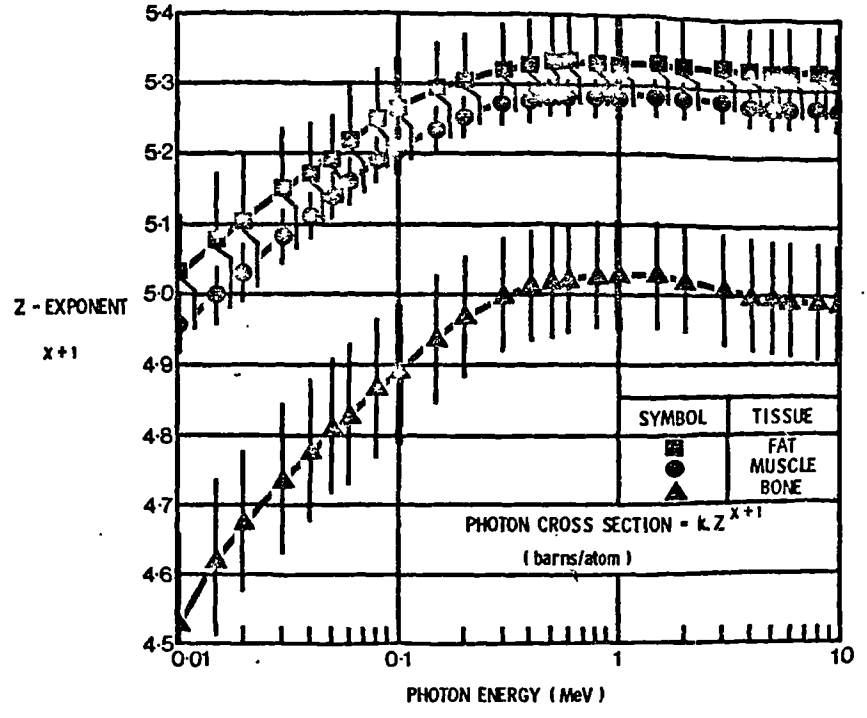

FIGURE 3.18 Z-EXPONENTS FOR PHOTOELECTRIC ATTENUATION PROCESS (WEIGHTED REGRESSION)

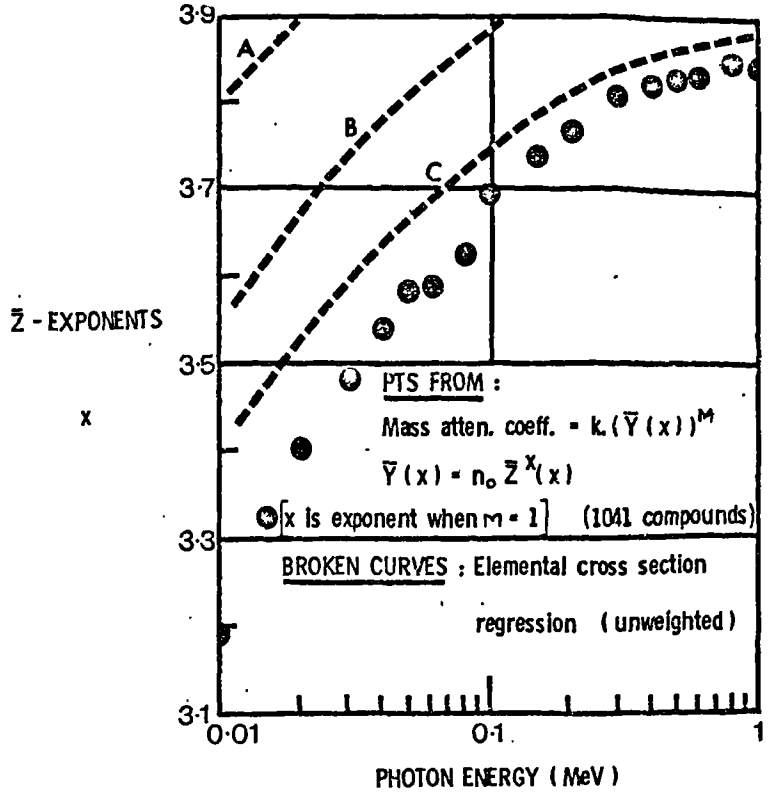

FIGURE 3.19 Z̄-EXPONENTS FOR PHOTOELECTRIC ATTENUATION PROCESS ('COMPOUND' REGRESSION)

result in a straight line of slope 'm'. This regression, using the calculated values of $\frac{\mu}{\rho}$ and $\overline{Y}(x)$ for the 1041 compounds, was computed for a number of values for x and the value which corresponded to 'm = 1' was interpolated. When 'm' was unity, the equation resolved into the conventional, $\frac{\mu}{\rho} = k.\overline{Y}(x)$.

The results of these calculations for photoelectric interactions are shown in FIGURE 3.19. Here the $\overline{Z}$-exponents, x, are plotted against energy. Each point represents the regression on the complete group of compounds and the associated $\overline{Y}(x)$ values. The unweighted elemental results are also plotted on the same scale. The lower exponents obtained in the compound analysis, was due to the fact that many of the compounds were completely devoid of hydrogen.

Because of the enormous quantities of data used, this method proved to be extremely tedious, even when fast digital computers were employed.

The combined results from these three methods for photoelectric, coherent and pair production attenuation processes are summarised in TABLE 3.5. The unweighted and weighted methods are seen to produce sets of data in close agreement. The influence of hydrogen is responsible for the higher photoelectric values obtained for weighted regression and the low values for the compound method. This effect is also the reason for the high exponents for pair

(a) PHOTOELECTRIC

	Z EXPONENTS		
DATA ANALYSED	10 keV	40 keV	150 keV
ELEMENTAL (NOT WEIGHTED)	4.39-4.80	4.63-4.99	4.78-5.11
ELEMENTAL (WEIGHTED)	4.53-5.03	4.78-5.17	4.94-5.29
COMPOUND	4.19	4.54	4.74

(b) COHERENT

	Z-EXPONENTS		
DATA ANALYSED	10 keV	40 keV	150 keV
ELEMENTAL (NOT WEIGHTED)	2.34-2.57	2.56-2.70	2.57-2.68
ELEMENTAL (WEIGHTED)	2.43-2.46	2.63-2.76	2.64-2,67
COMPOUND	2.45	2.55	2.65

(c) PAIR PRODUCTION

	Z-EXPONENTS		
DATA ANALYSED	5 MeV	10 MeV	20 MeV
ELEMENTAL (NOT WEIGHTED)	1.91-1.96	1.85-1.93	1.81-1.91
ELEMENTAL (WEIGHTED)	1.88-1.94	1.81-1.89	1.77-1.86
COMPOUND	1.96	1.93	1.91

TABLE 3.5 CALCULATED VALUES OF Z-EXPONENTS FOR (a) PHOTOELECTRIC, (b) COHERENT AND (c) PAIR PRODUCTION ATTENUATION DATA

production with the compound method.

Incoherent attenuation processes gave exponents within one percent of unity from 150 keV-100 MeV. The exponents decrease as the energy falls below 150 keV, being in the range 0.73-0.85 at 10 keV.

The remaining photon absorption and electron interactions were subsequently analysed using the first procedure, namely, unweighted linear regression. From the evidence obtained from the photon attenuation data analyses, it was apparent that this procedure would produce adequate and meaningful results. Some of the results are plotted in FIGURES 3.20-3.23 and a resumé of the exponents are shown in TABLES 3.6 and 3.7.

The regression for the photoelectric energy absorption process was confused by the fact that only two cross sections were available for hydrogen (10 and 15 keV). This caused discontinuities in the exponent versus energy curves that included hydrogen in the elemental grouping (FIGURE 3.20). The maximum exponent at 150 keV could not, therefore, be precisely recorded.

In general, the results for electron stopping powers (FIGURES 3.21 and 3.22) were poor, producing large exponent variations and large standard deviations, suggesting that simulation procedures based on this method would be inadequate for these interactions. Conversely, angular scattering powers yielded smaller exponent

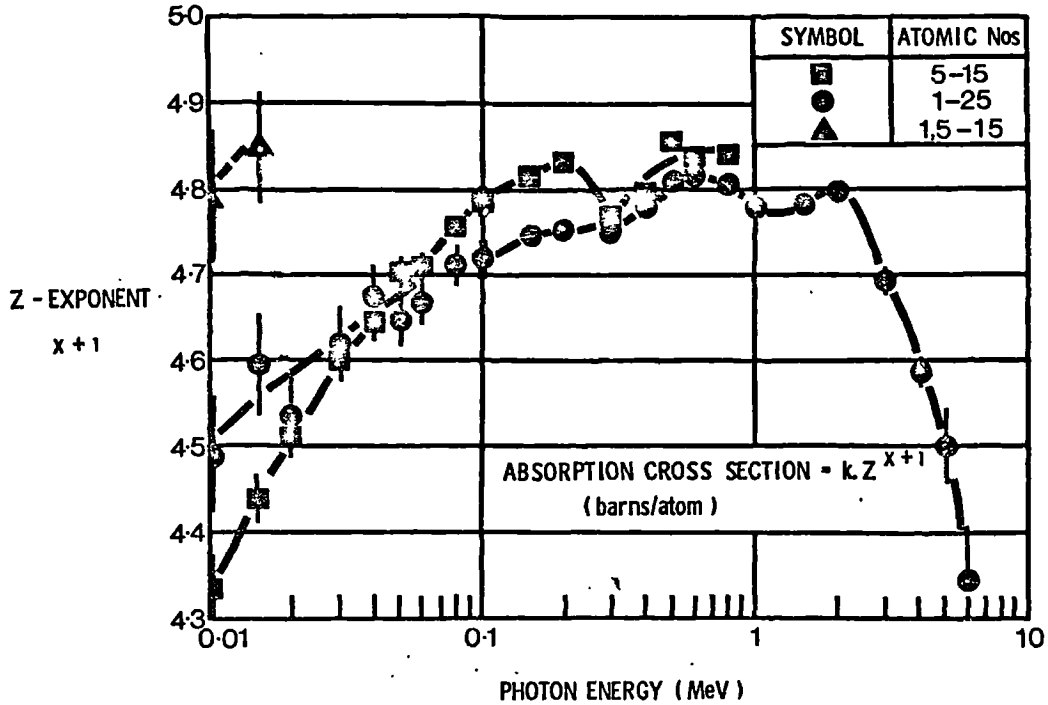

FIGURE 3.20 Z-EXPONENTS FOR PHOTOELECTRIC ENERGY ABSORPTION PROCESS (UNWEIGHTED REGRESSION)

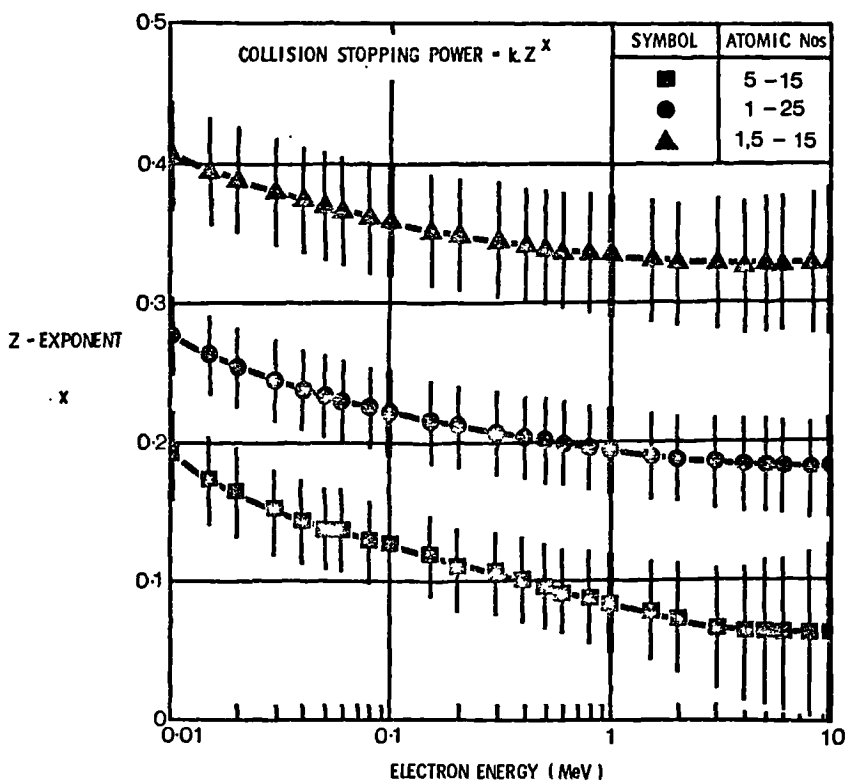

FIGURE 3.21 Z-EXPONENTS FOR ELECTRON COLLISION PROCESS (UNWEIGHTED REGRESSION)

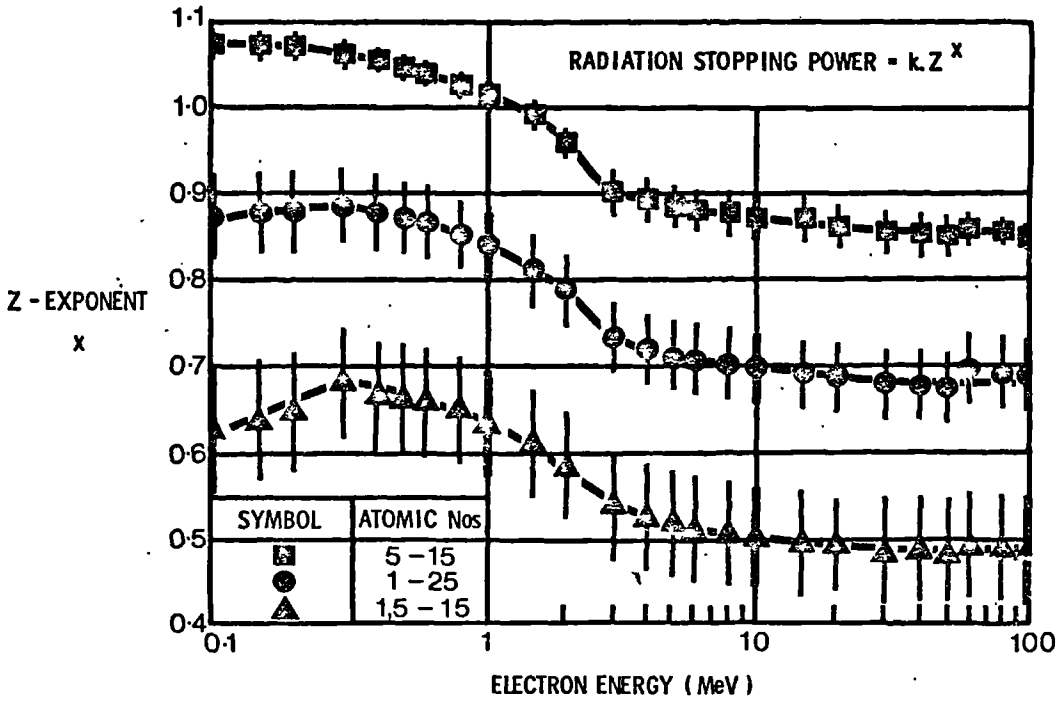

FIGURE 3.22 Z-EXPONENTS FOR ELECTRON RADIATION PROCESS (UNWEIGHTED REGRESSION)

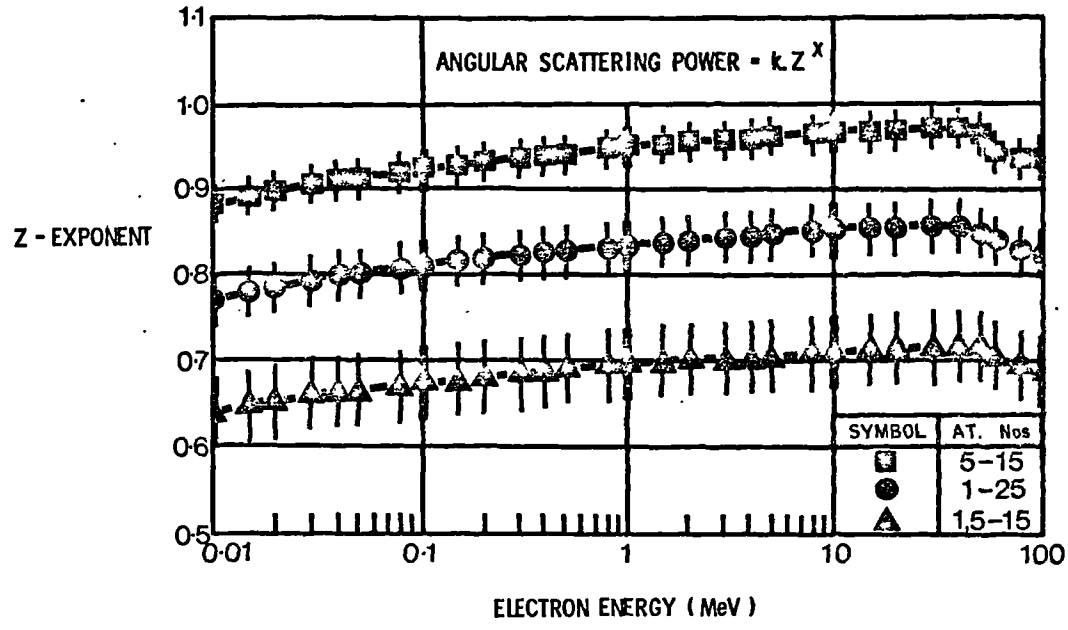

FIGURE 3.23 Z-EXPONENTS FOR ELECTRON ANGULAR SCATTERING PROCESS (UNWEIGHTED REGRESSION)

(a) PHOTOELECTRIC

	Z-EXPONENTS		
DATA ANALYSED	10 keV	40 MeV	150 keV
ELEMENTAL (NOT WEIGHTED)	4.33-4.79	4.64-4.67	4.74-4.82

(b) PAIR PRODUCTION

	Z-EXPONENTS		
DATA ANALYSED	5 MeV	10 MeV	20 MeV
ELEMENTAL (NOT WEIGHTED)	1.91-1.95	1.83-1.90	1.78-1.83

TABLE 3.6 CALCULATED VALUES OF Z-EXPONENTS FOR (a) PHOTOELECTRIC (b) PAIR PRODUCTION ENERGY ABSORPTION DATA

ELECTRON INTERACTION	Z-EXPONENTS				
	10 keV	100 keV	1 MeV	10 MeV	100 MeV
COLLISION STOPPING POWER	0.19-0.41	0.13-0.36	0.09-0.33	-	-
RADIATION STOPPING POWER	-	0.62-1.07	0.63-1.01	0.49-0.87	0.48-0.85
ANGULAR SCATTERING POWER	0.63-0.88	0.67-0.92	0.69-0.95	0.71-0.97	0.69-0.94

TABLE 3.7 CALCULATED VALUES OF Z-EXPONENTS FOR ELECTRON INTERACTIONS

variations and standard deviations (FIGURE 3.23).

Incoherent energy absorption interactions yielded Z-exponents within one percent of unity over the energy range 150 keV-3MeV. Outside this range the exponents decreased to be 0.73-0.80 at 10 keV and 0.72-0.83 at 100 MeV.

It appears from this investigation that the few Z-exponents published in the literature are not adequate for precise simulation procedures. This is particularly true in the important photoelectric region, where considerably higher exponents than the popular '2.94' are indicated. The results for most interactions vary widely with energy and elemental grouping, so simulation procedures based on the concept of effective atomic numbers will never produce formulations equivalent to those from the superior Basic Data Method. Unfortunately, neither method is applicable to high energy electrons, when the Addition Rule is not strictly obeyed. Despite these reservations, the two new methods described in this chapter have both produced many useful substitutes. The way in which these methods were applied in practice will be made the subject of the next chapter.

CHAPTER 4

THE PRACTICAL APPLICATION OF THE NEW SELECTION PROCEDURES

In the previous chapter, two selection procedures were introduced, namely, the BASIC DATA and the EXTENDED $\overline{Y}(x)$ METHODS. Formulae were developed which could be used for estimating the relative masses of the components of a substitute and selecting those compounds which would give pre-defined radiation characteristics over extended energy ranges. In the case of the Extended $\overline{Y}(x)$ Method, a thorough investigation of Z-dependence was made and data presented for all of the important photon and electron interactions.

This chapter will formalise these results and present them in a manner which will permit a relatively straightforward translation into workable computer programs.

4.1 FORMALISING THE NEW SELECTION PROCEDURES

(i) BASIC DATA METHOD

This procedure may be broken into six separate parts, each requiring a definite, but isolated mathematical action. At this stage the six steps will be applied to some 'general interaction', assuming that the material to be simulated and the base material for a two-component substitute have been selected.

(1) Select the FITTING RATIO, f .

(2) Calculate the limits of the slope of the substitute (m_s), using EQUATION 3.3 (FIGURE 3.5).

(3) Calculate the acceptable slopes of the added material (m_a), for a range of fractional weights (EQUATION 3.5 - FIGURE 3.7).

(4) Find a material which is COMPLEMENTARY to the base material (that is, if the base has coefficients, or powers, less than those for the material being simulated, the added compound MUST have correspondingly larger values).

(5) Calculate relative masses of base and added materials which together give perfect agreement for coefficients, or powers, at a mid-point energy (EQUATION 3.2).

(6) Check that the proposed added material has an acceptable slope (defined by (3)) for the fractional weights derived in (5). If this test is positive, the material is suitable for this interaction.

This procedure would have to be repeated for all of the other relevant effects.

In this study, three fitting modes were evaluated. ATTENUATION and ABSORPTION fitting considered partial photon interactions,

while ELECTRON fitting was devoted to electron stopping powers. The technique of selecting a given set of interactions and performing fitting manipulations on this aspect alone, leads to results which are more easily compared with theoretical predictions. The more complex technique of cascading the fitting through all of the partial interactions was rejected, although once the individual fitting modes are functioning correctly the transition to this technique would be fairly straightforward. In practice, the three fitting modes were extremely successful, especially in situations where certain interactions predominate, when the appropriate mode produced substitutes which were directly applicable.

For the two photon fitting modes, photoelectric and coherent (attenuation only) slopes were evaluated in the energy range 10-150 keV, with exact fitting at 40 keV. Pair production slopes were calculated over the energy range 5-20 MeV, with exact fitting at 10 MeV. Incoherent interactions were fitted at 1 MeV only.

The first choice for each formulation was the simulation, within the specified limits, for all of the interactions considered in the particular fitting mode. For example, photoelectric, coherent, incoherent, pair production attenuation processes were considered for the ATTENUATION fitting mode. If this condition was not met, then low, medium and high energy fitting was attempted. For photons, photoelectric and coherent interactions were considered

for low energies; incoherent process for medium energies; pair production and incoherent interactions for high energies. This method ensured that a useful list of formulae was always generated, even if no one compound could be found which was suitable for all of the interactions.

For electrons, three specific energies in the range 10 keV to 2 MeV were considered and the corresponding collision stopping powers analysed with respect to the Addition Rule (EQUATION 3.2). This simple procedure was found to give acceptable results.

4.1(ii) EXTENDED $\overline{Y}(x)$ METHOD

A similar sequence of six mathematical steps, as described in the first section, may be derived for the Extended $\overline{Y}(x)$ selection procedure. For a 'general interaction' and again assuming that the 'real' and base materials for a two-component substitute have been selected.

(1) Select the FITTING RATIO, f.

(2) Calculate the limits of the $\overline{Z}$-Power Ratio for the substitute, R_s (EQUATION 3.11 - FIGURE 3.12).

(3) Calculate the acceptable $\overline{Z}$-Power Ratios for the added material (R_B) for a range of electron fractions (EQUATION 3.12 - FIGURE 3.13).

(4) Find a material which is COMPLEMENTARY to the base material (that is, if the base has $\overline{Y}(x)$ values less than the material being simulated, the added material MUST have correspondingly larger values).

(5) Calculate electron fractions of base and added material which gives perfect $\overline{Y}(x)$ agreement with the 'real' material (EQUATION 3.8 - FIGURE 3.10).

(6) Check that the proposed added material has an acceptable $\overline{Z}$-Power Ratio (defined by (3)) for the electron fractions derived in (5). If this test is positive, the material is suitable for this interaction.

As for the Basic Data Method, the procedure would have to be repeated for all of the other relevant effects.

Only photon interactions, attenuation and absorption, were investigated by this method, due to the weak Z-dependence of stopping power data. The variations of Z-exponents with energy and elemental grouping, made the choice of exponents, even for photon interactions, extremely difficult. The possibility of having the Z-exponents governed by the type of material being simulated was considered. The higher values for photoelectric effect could be employed when materials of high hydrogen content were being simulated (FAT) and the lower values for materials having small quantities of hydrogen (BONE). This method appeared to be inappropriate in two-component substitutes having widely differing hydrogen contents. In these circumstances the photoelectric interactions of the components are characterised by different exponents.

The exponents that were finally used in this study are shown in TABLE 4.1. The values were based on a compromise selection and repeated practical tests in the final computer programs. In the table the photoelectric and coherent exponents corresponded to 10, 40 and 150 keV, while those for pair production were for 5, 10 and 20 MeV.

Incoherent interactions were analysed solely in terms of the magnitudes of electron densities (EQUATION 3.7 - FIGURE 3.9).

(a)

EFFECT	$\bar{Z}$-EXPONENT		
	10 keV	40 keV	150 keV
PHOTOELECTRIC (ATTENUATION)	3.5	3.7	3.8
PHOTOELECTRIC (ABSORPTION)	3.4	3.6	3.7
COHERENT (ATTENUATION)	1.4	1.6	1.7

(b)

EFFECT	$\bar{Z}$-EXPONENT		
	5 MeV	10 MeV	20 MeV
PAIR PRODUCTION (ATTENUATION)	0.94	0.92	0.88
PAIR PRODUCTION (ABSORPTION)	0.92	0.88	0.80

TABLE 4.1 THE $\bar{Z}$-EXPONENTS FOR (a) PHOTOELECTRIC, COHERENT, (b) PAIR PRODUCTION INTERACTIONS USED IN THE EXTENDED $\bar{Y}(x)$ SELECTION PROCEDURE

4.1(iii) THE COMPOUND LIBRARY

It was decided at the beginning of this study that a comprehensive library of compounds had to be compiled if the selection procedures were to be fully exploited. If the library was large enough to allow a number of equally acceptable substitutes to be formulated, then the final choice could be governed by ease of manufacture and availability of products. It was found in practice that, in certain circumstances, even when the library contained 400-500 compounds, the choice of suitable substitutes was frequently limited. For these reasons the number of compounds contained on the magnetic tape store was steadily increased throughout the study, whenever new polymers, resins or any materials of known composition were discovered in the literature.

The compounds may be divided into four groups, namely, INORGANIC, ORGANIC, POLYMERS/RESINS and LIQUIDS. As most of the inorganic and organic compounds were to be added to polymers and resins, it was necessary to restrict the choice according to the physical characteristics. As the added compounds normally had to be added in the solid phase, inert materials of high melting point were the most satisfactory.

The basic list of inorganic compounds was compiled from the HANDBOOK OF CHEMISTRY AND PHYSICS (1971-1972). Compounds were selected with melting points above 150°C, which would not

readily decompose and were not hygroscopic or deliquescent. The melting point restriction was relaxed if a compound had a formula which looked promising (for example, a high hydrogen content).

Similar reasoning was applied to organic materials, but due to the considerable number of formulae published it was thought prudent to further restrict the choice according to their availability. The excellent publication by the EASTMAN KODAK CO, 'ORGANIC CHEMICALS' was used to prepare the initial list. Although this limitation still resulted in many hundreds of formulae, it was comforting to know that all of the compounds were available, albeit at a price.

The list of polymers and resins was prepared from commercial literature and the advice of experts in the field (BRYDSON, 1971 and 1973; MARTIN, 1971 and 1973; CASS, 1971). This group was by far the hardest to compile due to the difficulty of obtaining reliable formulae from the relevant manufacturers.

The final group contained popular liquids and was prepared from the HANDBOOK OF CHEMISTRY AND PHYSICS (1971-1972) and the data presented by FRIGERIO & SAMPSON, 1969.

In the four groups, once the compound had been selected, computer data cards were prepared which recorded the following information:

COMPOUND NAME

MELTING POINT/BOILING POINT

SPECIFIC GRAVITY (IF KNOWN)

CHEMICAL FORMULA

The format of these data cards, which were used in conjunction with the magnetic tape writing programs ATTAPE and ZETAPE (APPENDIX 4), will be given in the next section.

Advice was sought on the toxicity and carcinogenic properties of the selected compounds (FRANCIS, 1973) and those which had dubious properties were rejected.

The most recent listing of the complete library of compounds is given in APPENDIX 3. The tabulation was, for convenience, generated via the CALCOMP 1670 microfilm plotter. The approximately 1040 compounds which are now stored on the magnetic tapes have proved to be invaluable in the formulation of many equivalent materials.

4.2 THE 'ZEDIT' SERIES OF COMPUTER PROGRAMS

(i) THE AIMS OF THE PROGRAMS

The two new selection procedures have been translated into two independent computer programs, called ZEDITA and ZEDITB (APPENDIX 4). Execution of each program requires the use of two magnetic tapes, one containing elemental attenuation and absorption cross sections and stopping powers; the other relevant compound data.

The principal aims of the programs were five-fold:

(1) The programs must strictly follow the theoretical selection procedures.

(2) Program execution time should be short to enable the complete library of compounds to be searched at each run.

(3) It must be possible to formulate one - or two - component substitutes.

(4) The systems should be simple to run with the minimum of 'user input' (i.e. input card data, etc).

(5) The structure of the programs must be flexible so that future modifications and improvements could easily be made.

In pursuit of these ideals the programs were written in Fortran IV, strictly according to the formulae developed in CHAPTER 3 and ultimately run on the complex of fast CDC computers housed at the University of London Computer Centre (U.L.C.C.). The speed of execution was important because a complete search of the compound library tapes during each run was highly desirable in order that useful formulations were not missed. A facility for re-positioning the magnetic tapes, and effectively rejecting a set number of initial compounds, was designed for the cases when the permitted time was too short for a complete run. In practice a Central Processor (CP) time of 120 seconds normally gave a complete search which allowed the jobs to be run under the ULCC 'J9' parameter. This gave a job turnaround of approximately one day: a longer CP time would have been categorised as a 'J12', with a subsequent turnaround of 1-2 weeks.

When the original versions of the ZEDIT series were designed, it was hoped that once a formulation was specified, a complete tabulation of coefficients and powers could be made. This was feasible when the numbers of derived formulae were below ten, but as the compound library increased in size, this thorough tabulation had to be abandoned. In its place a simplified tabulation was made of the basic formulation, expected specific gravity, energy ranges over which the coefficients and powers were within the specified Fitting Ratio and the maximum errors in these data. This necessitated a third program, TABLEC,

which gave a comprehensive compilation for the ten best formulations selected from the complete search of the compound library. TABLEC gives four print-out pages of data for each formula including $\overline{Y}(x)$ values, $\overline{Z}$-Powers, coefficients, powers and also the ratios of these quantities with those for the material being simulated.

When an extensive compound library was available, it was thought that many of these materials could be acceptable without any corrective additions. Consequently, the facility for searching the compound tapes for suitable materials was included in both programs.

Experience has shown that 'user input', the data card input required with each program, should be minimized. Large numbers of data cards ultimately find themselves out of their intended order, especially if the card deck is frequently run. Unless elaborate checking procedures are written into the program, the simplest solution is to keep these cards to below ten. In most of the runs with ZEDITA and ZEDITB only 7-9 data cards were required.

Finally, the structure of the programs was made as flexible as possible by the liberal use of subroutines, complete 'mini-programs' each having a definite computing function, called from the main program. This method allowed modifications to be performed without disruptive consequences to the rest of the program. The validity of this point was proved towards the end of the study when the programs were modified to take attenuation data directly

from tissue absorption measurements as the 'real' material characteristics. This had to by-pass the normal formula input and the subroutines responsible for coefficient computations.

More details of the structure of ZEDITA and ZEDITB will be given in the next section.

4.2(ii) THE BASIC STRUCTURE OF ZEDITA AND ZEDITB

Eahh ZEDIT has a main program and a number of subroutines. The function of each of these units is summarised below.

(a) ZEDITA (Photon Fitting Only)

This program is based upon the EXTENDED $\overline{Y}(x)$ METHOD and has, in addition to the main program, nine subroutines (ACALC, LIMITS, ZRANGE, ACHEKA, WRITAA, WRITAB, WRITAC, TABLE, ZCALC).

The sequence in the MAIN PROGRAM may be divided into 23 parts ----

START

(1) SET: 100 elemental names and atomic weights (Data Statements).

(2) SET: 33 energies (Data Statement).

(3) OUTPUT: Elemental names and atomic weights.

(4) INPUT(card): Fitting Mode (Attenuation, Absorption).

(5) SET: $\overline{Z}$-exponents.

(6) INPUT (Mag. Tape): Coefficients and powers for 30 elements.

(7) INPUT(card): Formula of material to be simulated.

(8) CALCULATE & STORE: Coefficients and powers for 'real' material (via subroutine ACALC).

(9) CALCULATE & STORE: $\overline{Z}$-Powers, etc (ZCALC).

(10) OUTPUT: $\overline{Z}$-Powers, coefficients, powers, etc (WRITAA, WRITAB, WRITAC).

(11) SET: Fitting Ratio.

(12) INPUT(card): Optional single material tabulation.

(13) IF: Single material tabulation required, search compound tape, find acceptable compounds and tabulate results (ACALC, LIMITS, TABLE).

(14) INPUT(card): Formula of base material.

(15) CALCULATE & STORE: Coefficients, powers, $\overline{Z}$-Powers, etc for base material (ACALC, ZCALC).

(16) OUTPUT: $\overline{Z}$-Powers, coefficients, powers, etc (WRITAA, WRITAB, WRITAC).

(17) INPUT(card): Number of initial compounds to be missed for tape repositioning.

(18) CALCULATE & STORE: Acceptable $\overline{Z}$-Power Ratios for range of electron fractions (ZRANGE).

(19) OUTPUT: Selection of stored $\overline{Z}$-Power Ratio data.

(20) INPUT(Mag. tape): Search tape to find acceptable compounds (ACHEKA).

(21) CALCULATE: New formula, coefficients and powers (ACALC).

(22) OUTPUT: Tabulate results (LIMITS, TABLE).

(23) OUTPUT: Number of compounds analysed.

END

Short descriptions of each SUBROUTINE now follows ----

ACALC: Calculates and stores coefficient data by the Addition Formula.

LIMITS: Calculates energy range over which coefficients and powers are within the limits specified by the Fitting Ratio. Maximum errors are also derived. The type of fitting is specified for low (LO), medium (MED), high (HI) or the complete range (ALL) of energies.

ZRANGE: Calculates and stores acceptable range of $\overline{Z}$-Power Ratios for 1000 electron fractions in the range 0.001-1.0. A selection of the stored data is tabulated.

ACHEKA: Checks compounds from the magnetic tape for photon interactions.

WRITAA: Tabulates name, formula, specific gravity and molecular weight for a compound.

WRITAB: Tabulate electron density, $\overline{Z}(x)$, $\left[\overline{Z}(x)\right]^x$, $\overline{Y}(x)$ and ratios of $\overline{Y}(x)$ for any material to those for the material being simulated. The exponent, x, has 30 values from 0.8-4.0).

WRITAC: Tabulates coefficient and power data in the energy range 10 keV-100 MeV. Partial and total attenuation coefficients, total energy absorption coefficients, partial and total electron stopping powers are given.

TABLE: Tabulates names and percentage weights of accepted added compounds. Energy ranges over which coefficients and powers are within the limits set by the Fitting Ratio are given together with the maximum error in the data corresponding to the Fitting Mode. The type of fitting is also indicated.

ZCALC: Calculates and stores $\overline{Z}$-Powers and electron densities.

(b) ZEDITB (Photon and electron Fitting)

This program uses the BASIC DATA METHOD and has a structure similar to ZEDITA. It is composed of a main program and nine subroutines (CALC, LIMITS, SRANGE, BCHEKA, WRITBA, BCHEKB, WRITBB, TABLE, ALINE).

The sequence in the MAIN PROGRAM may be divided into 22 sections ----

START

(1)-(4): As ZEDITA, but includes 'electron fitting', via (4).

(5) SET: Energy ranges over which coefficient and power slopes will be calculated.

(6)-(8): As ZEDITA [(8) calls subroutine CALC]

(9) OUTPUT: Coefficients and powers (WRITBA, WRITBB).

(10)-(13): As steps (11)-(14) in ZEDITA, with CALC replacing ACALC.

(14) CALCULATE & STORE: Coefficients and powers for base material (CALC).

(15) OUTPUT: Coefficients and powers for base material (WRITBA, WRITBB).

(16) : As (17) in ZEDITA.

(17) CALCULATE & STORE: Acceptable coefficient and power slopes for range of fractional weights (SRANGE).

(18) OUTPUT: Selection of stored slopes.

(19) INPUT (tape): Search compound tape to find acceptable compounds (BCHEKA, BCHEKB).

(20)-(22): As (21)-(23) in ZEDITA, CALC replacing ACALC.

END

The SUBROUTINES will now be described briefly ----

CALC: Calculates and stores coefficients and powers by the Addition Formula. The routine also initiates, via ALINE, the calculation and storage of coefficient and power slopes.

LIMITS: As for ZEDITA.

SRANGE: Calculate and stores acceptable coefficient or power slopes for 1000fractional weights in the range 0.001-1.0. A selection of the stored data is tabulated.

BCHEKA: Checks compounds from magnetic tape for photon interactions.

WRITBA: As for WRITAA used in ZEDITA, but with the addition of a table showing coefficient or power slopes.

BCHEKB: Checks compounds from magnetic tape for electron interactions.

WRITBB: As WRITAC in ZEDITA.

TABLE: As for ZEDITA.

ALINE: Computes linear regression for inputed data.

ZEDITA and ZEDITB both require approximately 31.5k of storage. The amount of storage for ZEDITA is abnormally high because it was considered necessary to input and store elemental coefficients and powers, so that direct comparisons could be made between the 'real' and new materials. If these comparisons had been omitted, then the amount of storage could have been drastically reduced.

The basic flow chart for these programs is shown in FIGURE 4.1. The chart gives some indication of the logic branching used which the summarised versions in the text could not specify.

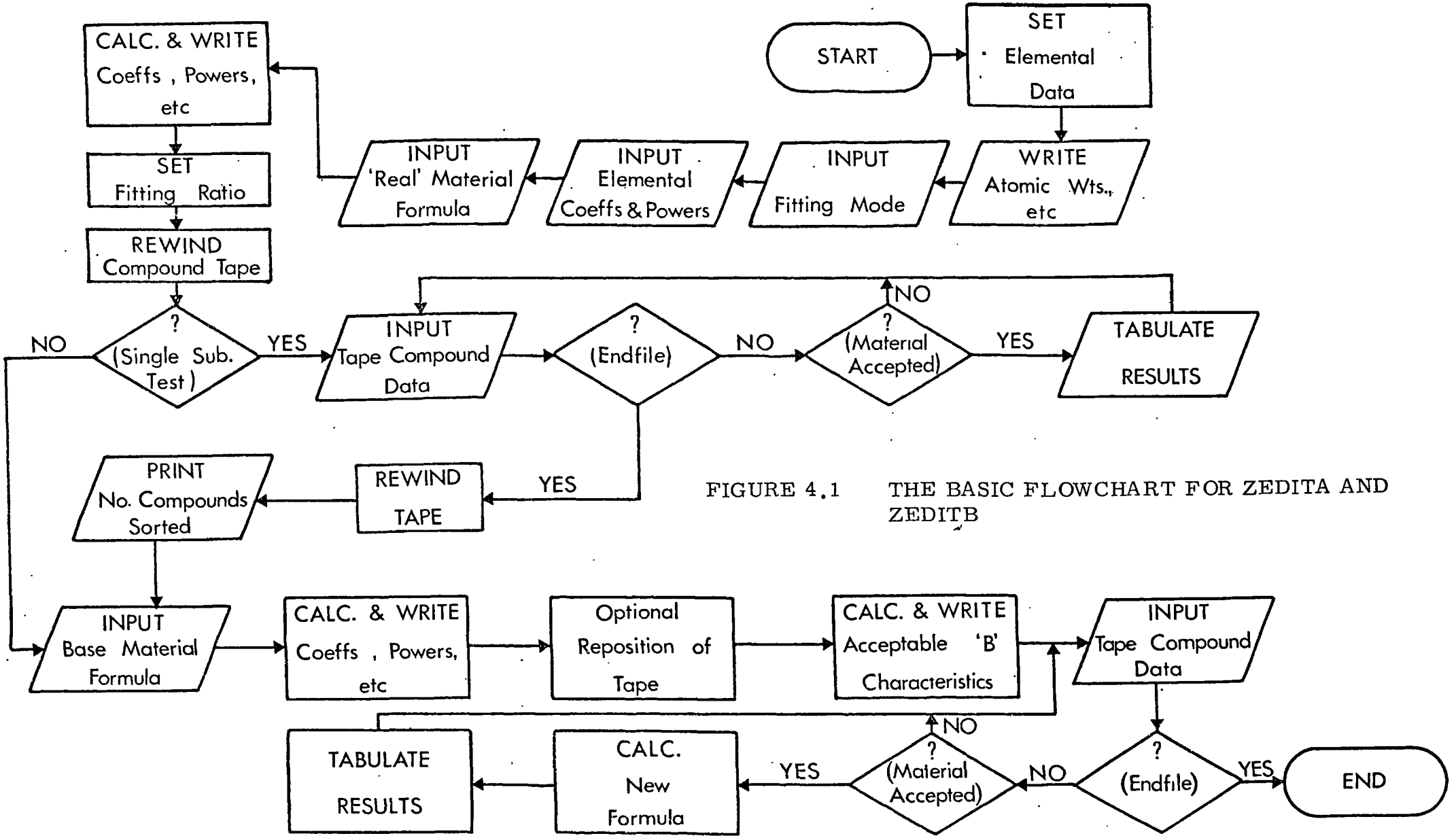

FIGURE 4.1 THE BASIC FLOWCHART FOR ZEDITA AND ZEDITB

4.2(iii) INPUT/OUTPUT SPECIFICATIONS

Two types of inputs were used in the computer programs ZEDITA and ZEDITB. These were magnetic tape input and card input.

To produce reasonably fast execution times it was necessary to generate two different compound data tapes, one for each of the ZEDIT programs. If one common tape had been employed, containing simply the chemical formula, specific gravity and melting (or boiling) point of each material, then before a screening check could be made to ascertain the acceptability of a given compound, the coefficients, powers, or $\overline{Y}(x)$ and $\overline{Z}$-Power Ratios would have to be calculated. Multiply these calculations by 1000 and many precious seconds are wasted. The problem was solved by generating two tapes, namely,

ZETAPE: This contained the chemical formula, specific gravity, melting or boiling point, electron density and 30 values of $\overline{Z}(x)$ and $\overline{Z}$-Powers for each compound.

ATTAPE: This contained chemical formula, specific gravity, melting or boiling point and the partial coefficients from 10 keV-100 MeV for each compound.

It was found in practice that these tapes significantly reduced the calculation times.

The other magnetic tape input, used in both programs, was COTAPE, which contained partial attenuation and energy absorption cross sections, collision and radiation stopping powers for the first 30 elements.

Both programs use limited card inputs. FIGURE 4.2 and TABLE 4.2 shows a typical set of seven data cards and their associated formats.

The first card selects the type of fitting procedure to be used. The three different types of Fitting Modes were denoted by ATT for attenuation coefficient fitting, ABS for energy absorption coefficient and ESP for electron stopping power procedures. All three modes were available with ZEDITB, but the electron procedure was omitted from ZEDITA.

The second and third cards specify the name, specific gravity (SG), melting/boiling point (MP) and formula of the material to be simulated. A similar card structure was used for the base material (cards 5 and 6). This format was employed throughout all the other computer programs which required similar compound input data.

Single material tabulation was selected by punching 'ONE' on card 4.

The last card set the number of initial compounds to be missed

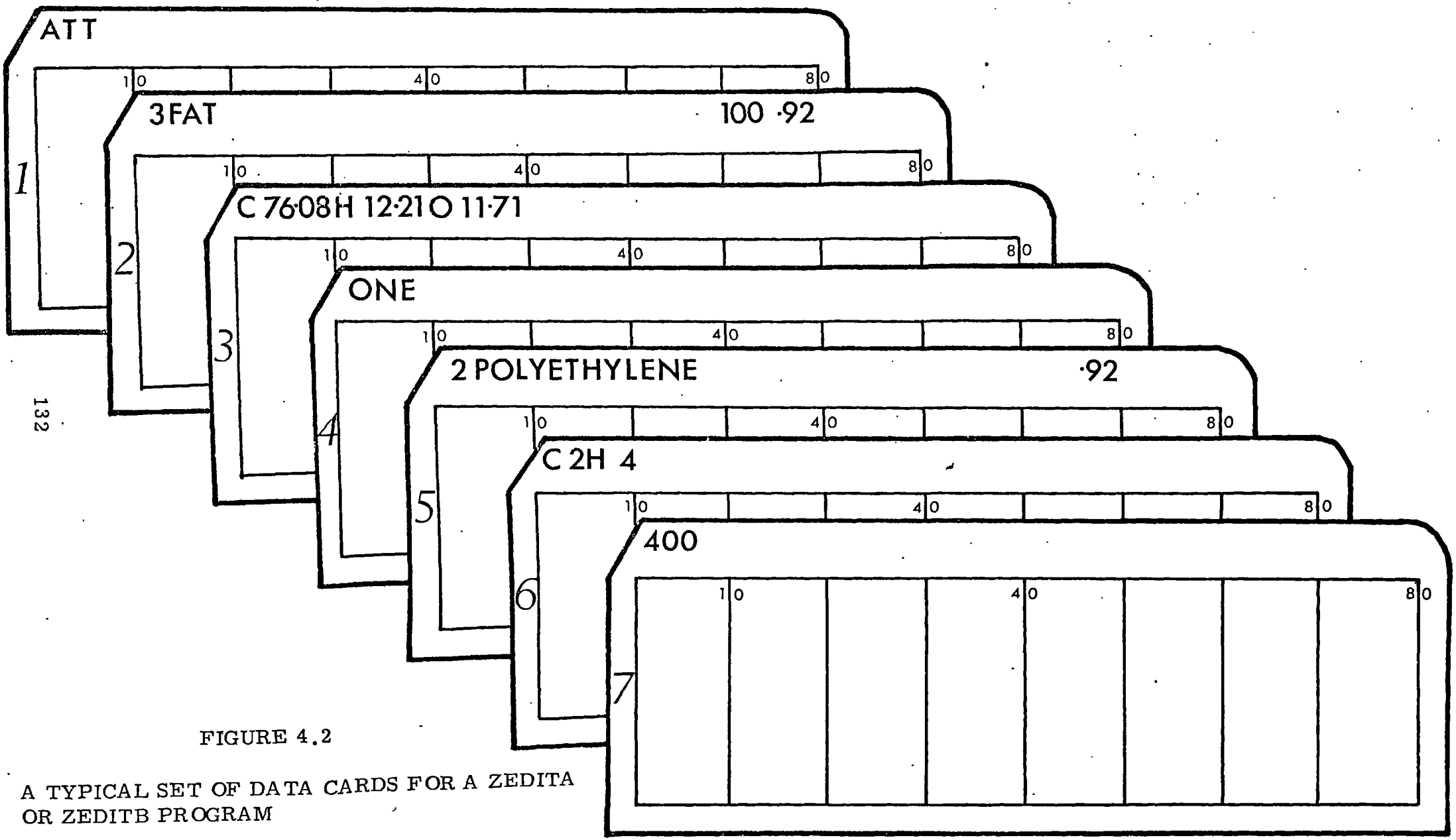

FIGURE 4.2

A TYPICAL SET OF DATA CARDS FOR A ZEDITA OR ZEDITB PROGRAM

CARD NO.	STRUCTURE	FORMAT
1	FITTING MODE (ATT, ABS, ESP)	(A3)
2	N, NAME, MODE, SG, MP N ≠ No. elements in 'real' material MODE = 0 : Integer atomic proportions MODE = 1 : Floating pt. atomic proportions MODE = 100 : Floating pt. percentage wts	(I2, 6A10, I3, 1X, F5.2, 1X, I4)
3	MODE = 0 : Element symbol, atomic prop. MODE = 1 : Element symbol, atomic prop. MODE = 100 : Element symbol, percentage wt	(A2, I3) (A2, F8.4) (A2, F8.4)
4	SINGLE MATERIAL SPECIFICATION - 'ONE' gives tabulation	(A3)
5	As card 2, but for base material	-
6	As card 3, but for base material	-
7	No. of rejected compounds for compound tape repositioning	(I3)

TABLE 4.2 THE FORMAT SPECIFICATIONS USED IN CARD INPUTS TO THE ZEDITA/ZEDITB PROGRAMS

from the compound magnetic tape if repositioning was necessary.

TABLE 4.3 illustrates the typical output tabulation which was common to both ZEDITA and ZEDITB. The table shows the results for fat simulation and photon attenuation fitting, using polyethylene as the base material. The first four columns gives the number and name of the added compound, its percentage weight and the molecular proportion, respectively. The next column gives the expected specific gravities for the indicated relative weights.

The next six columns give the energy ranges over which the attenuation coefficients, energy absorption coefficients and electron stopping powers are within the specified limits set in the program, in this case 1%. The last two columns indicate the maximum error in the data specified by the Fitting Mode, in this run attenuation coefficients, and the type of fitting that was used. As stated earlier, the programs always attempt to find a material and formula which gives an acceptable fit over all of the energies and interactions. If this is not possible, low, medium and high energy fits are attempted. The codes indicate that the following interactions are acceptable ----

ALL	-	All interactions
LO1	-	Photoelectric and coherent
LO2	-	Photoelectric only
MED	-	Incoherent only
HI1	-	Pair production and incoherent
HI2	-	Pair production only

PHOTON ATTENUATION FITTING (ZEDITA) SIMULATED MATERIAL WHITES FAT

BASE COMPOUND POLYETHYLENE

	ADDED SUBSTANCE	PERCENT-B	PROP-B	SG	ENERGY (MEV) - I O/O SIMULATION ATTENUATION	ABSORPTION	ELECTRONS	MAX O/O ERROR	TYPE
1	ALUMINIUM	11.9850	.1416	.999	0.150 - 6.000	0.200 - 6.000	0.010 - 60.00	100.5334	MED
2	ALUMINIUM	4.8615	.0508	.949	10.00 - 100.0	8.000 - 100.0	2.000 - 100.0	27.8435	HI2
3	ALUMINIUM CARBIDE	12.6174	.0281	.997	0.150 - 8.000	0.200 - 8.000	0.010 - 100.0	75.8128	MED
4	ALUMINIUM CARBIDE	6.0478	.0125	.955	0.400 - 100.0	0.600 - 100.0	1.000 - 100.0	26.7438	HI2
5	ALUMINIUM FLUORIDE	11.2652	.0425	.997	0.080 - 20.00	0.150 - 20.00	0.010 - 100.0	37.0133	MED
6	ALUMINIUM FLUORIDE	7.5002	.0271	.969	0.100 - 100.0	0.150 - 100.0	0.010 - 100.0	18.4186	HI2
7	ALUMINIUM NITRIDE	12.8773	.1012	1.014	0.150 - 8.000	0.200 - 8.000	0.010 - 60.00	68.7946	MED
8	ALUMINIUM NITRIDE	6.3278	.0462	.964	0.300 - 100.0	0.400 - 100.0	1.000 - 100.0	24.4327	HI2
9	ALUMINIUM OXIDE	13.2700	.0421	1.024	0.100 - 8.000	0.200 - 8.000	0.010 - 60.00	60.8928	MED
10	ALUMINIUM OXIDE	6.6127	.0195	.969	0.300 - 100.0	0.300 - 100.0	1.000 - 100.0	21.1009	HI2
11	ALUMINIUM PHENOXIDE	22.1185	.0260	.974	0.050 - 100.0	0.100 - 100.0	0.010 - 15.00	7.2526	MED
12	ALUMINIUM PHENOXIDE	25.7130	.0317	.984	0.050 - 100.0	0.100 - 100.0	0.010 - 5.000	11.4255	HI2
13	ALUMINIUM ORTHOPHOSPHATE	13.5428	.0360	1.008	0.150 - 8.000	0.200 - 8.000	0.010 - 50.00	78.7172	MED
14	ALUMINIUM ORTHOPHOSPHATE	6.2951	.0155	.958	0.600 - 100.0	4.000 - 100.0	1.500 - 100.0	25.8002	HI2
15	ALUMINIUM SILICATE (A)	13.8421	.0278	1.021	0.150 - 8.000	0.200 - 8.000	0.010 - 50.00	69.3403	MED
16	ALUMINIUM SILICATE (A)	6.4266	.0118	.964	3.000 - 100.0	4.000 - 100.0	1.500 - 100.0	22.3230	HI2
17	ALUMINIUM SILICATE (B)	13.7007	.0105	1.019	0.100 - 8.000	0.200 - 8.000	0.010 - 50.00	67.2530	MED
18	ALUMINIUM SILICATE (B)	6.4702	.0046	.964	0.600 - 100.0	0.600 - 100.0	1.500 - 100.0	22.0368	HI2
19	ALUMINIUM SULPHATE	14.4402	.0138	1.017	0.150 - 6.000	0.200 - 6.000	0.010 - 40.00	97.7732	MED
20	ALUMINIUM SULPHATE	5.9664	.0052	.958	8.000 - 100.0	8.000 - 100.0	3.000 - 100.0	29.5856	HI2
21	BORON	9.8377	.2831	.978	0.080 - 8.000	0.150 - 8.000	0.010 - 6.000	21.7878	MED
22	BORON NITRIDE	70.4534	2.6954	1.577	-	0.010 - 0.020	-	9.2533	LO2
23	BORON NITRIDE	12.2217	.1574	.992	0.060 - 10.00	0.100 - 10.00	0.010 - 20.00	15.4141	MED
24	BORON NITRIDE	60.9782	1.7665	1.439	-	-	-	7.7552	HI2
25	BORON OXIDE	18.9748	.0944	1.044	0.010 - 100.0	0.010 - 100.0	0.200 - 100.0	.9067	LO2
26	BORON OXIDE	12.9431	.0598	1.001	0.040 - 30.00	0.080 - 30.00	0.010 - 100.0	8.0731	MED
27	BORON OXIDE.	21.2411	.1087	1.061	0.020 - 100.0	0.050 - 100.0	30.00 - 100.0	1.8466	HI2
28	BORON TRISULPHIDE	13.5963	.0375	.974	0.200 - 5.000	0.300 - 5.000	0.050 - 40.00	202.5612	MED
29	BORON TRISULPHIDE	3.9490	.0098	.935	20.00 - 100.0	15.00 - 100.0	4.000 - 100.0	45.7599	HI2
30	CALCIUM ALUMINATE (A)	13.8163	.0285	1.017	0.150 - 6.000	0.300 - 5.000	0.010 - 30.00	171.9827	MED
31	CALCIUM ALUMINATE (A)	4.6554	.0087	.951	15.00 - 100.0	15.00 - 100.0	5.000 - 100.0	46.7332	HI2
32	CALCIUM METABORATE	13.7617	.0356	—	0.150 - 6.000	0.300 - 6.000	0.010 - 40.00	160.5773	MED
33	CALCIUM METABORATE	5.7644	.0137	—	8.000 - 100.0	8.000 - 100.0	3.000 - 100.0	56.5539	HI2
34	CALCIUM TETRABORATE	13.4583	.0223	—	0.150 - 10.00	0.200 - 10.00	0.010 - 60.00	98.8116	MED
35	CALCIUM TETRABORATE	7.7867	.0121	—	0.200 - 100.0	0.300 - 100.0	0.300 - 100.0	49.4053	HI2
36	CALCIUM CARBIDE	14.9155	.0767	1.008	0.200 - 4.000	0.300 - 4.000	0.100 - 30.00	341.4438	MED
37	CALCIUM CARBIDE	3.6252	.0165	.940	20.00 - 100.0	15.00 - 100.0	6.000 - 100.0	69.0419	HI2
38	CALCIUM CARBONATE (ARGONITE)	14.9896	.0494	1.025	0.200 - 5.000	0.300 - 5.000	0.010 - 20.00	224.0563	MED
39	CALCIUM CARBONATE (ARGONITE)	4.6973	.0138	.951	15.00 - 100.0	15.00 - 100.0	6.000 - 100.0	57.5624	HI2
40	CALCIUM CARBONATE (CALCITE)	14.9896	.0494	1.021	0.200 - 5.000	0.300 - 5.000	0.010 - 20.00	224.0563	MED

TABLE 4.3 THE FIRST PAGE OF THE COMPUTER PRINTOUT FOR ZEDITA AND FAT SIMULATION USING POLYETHYLENE AS THE BASE MATERIAL

This particular fitting procedure (ATT) was found to be the most useful one for both ZEDITA and ZEDITB, and has been used extensively for many combinations of materials.

4.3 COMPARING THE NEW PROCEDURES

The precision of the two selection procedures will be evident when, in the next chapter, some new substitutes are presented simulating a number of different materials and the radiation characteristics are calculated. At this juncture it is constructive to consider the results of the two methods when applied to the same problem.

The problem chosen was the simulation of muscle using polyethylene as the base material. Two identical sets of data were processed through the ZEDIT programs simulating for photon attenuation interactions. TABLE 4.4 shows the first page of results from each run. The outputs were obtained in the form of microfilm for this and the previous table.

It can be seen that the agreement between the two sets of data is remarkably good, the same compounds being selected and fitted for the same interactions. In the majority of cases the percentage weights differ by less than 1%. This type of result is not atypical and has been repeated frequently with many different materials.

These versions of ZEDITA and ZEDITB have been successfully operating for over a year and have indicated more than fifty substitutes with characteristics superior to existing systems. In a number of cases substitutes have been produced simulating materials which have not been adequately considered in the past. These new substitutes and their calculated properties will be discussed in the next chapter.

(a)

PHOTON ATTENUATION FITTING (ZEDITA) SIMULATED MATERIAL ICRU MUSCLE

BASE COMPOUND POLYETHYLENE

	ADDED SUBSTANCE	PERCENT-B	PROP-B	SG	ENERGY (MEV) - I O/O SIMULATION ATTENUATION	ABSORPTION	ELECTRONS	MAX O/O ERROR	TYPE
1	ALUMINIUM	22.9124	.3090	1.084	0.150 - 15.00	0.200 - 10.00	0.010 - 0.500	46.3890	MED
2	ALUMINIUM	25.8411	.3567	1.106	0.150 - 100.0	0.200 - 80.00	-	58.0616	MI2
3	ALUMINIUM CARBIDE	24.1214	.0620	1.079	0.100 - 6.000	0.200 - 6.000	0.010 - 0.600	25.1642	MED
4	ALUMINIUM CARBIDE	33.1357	.0966	1.153	0.100 - 100.0	0.150 - 0.200	-	55.2842	MI2
5	ALUMINIUM FLUORIDE	21.5745	.0919	1.078	0.080 - 5.000	0.150 - 4.000	0.010 - 0.800	12.5464	MED
6	ALUMINIUM FLUORIDE	41.0945	.2331	1.277	0.080 - 100.0	-	-	32.5332	MI2
7	ALUMINIUM NITRIDE	24.8184	.2235	1.117	0.080 - 6.000	0.150 - 6.000	0.010 - 0.600	18.9368	MED
8	ALUMINIUM NITRIDE	34.6699	.3632	1.225	0.100 - 100.0	0.150 - 0.200	-	48.2693	MI2
9	ALUMINIUM OXIDE	25.3690	.0935	1.143	0.080 - 6.000	0.150 - 6.000	0.010 - 0.600	11.6770	MED
10	ALUMINIUM OXIDE	36.2320	.1563	1.275	0.080 - 100.0	0.150 - 80.00	-	40.3798	MI2
11	ALUMINIUM PHENOXIDE	42.2654	.0871	1.030	0.150 - 4.000	0.150 - 3.000	0.080 - 0.800	38.0743	MED
12	ALUMINIUM ORTHOPHOSPHATE	25.8906	.0804	1.103	0.100 - 8.000	0.200 - 6.000	0.010 - 0.600	25.7648	MED
13	ALUMINIUM ORTHOPHOSPHATE	34.4918	.1211	1.182	0.100 - 100.0	0.200 - 80.00	-	52.7142	MI2
14	ALUMINIUM SILICATE (A)	26.4628	.0823	1.135	0.080 - 8.000	0.150 - 8.000	0.010 - 0.600	18.8915	MED
15	ALUMINIUM SILICATE (A)	36.2126	.0941	1.231	0.100 - 100.0	0.150 - 80.00	-	43.4405	MI2
16	ALUMINIUM SILICATE (B)	26.1926	.0234	1.130	0.080 - 8.000	0.150 - 8.000	0.010 - 0.600	17.1089	MED
17	ALUMINIUM SILICATE (B)	36.4513	.0362	1.229	0.100 - 100.0	0.150 - 80.00	-	42.7238	MI2
18	ALUMINIUM SULPHATE	27.8063	.0313	1.125	0.150 - 10.00	0.200 - 10.00	0.010 - 0.600	44.7805	MED
19	ALUMINIUM SULPHATE	32.8908	.0398	1.173	0.150 - 100.0	0.200 - 100.0	-	63.1923	MI2
20	BORON	18.8074	.8011	1.039	0.150 - 3.000	0.200 - 3.000	0.400 - 1.000	84.9812	MED
21	BORON NITRIDE	23.3650	.3446	1.067	0.150 - 3.000	0.200 - 3.000	0.300 - 1.000	98.2787	MED
22	BORON OXIDE	24.7442	.1325	1.089	0.150 - 3.000	0.200 - 3.000	0.300 - 1.000	80.9830	MED
23	BORON TRISULPHIDE	25.0328	.0836	1.029	0.200 - 8.000	0.300 - 100.0	0.030 - 0.20	138.4760	MED
24	BORON TRISULPHIDE	21.6372	.0857	1.009	0.300 - 100.0	0.400 - 80.00	0.010 - 0.800	105.9951	MI2
25	CALCIUM ALUMINATE (A)	26.4136	.0837	1.126	0.900 - 100.0	0.300 - 100.0	0.010 - 0.500	112.9406	MED
26	CALCIUM ALUMINATE (A)	25.5078	.0808	1.117	0.200 - 100.0	0.300 - 40.00	0.010 - 0.600	107.1693	MI2
27	CALCIUM METABORATE	26.3092	.0797	—	0.200 - 10.00	0.300 - 10.00	0.010 - 0.600	104.8171	MED
28	CALCIUM METABORATE	31.5839	.1030	—	0.150 - 100.0	0.300 - 15.00	-	136.5698	MI2
29	CALCIUM TETRABORATE	25.7291	.0498	—	0.150 - 5.000	0.300 - 5.000	0.010 - 0.800	48.7252	MED
30	CALCIUM TETRABORATE	42.8643	.1068	—	0.150 - 100.0	0.200 - 0.200	-	117.2318	MI2
31	CALCIUM CARBIDE	26.5148	.1748	1.104	0.300 - 5.000	0.400 - 5.000	0.100 - 0.150	268.7021	MED
32	CALCIUM CARBIDE	19.8632	.1095	1.041	0.600 - 100.0	4.000 - 40.00	0.300 - 1.000	170.3804	MI2
33	CALCIUM CARBONATE (ARGONITE)	26.6565	.1126	1.145	0.200 - 10.00	0.300 - 100.0	0.010 - 0.500	161.6225	MED
34	CALCIUM CARBONATE (ARGONITE)	25.7374	.0871	1.117	0.300 - 100.0	0.400 - 40.00	0.010 - 0.800	139.5201	MI2
35	CALCIUM CARBONATE (CALCITE)	26.6565	.1126	1.135	0.200 - 10.00	0.300 - 100.0	0.010 - 0.500	161.6225	MED
36	CALCIUM CARBONATE (CALCITE)	25.7374	.0871	1.108	0.300 - 100.0	0.400 - 40.00	0.010 - 0.800	139.5201	MI2
37	CALCIUM FLUORIDE	24.2519	.1150	1.112	0.300 - 8.000	0.400 - 100.0	0.010 - 0.400	183.0381	MED
38	CALCIUM FLUORIDE	20.5144	.0927	1.077	0.300 - 100.0	0.400 - 40.00	0.010 - 1.000	146.2990	MI2
39	CALCIUM HYDRIDE	42.5087	.4828	1.178	0.400 - 2.000	0.500 - 2.000	30.00 - 30.00	678.9700	MED
40	CALCIUM HYDRIDE	13.5434	.1044	.988	60.00 - 100.0	20.00 - 50.00	1.500 - 3.000	178.6032	MI2

(b)

PHOTON ATTENUATION FITTING (ZEDITB) SIMULATED MATERIAL ICRU MUSCLE

BASE COMPOUND POLYETHYLENE

	ADDED SUBSTANCE	PERCENT-B	PROP-B	SG	ENERGY (MEV) - I O/O SIMULATION ATTENUATION	ABSORPTION	ELECTRONS	MAX O/O TYPE	
1	ALUMINIUM	23.1978	.3141	1.086	0.150 - 50.00	0.200 - 10.00	0.010 - 0.400	47.6565	MED
2	ALUMINIUM	24.9747	.3461	1.101	0.150 - 100.0	0.200 - 20.00	0.080 - 0.150	55.5465	MI2
3	ALUMINIUM CARBIDE	24.5457	.0634	1.082	0.100 - 8.000	0.200 - 8.000	0.010 - 0.500	26.5804	MED
4	ALUMINIUM CARBIDE	32.5328	.0940	1.148	0.100 - 100.0	0.150 - 0.200	-	53.2419	MI2
5	ALUMINIUM FLUORIDE	25.5327	.1145	1.113	0.015 - 3.000	0.040 - 3.000	0.010 - 0.300	8.8330	LO2
6	ALUMINIUM FLUORIDE	21.9907	.0942	1.082	0.080 - 4.000	0.150 - 4.000	0.010 - 0.800	11.8921	MED
7	ALUMINIUM FLUORIDE	40.8240	.2305	1.274	0.060 - 100.0	-	-	31.9547	MI2
8	ALUMINIUM NITRIDE	25.0432	.2287	1.122	0.080 - 6.000	0.150 - 6.000	0.010 - 0.600	20.2188	MED
9	ALUMINIUM NITRIDE	34.1573	.3552	1.219	0.100 - 100.0	0.150 - 0.200	-	47.7528	MI2
10	ALUMINIUM OXIDE	25.7941	.0956	1.147	0.080 - 6.000	0.150 - 6.000	0.010 - 0.600	12.8002	MED
11	ALUMINIUM OXIDE	35.7990	.1534	1.269	0.080 - 100.0	0.150 - 0.200	-	39.2360	MI2
12	ALUMINIUM PHENOXIDE	43.5473	.0707	1.033	0.150 - 4.000	0.200 - 3.000	0.030 - 0.800	38.3912	MED
13	ALUMINIUM ORTHOPHOSPHATE	26.3154	.0822	1.107	0.100 - 8.000	0.200 - 6.000	0 010 - 0.600	27.0959	MED
14	ALUMINIUM ORTHOPHOSPHATE	34.0146	.1186	1.177	0.100 - 100.0	0.200 - 10.00	-	51.2183	MI2
15	ALUMINIUM SILICATE (A)	26.8870	.0637	1.140	0.080 - 8.000	0.150 - 8.000	0.010 - 0.600	20.0815	MED
16	ALUMINIUM SILICATE (A)	34.7856	.0923	1.226	0.100 - 100.0	0.150 - 10.00	-	42.2425	MI2
17	ALUMINIUM SILICATE (B)	26.8171	.0239	1.134	0.080 - 6.000	0.150 - 8.000	0.010 - 0.600	18.2834	MED
18	ALUMINIUM SILICATE (B)	35.0228	.0355	1.224	0.100 - 100.0	0.150 - 10.00	-	41.5306	MI2
19	ALUMINIUM SULPHATE	28.1843	.0322	1.130	0.150 - 10.00	0.200 - 10.00	0.010 - 0.600	46.8568	MED
20	ALUMINIUM SULPHATE	32.1598	.0389	1.168	0.150 - 100.0	0.200 - 40.00	-	61.2748	MI2
21	BORON	18.5989	.6329	1.044	0.150 - 3.000	0.200 - 3.000	0.400 - 1.000	65.0874	MED
22	BORON NITRIDE	24.2072	.3610	1.074	0.150 - 3.000	0.200 - 3.000	0.300 - 1.000	59.1828	MED
23	BORON OXIDE	25.5025	.1379	1.095	0.150 - 3.000	0.200 - 3.000	0.200 - 1.000	50.6156	MED
24	BORON TRISULPHIDE	26.7155	.0868	1.032	0.200 - 8.000	0.300 - 6.000	0.100 - 0.150	143.6645	MED
25	BORON TRISULPHIDE	20.9867	.0832	1.006	0.300 - 100.0	0.400 - 40.00	0.010 - 0.800	101.1442	MI2
26	CALCIUM ALUMINATE (A)	26.8584	.0852	1.130	0.200 - 80.00	0.300 - 100.0	0.010 - 0.400	115.7748	MED
27	CALCIUM ALUMINATE (A)	24.8878	.0588	1.111	0.200 - 100.0	0.300 - 20.00	0.010 - 0.600	103.2182	MI2
28	CALCIUM METABORATE	26.9659	.0824	—	0.200 - 10.00	0.300 - 10.00	0.010 - 0.600	108.5137	MED
29	CALCIUM METABORATE	30.8486	.0998	—	0.150 - 100.0	0.300 - 15.00	0.010 - 0.150	132.1018	MI2
30	CALCIUM TETRABORATE	26.4260	.0516	—	0.150 - 5.000	0.300 - 5.000	0.010 - 0.800	51.5442	MED
31	CALCIUM TETRABORATE	42.0271	.1041	—	0.150 - 100.0	0.200 - 0.200	-	114.6540	MI2
32	CALCIUM CARBIDE	29.1710	.1802	1.110	0.300 - 5.000	0.400 - 5.000	-	276.1597	MED
33	CALCIUM CARBIDE	19.1813	.1038	1.036	6.000 - 100.0	4.000 - 20.00	0.400 - 1.500	162.6316	MI2
34	CALCIUM CARBONATE (ARGONITE)	29.2662	.1160	1.151	0.200 - 10.00	0.300 - 100.0	0.010 - 0.400	166.2388	MED
35	CALCIUM CARBONATE (ARGONITE)	25.0548	.0937	1.111	0.300 - 100.0	0.400 - 20.00	0.010 - 1.000	134.3520	MI2
36	CALCIUM CARBONATE (CALCITE)	29.2662	.1160	1.140	0.200 - 10.00	0.300 - 100.0	0.010 - 0.400	166.2388	MED
37	CALCIUM CARBONATE (CALCITE)	25.0548	.0937	1.102	0.300 - 100.0	0.400 - 20.00	0.010 - 1.000	134.3520	MI2
38	CALCIUM FLUORIDE	24.7116	.1178	1.116	0.300 - 8.000	0.400 - 100.0	0.015 - 0.300	187.9573	MED
39	CALCIUM FLUORIDE	19.8875	.0893	1.072	0.400 - 100.0	0.500 - 20.00	0.010 - 1.000	140.2354	MI2
40	CALCIUM HYDRIDE	42.7408	.4875	1.180	0.400 - 2.000	0.500 - 2.000	30.00 - 30.00	682.9817	MED

TABLE 4.4 THE FIRST PAGES OF RESULTS FROM (a) ZEDITA AND (b) ZEDITB FOR MUSCLE SIMULATION, POLYETHYLENE AS BASE MATERIAL AND PHOTON ATTENUATION FITTING

CHAPTER 5

THE CALCULATED PROPERTIES OF A RANGE OF TISSUE AND AIR SUBSTITUTES

5.1 SOME GENERAL COMMENTS

The new selection procedures described previously have been extensively applied to the formation of a range of tissue and air substitutes. The formulations were produced by the use of the two computer programs ZEDITA AND ZEDITB, which in most cases were run simultaneously for each simulation exercise. Many hundreds of two-component substitutes were generated during the course of the study, and from these some thirty were selected for manufacture.

The choice of formulae depended upon the agreement between the relevant radiation characteristics for the 'real' material and substitute, and the subsequent application. An example was the development of a breast tissue substitute designed for mammography dosimetry. The substitute was required to have acceptable low energy photon attenuation and absorption characteristics and be suitable for casting large, air free sections.

The base materials that were considered included wax, polyethylene, TPX, P.V.C., epoxy resins, polyurethane foams and, of course, water. There was a gradual trend during the study from polymer-based substitutes which required elaborate equipment not available on site, towards epoxy resin based materials. With these resins, the manufacturing procedures could be easily

performed within any conventional laboratory equipped with modest vacuum and stirring apparatus (described in CHAPTER 6). These comments similarly applied to polyurethane foams used as lung substitutes.

A problem that was always present was the accuracy of the formulae available for the many materials investigated. This was particularly important with the base materials which were often commercial polymers. The large manufacturing organisations such as I.C.I., SHELL and CIBA-GEIGY were exceptionally helpful in this respect, but sometimes the advice was vague and apparently shrouded in commercial secrecy. All too frequently a formula would be quoted as being basically correct, except for the addition of 'a small percentage of a stabilizing agent'. The formula of the stabilizing agent was always highly classified.

Another similar situation occurred with the'unknown' impurities contained within many inorganic compounds. High purity chemicals, such as ANALAR grades, were always used when these were available. If it was thought that a material was contaminated or had an unknown composition, other methods of identification were pursued. These methods included chemical analysis and high precision, low energy photon attenuation measurements. The latter technique, which successfully indicates small quantities of high-Z contaminants, is described in CHAPTER 7.

5.2 THE SIMULATED MATERIALS

When the different types of materials to be simulated were being considered, three factors tended to influence the selection. The first was historical. During 60 years of dosimetric measurements, the many diverse problems that were encountered obviously forced the evolution of the existing substitutes. In this period the demand was predominantly for muscle, lung, bone and air substitutes. As the analysis of existing substitutes showed that in most cases the radiation characteristics were unacceptable, then all of these materials should be simulated, in the light of standards set in this study.

The second influencing factor involved the current demand for substitutes. During the course of the work, inconsistencies relating to the dosimetry of mammographic techniques has resulted in the production of substitutes that simulate the tissues found in the human breast. A great deal of effort was put into the search for a reliable formula representing 'average' breast tissue, which was unsuccessful except that it established the variations of the composition with age and subject. Apparently the tissue varies between the extremes of fat and water. 'Average' breast tissue was quoted as being composed of a mixture of fat/water in the proportions from 25:75 to 75:25. To resolve the dilemma the measurements were performed on three test objects, constructed of a fat substitute, a muscle substitute and a 'breast' tissue material based on fat (50); water (50).

The shortage of 'European sized' skeletons in the manufacture of body phantoms (STACEY, 1971) has given impetus to the development of bone substitutes. From data supplied by SPIERS (1971), an 'inner bone' formula was calculated which had the average composition of a mixture of hard bone and soft tissue. The formula, which takes into account the average ratio of hard bone to red marrow in trabecular bone structures, was based on the ratio of 22.4% bone to 77.6% soft tissue (by weight). Bones made with this mixture need only be coated with an outer layer of a hard bone substitute, to simulate real bones on a macroscopic scale.

Similarly, the continued search for more 'tissue equivalent' thermoluminescent dosemeters, has stimulated the investigation of mixtures of phosphors and inert powders that have improved radiation properties.

The third influencing factor was a preprint of an ICRP document on Reference Man which was received in 1970 (TIPTON, 1970). The document contained an elemental analysis of some 80 tissues and organs, with data covering 64 elements. This treatment will ultimately replace a similar, but less extensive, ICRP publication of 1959. Unfortunately the new document contains a number of numerical anomalies and amended 'final' versions are still being written.

It was realised that an adequate evaluation of this mass of data could only be performed by computer, so the formulae have been compiled on to magnetic tape in the same way as the data for compounds was stored (ATTAPE and ZETAPE - APPENDIX 4). When amendments are received, the tapes are updated.

The influence of this source of data has arisen from the discrepancies between photon energy absorption coefficients calculated for these tissues, and those for the formulae published by ICRP in 1959. An analysis of the 1959 data was given by the ICRU (National Bureau of Standards, 1963) who pointed out that the high atomic number elements in the thyroid, liver and spleen would result in increased energy absorption compared to muscle. In the energy range 10-50 keV, thyroid and spleen were stated to give approximately 10%, and liver as much as 30% increased absorption.

Attenuation and energy absorption coefficients, stopping and angular scattering powers have been tabulated for all of the 80 tissues and organs and these high absorption values with respect to muscle, have not been recorded.

The differences appear to be due to the interpretation of the 1959 data. In the original ICRP document, tables of elemental concentrations (in μg/g wet tissue) for 44 elements are given from silver (Ag) through to Zirconium (Zr) omitting, among others, the elements carbon, hydrogen, nitrogen and oxygen. The ICRU

calculations were made on a muscle based material having these trace elements. The new ICRP document includes the C, H, N, O group of elements and shows that each tissue or organ is composed of WATER + FAT + PROTEIN + TRACE ELEMENTS and not simply WATER (or MUSCLE) + TRACE ELEMENTS as ICRU reasoned. The result of this is that the coefficients are much lower than previously reported because of the reduction caused by the fat and protein components.

The calculated values of mass energy absorption coefficient ratios, for a few tissues and organs quoted in the new Reference Man document, compared to muscle, are shown in FIGURE 5.1. The low absorption ratios for thyroid, liver and spleen are illustrated in the figure.

The new ICRP document stimulated the production of skin, liver and thyroid substitutes and should pave the way for the simulation of many more tissues once the numerical discrepancies have been eliminated from the data.

The new substitutes, and their calculated radiation characteristics, will be discussed in the next two sections. The first of these will deal with the tissue and organ substitutes, namely MUSCLE, FAT, LUNG, BONE, SKIN, BREAST, LIVER and THYROID. The last section in this chapter will deal with 'miscellaneous' substitutes, in particular those for AIR and thermoluminescent dosimetry (TLD) systems. For reference

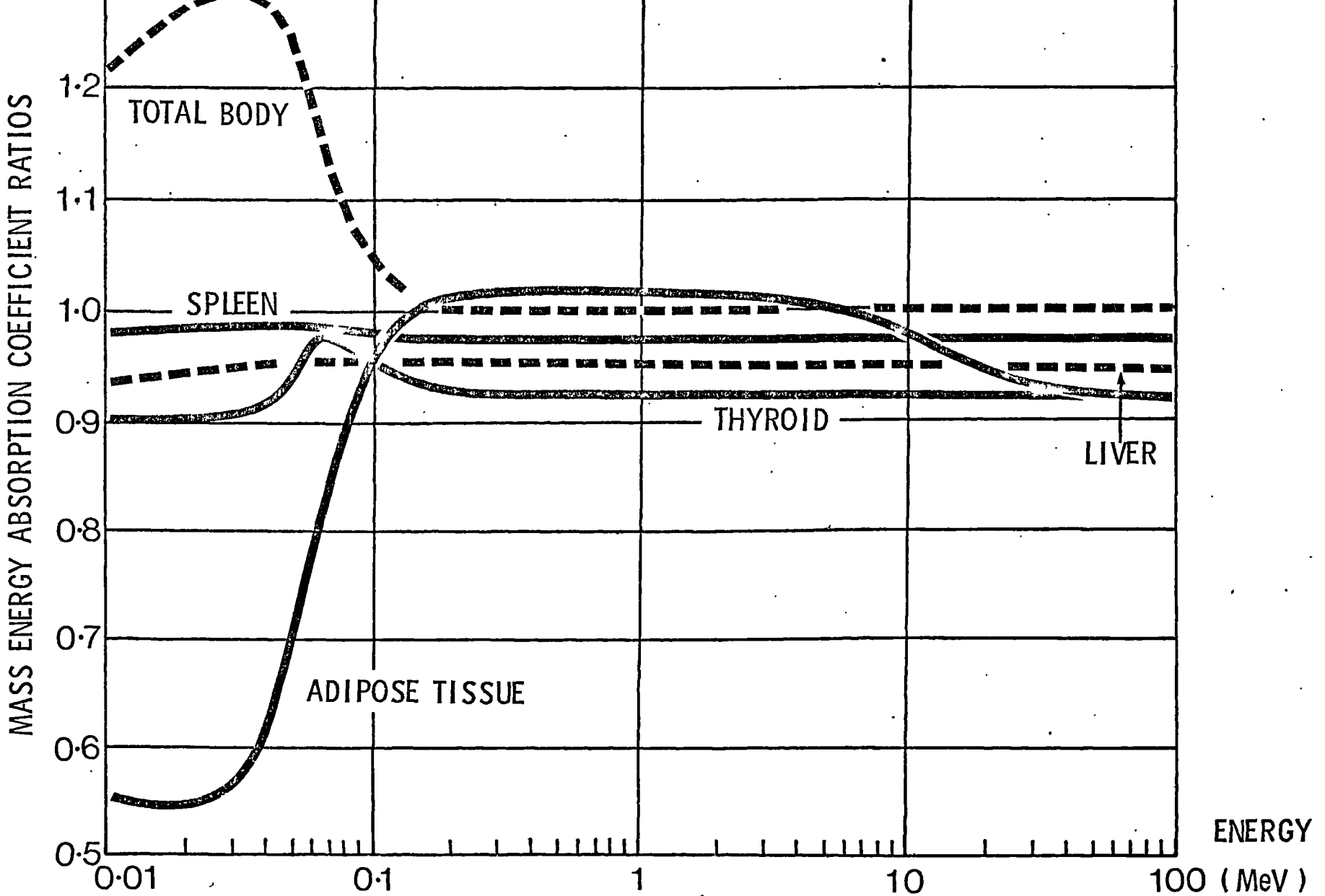

FIGURE 5.1 MASS ENERGY ABSORPTION COEFFICIENT RATIOS FOR A NUMBER OF BIOLOGICAL TISSUES COMPARED TO MUSCLE

purposes, the chemical compositions and specific gravities of all these simulated materials are grouped together in TABLE 5.1. The formula for red marrow was supplied by APSDEN (1973).

MATERIAL	CHEMICAL COMPOSITION (PERCENTAGE WEIGHTS)	S G
MUSCLE	H(10.2);C(12.3); N(3.5); O(72.893); Na(0.08); Mg(0.02); P(0.2); S(0.5); K(0.3); Ca(0.007)	1.0 – 1.05
FAT	H(12.21); C(76.08); O(11.71)	0.92
LUNG	AS MUSCLE	0.26 – 1.05
HARD BONE	H(3.39); C(15.5); N(3.97); O(44.1); Na(0.06); Mg(0.21); P(10.2); S(0.31); Ca(22.2)	1.85
INNER BONE	H(8.67); C(13.0); N(3.6); O(66.40); Na(0.08); Mg(0.06); P(2.43); S(0.46); K(0.23); Ca(4.96)	1.12
SKIN	H(10.0); C(22.7); N(4.62); O(61.5); Na(0.181); Mg(0.0058); P(0.0327); S(0.158); Cl(0.265); K(0.0846); Ca(0.015)	1.10
BREAST	H(11.70); C(38.04); O(50.26)	0.96
LIVER	H(10.0); C(14.4); N(2.83); O(66.7); Na(0.1); Mg(0.0172); P(0.261); S(0.289); Cl(0.2); K(0.25); Ca(0.005); Fe(0.0178)	1.07
THYROID	H(10.0); C(10.6); N(2.19); O(68.8); Na(0.219); Mg(0.01); P(0.075); Cl(0.169); K(0.119); Ca(0.035); I(0.06)	1.05
AIR	N(75.5); O(23.2); Ar(1.3)	–
RED MARROW	H(10.18); C(47.48); N(2.18); O(36.04); Na(0.008); Mg(0.0024); P(0.028); S(0.154); Cl(0.1); K(0.174);Ca(0.0004); Fe(0.01); Zn(0.009)	1.03

TABLE 5.1 THE CHEMICAL COMPOSITIONS AND SPECIFIC GRAVITIES OF THE MATERIALS SIMULATED IN THIS STUDY

5.3 TISSUE AND ORGAN SUBSTITUTES

(i) MUSCLE

The first action in the development of this, and all the other groups of substitutes, was to check the compound library to see whether any materials, without additives, were suitable. This normally produced a few interesting materials, useful over limited energy ranges, but rarely produced ideal systems. In the case of muscle a compound in powder form was found.

The next step was to decide upon the base materials. This choice was, of course, governed by the subsequent use of the material. The diversity of the applications for muscle substitutes was such that six base materials had to be considered. These bases were paraffin wax, polyethylene, TPX, nylon, water and epoxy resin formulations. This choice covered most, if not all, of the possible uses of muscle substitutes, capable of being cast in large or small volumes, poured, moulded and machined to any desired shape.

Once the most promising formulae had been selected from the tabulations produced by the ZEDIT programs, a complete listing of coefficients, powers and other important data was derived via the program TABLEC (APPENDIX 4).

TABLE 5.2 presents the fifteen best formulae that were derived as muscle substitutes. Here, the constituents are tabulated, together with the percentage weights bracketed after

MUSCLE SUBSTITUTES

No.	CONSITUENTS AND PERCENTAGE WEIGHTS	CODE
1	ALUMINIUM ACETYLACETONATE (100)	-
2	ALUMINIUM BUTOXIDE (100)	-
3	POLYETHYLENE (72.66); MAGNESIUM OXIDE (27.34)	MS1
4	TPX (76.26); MAGNESIUM OXIDE (23.74)	-
5	TPX (74.47); ALUMINIUM FLUORIDE (25.53)	-
6	PARAFFIN WAX (70.65); MAGNESIUM OXIDE (23.55); LITHIUM CARBONATE (5.80)	MS2
7	EPOXY CB1/4PMS (72.24); SODIUM FLUORIDE (27.76)	MS3
8	EPOXY CB1/4PMS (78.87); MAGNESIUM OXIDE (21.13)	MS4
9	EPOXY CB1/3PMS (84.87); P.V.C. (7.13); P.T.F.E. (8.00)	MS5
10	EPOXY CB2/4PMS (78.55); ALUMINIUM FLUORIDE (21.45)	-
11	EPOXY CB2/4PMS (80.14); MAGNESIUM OXIDE (19.86)	-
12	NYLON-6 (64.97); MAGNESIUM CARBONATE (35.03)	MS6
13	NYLON-6 (73.77); SODIUM FLUORIDE (26.23)	-
14	WATER (99.83); MANGANESE FLUORIDE (0.17)	-
15	WATER (88.60); SODIUM ACETATE (11.40)	-

TABLE 5.2 SOME NEW MUSCLE SUBSTITUTES

each compound. The formulae are numbered for easy reference and specific ones are also coded (MS1, MS2, etc). These are materials which have been manufactured and evaluated experimentally. Those which are uncoded have not been manufactured but, from the experience gained in this study, are considered to be practically viable.

Many of the points discussed in this section will be applicable to the other substitutes, so some space will be devoted to descriptions of these formulae and the philosophy behind their design. For convenience they will be discussed in the groupings indicated in the table.

The first two materials were found from a 'single material' search of the complete compound library magnetic tape and may have applications as bolus systems in Radiotherapy treatments. Variable packing, often encountered with powders, might prove troublesome with this type of product.

The next four substitutes were based on the polyolefin family, namely polyethylene $(C_2H_4)_n$ and TPX $(C_6H_{12})_n$, together with polypropylene $(C_3H_6)_n$ and, to a good approximation, paraffin wax $(C_{25}H_{52})$. It was found that a formula of the form CH_2 was adequate for the four materials, yielding essentially the same coefficients and powers. The specific gravities for these materials ranged from 0.83 to 0.92 which made for a very useful flexibility in terms of the density of the final product. Once a suitable system was derived for the CH_2 formula, based upon the

agreement between coefficients and powers, the specific gravity of the final product could be adjusted as required by choosing different bases. This was evident with numbers 3 and 4. Number 3, or MS1, was one of the first substitutes to be devised and was based on polyethylene, with subsequently a high specific gravity (1.15). Number 4 was an improved formulation derived with the latest versions of ZEDIT and used the lower density, TPX, resulting in a specific gravity of 1.02. Formula 6 was an attempt to improve the agreement of the coefficients and powers by including a third additive. The problem was still analysed as a two-component system, by using WAX + MgO, in the proportion (by weight) of 75:25, as the base material when lithium carbonate was indicated as the best additive.

Formulae 7-11 were epoxy resin based materials. Two resin systems were investigated:-

CB1: CIBA MY750, a liquid bisphenol A epoxy resin, is added to the low viscosity liquid amino-amide hardener, XD593, in the proportions (by weight) of 100:60. Theoretical formula: C(72.35); H(8.97); N(5.62); O(13.07).

CB2: CIBA MY750 is added to 2-ethylhexy glycidyl ether, EP-587 and a mixture of 2, 4, 4 - and 2, 2, 4 - trimethylhexane - 1, 6 - diamines, XD555, in the proportions (by weight) of 100:50:31. Theoretical formula: C(71.25); H(9.54); N(3.03); O(16.18).

The specific gravities of these resins were approximately 1.1, which resulted in unacceptably high density muscle substitutes. To reduce these values, low density 'microspheres', microfine powders made up of hollow, gas-filled, spheres, were added to the resins. Two types of microspheres were used:-

PMS: BXL phenolic microspheres (BJO 0930) of specific gravity ~0.13. Mean particle size: 50 μm. Theoretical formula: C(78.23); H(7.88); O(13.89).

SMS: 'SARAN' microspheres, a copolymer of vinylidene chloride and acrylonitrile developed by the Dow Chemical Co., of specific gravity ~0.03. Particle distribution: 10-100 μm. Theoretical formula: C(29.97); H(2.52); N(3.18); Cl(64.33).

Relatively small quantities of these microspheres added to the resins reduced the bulk specific gravities to below unity; for example, 4% (by weight) of the phenolic microspheres reduced the specific gravities to 0.85, while less than 1% of 'SARAN' was required to produce the same reduction.

In the tabulation the percentage of added microspheres are indicated immediately before the coding; 'CB1/4PMS' describes a mixture of resin and phenolic microspheres in the proportion (by weight) of 96% CB1 and 4% PMS.

In general, using the resin/microsphere mixture as the base material, only one added compound was required to produce useful

substitutes. An exception was MS5, a special system having two additives, one controlling viscosity and the other correcting the radiation characteristics. This procedure will be discussed in greater detail in the next chapter.

Formulae 12 and 13 use nylon-6 as a base and were designed as possible Radiotherapy bolus materials. A high density product was intentional in order that the effective density of the particulate form was close to that for muscle. This type of material, if manufactured in small, identical spheres should have smaller packing problems than the powders described earlier.

Although water has excellent properties as a muscle substitute, differences of some 4% occurs in the mass energy absorption coefficients. The ZEDIT programs were used in an attempt to improve this divergence by the addition of suitable compounds. Unfortunately, a number of the best additives produced by the programs giving coefficient and power agreement within 1%, could not be used because of their insolubility in water. Two acceptable materials were located and are tabulated as numbers 14 and 15. Formula 14, due to the extremely small quantity of material added and the corresponding problems of uniform dispersion, probably has limited applications.

As most of the substitutes described in this chapter were categorised as class A materials with coefficient or power errors below 5%, a tabulation technique is used to illustrate the

variations in the relevant data. TABLE 5.3 shows the ratios, between the fifteen muscle substitutes and muscle, of mass attenuation and energy absorption coefficients, electron mass stopping and angular scattering powers at three energies, 10 keV, 1 MeV and 100 MeV. For the coefficients, the ratio indicating the largest error in the range 10-40 keV is quoted if the ratios peak in this range. An inspection of the complete curves of coefficient and power ratios in Chapter 2, will show that this method effectively describes the response of the substitutes, as the maximum errors occur at low and high energies, while the 1 MeV ratios characterise the magnitudes of the errors in the broad medium energy region. This concise method of display is useful if specific characteristics are required for a definite application. The last column gives the calculated specific gravity of the substitute.

It can be seen from the table that the errors are generally low, and frequently have the CLASS A category for either photons or electrons.

No.	ATTENUATION RATIOS			ABSORPTION RATIOS			STOPPING POWER RATIOS			ANG. SCATTERING RATIOS			S.G.
	10 keV (or max)	1 MeV	100 MeV	10 keV (or max)	1 MeV	100 MeV	10 keV	1 MeV	100 MeV	10 keV	1 MeV	100 MeV	
1	0.99	0.96	0.96	0.99	0.96	0.97	0.95	0.96	0.94	0.96	0.96	0.96	1.27
2	1.05	1.00	0.95	1.03	1.00	0.96	1.01	1.01	0.97	0.93	0.93	0.93	1.02
3	1.07	1.00	0.96	1.09	1.00	0.96	1.00	1.00	0.97	0.94	0.94	0.94	1.15
4	0.96	1.01	0.94	0.96	1.01	0.95	1.01	1.01	0.97	0.92	0.92	0.92	1.02
5	0.97	0.99	0.93	0.97	0.99	0.95	0.99	0.99	0.96	0.92	0.91	0.91	1.01
6	0.98	1.00	0.94	0.98	1.00	0.95	1.00	1.00	0.96	0.93	0.93	0.93	1.15
7	1.01	0.95	0.97	1.01	0.95	0.97	0.93	0.93	0.91	0.97	0.97	0.97	1.04
8	0.98	0.97	0.96	1.02	0.97	0.97	0.95	0.96	0.95	0.96	0.96	0.96	1.00
9	1.03	0.98	0.93	1.06	0.98	0.94	0.97	0.97	0.94	0.91	0.91	0.91	1.00
10	0.98	0.97	0.95	0.98	0.97	0.96	0.95	0.96	0.94	0.95	0.95	0.95	1.00
11	0.97	0.98	0.96	0.97	0.98	0.96	0.96	0.97	0.95	0.95	0.95	0.95	1.00
12	0.98	0.96	0.97	0.98	0.96	0.98	0.95	0.95	0.92	0.97	0.97	0.97	1.44
13	1.00	0.96	0.97	1.00	0.96	0.97	0.94	0.95	0.95	0.97	0.97	0.97	1.32
14	1.01	1.01	1.02	1.01	1.00	1.01	1.01	1.01	1.02	1.02	1.02	1.02	1.00
15	1.03	1.00	1.02	1.03	1.00	1.01	1.00	1.00	1.01	1.02	1.03	1.03	1.04

TABLE 5.3 COEFFICIENT RATIOS, POWER RATIOS AND SPECIFIC GRAVITIES OF THE NEW MUSCLE SUBSTITUTES

5.3(ii) FAT

Fat, which makes up some 19%, by weight, of the total human body (TIPTON, 1970), has been rather neglected with respect to simulation. In this study twelve fat substitutes have been formulated and are described in TABLE 5.4 and the corresponding calculated coefficient and power ratios are shown in TABLE 5.5. The coding for manufactured substitutes is 'FT' (i.e. FT1, FT2, etc).

The first five materials all have useful characteristics without the addition of any corrective compound. Number 1 is a copolymer of ethylene and vinyl acetate, called 'EVA'. When added in the correct proportions, the coefficients and powers differ by only a maximum of 2% compared to those for fat, over the entire energy range. EVA-28 is the commercial grade which corresponds to these results. The specific gravity of EVA-28 is higher than required at 0.95. Formulae 2 and 3 are powders while 4 and 5 are commercially available polymers. These four materials are within 1% of fat, except for the high specific gravities of the polymers. (The specific gravities of the powders were not readily available in the literature).

TPX, with its low mass density, is ideal as a base for fat substitutes, and formulae 6-9 were based on this material. Maximum errors are generally below 2%; formula 9 is exceptional as it had exactly the same coefficients and powers as fat.

FAT SUBSTITUTES

No.	CONSITUENTS AND PERCENTAGE WEIGHTS	CODE
1	EVA-28 (100)	FT2
2	LITHIUM MYRISTATE (100)	-
3	LITHIUM PALMITATE (100)	-
4	NYLON-11 (100)	-
5	NYLON-12 (100)	-
6	TPX (81,42); LITHIUM CARBONATE (18.58)	FT1
7	TPX (79.68); LITHIUM CARBONATE (20.32)	-
8	TPX (95.87); SODIUM FLUORIDE (4.13)	FT3
9	TPX (72.66); ACETYLUREA (27.34)	-
10	EPOXY CB1/2PMS (70.63); TPX (29.37)	FT4
11	EPOXY CB1/0.5SMS (70.63); TPX (29.37)	FT5
12	EPOXY CB1/2PMS (45); TPX (55)	FT6

TABLE 5.4 SOME NEW FAT SUBSTITUTES

No.	ATTENUATION RATIOS			ABSORPTION RATIOS			STOPPING POWER RATIOS			ANG. SCATTERING RATIOS			S.G.
	10 keV	1 MeV	100 MeV	10 keV (or max)	1 MeV	100 MeV	10 keV	1 MeV	100 MeV	10 keV	1 MeV	100 MeV	
1	0.98	1.00	1.00	0.98	1.00	1.00	1.00	1.00	1.00	1.00	1.00	1.00	0.95
2	1.01	0.99	0.99	1.01	0.99	0.99	0.99	0.99	0.99	0.99	0.99	0.99	-
3	0.99	0.99	0.99	0.99	0.99	0.99	1.00	0.99	0.99	0.99	0.99	0.99	-
4	1.01	0.99	1.00	1.01	0.99	1.00	0.99	0.99	1.00	1.01	1.01	1.01	1.04
5	0.99	1.00	1.00	0.99	1.00	1.00	0.99	0.99	1.00	1.00	1.00	1.00	1.02
6	0.98	0.99	0.99	0.98	0.99	0.99	0.99	0.99	0.99	0.98	0.98	0.98	0.95
7	1.00	0.99	0.99	1.00	0.99	0.99	0.99	0.99	0.99	0.99	0.99	0.99	0.96
8	0.99	1.01	0.99	0.98	1.01	0.99	1.02	1.02	1.00	0.98	0.98	0.98	0.86
9	1.00	1.00	1.00	1.00	1.00	1.00	1.00	1.00	1.00	1.00	1.00	1.00	-
10	1.00	0.99	1.00	1.00	0.99	1.00	0.98	0.98	0.99	1.01	1.01	1.01	0.92
11	1.00	0.99	1.00	1.00	0.99	1.00	0.98	0.98	0.99	1.01	1.01	1.01	0.92
12	0.93	1.00	0.99	0.92	1.00	0.99	1.00	1.00	0.99	0.99	0.99	0.99	0.89

TABLE 5.5 THE COEFFICIENT RATIOS, POWER RATIOS AND SPECIFIC GRAVITIES OF THE NEW FAT SUBSTITUTES

The last three substitutes (10-12) are epoxy resin based, with TPX as additives. Number 12 was a special formulation made after some low energy photon attenuation measurements had indicated that the theoretical formula of the resin might have a small, but detectable, error.

Although, admittedly, fat is a relatively simple material to simulate, these results illustrate the potential of the new selection procedures. Ignoring number 12, which was not evolved through the selection procedures, the largest coefficient and power error for eleven materials is 2% while many are within 1% or even less of the real values.

5.3(iii) LUNG

It was shown earlier that existing lung substitutes are very poor, when for photons no class A, or even class B materials were evident from a search of the literature. Two systems were analysed, one based on polyurethane foams and the other on epoxy resin/microsphere syntactic foams. Both materials present manufacturing problems (described in detail in the next chapter) when the low density substitutes are required. For polyurethanes, lung specific gravities of 0.26 fall between the low values for flexible foams (sg :~0.03) and the relatively high values for rigid foams (sg :~0.5). Fortunately I.C.I. were able to suggest a semi-rigid material which proved to be quite useful. With mixtures of epoxy resin and microspheres, the problem was finding a grade of microspheres with the distribution of particle size such that large quantities of spheres may be added to reduce the density to the levels required. Specific gravities down to 0.5-0.6 were feasible with the phenolic microspheres quoted earlier.

The polyurethane system is described below.

PU1: I.C.I. ACTIVATOR HM 10, a stable blend of catalysts, surfactants, foam stabilisers, polyols and water, is added to a mixture of DALTOCEL SF, a cross-linked polyester, and SUPRASEC DN, a diphenylmethane diisocyanate composition. The proportions, by weight, of DALTOCEL SF, SUPRASEC DN and ACTIVATOR HM 10, were 100 : 85 : 40. Theoretical formula: C(60); H(7); N(5); O(28).

Due to the complexity of this composition, only the approximate theoretical formula quoted was available.

Three formulations based on polyurethane foams and two based on the epoxy resin/microspheres are described in TABLE 5.6, together with their calculated coefficient and power ratios in TABLE 5.7. The manufactured materials are coded 'LN'.

The ratios given in TABLE 5.7 show that the agreement between the substitutes and lung tissue is extremely good, although it must be borne in mind that errors could be introduced in the polyurethane data if the chemical formula differs appreciably from the one quoted.

The specific gravities for the polyurethane based substitutes are measured values and not theoretical ones. Measured values had to be given because the foams were not allowed to rise freely but were contained within aluminium moulds and forced to 'over-pack' to achieve the required densities.

LUNG SUBSTITUTES

No.	CONSTITUENTS AND PERCENTAGE WEIGHTS	CODE
1	PU1 (85.73); ALUMINIUM OXIDE (14.27)	LN1
2	PU1 (68.89); MAGNESIUM CARBONATE (31.11)	-
3	PU1 (83.13); MAGNESIUM OXIDE (16.87)	-
4	EPOXY CB2/16.2 PMS (78.48); ALUMINIUM FLUORIDE (21.52)	LN2
5	EPOXY CB2/16.2 PMS (91.89);P.V.C.(8.11)	LN3

TABLE 5.6 SOME NEW LUNG SUBSTITUTES

No.	ATTENUATION RATIOS			ABSORPTION RATIOS			STOPPING POWER RATIOS			ANG. SCATTERING RATIOS			S.G.
	10 keV (or max)	1 MeV	100 MeV	10 keV (or max)	1 MeV	100 MeV	10 keV	1 MeV	100 MeV	10 keV	1 MeV	100 MeV	
1	0.97	0.96	0.96	0.98	0.96	0.97	0.94	0.95	0.94	0.96	0.96	0.96	0.30
2	0.99	0.95	0.98	0.99	0.95	0.98	0.92	0.94	0.94	0.99	0.99	0.99	0.30
3	0.97	0.96	0.97	0.98	0.96	0.97	0.94	0.95	0.94	0.98	0.97	0.97	0.30
4	0.97	0.96	0.95	0.98	0.96	0.96	0.95	0.96	0.94	0.95	0.95	0.95	0.61
5	1.04	0.99	0.92	1.08	0.99	0.94	0.99	0.99	0.94	0.90	0.90	0.90	0.53

TABLE 5.7 THE COEFFICIENT RATIOS, POWER RATIOS AND SPECIFIC GRAVITIES OF THE NEW LUNG SUBSTITUTES

5.3(iv) BONE

A similar situation exists with bone substitutes as with lung, in that no class A materials have been apparently recorded in the literature for photon interactions.

TABLE 5.8 shows six formulae of hard bone substitutes (manufactured materials coded 'SB') and five inner bone formulations (coded 'IB'). The calculated coefficient and power ratios for the substitutes compared to the bone tissue are given in TABLE 5.9.

The base materials chosen for bone simulation were polyethylene, epoxy resins, acrylics, P.V.C. and water.

For hard bone, the epoxy resins (without microspheres) were ideal systems giving agreement within a few percent for most interactions. Due to the densities of resin and added materials, and their relative masses in the formulations, the resultant specific gravities were very close to the required value. Formula 4 was exceptionally good, having exactly the same coefficients and powers as hard bone. Formula 6 was a P.V.C. formulation manufactured by Plastic Coatings Ltd. The original formula, having acceptable radiation characteristics, could not be manufactured by the firm so the rather inferior form shown was produced as a compromise.

Formulae 7-11 were for inner bone. With the acrylic and epoxy based substitutes, agreement was again within a few percent. Water based formulae again suffered from the problem of insolubility of the best additives, although Number 11 appears promising.

BONE SUBSTITUTES

No.	CONSTITUENTS AND PERCENTAGE WEIGHTS	CODE
	(a) HARD BONE	
1	POLYETHYLENE (32.55); VINYLIDENE CHLORIDE POLYMER (67.45)	-
2	POLYETHYLENE (35.78); CALCIUM METASILICATE (64.22)	-
3	EPOXY CB1 (32.71); CALCIUM CARBONATE (67.29)	SB1
4	EPOXY CB1 (36.62); CALCIUM METASILICATE (63.38)	-
5	EPOXY CB2 (32.66); CALCIUM CARBONATE (67.34)	SB3
6	'PLASTISOL' P.V.C. (60); CALCIUM ALUMINATE (40)	SB2
	(b) INNER BONE	
7	EPOXY CB1 (74.50); P.V.C. (25.50)	IB1
8	ACRYLICS (84.96); HEXACHLOROETHANE (15.04)	-
9	ACRYLICS (75.92); P.V.C. (24.08)	IB2
10	WATER (83.0); SODIUM CHLORIDE (17.0)	
11	WATER (70.26); POTASSIUM SORBATE (29.74)	

TABLE 5.8 SOME NEW BONE SUBSTITUTES

No.	ATTENUATION RATIOS			ABSORPTION RATIOS			STOPPING POWER RATIOS			ANG. SCATTERING RATIOS			S.G.
	10 keV (or max)	1 MeV	100 MeV	10 keV (or max)	1 MeV	100 MeV	10 keV	1 MeV	100 MeV	10 keV	1 MeV	100 MeV	
1	1.02	1.01	1.00	1.06	1.01	1.00	1.01	1.01	1.03	1.00	1.00	1.00	1.31
2	1.00	1.02	0.99	1.00	1.02	0.99	1.03	1.02	1.01	0.99	0.99	0.99	1.55
3	1.00	1.00	0.97	1.02	1.00	0.98	1.01	1.00	0.98	0.96	0.96	0.96	1.90
4	1.00	1.00	1.00	1.00	1.00	1.00	1.00	1.00	1.00	1.00	1.00	1.00	1.82
5	1.01	1.00	0.97	1.02	1.00	0.98	1.01	1.00	0.98	0.97	0.96	0.96	1.82
6	0.83	1.00	0.95	0.83	1.01	0.97	1.01	1.01	0.98	0.94	0.94	0.94	1.73
7	1.04	0.99	0.95	1.05	0.99	0.96	0.99	0.99	0.96	0.93	0.93	0.93	1.15
8	0.99	0.98	0.96	1.03	0.98	0.97	0.97	0.98	0.96	0.96	0.96	0.96	-
9	0.98	0.99	0.94	1.02	0.99	0.95	0.98	0.98	0.95	0.93	0.93	0.93	1.21
10	1.06	1.00	1.04	1.10	1.00	1.03	0.99	1.00	1.03	1.05	1.06	1.05	1.10
11	1.01	1.01	1.00	1.01	1.01	1.00	1.01	1.01	1.00	1.00	1.00	1.00	1.09

TABLE 5.9 THE COEFFICIENT RATIOS, POWER RATIOS AND SPECIFIC GRAVITIES OF THE NEW BONE SUBSTITUTES

5.3(v) OTHER BIOLOGICAL TISSUES

TABLES 5.10-5.14 show the formulae and characteristics of materials devised to simulate skin,'breast tissue', liver and thyroid; the codes for manufactured substitutes were 'SK', 'BR', 'LV' and 'TH', respectively. Acrylic, epoxy resin and water based substitutes have been formulated, again with reasonable success. The tables are self-evident, but the formulae for 'breast tissue' requires some comment.

The breast series, coded 'BR' were devised for low energy photon mammography measurements. Formulae BR1 to BR6 were the results of an experimental investigation to find a formulation which would stand up to the severe restrictions laid down in the manufacturing requirements (chapter 6). Although the complete set of coefficient and power ratios are quoted (TABLE 5.12), the important values in this particular application were the photon attenuation and energy absorption coefficient ratios below 40 keV.

SKIN SUBSTITUTES

No.	CONSTITUENTS AND PERCENTAGE WEIGHTS	CODE
1	ACRYLICS (83.78); MAGNESIUM FLUORIDE (16.22)	-
2	ACRYLICS (56.79); P.T.F.E. (43.21)	-
3	EPOXY CB1/2PMS (82.98); ALUMINIUM FLUORIDE (17.02)	SK1
4	EPOXY CB1/2PMS (71.55); MAGNESIUM CARBONATE (28.45)	-
5	EPOXY CB1/2PMS (78.58); SODIUM FLUORIDE (21.42)	-

TABLE 5.10 SOME SKIN SUBSTITUTES

'BREAST TISSUE' SUBSTITUTES

No.	CONSTITUENTS AND PERCENTAGE WEIGHTS	CODE
1	EPOXY CB1/4PMS (70.14);P.T.F.E.(29.86)	BR1
2	EPOXY CB1/2PMS (96.36); P.V.C. (3.64)	BR2
3	EPOXY CB1/3PMS (85.86); P.V.C. (2.14); P.T.F.E. (12.00)	BR3
4	EPOXY CB1/1PMS (95.79); P.V.C. (3.71); P.T.F.E. (0.50)	BR4
5	EPOXY CB1/2PMS (92.89); P.V.C. (3.11); P.T.F.E. (4.00)	BR5
6	EPOXY CB1/3PMS (89.44); P.V.C. (2.56); P.T.F.E. (8.00)	BR6

TABLE 5.11 SOME 'BREAST TISSUE' SUBSTITUTES

No.	ATTENUATION RATIOS			ABSORPTION RATIOS			STOPPING POWER RATIOS			ANG. SCATTERING RATIOS			S.G.
	10 keV	1 MeV	100 MeV	10 keV (or max)	1 MeV	100 MeV	10 keV	1 MeV	100 MeV	10 keV	1 MeV	100 MeV	
SKIN													
1	1.05	0.97	0.99	1.05	0.97	0.99	0.95	0.96	0.96	0.99	1.00	0.99	-
2	1.03	0.94	0.99	1.04	0.94	0.99	0.90	0.92	0.94	1.01	1.01	1.01	1.45
3	0.98	0.97	0.96	0.99	0.97	0.97	0.96	0.96	0.95	0.96	0.96	0.96	1.08
4	0.98	0.97	0.98	1.02	0.97	0.98	0.95	0.96	0.95	0.98	0.98	0.98	1.19
5	1.02	0.97	0.97	1.02	0.97	0.98	0.95	0.95	0.95	0.98	0.98	0.98	1.11
BREAST													
1	0.96	0.94	0.98	1.03	0.94	0.98	0.91	0.93	0.94	1.00	1.00	1.00	1.03
2	0.98	0.97	0.95	1.06	0.97	0.96	0.97	0.97	0.95	0.95	0.95	0.95	0.97
3	0.98	0.96	0.97	1.03	0.96	0.97	0.94	0.95	0.95	0.97	0.97	0.97	0.98
4	1.03	0.97	0.95	1.07	0.97	0.96	0.96	0.97	0.95	0.95	0.95	0.95	0.99
5	1.02	0.97	0.96	1.05	0.97	0.97	0.96	0.96	0.95	0.96	0.95	0.95	0.99
6	0.98	0.97	0.96	1.03	0.96	0.97	0.95	0.96	0.95	0.96	0.96	0.96	0.96

TABLE 5.12 THE COEFFICIENT RATIOS, POWER RATIOS AND SPECIFIC GRAVITIES OF THE SKIN AND BREAST TISSUE SUBSTITUTES

LIVER AND THYROID SUBSTITUTES

No.	CONSTITUENTS AND PERCENTAGE WEIGHTS	CODE
	(a) LIVER	
1	EPOXY CB1/4PMS (84.47); ALUMINIUM OXIDE (15.53)	LV1
2	EPOXY CB1/4PMS (72.47); SODIUM CARBIDE (27.53)	-
3	WATER (60); LITHIUM NITRATE (40)	LV2
	(b) THYROID	
4	EPOXY CB1/3PMS (83.48); ALUMINIUM FLUORIDE (16.52)	-
5	EPOXY CB1/0.5SMS (79.48); SODIUM FLUORIDE (20.52)	TH1

TABLE 5.13 SOME LIVER AND THYROID SUBSTITUTES

No.	ATTENUATION RATIOS			ABSORPTION RATIOS			STOPPING POWER RATIOS			ANG. SCATTERING RATIOS			S.G.
	10 keV	1 MeV	100 MeV	10 keV (or max)	1 MeV	100 MeV	10 keV	1 MeV	100 MeV	10 keV	1 MeV	100 MeV	
LIVER													
1	0.97	1.02	0.99	0.98	1.02	1.01	0.96	0.96	0.94	0.99	0.98	0.98	0.97
2	1.01	1.01	1.00	1.00	1.01	1.01	0.94	0.94	0.94	1.01	1.00	1.00	0.97
3	1.02	1.01	1.06	1.02	1.01	1.05	0.95	0.95	0.97	1.07	1.08	1.08	1.30
THYROID													
1	1.03	1.04	1.01	0.98	1.04	1.03	0.95	0.95	0.93	1.01	1.01	1.01	0.96
2	1.03	1.04	1.03	0.99	1.04	1.04	0.94	0.95	0.93	1.02	1.02	1.02	0.99

TABLE 5.14 THE COEFFICIENT RATIOS, POWER RATIOS AND SPECIFIC GRAVITIES FOR THE LIVER AND THYROID SUBSTITUTES

5.4 MISCELLANEOUS MATERIALS

Two other groups of substitutes have been analysed, namely air substitutes and those based on the thermoluminescent phosphor, lithium borate.

The air substitutes are described in the same format as before, in TABLES 5.15 and 5.16, with the manufactured materials coded 'AR'. Numbers 1 and 2 are powders, formulae 3-8 are based on the polymer P.T.F.E. and the remainder on acrylics, bakelite and epoxy resin . No attempt was made to specify the electrical conduction properties of the products, although this could easily be achieved by including a fixed amount of carbon with the chosen base material.

P.T.F.E. is a particularly interesting base because it is composed of carbon and fluorine, whose atomic numbers conveniently straddle the important atomic numbers of the components of air - nitrogen and oxygen. As P.T.F.E. has the formula C_2F_4 , the fluorine contribution to the coefficients at low energies causes them to be more than 30% higher than those of air. The addition of a material containing predominantly lower atomic numbers should improve this situation. This is illustrated in formulae 3 and 4. Number 4 was shown by the ZEDIT programs to have errors ~10%, but it was thought that the material warranted some investigation. Number 3, or AR1, was found to be commercially available, with percentage weights close to those of formula 4.

AIR SUBSTITUTES

No.	CONSTITUENTS AND PERCENTAGE WEIGHTS	CODE
1	LITHIUM NITRATE (100)	-
2	OXALIC ACID (100)	-
3	P.T.F.E. (75); CARBON (25) (FLUON VP25)	AR1
4	P.T.F.E. (71.63); CARBON (28.37)	-
5	P.T.F.E. (58.45); ACETAMIDOQUINOLINE (41.55)	-
6	P.T.F.E. (59.43); ANTHRACENE (40.57)	-
7	P.T.F.E. (47.39); MELAMINE FORMALDEHYDE (52.61)	-
8	P.T.F.E. (59.16); NYLON-11 (40.84)	-
9	ACRYLICS (47.62); LITHIUM FLUORIDE (52.38)	-
10	BAKELITE (40.20); P.T.F.E. (59.80)	AR2
11	BAKELITE (67.59); MAGNESIUM CARBONATE (32.41)	-
12	EPOXY CB1 (56.87); SODIUM METABORATE (43.13)	-

TABLE 5.15 SOME NEW AIR SUBSTITUTES

No.	ATTENUATION RATIOS			ABSORPTION RATIOS			STOPPING POWER RATIOS			ANG. SCATTERING RATIOS			S.G.
	10 keV (or max)	1 MeV	100 MeV	10 keV (or max)	1 MeV	100 MeV	10 keV	1 MeV	100 MeV	10 keV	1 MeV	100 MeV	
1	0.95	0.99	0.99	0.93	0.99	0.98	1.00	0.99	0.99	0.99	0.99	0.99	2.38
2	0.94	1.02	1.00	0.92	1.02	1.00	1.04	1.03	1.02	1.00	1.00	1.00	1.65
3	1.14	0.97	1.00	1.16	0.97	0.99	0.95	0.96	0.99	1.01	1.01	1.01	2.10
4	1.11	0.97	1.00	1.12	0.97	0.99	0.95	0.96	0.98	1.00	1.00	1.00	2.01
5	1.02	1.00	0.98	1.03	1.00	0.98	1.00	1.00	1.00	0.97	0.97	0.97	-
6	0.98	1.00	0.97	0.95	1.00	0.97	1.00	1.00	0.99	0.96	0.96	0.96	1.67
7	1.01	1.00	0.99	0.97	1.00	0.99	1.00	1.00	1.00	0.98	0.98	0.98	1.72
8	1.01	1.02	0.98	0.97	1.02	0.98	1.04	1.03	1.02	0.96	0.96	0.96	1.48
9	0.95	1.00	0.93	0.92	1.00	0.94	1.03	1.01	0.97	0.91	0.90	0.90	1.65
10	1.04	1.00	0.98	1.05	1.00	0.98	1.00	1.00	1.00	0.98	0.98	0.98	1.65
11	1.03	1.04	0.97	1.00	1.04	0.98	1.06	1.05	1.02	0.95	0.95	0.95	1.54
12	1.03	1.04	0.97	1.03	1.04	0.98	1.07	1.05	1.02	0.95	0.95	0.95	1.44

TABLE 5.16 THE COEFFICIENT RATIOS, POWER RATIOS AND SPECIFIC GRAVITIES OF THE NEW AIR SUBSTITUTES

The use of these materials in ionization chambers requires ideally that the substitute be made up of elements having similar atomic numbers as those found in air, in order that the electron emission is comparable (SPIERS, 1972). For this reason the choice of additives was further restricted.

Another application of the selection procedures has been in the formulation of TLD based mixtures (coded 'TL') of powders which have radiation characteristics corresponding to muscle, bone, liver and red marrow (TABLE 5.17). These formulations have greatly improved coefficient and power ratios (TABLE 5.18) over the basic material and should improve the accuracy of dosimetric investigations. An example of this improvement would be low energy photon measurements, when the volumes of powder normally employed could seriously distort the photon and electron energy spectra from that distribution which a perfect equivalent powder would produce.

Formulae 3 and 4 are bone substitutes and, together with formula 6, a formulation simulating red marrow, could be used to derive information of interest in trabecular bone dosimetry.

The substitutes introduced in this chapter have, from their calculated properties, advantages over existing substitutes. They have well defined and more precise radiation characteristics for photons and electrons, are diverse in composition and, as will be seen later, are reasonably easy to manufacture. In some cases the

No.	TLD FORMULATIONS		SIMULATED MATERIAL	CODE
	CONSTITUENTS AND PERCENTAGE WEIGHTS			
	LITHIUM BORATE + 0.1% Mn	ADDED MATERIAL		
1	96.19	ALUMINIUM (3.81)	MUSCLE	TL1
2	58.17	P.T.F.E. (41.83)	MUSCLE	TL2
3	50.66	CALCIUM FLUORIDE (49.34)	BONE	-
4	36.14	CALCIUM SULPHATE (63.86)	BONE	-
5	98.30	CALCIUM CARBONATE (1.70)	LIVER	TL3
6	77.26	BORON (22.74)	RED MARROW	-

TABLE 5.17 TLD (LITHIUM BORATE) FORMULATIONS

No.	ATTENUATION RATIOS			ABSORPTION RATIOS			STOPPING POWER RATIOS			ANG. SCATTERING RATIOS		
	10 keV	1 MeV	100 MeV	10 keV (or max)	1 MeV	100 MeV	10 keV	1 MeV	100 MeV	10 keV	1 MeV	100 MeV
1	0.98	0.88	0.94	0.98	0.88	0.94	0.85	0.86	0.87	0.96	0.96	0.96
2	1.02	0.88	0.97	1.03	0.88	0.96	0.83	0.85	0.88	1.00	1.00	1.00
3	0.98	0.94	0.97	0.99	0.94	0.97	0.92	0.93	0.93	0.97	0.97	0.97
4	1.01	0.96	1.01	1.01	0.96	1.00	0.94	0.95	0.96	1.02	1.02	1.02
5	1.00	0.93	0.98	0.99	0.92	0.99	0.85	0.86	0.86	1.01	1.01	1.01
6	0.99	0.90	0.98	1.00	0.90	0.98	0.83	0.85	0.87	1.01	1.01	1.01

TABLE 5.18 THE COEFFICIENT AND POWER RATIOS FOR THE TLD FORMULATIONS

new materials simulate tissues which have been poorly served in the past and, in a few instances, break new ground. The epoxy resin based substitutes, in particular MS5, FT5, LN3, SB3, IB1 and BR6, have proved in practice to be extremely useful in many dosimetric situations.

After the manufacturing techniques and quality control tests have been described in the next chapter, the measured radiation properties of selected materials will be compared with these calculated results.

CHAPTER 6

THE MANUFACTURING AND QUALITY TESTING TECHNIQUES DEVELOPED FOR THE NEW SUBSTITUTES

In this chapter the various methods evolved for manufacturing the new substitutes will be described, together with the physical investigations that were used for quality testing each batch of materials. The chapter falls naturally into two sections dealing respectively with the manufacturing and the physical testing procedures.

6.1 THE MANUFACTURING TECHNIQUES

It was stated earlier that the trend throughout the study was away from the polymers which required elaborate manufacturing procedures, to the more amenable epoxy resin systems. From the tables of new materials introduced in the last chapter, it was evident that these resins were extensively applied in many simulation studies. Before the practical experience in this aspect of the study is evaluated, wax and polyolefin based substitutes will be considered.

6.1(i) WAX

Historically, this material has found universal acceptance, either on its own, or, with additives that were claimed to improve the radiation properties.

The melting point of paraffin wax is 49-63°C, so it is a fairly simple task to either mould, or cast, a pure wax sample. Problems arise when additives (called 'fillers') are introduced as powders, into the molten wax. If the time taken for the material to solidify is prolonged after the fillers are added, then the wax and fillers will separate according to their relative mass densities and the particle size of the powder.

The only method of eliminating this effect is to stir the mixture continuously until the solidification process is almost complete, so that the increasing viscosity results in the particulate filler being 'held' in position. This technique unfortunately produces a large quantity of trapped air within the sample which is difficult to remove.

A possible solution to some of these problems would be to stir, or tumble, the molten mixture of wax and filler within an evacuated chamber, allowing the material to cool and partially solidify. Transfering the mixture to moulds or trays is always difficult, whatever method is adopted. Pouring necessitates a low viscosity mixture with subsequent settling-out defects, while the use of a spatula with high viscosity mixtures introduces large quantities of

trapped air into the final product.

Some of the defects which may result from these procedures are illustrated in the Xeroradiograph shown in FIGURE 6.1. A breast shaped phantom was manufactured using MS2, a mixture of paraffin wax and finely ground powders of magnesium oxide and lithium carbonate. Extreme care was taken to exclude air and to transfer the material into a silicon rubber mould, by pouring at the last possible moment before the process of solidification inhibited the flow. The solidified phantom was xeroradiographed at 50 kV on the Siemens 'Mammomat' X-ray machine at the Royal Marsden Hospital, London. This method was chosen for its fine resolution and corresponding ability to demonstrate small differences in composition. Due to the reversal process produced during the xeroradiographic technique, the light areas are due to trapped air and the dark areas to absorption in conglomerates of filler. It is clear from these results that, despite the extreme care taken during its manufacture, the breast phantom shown in the figure is far from homogeneous.

A further characteristic which leads to poor results is the rapid shrinkage as crystallisation occurs during cooling. Differential cooling in wax phantoms of large volume have been purported to produce such enormous stresses that explosions have frequently occurred (STACEY, 1973).

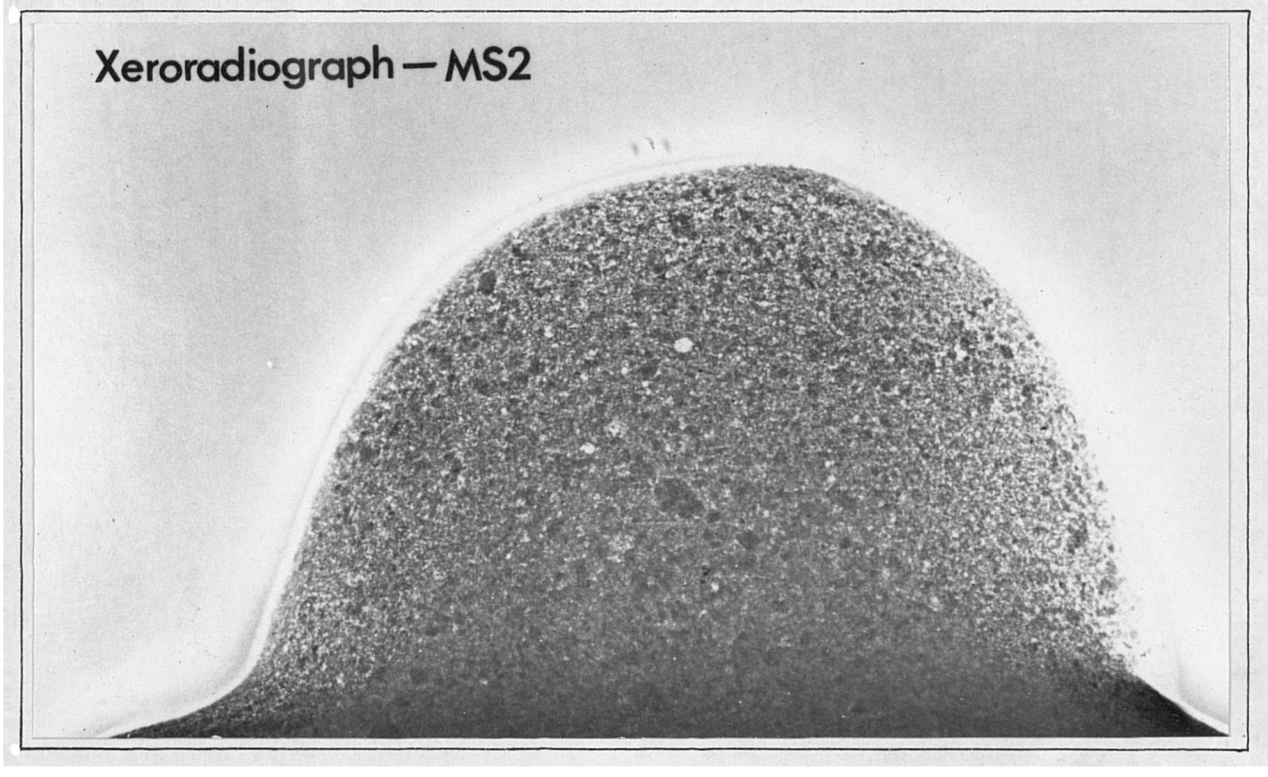

FIGURE 6.1 A XERORADIOGRAPH OF A BREAST PHANTOM MANUFACTURED FROM THE WAX BASED SUBSTITUTE MS2

Once the material has been manipulated into the desired shape, there still exist severe handling problems. Wax phantoms, although cheap, are fragile and often brittle, they will warp and often distort if handled excessively.

In short, although it is a simple procedure to heat a volume of wax, add a filler and pour the mixture into a mould; it is exceedingly difficult to produce an air-free, homogeneous sample, which maintains its shape with continued use.

6.1(ii) POLYOLEFINS

Some of the problems inherent with wax based substitutes were solved in 1949 when JONES AND RAINE introduced MIX D. Realizing that paraffin wax and polyethylene were similar as regards photon attenuation, a mixture of these two materials was used as the base and magnesium oxide and titanium dioxide added to improve the radiation properties. The authors stated in their paper that the mixture 'ensured that when molten the wax pours easily and is yet viscous enough to keep the Mg O - TiO_2 filler in homogeneous suspension'.

MIX D was an improvement, but the disadvantages of samples warping, shrinking and shattering easily still existed. Added to this, inspection of typical samples of MIX D has shown poor dispersion of filler, when,even by visual observation, large masses of filler are clearly visible.

An obvious solution is to eliminate wax completely, and to base the substitute on either polyethylene, TPX or polypropylene. Theoretically, a mixture such as the German M3, based on one of these polyolefins instead of wax, should be extremely good. TPX offers the most advantages due to its superb machining properties, especially compared to polyethylene, and its low specific gravity that would result in a substitute (TPX + fillers) having a bulk density approaching unity.

These polymers may be processed by a variety of techniques (BRYDSON, 1970). With COMPRESSION MOULDING the polymer is heated in a mould, compressed to shape and cooled. This method is often used to produce large, strain-free objects. With INJECTION MOULDING, the polymer is melted and injected, often under great pressure, into a mould which is at a temperature below the freezing point of the polymer so that the latter can solidify. Because of the tendency for crystallisation to occur, high shrinkage may take place. Another method is EXTRUSION MOULDING, when the molten polymer it extruded into a mould and left to set.

When fillers are added to a polymer, frequently a two-roll mill is used. In this equipment the powdered polymers and fillers, after being thoroughly mixed in 'powder blenders', are fed on to two heated rotating cylinders. The polymer melts and by suitable temperature controls, a leathery hide is formed round one of the rolls. On cooling, the hide is removed, pulverised and moulded by one of the above processes into the desired shape. A mill specially designed to produce good particle dispersion and uniformity, essential in the manufacture of substitutes, was described by SHONKA et al.(1958) in connection with their work on conducting plastics.

At the temperatures required to melt these polymers, oxidation is likely to occur unless air is excluded from the molten material,

or special antioxidants are added. The range of processing temperatures are from 150°C for polyethylene, 210-250°C for polypropylene to 270°C with TPX. The high temperatures required for TPX present problems when roll mills constructed of stainless steel are employed.

Unfortunately the equipment outlined here is extremely costly and rarely found in Hospital environments. Even in some University Departments specialising in Polymer Research, only the plastics requiring low processing temperatures can be manipulated and consequently TPX cannot be considered. (This latter comment similarly applies to P.T.F.E., which is normally sintered at temperatures ~370°C).

Large commercial organisations can, of course, perform all of these functions. I.C.I. has, without any charges being made, produced a number of the polyolefin based substitutes, including the TPX materials FT1 and FT3. All of the I.C.I. manufactured substitutes had excellent dispersions of filler. Some smaller organisations were able to produce these materials, but the cost was often prohibitive.

The advantages of using TPX based substitutes are numerous. Excellent samples may be made having good filler dispersion, small shrinkage, are easy to machine and clean to handle and have good radiation characteristics. The disadvantages appear to revolve around the problems of manufacture and the technical difficulties when large, air-free sections are required.

6.1(iii) EPOXY RESINS

The problem of producing substitutes in a conventional hospital laboratory was solved by the use of epoxy resin systems. Using these resins it was possible to manufacture both small and large objects, completely air-free with good dispersion of fillers and small shrinkage on curing.

The apparatus used for their manufacture is shown in FIGURE 6.2(a).

Accurately measured quantities of liquid resin and hardener, microspheres (if required) and filler were poured into the reaction vessel (500 ml) and the specially ground lid attached. A twin bladed rotor was passed through the central stirrer gland and connected to the variable speed electric stirrer. The components were then thoroughly mixed by ensuring that the blades of the rotor were deep in the fluid. Once the desired degree of mixing had been achieved, the blades were raised to just below the top surface of the fluid. While still stirring the mixture, the system was evacuated. The pressure reduction caused the fluid to rise in the vessel, but the rotating blades soon broke the resulting foam, allowing the trapped gases to escape. After approximately 3-5 minutes, depending upon the viscosity of the mixture, the foam would collapse and contract. At this point the rotor was lowered into its previous position deep in the fluid and the mixing and evacuation continued for 20 minutes. At the end of this time,

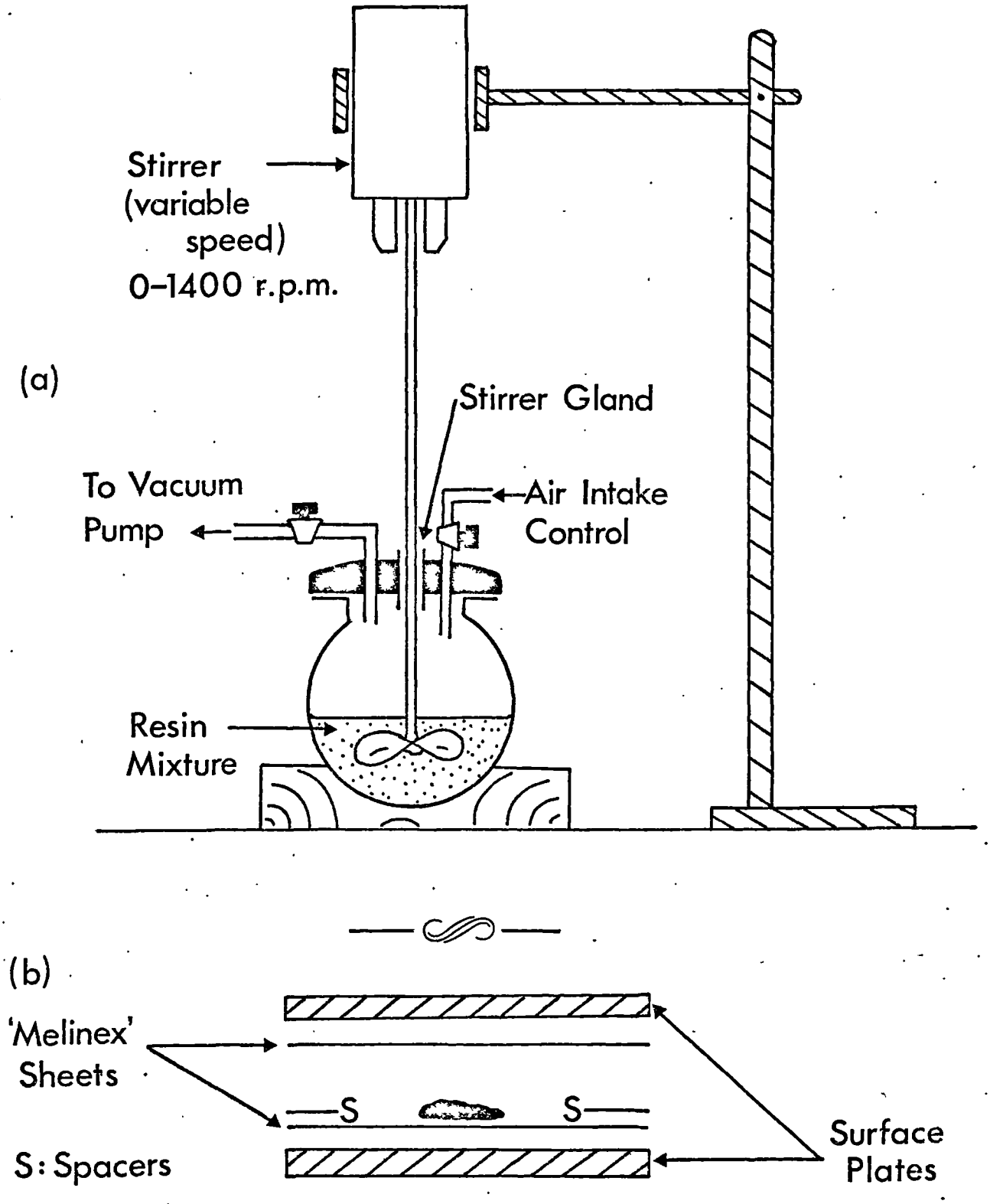

FIGURE 6.2 (a) APPARATUS FOR MANUFACTURING EPOXY RESIN BASED SUBSTITUTES

(b) TECHNIQUE USED FOR PRODUCING EPOXY RESINS IN SHEET FORM

the mixture was generally air-free and could be poured into moulds or trays. The samples were left at room temperature for 15-20 hours to complete the hardening process.

The problem of filler separation was still present with these systems but could virtually be eliminated by a suitable adjustment of the viscosity of the mixture. If a small loading of filler (that is, below 5%, by weight) had to be added, it was found that the viscosity of the resin ($\sim 25\ Ns/m^2$) was not great enough to hold the particles in position. The situation could be improved to a small extent by using finely ground powdered fillers, thus increasing the surface area presented to the resin. Another, and more useful approach was to stir and evacuate the mixture as outlined previously, and then to delay the pouring for approximately two hours, so that the hardening reaction increased the viscosity. Stirring during this waiting period was essential to inhibit filler separation. Normally low speed agitation was adequate throughout this period, ending with the normal high speed stirring immediately before the pouring stage.

The combined use of delayed pouring and finely ground additives proved extremely successful when small quantities of fillers were used.

A factor which limited the application of these mixtures was the production of heat during the chemical reaction, called the exotherm.

When these masses, greater than 1 kg were cast, the exotherm was so excessive with unfilled resins or those containing small quantities of filler, that the samples were often distorted and discoloured and occasionally shattered. It must be stressed that this occurred with quantities of filler below 5%, by weight (e.g. BR2).

With larger amounts of filler the problem was the efficient removal of air from a high viscosity, or sometimes dough-like, mixture (e.g. SB1) . In these cases little filler separation and a reduced exotherm occurred. To effectively extract the air it was found that a large reaction vessel (5 litres) gave acceptable results as it produced a large surface area from which gas could be removed. In addition an increased evacuation time (30-60 minutes) assisted the process. Particle size was also an important consideration, as a finely ground powder would increase the viscosity more than the same mass of a coarse powder.

Substitutes BR2 with only 3.64% filler and SB1 with 67.29% illustrate the extremes of the additive proportions, while most formulations were in the range 20-30% which yielded manageable mixtures. The addition of microspheres as density correction agents produced increased viscosities due to their small particle size. This was particularly true with 'Saran' microspheres which, in quantities of only a few percent produced unworkable systems. Some chemical reaction between 'Saran' and the epoxy resin was also recorded, leading to higher density final products than theoretically predicted.

An attempt to produce a 'perfect' epoxy resin formulation, having a viscosity large enough to hold the filler in position, but still be able to allow gas to escape, resulted in the series BR2 to BR6. P.T.F.E., which was available as a fine powder (mean particle diameter - 5 μm), was used as the principal thickening agent. Powdered P.V.C. was employed for correcting the coefficients and powers, while the microspheres corrected for mass density and also produced some increase in viscosity. The relative proportions arrived at finally in BR6 produced a system that could be used to cast large, air-free, homogeneous phantoms.

At this stage it would be appropriate to consider the methods of manufacturing different types of test objects. Thin films of epoxy based substitutes were produced when a series of low energy photon attenuation measurements were performed. A number of different techniques were tested, including sandwiching the material in the liquid phase between horizontal plates. Plates constructed from glass, aluminium, P.T.F.E., perspex, 'melinex' and polystyrene were evaluated. The method finally adopted is shown in FIGURE 6.2(b). An accurately ground surface plate was covered with a sheet of 'melinex' and four spacers of the same thickness as the required sample, were placed around the periphery. A small quantity of the stirred and de-gassed resin was poured on to the centre of the 'melinex'. Another sheet of 'melinex' was used to cover the lower plate and a second surface plate placed on the top. By applying

suitable pressure the mixture was squashed between the plates into the required thickness. The whole system was left undisturbed until the resin hardened, when the top plate was removed and the 'melinex' easily peeled from the sample. Films down to 0.1 mm have been manufactured by this method.

Certain materials were found to have excellent release properties, notably polyethylene, 'melinex', P.T.F.E., polystyrene and silicon rubber. The release of the hardened resins from perspex, glass and aluminium was poor.

For large resin based samples polystyrene petri dishes and trays were used to cast either discs or sheets up to a few centimetres thick. For body sections silicon rubber moulds have proved to be extremely useful and, with care, may be re-used many times. A suitable product was found to be 'SILASTIC', sold as a low viscosity solution (3110 R.T.V) and a thixotropic gel (504 R.T.V.). Large quantities of heat may be evolved when in this type of application only small amounts of fillers are added.

These procedures have been found to be capable of producing high quality samples during some eighteen months of investigation and are well within the scope of most Hospital Physics Departments.

6.1(iv) POLYURETHANE FOAMS

Polyurethane foams were used in the manufacture of low density lung substitutes (specific gravity - 0.3). A semi-rigid formulation was specified by I.C.I. (5.3(iii)) which could be manufactured at this density level.

The principal constituents of the foam, DALTOCEL SF, SUPRASEC DN and the filler were thoroughly mixed together in the required proportions and de-gassed. The ACTIVATOR HM 10 was then added and stirred quickly into the mixture. As the chemical foaming action started 10-15 seconds after the activator was added, the constituents were mixed in the moulding container. Strong aluminium moulds were necessary because to attain the desired density the foam, normally a much lower density, was contained and forced to overpack, which consequently caused considerable pressures to develop. To withstand these forces, the cylindrical moulds were capped, top and bottom, by brass plates, and clamped in a mechanical press. Wax treatment of the metal surfaces ensured good release properties.

The short time available for stirring after the activator was added, precluded the use of evacuation, so a certain amount of trapped air was always present. The air above the unfoamed mixture in the mould was allowed to escape via a small hole in the upper retaining plate, when the foam expanded. This hole was plugged when all of the air had been ejected.

Filler separation was not a problem, as the mixture had a high viscosity.

The maximum thickness sample that could be produced by this method was one centimetre. Larger thicknesses reduced the amount of overpacking and resulted in non-uniform foams having unacceptably low bulk densities.

6.1(v) MISCELLANEOUS SYSTEMS

To complete this section a few words will be devoted to the remaining base materials that have been used in this study.

The other polymer based substitutes mentioned in the formulae quoted in Chapter 5 were nylon-6, P.T.F.E., bakelite and P.V.C. The comments given in 6.1(ii) again apply to these substances, with the degree of difficulty in the manufacturing procedures depending upon the individual material. Milling, extrusion and injection moulding and sintering techniques were employed.

The P.V.C. 'Plastisol' bone substitute, SB2, was an attempt to produce a liquid P.V.C. mixture which could be used for coating cores of 'inner bone' (IB1, IB2). The liquid mixture contains a solvent which evaporates on contact with the air. A formula, suggested by Plastic Coatings Ltd, was based on a P.V.C. resin, a phthalate plasticiser and a stabiliser. It was found that when the filler, calcium aluminate, was added to the liquid P.V.C. formulation suggested, the filler inhibited the action of the plasticiser, which had to be increased in concentration. This modification obviously ruined the agreement in the coefficient and power data which were based on the original P.V.C. formula. Added to this, the high viscosity of the mixture resulted in poor air release and, subsequently inferior samples.

The other system tested was the two-component acrylic product,

I.C.I. 'Tensol No.7'. It was found that the recommended quantity of catalyst that was to be added to the monomer had to be reduced from 4% to 1% (by weight), so that the hardening time could be increased from a few minutes to 10-20 minutes. This permitted the mixture of acrylic and P.V.C. (IB2) to be adequately de-gassed. The speed of hardening eliminated any filler separation problems. It was noted that the addition of P.V.C. apparently acted as a catalyst and decreased the hardening time.

The manufacturing procedures utilized for each of the new substitutes are summarized in TABLE 6.1. On the same table are quoted details of the appearance of each material and the machining properties. These latter comments are obviously subjective and cannot be specified precisely.

CODE	PRODUCTION	COLOUR	RIGID/ FLEXIBLE	MACHIN-ING PROPS
MS1	MILLED/EXTRUDED	CREAM	FLEXIBLE	POOR
MS2	CAST	WHITE	RIGID	"
MS3	"	BROWN	"	FAIR
MS4	"	"	"	GOOD
MS5	"	"	"	"
MS6	MILLED/EXTRUDED	CREAM	FLEXIBLE	FAIR
FT1	MILLED/EXTRUDED	WHITE	RIGID	GOOD
FT2	"	GREY	FLEXIBLE	POOR
FT3.	"	WHITE	RIGID	GOOD
FT4	CAST	BROWN	"	"
FT5	"	YELLOW	"	"
FT6	"	BROWN	"	FAIR
LN1	FOAMED	YELLOW	FLEXIBLE	POOR
LN2	CAST	BROWN	RIGID	GOOD
LN3	"	"	"	"
SB1	CAST	CREAM	RIGID	V.GOOD
SB2	"	GREY-BROWN	"	POOR
SB3	"	CREAM	"	V.GOOD
IB1	CAST	ORANGE	RIGID	GOOD
IB2	"	WHITE	"	"
SK1	CAST	BROWN	RIGID	FAIR
BR-SERIES	CAST	BROWN	RIGID	GOOD
LV1	CAST	BROWN	RIGID	GOOD
LV2		"	"	"
TH1	CAST	YELLOW	RIGID	FAIR
AR1	SINTERED	BLACK	RIGID	GOOD
AR2	MILLED/INJECTION MOULDED	YELLOW	"	POOR

TABLE 6.1 THE MANUFACTURING PROCEDURES AND SOME PROPERTIES OF THE NEW SUBSTITUTES

6.2 SOME PHYSICAL INVESTIGATIONS FOR QUALITY TESTING

(i) SPECIFIC GRAVITY DETERMINATIONS

Specific gravity measurements were performed on all of the manufactured substitutes and also on a range of polymers, existing substitutes and TLD materials. These values were subsequently used in a series of determinations of photon mass attenuation coefficients described in detail in the next chapter.

A selection of these materials were accurately machined into small discs,2.2 cm diameter and 1 cm thick. The discs permitted the measurement of specific gravity with high precision by a direct determination of mass and volume. In the cases when accurately machined discs could not be made, a 40 ml Hubbard Density Bottle was employed. This latter technique was necessary for such materials as 'Temex' rubber and the thin films of 'Melinex' and 'Kapton'.

TABLES 6.2 and 6.3 list the measured and, where appropriate, the published or calculated specific gravities of all the materials used in the attenuation measurements. Suppliers and the types of materials are also indicated on the tables. The standard error of measurement was 0.5%.

The agreement between the two sets of data is generally good, especially with the polymers. Some disagreement occurred with the new substitutes when different grades of fillers were used

MATERIAL	SPECIFIC GRAVITIES		SUPPLIER/GRADE
	MEASURED	PUBLISHED	
CB1	1.11	1.10	CIBA-GEIGY (UK) LTD
CB2	1.08	1.10	CIBA-GEIGY (UK) LTD
MELINEX	1.39	1.40	I.C.I. LTD - TYPE 'S'
NYLON-6	1.13	1.13	NYLONIC ENGINEERING CO.LTD
PERSPEX	1.10-1.18	1.17-1.20	I.C.I. LTD - 'CLEAR'
POLYETHYLENE	0.92	0.92-0.97	I.C.I. LTD; TELCON PLASTICS LTD
POLYCARBONATE	1.20	1.20	BAYER CHEMICALS LTD
POLYMIDE	1.41	1.42	DUPONT CO LTD - 'KAPTON'
POLYSTYRENE	0.95-1.05	0.98-1.11	A. WARNE & CO.LTD; BORST BROS LTD - 'POLYFLEX' - 'CLEAR'
P.T.F.E.	2.15	2.10-2.30	PAMPUS FLUOROPLAST LTD
P.V.C.	1.33	1.35	I.C.I. LTD - 'DARVIC'
T P X	0.85	0.83	I.C.I. LTD
ALDERSON FAT	0.88	-	ALDERSON RESEARCH LABORATORIES, INC.
ALDERSON MUSCLE	1.03	0.985	ALDERSON RESEARCH LABORATORIES, INC.
ALDERSON LUNG	0.32	0.32	ALDERSON RESEARCH LABORATORIES, INC.
M3	1.00	1.05	ST BARTHOLOMEW'S HOSPITAL
MIX D	0.97	0.99	KENT and CANTERBURY HOSPITAL
PRESSDWOOD	0.96	-	ST BARTHOLOMEW'S HOSPITAL
PYREX	2.22	2.2	GOOCH & HOUSEGO LTD
SHONKA A-150	1.12	1.12	BENEDICTINE COLLEGE, ILLINOIS
SHONKA C-552	1.78	1.76	BENEDICTINE COLLEGE, ILLINOIS
TEMEX	1.00	1.01	JAMES GIRDLER & CO.LTD
ALUMINIUM	2.69	2.70	A.E.R.E., HARWELL
CARBON	1.74	1.5-1.9	MORGANITE CRUCIBLE CO.LTD
PARAFFIN WAX	0.86	0.90-0.93	POTH HILLE & CO.LTD
WATER	-	1.00	ST BARTHOLOMEW'S HOSPITAL
LITHIUM BORATE/CARBON	1.57	-	BRITISH NUCLEAR FUELS LTD
CARBON/RESIN	1.84	-	BRITISH NUCLEAR FUELS LTD
LITHIUM BORATE/P.T.F.E.	2.13	-	D.A. PITMAN LTD
LITHIUM FLUORIDE	2.63	2.64	NATIONAL PHYSICAL LABORATORY

TABLE 6.2 THE SPECIFIC GRAVITIES, GRADES AND SUPPLIERS OF THE INVESTIGATED MATERIALS

SUBSTITUTE	SPECIFIC GRAVITIES	
	MEASURED	CALCULATED
MS1	1.00	1.15
MS2	1.00	1.15
FT2	0.95	0.95
FT3	0.84	0.86
FT4	0.92	0.92
FT5	0.92	0.92
FT6	0.83	0.89
SB1	1.85	1.90
SB2	2.39	1.73
IB1	1.17	
IB2	1.18	1.21
SK1	1.14	1.08
AR1	1.94	2.10

TABLE 6.3 THE SPECIFIC GRAVITIES OF SOME OF THE NEW SUBSTITUTES

during the manufacture. The wax used in the manufacture of M3 and MS2 had a lower specific gravity than published and resulted in the reduced value. TABLE 6.4 summarizes the grades and suppliers of all the powdered fillers used.

The measurement of specific gravity provided a quick and effective means of detecting density anomalies in the constituents of the new substitutes or dispensing errors in their manufacture.

POWDER	GRADE	SUPPLIER
ALUMINIUM	STANDARDISED LAB. REAGENT	COMAK CHEMICALS LTD
ALUMINIUM FLUORIDE	LABORATORY REAGENT	HOPKIN and WILLIAMS LTD
ALUMINIUM OXIDE	LABORATORY REAGENT	B.D.H. LTD
CALCIUM ALUMINATE	CA-31	EASTMAN KODAK CO.
CALCIUM CARBONATE	OMYA BLR/2; OMYA BL	MELBOURN CHEMICALS LTD
CALCIUM FLUORIDE	GENERAL PURPOSE REAGENT	HOPKIN and WILLIAMS LTD
CALCIUM SULPHATE	LABORATORY REAGENT	HOPKIN and WILLIAMS LTD
LITHIUM CARBONATE	LABORATORY REAGENT	HOPKIN and WILLIAMS LTD
LITHIUM NITRATE	GENERAL PURPOSE REAGENT	HOPKIN and WILLIAMS LTD
MAGNESIUM CARBONATE	PURE B.P.	KOCH-LIGHT LABORATORIES LTD
MAGNESIUM OXIDE	ANALAR	HOPKIN and WILLIAMS LTD
P.T.F.E.	G163(COARSE); L169B(FINE)	I.C.I. LTD
P.V.C.	'CORVIC'-D50/16(COARSE); P65/55(FINE)	I.C.I. LTD
SODIUM FLUORIDE	ANALAR	HOPKIN AND WILLIAMS LTD
TPX	RT-418	I.C.I. LTD

TABLE 6.4 THE GRADES AND SUPPLIERS OF THE POWDERED FILLERS USED IN THE MANUFACTURED MATERIALS

6.2(ii) HOMOGENEITY TESTS

Four different tests were used to investigate the homogeneity of the manufactured substitutes and, indeed, some of the existing substitutes. These were respectively xeroradiography and three types of microscopy, namely optical transmission, optical reflection and electron scanning microscopy.

The results of xeroradiography have already been illustrated (6.1(i)). The method is superior to conventional radiography; even high resolution radiography does not yield as much information. The smallest detectable particle size with the system at the Royal Marsden Hospital was 100 μm. Particles of this size were observed from a series of xeroradiographs of large test objects containing particles of different diameters. This method is the best one for indicating air volumes within a sample.

Optical transmission microscopy could only be used if the sample could be manufactured into a thin optically translucent film. This excluded such materials as opaque rubbers ('Temex') and resins filled with large quantities of additives (e.g. SB1, with its large loading of calcium carbonate, or Alderson lung substitute with its loading of phenolic microspheres). FIGURES 6.3 and 6.4 show typical results with specially prepared thin samples of IB2 and FT6. The magnification in each case was X150. Both of these illustrate the uniformity possible with the epoxy resin systems. IB2 has P.V.C. as a filler with mean particle sizes of 100 μm. FT6

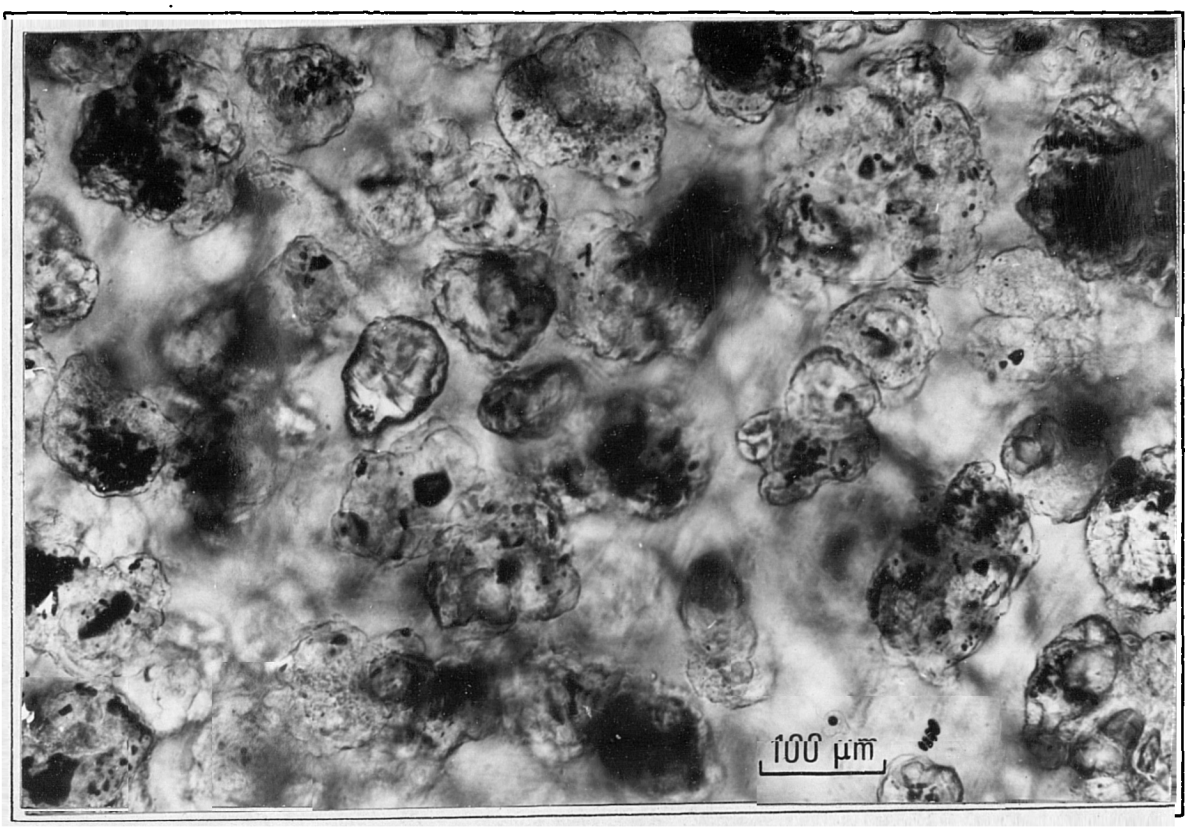

FIGURE 6.3 OPTICAL TRANSMISSION MICROSCOPY - IB2

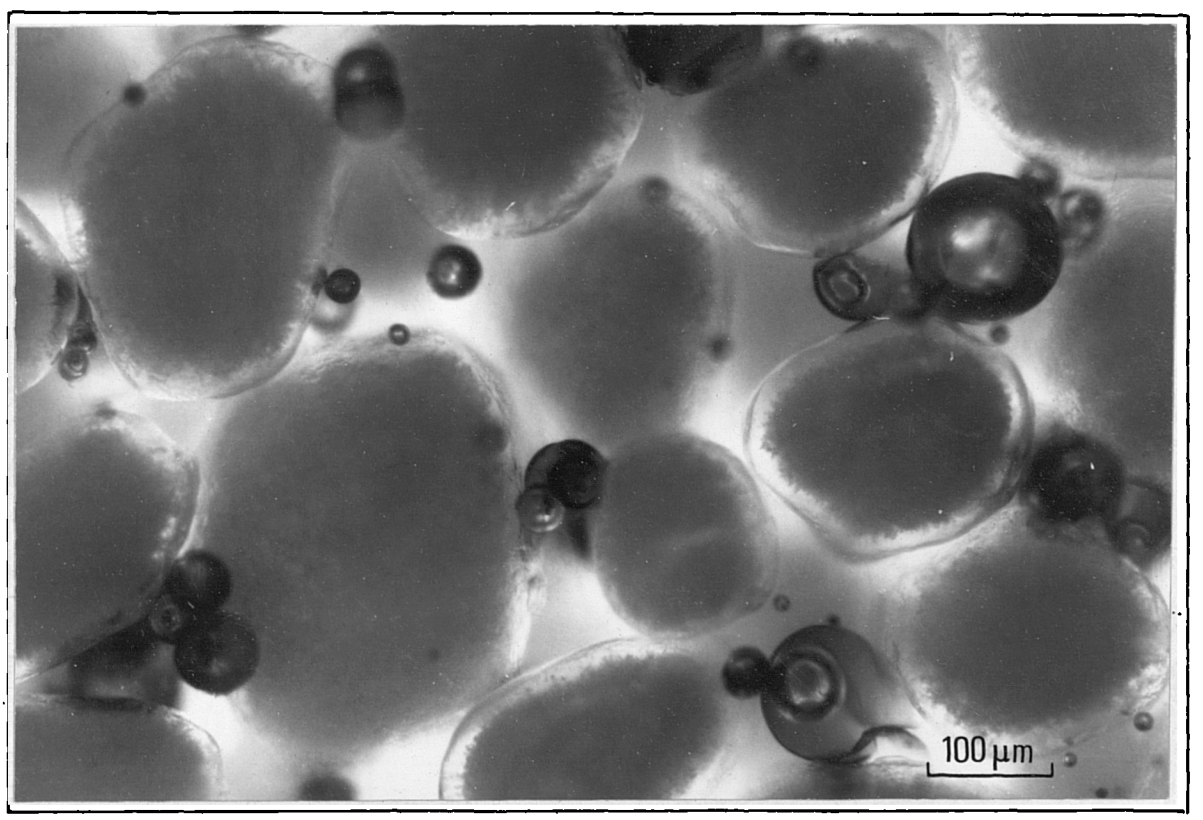

FIGURE 6.4 OPTICAL TRANSMISSION MICROSCOPY - FT6

has TPX powder added to the resin, together with phenolic microspheres. The distribution of the large TPX particles with the smaller microspheres dispersed amongst them is still very uniform. The mean diameter of the TPX particles is 250 μm.

Optically opaque materials may be investigated by reflection microscopy. Tests made on a suitable apparatus at the City University (PHILLIPS, 1973) showed that the technique was effective, providing the sample was carefully ground on the surface of interest.

The last and rather elaborate method which was investigated was electron microscopy. Attempts to produce samples suitable for transmission studies failed so a scanning electron microscope was used and produced spectacular results. FIGURES 6.5 and 6.6 show the scans for Alderson lung and SB1. Magnification varied from X200 for the lung material to X1000 for SB1. Fractured and prepared (ground) surfaces were analysed, the latter producing slightly better results. The samples, in the form of cubes of side 4mm, were first coated with carbon and then gold before being scanned.

A single phenolic microsphere is clearly visible in the centres of FIGURE 6.5(a) and the electronically magnified scan shown in FIGURE 6.5(b). The numerous craters are apparently made by the spheres removed when the sample was ground. Increased

(a)

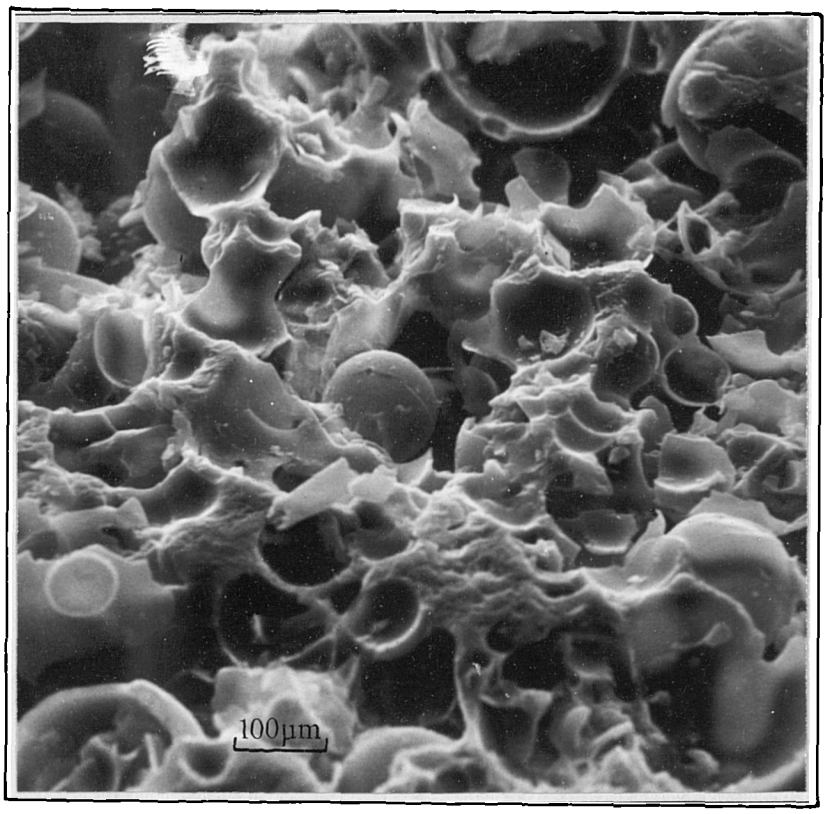

(b)

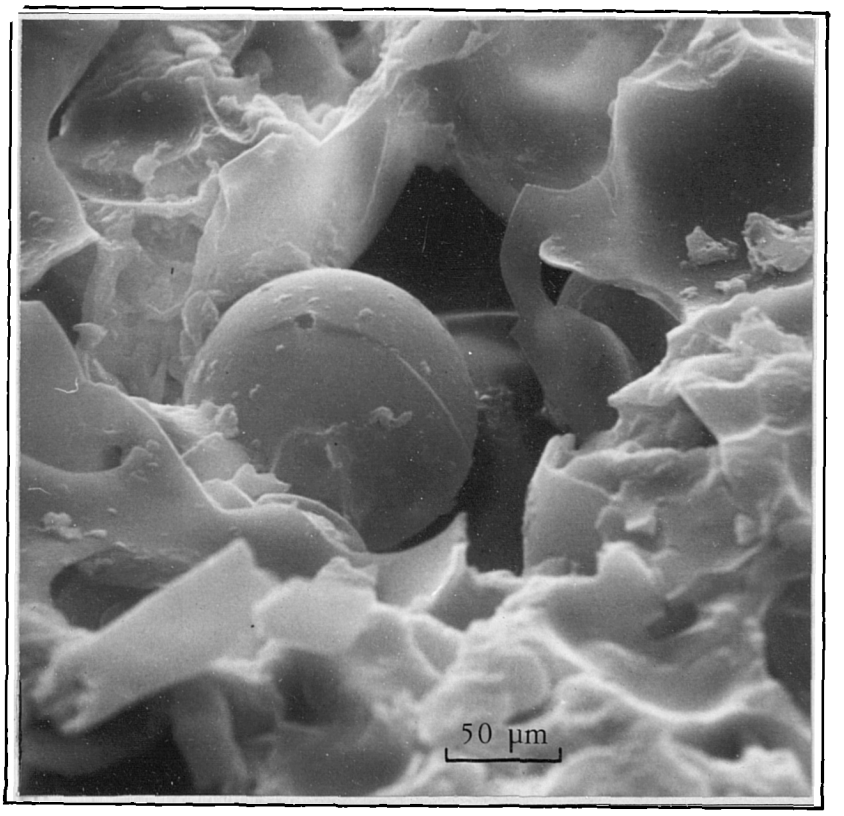

FIGURE 6.5 ELECTRON MICROSCOPE SCANS OF A SAMPLE OF ALDERSON LUNG MATERIAL

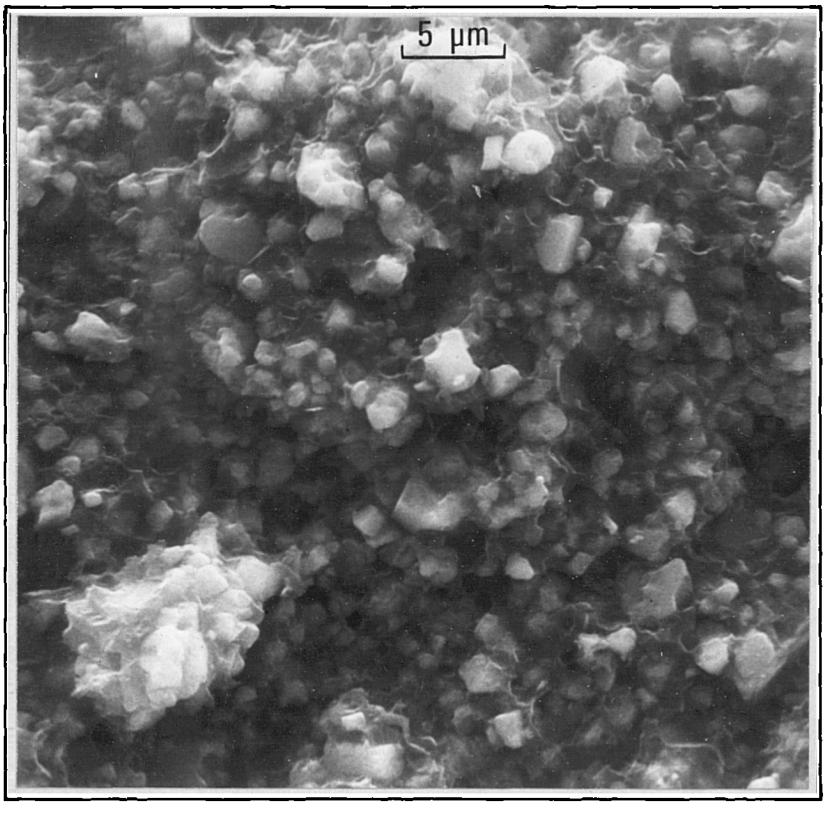

FIGURE 6.6 ELECTRON MICROSCOPE SCANS OF A SAMPLE OF SB1

magnification could not locate any other particulate filler within the crater walls.

FIGURE 6.6 shows the distribution of calcium carbonate in SB1 and illustrates that aggregates of the fillers can be formed within these mixtures.

The scans were produced on the S4 STEREOSCAN Scanning Electron Microscope at University College, London, (MILLEDGE, 1973).

The four methods described in this section appear to be complementary, but the choice of test will often depend upon whether the material is optically opaque or translucent and the degree of homogeneity required; the latter frequently being governed by the subsequent use of the substitute. If it is thought that trapped air is present, then the optical and electron methods are not suitable and Xeroradiography should be used. If a high degree of particulate uniformity is required, the scanning electron microscope offers a quick and elegant solution. The fact that special procedures have to be adopted to prepare a sample for analysis, (for example, grinding) always result in uncertainties regarding the modification or destruction of important characteristics. Techniques which were not dependent upon such preparative procedures were always employed whenever possible.

CHAPTER 7

PHOTON ATTENUATION MEASUREMENTS ON SELECTED SUBSTITUTES AND ALLIED MATERIALS

7.1 INTRODUCTION

The validity of the theoretical data presented in Chapter 5 was investigated experimentally by a series of 'narrow beam' photon attenuation measurements. These measurements were made on 30-40 materials including a selection of the new substitutes, some important existing substitutes, the common polymers and a few thermoluminescent materials. Carbon and aluminium samples, together with water, were also considered as a means of establishing the reliability of the measuring techniques.

It was decided at an early stage in the experiments that the photon energies used must extend from 10 keV to at least 1 MeV so that calculated data in the predominant photoelectric and incoherent scattering ranges could be adequately assessed. The lower energies were particularly important as the strong Z-dependence of the photoelectric process allowed both the elemental compositions of the materials and the precision of the selection procedures, to be probed.

Attenuation measurements with Americium-241 and Cobalt-60 were made at St. Bartholomew's Hospital, as convenient sources and nucleonic equipment were readily available. These radionuclides provided photons of 59.57 keV (^{241}Am), 1.1732 and 1.3325 MeV (^{60}Co). Low energy measurements were made at

Berkeley Nuclear Laboratories using characteristic X-radiation from germanium and molybdenum targets. These provided essentially monoenergic beams with the following mean energies:-

Germanium	K_α	9.8709 keV
	K_β	11.0415 keV
Molybdenum	K_α	17.4268 keV
	K_β	19.7868 keV

Equipment for the latter experiments was made available by the Environmental and Medical Sciences Division of A.E.R.E., Harwell.

The manufacture of the absorbers for these measurements presented a number of problems. As the photon energies were nominally from 10 keV to 1 MeV, a wide range of absorber thicknesses had to be produced. TABLE 7.1 shows the Half Value Thickness (H.V.T.) for each of the tissues, lung, fat, muscle and bone at 10 keV, 20 keV, 60 keV and 1 MeV. To obtain reliable results it was decided that whenever possible, a series of the transmission readings would be taken from zero thickness to at least one H.V.T. For bone substitutes this necessitated the manufacture of thin slices below 0.1 mm thick for use at 10 keV to centimetre thick absorbers at 1 MeV. At the other extreme lung substitutes required centimetre thicknesses at 10 keV to tens of centimetres at 1 MeV. The wide range materials analysed (listed earlier in TABLES 6.2 and 6.3) similarly produced technical difficulties. The mechanical properties of, say, wax and pyrex or epoxy resin and single crystals of lithium fluoride required completely different manufacturing techniques.

TISSUE	S.G.	H.V.T. (mm)			
		10 keV	20 keV	60 keV	1 MeV
LUNG	0.26	5.1	34	130	380
FAT	0.92	3.1	16	38	110
MUSCLE	1.00	1.3	8.8	34	99
BONE	1.85	0.13	0.96	12	57

TABLE 7.1 THE H.V.T's FOR LUNG, FAT, MUSCLE AND BONE TISSUES FOR PHOTON ENERGIES FROM 10 keV-1 MeV

FIGURE 7.1(a) shows a few of the 500 absorbers manufactured for this study. Absorbers from 0.05 to 1 mm thick were mounted in 35 mm transparency frames and are shown in the slide box to the right of the photograph. Disc absorbers, 22 mm diameter, 5 and 10 mm thick are shown stored in polystyrene tubes to the left of the photograph.

FIGURE 7.1(b) shows the perspex holder used to position the absorbers in the photon beam. The holder was constructed such that the narrow beam passed unimpeded through its central section. Slots in the inner walls of the holder allowed a maximum of ten thin absorbers in the transparency frames to be placed in the beam. The thicker disc absorbers were positioned centrally in the beam by placing the 'V-block' assembly (front left of photograph) in the main holder.

Each absorber was uniquely coded so that anomalous readings could be traced to a specific sample.

Attenuation measurements on water were performed using the cells shown in FIGURE 7.2. Three annular perspex holders were constructed, such that the central sections, of diameter 22 mm, contained tensioned 'melinex' walls, 0.06 mm thick, separated by 1, 5 and 10 mm spacers. Holes at the top of each spacer allowed water to be injected into the void between the 'melinex' windows producing water absorbers of thicknesses nominally equal to those of the spacers.

(a)

(b)

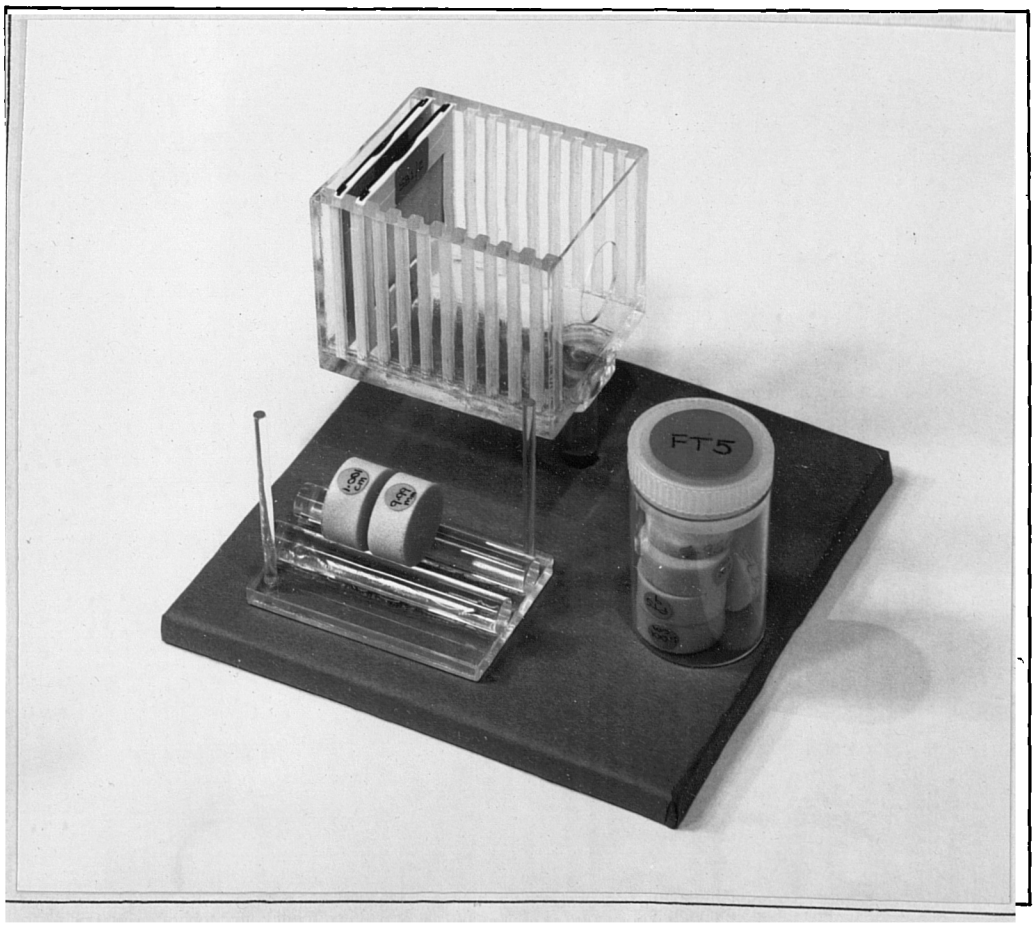

FIGURE 7.1 THE ABSORBERS AND HOLDER USED IN THE ATTENUATION MEASUREMENTS

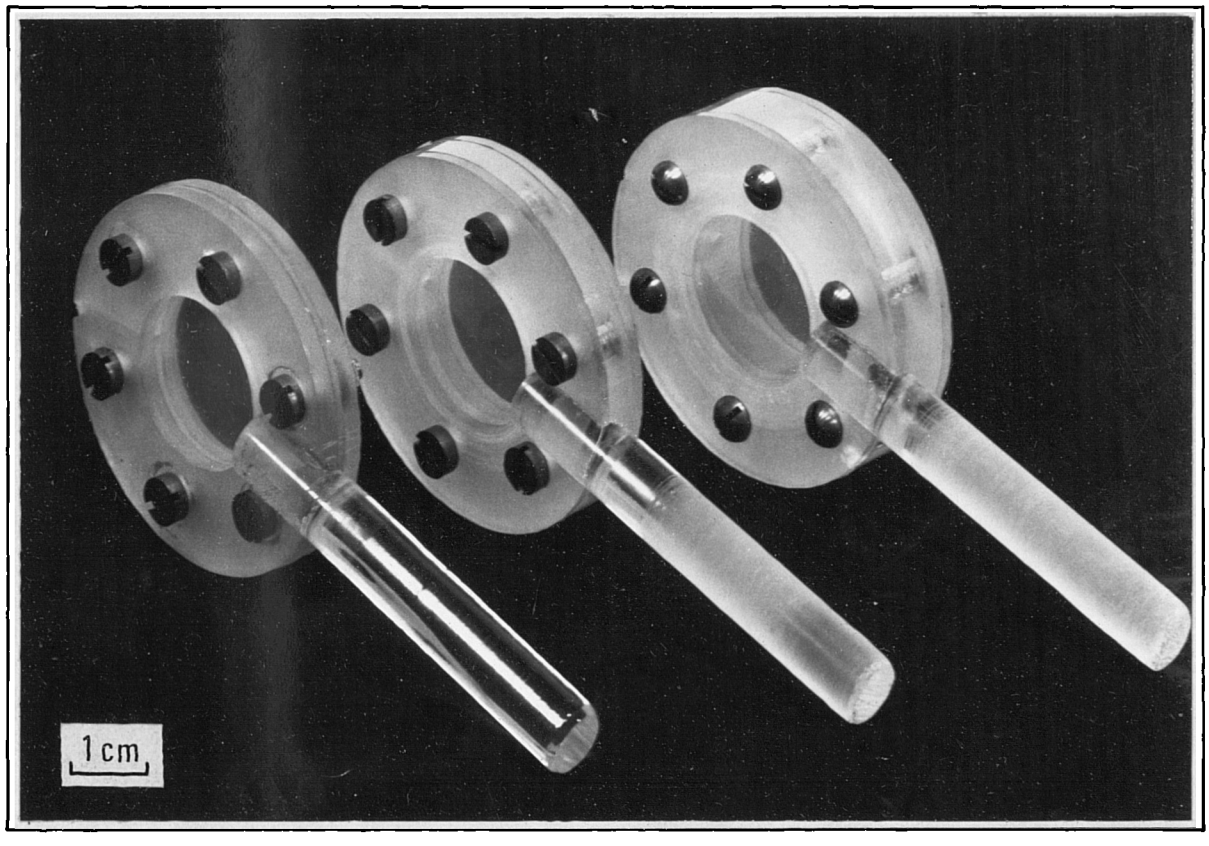

FIGURE 7.2 'MELINEX'-WALLED CELLS USED FOR ATTENUATION MEASUREMENTS ON LIQUIDS

The thicknesses of all the absorbers were carefully measured with precision micrometers. The thicknesses of one hundred of the most important samples were checked at the Mullard's Standards Laboratory. A Johansson Mikrokator, with 41 cm radius anvils and a measuring pressure of 10 g, was used for the solid absorbers and an optical feeler microscope for the three (filled) water cells. The absorbers were measured at a central position, corresponding to the region traversed by the radiation beam. Uncertainties were, at best, ± 0.005 mm but a few samples (rubbers, cleaved crystals and waxes) gave uncertainties of ± 0.010 mm.

These absorbers and the methods of positioning them in the narrow beams have proved in practice to be completely successful for all the photon attenuation measurements.

7.2 THE EXPERIMENTAL TECHNIQUES

Although the general approach to the measurements, using both radionuclide sources and characteristic X-rays, were similar, the differences in the experimental apparatus require a short description.

FIGURE 7.3 depicts schematically the apparatus used for the radionuclide measurements (^{241}Am and ^{60}Co). An encapsulated 'point' source, 2 mm diameter and of activity varying from 2.5 mCi for ^{60}Co to 14 mCi for ^{241}Am, was fitted into the lower end of the lead collimator A. Lead collimator B was fixed co-axially above A, the facing surfaces of the collimators being 80 cm apart. Collimator B was manufactured such that a 2.5 cm Sodium Iodide scintillation assembly could be located vertically above its upper surface. Absorbers were placed, midway between the collimators, on a perspex platform which had a 2 cm hole co-axial with the collimators. The effective beam diameter at the sample was 5.6 mm. The whole assembly was held in a rigid metal frame.

The scintillation assembly was connected to a Nuclear Enterprise SR3 scaler, analyser and H.T. unit. Maximum count-rates, integrated over the channels giving the 'peak' response, when no absorber was present in the beam ('zero thickness') was 22,000 counts/minute for ^{241}Am (59.57 keV) and 20,000 counts/minute for ^{60}Co (1.1732 MeV). The standard deviations on these count-rates, during the complete series of

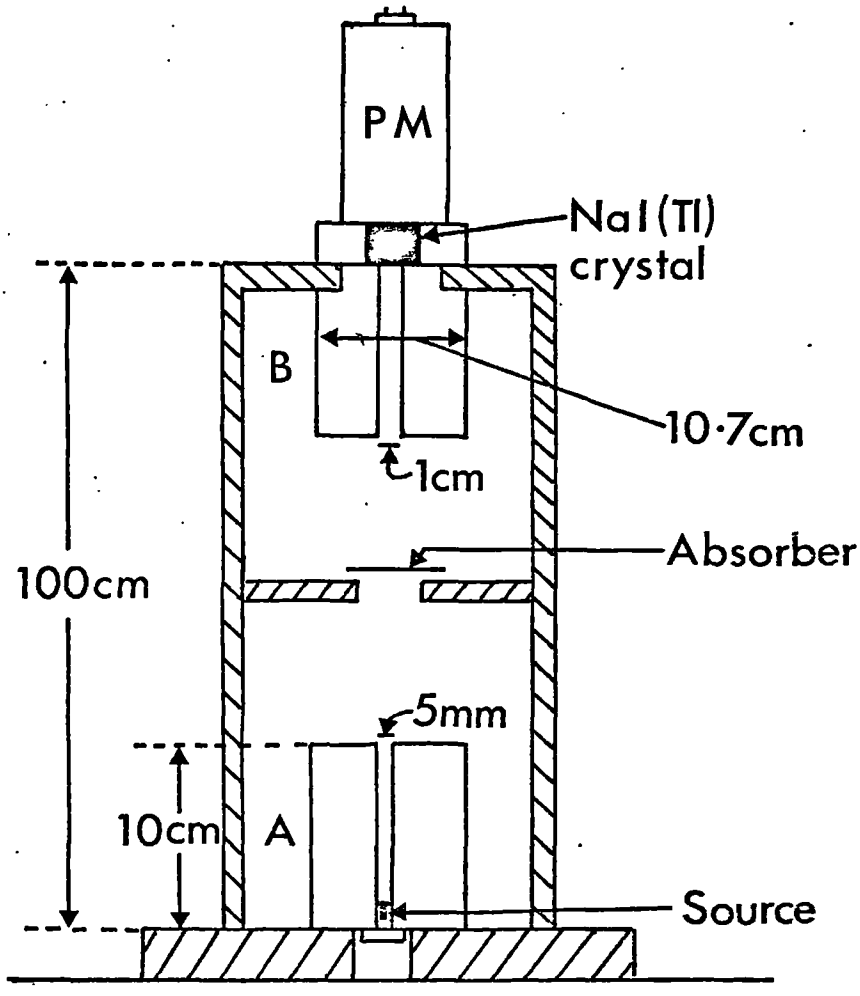

FIGURE 7.3 SCHEMATIC DIAGRAM OF THE ATTENUATION APPARATUS USED WITH RADIONUCLIDE SOURCES

measurements, amounted to approximately 0.7% for ^{241}Am and 0.9% for ^{60}Co.

FIGURE 7.4 shows the Harwell/Berkeley apparatus which was used for the measurements with characteristic X-rays from germanium and molybdenum targets. Characteristic radiation, emitted at right angles to a beam of primary X-rays (80-100 kV) was allowed to pass through three lead collimators, X, Y, Z, to fall on to a lithium drifted germanium detector. The dimensions of the collimating system were as shown in the figure. To reduce the amount of scattered radiation falling on the detector, the whole system was housed within a 5.5 mm lead surround. The output from the X-ray machine was monitored by a Victoreen 1LA ionization chamber (M), placed inside the entrance port machined in the surround. The beam diameter at the absorbers, which were placed before collimator Y in the perspex holder, was approximately 4.5 mm. Signals from the germanium detector were fed into a Harwell designed nucleonic counting unit, which included a multichannel analyser with computer compatible paper-tape output.

Typical spectra obtained with this equipment are shown in FIGURE 7.5. The K_α and K_β lines for germanium and molybdenum were plotted after the beams had traversed different absorber thicknesses. In both cases the K_α lines produced large count-rates, when zero thickness rates, integrated over the channels spanning the peaks, amounted to 23,000 counts/minute with germanium and 31,000 counts/minute with molybdenum. The standard deviations in these

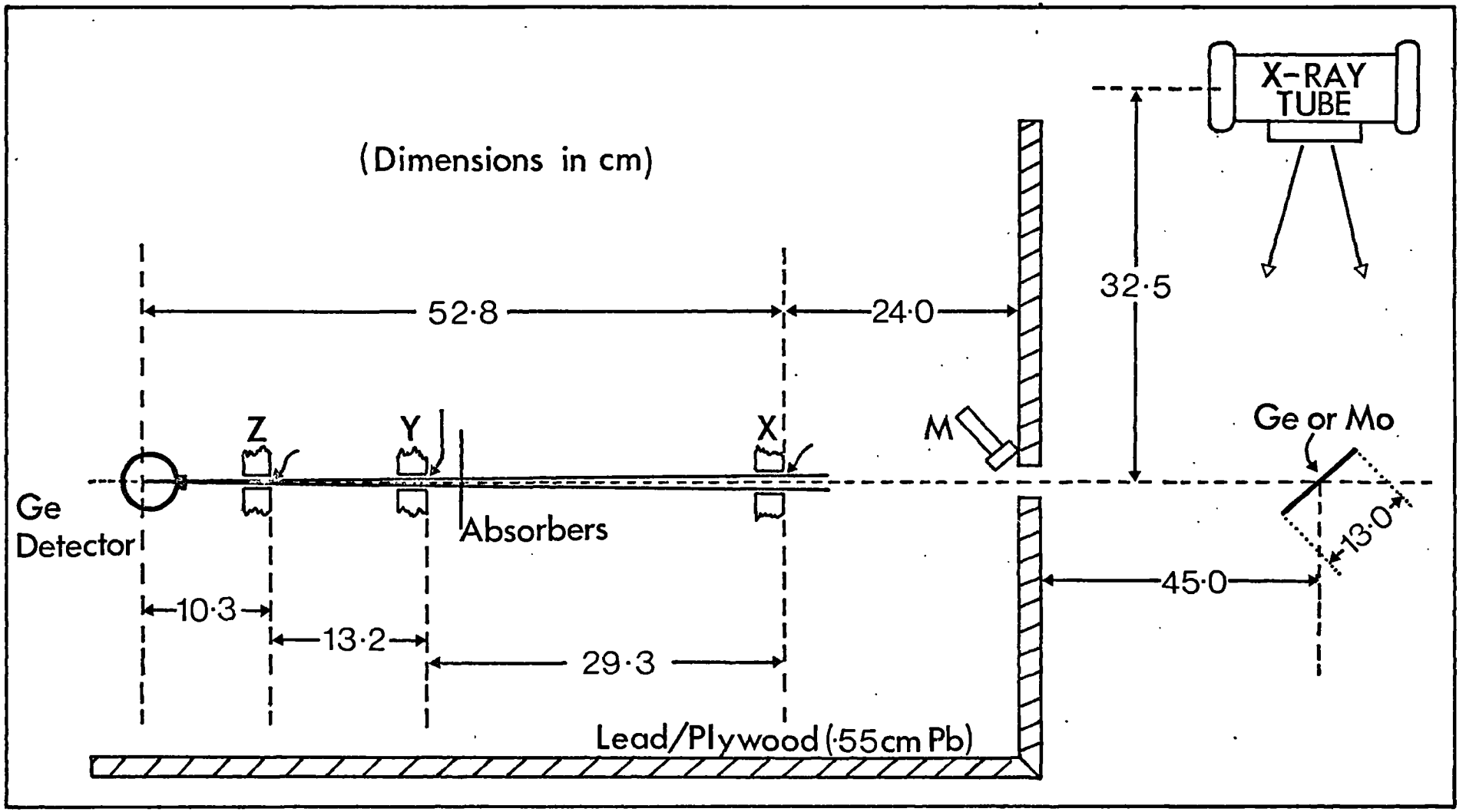

FIGURE 7.4 SCHEMATIC DIAGRAM OF THE ATTENUATION APPARATUS USED WITH CHARACTERISTIC X-RAYS

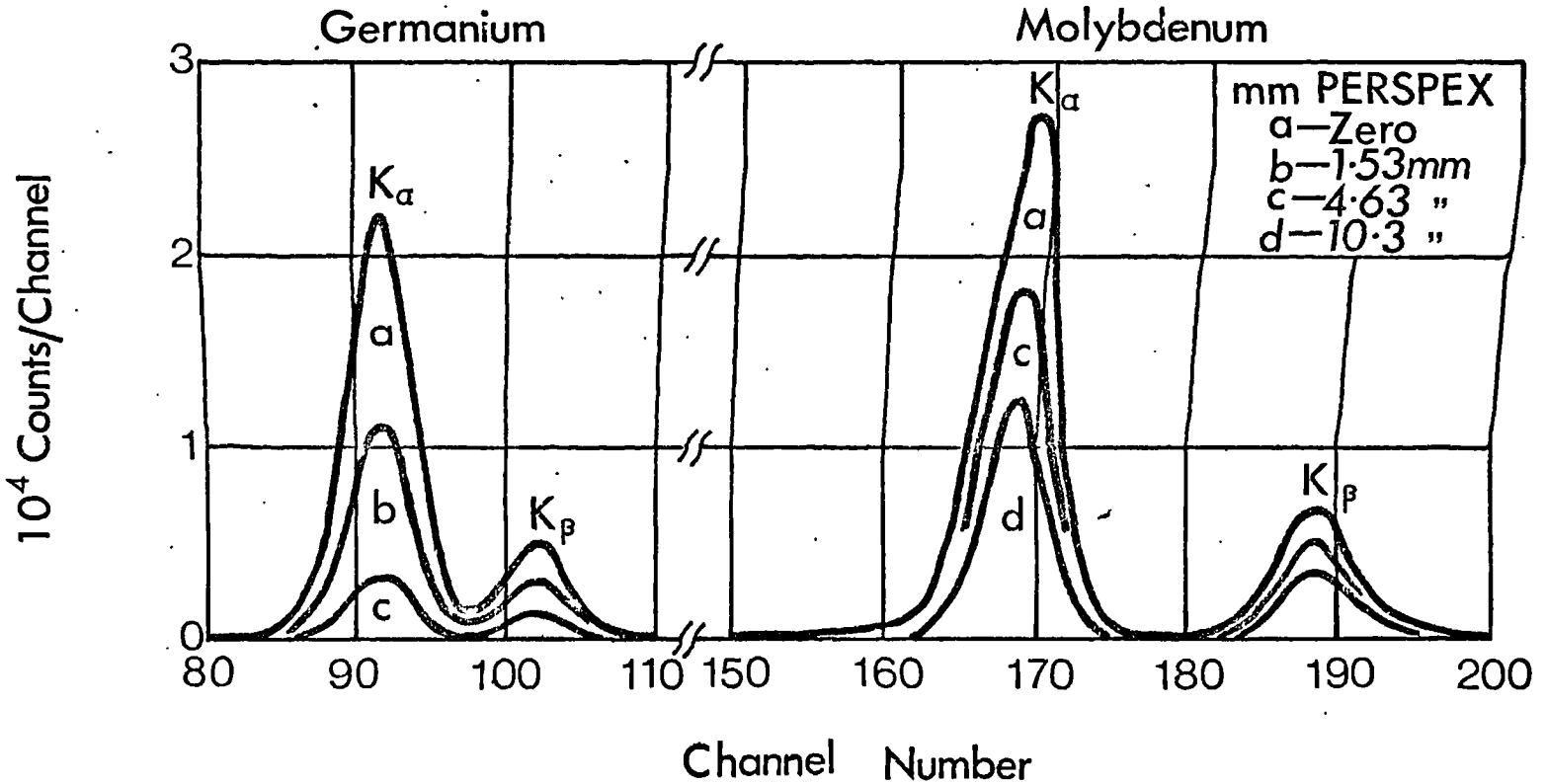

FIGURE 7.5 GERMANIUM AND MOLYBDENUM CHARACTERISTIC X-RAY SPECTRA OBTAINED WITH DIFFERENT ABSORBER THICKNESSES

'zero' values, during the complete period of the measurements, amounted to approximately 0.5%.

At the beginning of this section it was stated that the general approach to the measurements was similar in the two experimental procedures. In both cases the zero thickness count-rate was determined at the start of each run. Absorbers of one material were then added and count-rates measured until the readings were reduced by 50%. After appropriate corrections for deadtime and X-ray output variations had been made, the integrated count-rates over the peak were converted to percentage transmissions, giving the zero thickness rate the 100% value. The regression of log (transmission) versus absorber thickness was then computed and the slope or narrow beam linear attenuation coefficient (μ) derived. Whenever possible, zero thickness readings were repeated at the beginning and end of each series of measurements on a particular material, and the mean value used in the computation. In the few cases when only one suitable absorber thickness was available, this procedure could not be followed and the linear attenuation coefficient was calculated from the zero and single thickness readings.

Typical transmission curves for the K_α and K_β lines from germanium and molybdenum are shown in FIGURE 7.6. In the figure the data for perspex, presented in the previous figure, are drawn on a log-linear plot. Due to the lower count-rates produced by the K_β lines and the associated reduction in the overall precision for the derived attenuation coefficients, data for these lines will not be presented in this analysis.

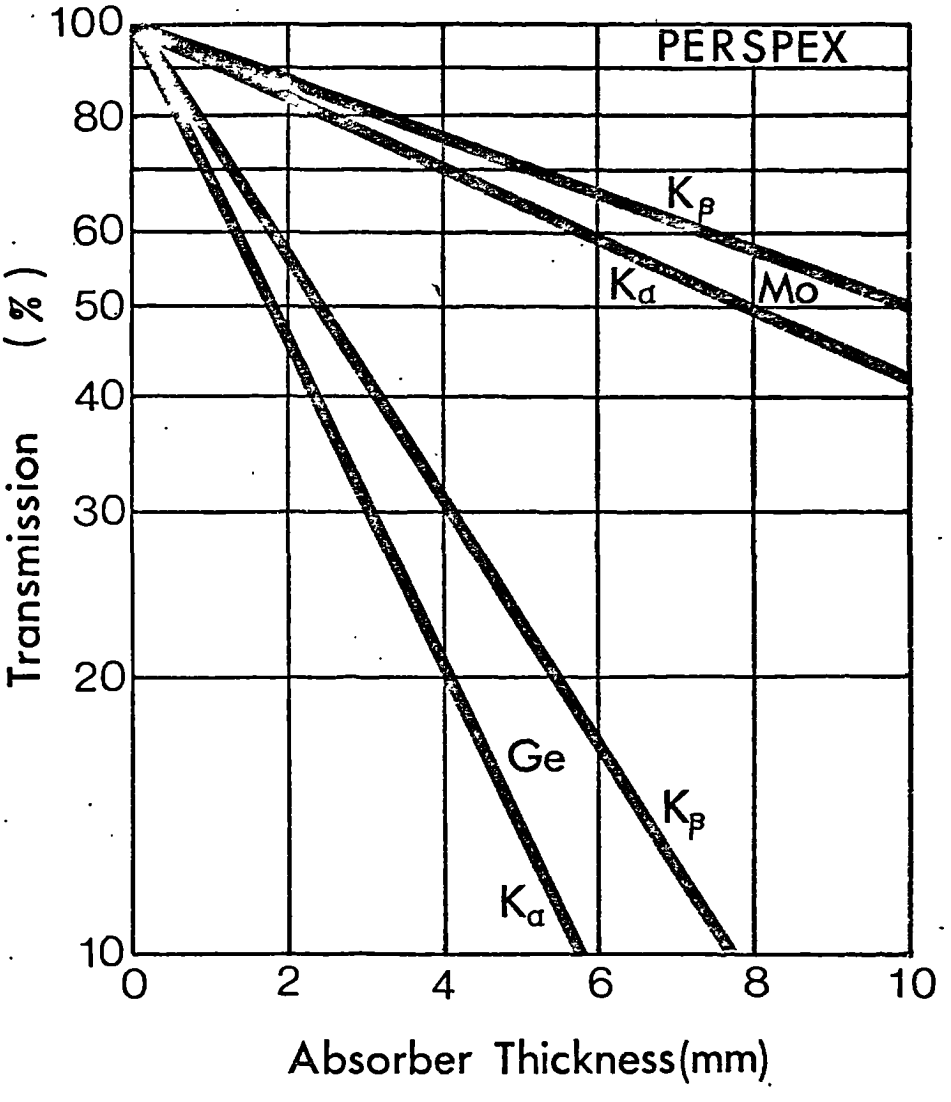

FIGURE 7.6 TRANSMISSION CURVES FOR PERSPEX (K_α, K_β, CHARACTERISTIC X-RAYS FROM Ge AND Mo)

Before the results of the measurements are compiled, a short description will be given of the computation procedure adopted for the evaluation of mass attenuation coefficients at the 'non-standard' energies employed. These calculated coefficients were required so that a direct comparison could be made with the measured data.

7.3 CALCULATED DATA

Mass attenuation coefficients for compounds were generally calculated, from elemental cross section data, at 33 energy points. These 'standard' energies covered the range 10 keV to 100 MeV, having repeated increments as shown below:-

.01, .015, .02, .03, .04, .05, .06, .08, .1, .15, .2, ----100(MeV)

The coefficients of the materials used in the attenuation measurements had to be calculated at 'non-standard' energies, for example, at 9.8709 keV instead of 10 keV, so suitable interpolation and extrapolation procedures were required.

Curve fitting techniques were adopted, fitting to the basic data polynomial expressions of the form, $\ln C = \sum_{i=0}^{n} a_i (\ln E)^i$, where the mass attenuation coefficients (C) for a material at different 'standard' energies (E), were used to establish the values of a_i . Once the polynomial expression had been produced, substitution of a 'non-standard' energy readily yielded the required mass attenuation coefficient.

FIGURE 7.7 shows the errors in the 'true' and 'fitted' total mass attenuation coefficients for muscle, when (a) the polynominal fitting procedure was applied to TOTAL attenuation coefficients and (b) the procedure was applied to the individual PARTIAL effects and the total attenuation coefficients found by summation. In both cases the total mass attenuation coefficients at the 'standard' energies,

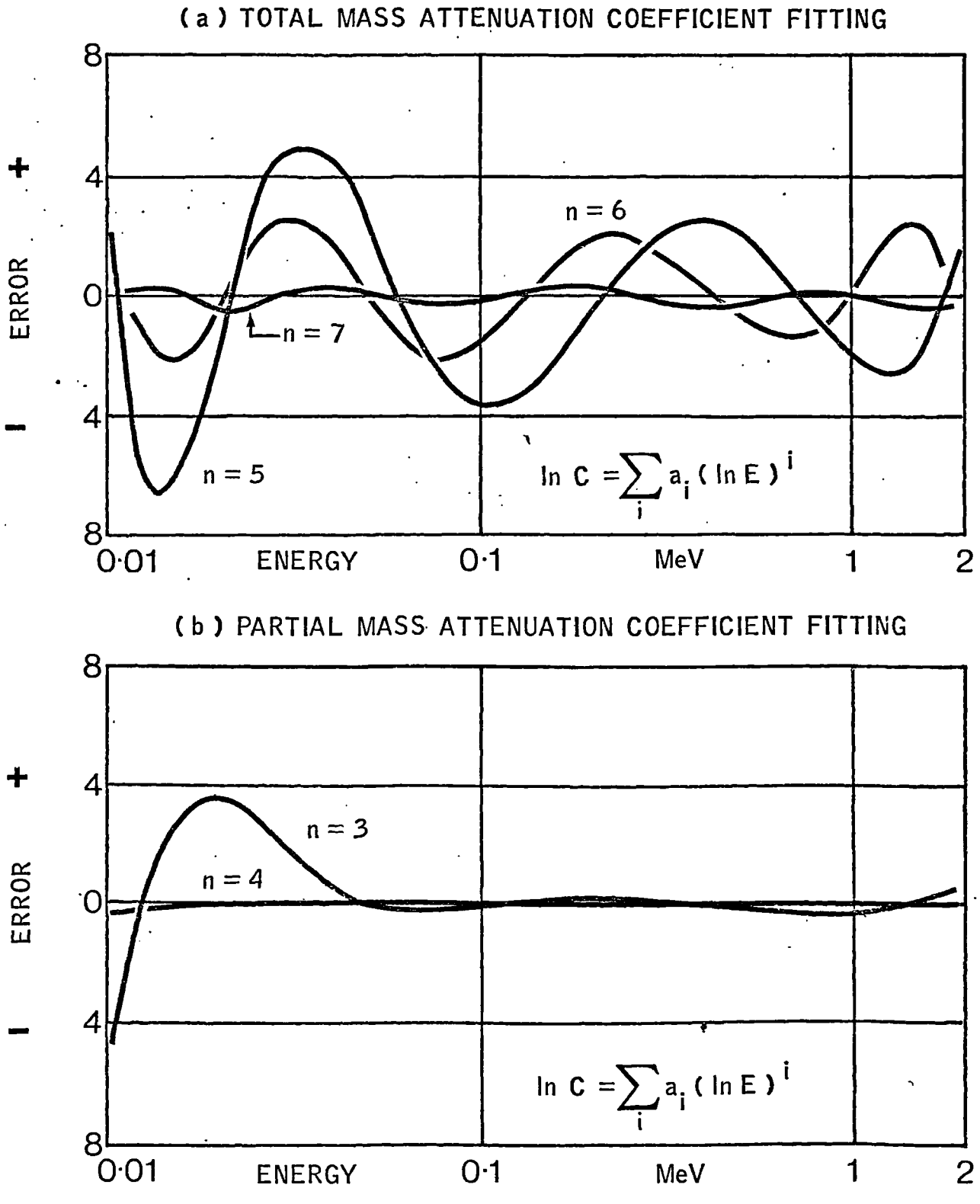

FIGURE 7.7 POLYNOMIAL FITTING ERRORS IN TOTAL COEFFICIENTS FOR MUSCLE

from 10 keV to 2 MeV, were compared with the coefficients calculated at the same energies by substitution into the derived polynomial expression. This was repeated for expressions of different degrees until errors below 1% were obtained.

It was found that to achieve comparable results, higher degree polynomials were necessary when the expressions were fitted to the total coefficients, than when partial coefficient fitting was employed. Subsequently, total mass attenuation coefficients at the 'non-standard' energies were taken as means of the coefficients computed by the two methods, when polynomials of degree 7 for total coefficient fitting and degree 4 for partial coefficient fitting were adopted. Agreement between the two methods was generally better than 0.5%.

7.4 THE EXPERIMENTAL RESULTS

TABLES 7.2-7.5 summarize the experimental results obtained from ^{60}Co, ^{241}Am and the K_α lines of germanium and molybdenum, respectively. Each table comprises of five columns:-

The FIRST column, on the extreme left, lists the names of the materials being tested.

The SECOND column lists the measured values of the narrow beam linear attenuation coefficients, μ (m^{-1}). The standard deviation is given in the cases where a number of transmission measurements were made enabling a regression computation to be made.

The THIRD column quotes the measured values of mass attenuation coefficients, $\frac{\mu}{\rho}$ (m^2/kg). These values were calculated from the linear attenuation coefficients given in the previous column and the measured specific gravities listed in Chapter 6 (TABLES 6.2 and 6.3).

The FOURTH column quotes the values of the mass attenuation coefficients, $\frac{\mu}{\rho}$ (m^2/kg) calculated by the polynomial fitting routines described in section 7.3 .

The FIFTH and final column presents the ratios of the measured mass attenuation coefficients to the calculated values.

In TABLE 7.2 the results for 31 materials are summarized, when the 1.1732 MeV gamma radiation from ^{60}Co was used. Maximum differences between calculated and measured data was 5%, although the agreement was generally below 2%. The random errors associated with these measurements were due to counting statistics, uncertainties in sample thickness and the unknown impurities present. An indication of the size of these errors is given by the quoted standard deviations, which were typically in the range 2-3%.

TABLE 7.3 shows the results for the same 31 materials when the 59.57 keV gamma radiation from ^{241}Am was selected. Excellent agreement between calculated and measured coefficients was found for most materials, when the standard deviations computed from the regression data were typically in the range 0.5-1%. The higher precision of these results compared to those for ^{60}Co was thought to be due, in part, to the better collimation produced by the apparatus at the lower energy, and the difficulty in obtaining ^{60}Co transmission curves down to 50% attenuation for all of the materials, with the available absorbers.

For both ^{241}Am and ^{60}Co the measured results for water and the elements aluminium and carbon were within 2% of the calculated values, which lends confidence to the experimental method. Excellent agreement between measured and calculated data was achieved for the new substitutes, indicating the high precision of

MATERIAL	$\mu(m^{-1})$ MEAS.	μ/ρ (m^2/kg) MEAS.	μ/ρ (m^2/kg) CALC.	RATIO
CB1	7.23 ± .17	.00651	.00638	1.02
NYLON-6	7.26 ± .24	.00642	.00645	1.00
PERSPEX	6.80 ± .16	.00618	.00638	0.97
POLYETHYLENE	6.33 ± .06	.00688	.00671	1.03
POLYCARBONATE	7.42 ± .13	.00618	.00620	1.00
POLYSTYRENE	6.20 ± .12	.00652	.00632	1.03
P.T.F.E.	12.0 ± .3	.00558	.00565	0.99
P.V.C.	8.17 ± .14	.00614	.00603	1.02
TPX	5.52 ± .13	.00649	.00671	0.97
ALDERSON FAT	5.16 ± .21	.00586	-	-
ALDERSON MUSCLE	5.90 ± .11	.00573	-	-
ALDERSON LUNG	1.75 ± .06	.00547	-	-
M3	6.83 ± .13	.00683	.00653	1.05
MIX D	6.47 ± .17	.00667	.00664	1.00
PYREX	13.3	.00599	.00585	1.02
SHONKA A-150	7.16 ± .14	.00639	.00637	1.00
SHONKA C-552	10.5 ± .1	.00590	.00587	1.01
TEMEX	6.68 ± .15	.00668	.00639	1.05
ALUMINIUM	15.2 ± .3	.00565	.00567	1.00
CARBON	10.4 ± .1	.00598	.00588	1.02
WATER	6.65	.00665	.00652	1.02
MS2	6.58 ± .26	.00658	.00646	1.02
FT1	6.01 ± .14	.00660	.00652	1.01
FT2	6.40 ± .15	.00674	.00659	1.02
FT3	5.64 ± .02	.00671	.00666	1.01
FT4	6.06 ± .17	.00659	.00649	1.02
FT5	6.02 ± .04	.00654	.00649	1.01
SB1	11.4 ± .1	.00616	.00605	1.02
IB1	7.69 ± .17	.00657	.00630	1.04
IB2	7.41 ± .35	.00628	.00628	1.00
SK1	7.34 ± .13	.00644	.00627	1.03

TABLE 7.2 NARROW BEAM ATTENUATION RESULTS - ^{60}Co

- 1.1732 MeV -

MATERIAL	μ (m^{-1}) MEAS.	μ/ρ (m^2/kg)		RATIO
		MEAS.	CALC.	
CB1	21.74 ± .14	.0196	.0191	1.03
NYLON-6	22.23 ± .20	.0197	.0193	1.02
PERSPEX	20.54 ± .15	.0187	.0193	0.97
POLYETHYLENE	18.26 ± .14	.0198	.0197	1.01
POLYCARBONATE	22.51 ± .19	.0188	.0187	1.01
POLYSTYRENE	18.10 ± .29	.0191	.0187	1.02
P.T.F.E.	40.11 ± .24	.0187	.0188	0.99
P.V.C.	45.67 ± .45	.0343	.0337	1.02
TPX	16.22 ± .17	.0191	.0197	0.97
ALDERSON FAT	16.00 ± .13	.0182	-	-
ALDERSON MUSCLE	19.10 ± .18	.0185	-	-
ALDERSON LUNG	6.00 ± .03	.0188	-	-
M3	21.02 ± .11	.0210	.0207	1.01
MIX D	20.14 ± .14	.0208	.0208	1.00
PYREX	53.68	.0242	.0245	0.99
SHONKA A-150	22.26 ± .16	.0200	.0198	1.01
SHONKA C-552	33.02 ± .21	.0186	.0189	0.98
TEMEX	21.32 ± .27	.0213	.0202	1.06
ALUMINIUM	75.13 ± .09	.0279	.0284	0.98
CARBON	30.42 ± .22	.0175	.0176	0.99
WATER	20.30	.0203	.0206	0.99
MS2	20.41 ± .15	.0204	.0205	1.00
FT1	17.47 ± .29	.0192	.0195	0.98
FT2	18.82 ± .13	.0198	.0196	1.01
FT3	16.66 ± .24	.0198	.0198	1.00
FT4	17.87 ± .10	.0194	.0193	1.01
FT5	17.63 ± .12	.0192	.0194	0.99
SB1	59.78 ± .29	.0321	.0319	1.01
IB1	27.39 ± .12	.0234	.0230	1.02
IB2	27.29 ± .26	.0231	.0228	1.01
SK1	22.82 ± .23	.0200	.0196	1.02

TABLE 7.3 NARROW BEAM ATTENUATION RESULTS - ^{241}Am

- 59.57 keV -

the selection and manufacturing procedures.

The acceptability of the new substitutes was only put in question when the results at lower energies were analysed. TABLE 7.4 presents the results for the K_α line from molybdenum (17.4268 keV) for 30 materials and TABLES 7.5(a), 7.5(b) the results from germanium (9.8709 keV) for 43 materials. The standard deviations on these measurements were generally in the range 1-2% for molybdenum and 0.5-1% for germanium.

Although the data for the TPX, polyethylene, perspex and P.T.F.E. based substitutes (FT2, FT3, IB2, AR1) showed good agreement with calculated values, the epoxy resin based substitutes (FT4, FT5, SB1, IB1, SK1) showed both positive and negative discrepancies in excess of 5%. Positive discrepancies were also noted in the measurements on the unfilled resins CB1 and CB2, indicating that either the basic 'CHNO' theoretical formula was incorrect or, more probably, that a contaminant of high atomic number was present. Discussions with the manufacturers, CIBA-GEIGY (UK) LTD (MARTIN, 1974), have established that a small percentage of chlorine is always present in the raw materials, ranging from 0.1-0.2% at its lowest concentration, to 0.8% at its maximum. Most resins were stated as having 0.4-0.5% concentrations of chlorine. Calculations have shown that chlorine concentrations of 0.25% produce discrepancies of 5% at 10 keV, while 5% chlorine produce 10% errors.

MATERIAL	$\mu(m^{-1})$ MEAS.	μ/ρ (m^2/kg) MEAS.	μ/ρ (m^2/kg) CALC.	RATIO
CB1	75.08 ± 1.22	.0676	.0635	1.06
PERSPEX	87.93 ± 1.60	.0745	.0735	1.01
POLYETHYLENE	48.92 ± .28	.0531	.0534	0.99
POLYSTYRENE	51.38	.0541	.0546	0.99
P.T.F.E.	286.7	.133	.134	0.99
TPX	44.78 ± .26	.0527	.0534	0.99
ALDERSON FAT	42.55 ± 1.14	.0484	-	-
ALDERSON MUSCLE	85.75 ± 2.48	.0833	-	-
ALDERSON LUNG	22.88 ± .12	.0715	-	-
M3	113.1	.113	.111	1.02
MIX D	97.99	.101	.102	0.99
SHONKA A-150	106.2 ± .5	.0948	.0925	1.02
SHONKA C-552	190.0 ± 2.1	.107	.106	1.01
TEMEX	104.9 ± .8	.105	.0999	1.05
ALUMINIUM	1407 ± 6	.523	.508	1.03
CARBON	97.09 ± .74	.0558	.0560	1.00
PARAFFIN WAX	46.09	.0536	.0533	1.01
WATER	107.2	.107	.107	1.00
LITHIUM BORATE/ P.T.F.E.	266.6	.125	.121	1.03
LITHIUM FLUORIDE	298.8 ± .4	.114	.121	0.94
MS2	109.7	.110	.110	1.00
FT2	57.26 ± .51	.0603	.0600	1.01
FT3	50.66	.0603	.0606	1.00
FT4	58.92	.0640	.0606	1.06
FT5	59.78 ± .49	.0650	.0606	1.07
FT6	49.11	.0592	-	-
SB1	1000	.0541	.0584	0.93
IB2	263.6	.215	.216	1.00
SK1	108.1	.0948	.0985	0.96
AR1	224.2	.116	.114	1.02

TABLE 7.4 NARROW BEAM ATTENUATION RESULTS - Mo(K_α)

- 17.4268 keV -

MATERIAL	$\mu(m^{-1})$ MEAS.	μ/ρ (m^2/kg)		RATIO
		MEAS.	CALC.	
CB1	332.5 ± 4.2	.300	.275	1.09
CB2	325.3 ± 2.6	.301	.281	1.07
MELINEX	502.4 ± 4.9	.361	.349	1.03
NYLON-6	300.7 ± 1.8	.293	.287	1.02
PERSPEX	401.5 ± .7	.340	.337	1.01
POLYETHYLENE	190.7 ± 1.1	.207	.208	1.00
POLYCARBONATE	347.3 ± 1.1	.289	.294	0.98
POLYIMIDE	455.6 ± 4.0	.323	.318	1.02
POLYSTYRENE	233.6 ± 2.4	.222	.222	1.00
P.T.F.E.	1481 ± 9	.689	.702	0.98
P.V.C.	4747	3.57	3.42	1.04
TPX	173.4 ± 1.2	.204	.208	0.98
ALDERSON FAT	177.2 ± 1.8	.201	-	-
ALDERSON MUSCLE	406.4 ± 3.5	.395	-	-
ALDERSON LUNG	98.5 ± 3.3	.308	-	-
M3	548.9 ± 9.1	.549	.534	1.03
MIX D	421.9 ± 1.3	.435	.456	0.95
PRESSDWOOD	568.6	.592	-	-
PYREX	3009	1.36	1.77	0.77
SHONKA A-150	481.7 ± 4.4	.430	.421	1.02
SHONKA C-552	933.8 ± 4.1	.558	.532	1.05
TEMEX	455.0 ± 4.3	.455	.440	1.03
ALUMINIUM	7489 ± 63	2.78	2.73	1.02
CARBON	396.0 ± 5.6	.228	.237	0.96
PARAFFIN WAX	179.7	.209	.207	1.01
WATER	530.2	.530	.536	0.99
LITHIUM BORATE/ CARBON	606.6	.386	-	-
CARBON/RESIN	515.4	.280	-	-
LITHIUM BORATE/ P.T.F.E.	1351	.634	.625	1.01
LITHIUM FLUORIDE	1539	.585	.633	0.92

TABLE 7.5(a) NARROW BEAM ATTENUATION RESULTS - Ge(K_α)

- 9.8709 keV -

MATERIAL	$\mu(m^{-1})$ MEAS.	μ/ρ (m^2/kg)		RATIO
		MEAS.	CALC.	
MS1	490.0	.490	.569	0.86
MS2	576.2 $\pm$ 1.8	.576	.534	1.08
FT2	243.7 $\pm$ 1.1	.257	.250	1.03
FT3	211.0 $\pm$ 1.5	.251	.253	0.99
FT4	254.3 $\pm$ .7	.278	.255	1.09
FT5	255.6 $\pm$ 1.3	.278	.255	1.09
FT6	215.8 $\pm$ 2.1	.260	-	-
SB1	5140	2.78	3.00	0.93
SB2	2398 $\pm$ 34	1.00	2.49	0.40
IB1	1062 $\pm$ 10	0.908	1.10	0.83
IB2	1299 $\pm$ 25	1.10	1.07	1.03
SK1	489.3 $\pm$ 6.9	.429	.475	0.90
AR1	1134 $\pm$ 6	.585	.586	1.00

TABLE 7.5(b) NARROW BEAM ATTENUATION RESULTS - Ge(K_α)

- 9.8709 keV -

The positive errors in FT5 and FT4 were probably due to this chlorine contamination. Substitute FT6 was specially formulated to take into account the large measured coefficients for the resins and yielded mass attenuation coefficients of 0.260 m^2/kg for germanium K_α radiation. This corresponded very favourably to the value of 0.255 m^2/kg calculated at the same energy for fat.

It is thought that poor sample preparation was the cause of the low values for SB1, IB1 and SK1, which were visually inferior to the other samples. In particular, substitute SB1, which had a high initial viscosity, was extremely difficult to compress into the thin absorbers required for these tests.

For reliable systems based on epoxy resins these results show that attenuation measurements, preferably around 10 keV, must be made on the raw materials. Once the characteristics of the unfilled resins have been established, resulting substitutes should be similarly checked by attenuation investigations.

Poor sample preparation was also responsible for the anomalous results obtained with the substitute MS2, a wax based material manufactured at St Bartholomew's Hospital, and the polymer based substitutes MS1 and SB2 which were manufactured commercially.

The calculated coefficients for pyrex were derived from the Corning 7740 formula which the manufacturers claimed applied to their product. The significantly low values measured indicated

that this formula [B(4.01); O(53.96); Na(2.82); Al(1.16); Si(37.72); K(0.33)] was not applicable.

Excellent results were obtained with most of the polymers, elements and water. The measured data for the lithium borate and resin coated carbon TLD discs (BRUNSKILL, 1973) could not be compared with any calculated values due to the unknown formulation of the high temperature resin employed. The cleaved single crystals of lithium fluoride had measured coefficients 6-8% below the calculated values.

To allow the data for the commercial products to be assessed, TABLE 7.6 summarizes the measured mass attenuation coefficients for the products and the calculated coefficients for the materials being simulated. TABLE 7.7 gives the ratios of the measured coefficients to the calculated values of the 'real' material. In both tables data for the four energies are presented. The Alderson materials gave particularly poor results, the popular muscle substitute producing errors exceeding 25% at 10 keV. 'Temex' was better than predicted but still gave errors in excess of 15% at low energies.

	MATERIAL	MASS ATTENUATION COEFFICIENTS μ/ρ (m^2/kg)			
		9.8709 keV	17.4268 keV	59.57 keV	1.1732 MeV
(a)	ALDERSON FAT	.201	.0484	.0182	.00586
	ALDERSON MUSCLE	.395	.0833	.0185	.00573
	ALDERSON LUNG	.308	.0715	.0188	.00547
	SHONKA A-150	.430	.0948	.0200	.00639
	SHONKA C-552	.558	.107	.0186	.00590
	TEMEX	.455	.105	.0213	.00668
(b)	FAT	.255	.0608	.0196	.00658
	MUSCLE	.546	.110	.0205	.00647
	AIR	.518	.104	.0188	.00587

TABLE 7.6 THE (a) MEASURED AND (b) CALCULATED MASS ATTENUATION COEFFICIENTS FOR SOME COMMERCIAL PRODUCTS SIMULATING FAT, MUSCLE AND AIR

MATERIAL	MASS ATTENUATION COEFFICIENT RATIOS			
	9.8709 keV	17.4268 keV	59.57 keV	1.1732 MeV
ALDERSON FAT	0.79	0.80	0.93	0.89
ALDERSON MUSCLE	0.72	0.76	0.90	0.89
ALDERSON LUNG	0.56	0.65	0.92	0.85
SHONKA A-150	0.79	0.86	0.98	0.99
SHONKA C-552	1.08	1.03	0.99	1.01
TEMEX	0.83	0.95	1.04	1.03

TABLE 7.7 THE RATIOS OF THE MEASURED MASS ATTENUATION COEFFICIENTS FOR THE COMMERCIAL PRODUCTS TO THE CALCULATED COEFFICIENTS OF THE 'REAL' MATERIALS

TYPE	CONSTITUENTS AND PERCENTAGE WEIGHTS	% Cl
MS5	CB1/3PMS(84.87); P.V.C.(7.13); P.T.F.E.(8.00)	ZERO
	CB1/3PMS(85.23); P.V.C.(6.77); P.T.F.E.(8.00)	0.25
	CB1/2.5PMS(85.60); P.V.C.(6.40); P.T.F.E.(8.00)	0.50
FT5	CB1/0.5SMS(70.63); TPX(29.37)	ZERO
	CB1/0.35SMS(58.44); TPX(41.56)	0.25
	CB1/0.20SMS(50.00); TPX(50.00)	0.50
LN3	CB2/18PMS(91.89); P.V.C.(8.11)	ZERO
	CB2/18PMS(91.94); P.V.C.(8.06)	0.25
	CB2/18PMS(92.37); P.V.C.(7.63)	0.50
SB3	CB2(32.66); CALCIUM CARBONATE(67.34)	ZERO
	CB2(32.78); CALCIUM CARBONATE(67.22)	0.25
	CB2(32.89); CALCIUM CARBONATE(67.11)	0.50
IB1	CB1(74.50); P.V.C.(25.50)	ZERO
	CB1(74.84); P.V.C.(25.16)	0.25
	CB1(75.17); P.V.C.(24.83)	0.50
BR6	CB1/3PMS(89.44); P.V.C.(2.56); P.T.F.E.(8.00)	ZERO
	CB1/3PMS(89.84); P.V.C.(2.16); P.T.F.E.(8.00)	0.25
	CB1/3PMS(90.23); P.V.C.(1.77); P.T.F.E.(8.00)	0.50

TABLE 7.8 FORMULATIONS BASED ON EPOXY RESINS CONTAINING DIFFERENT CHLORINE CONCENTRATIONS

It was concluded from these measurements that the polymer based substitutes, provided the manufactured samples have good dispersion of fillers and are free from trapped air, yield excellent products. Epoxy resin systems can produce comparable results if the attenuation properties of the unfilled resins are first established.

The corrections in the theoretical filler proportions for epoxy resins containing differing chlorine levels are given in TABLE 7.8, and cover the formulations which have proved to be most useful in practical applications. In most cases the modifications are minimal; an example being SB3, requiring 67.34% calcium carbonate if the resin is chlorine-free, or 67.11% if 0.5% chlorine is present.

CHAPTER 8

SOME APPLICATIONS OF THE NEW SUBSTITUTES

In this chapter some of the possible applications of the substitutes will be explored and examples given of the dosimetric studies that have already been initiated. Detailed descriptions of individual studies will not be given, but a more general approach will be adopted in order that the diversity of the new systems is adequately covered.

8.1 THERMOLUMINESCENT DOSIMETRY

One of the attractions of the thermoluminescent dosimetry materials lithium fluoride and lithium borate has been their much publicised 'tissue equivalence' for photon interactions. This is particularly true of lithium borate systems which are frequently said to have superior equivalence to muscle than lithium fluoride. Their relative merits are put into perspective if the ratios of the calculated mass energy absorption coefficients of the dosimetry materials to those for muscle are derived. TABLE 8.1 shows these ratios for the two systems described above, together with those for two popular teflon (P.T.F.E.) disc dosemeters. It can be seen that discrepancies at low energies approaching 20% are found with the basic materials while the teflon loaded discs have similar discrepancies of 30%.

Six TLD formulations using lithium borate (0.1% Mn) as the basic material, were presented in Chapter 5 (TABLES 5.17 and 5.18). These were mixtures of the powdered lithium borate phosphor and

MATERIAL	COEFFICIENT RATIO		
	10 keV	1 MeV	100 MeV
LITHIUM BORATE ($Li_2B_4O_7$)	0.79	0.88	0.93
LITHIUM FLUORIDE (LiF)	1.19	0.84	0.92
TEFLON/5% LITHIUM BORATE	1.30	0.87	1.01
TEFLON/5% LITHIUM FLUORIDE	1.31	0.87	1.01

TABLE 8.1 MASS ENERGY ABSORPTION COEFFICIENT RATIOS FOR SOME TLD SYSTEMS COMPARED TO MUSCLE

a number of different powdered fillers, producing particulate systems simulating muscle, bone, liver and red marrow.

TL1 using aluminium (3.81%) & TL3 using calcium carbonate (1.7%)were found to be completely satisfactory in practice, giving essentially the same light output as the basic powder. TL1 was a muscle substitute, while TL3 represented liver.

TL2, another muscle substitute, was found to be difficult to produce due to the large quantity of P.T.F.E. (41.83%)making mixing difficult. An extremely useful dosemeter would be produced, particularly for low energy studies if solid teflon discs could be manufactured with the loading of lithium borate (58.17%) giving these relative proportions.

The bone substitutes, having the fillers calcium fluoride (49.34%) and calcium sulphate (63.86%)appear interesting and, if the TLD forms are used, could lead to useful data applicable to trabecular bone dosimetry.

Mixing the powders adequately will always be a difficult problem, especially as, with repeated use, the components tend to separate according to their relative mass densities and the dimensions of the particles. Despite these limitations the particulate systems could prove to be superior in low energy studies when the absorption properties of the dosemeter might strongly influence the results.

8.2 RADIATION DOSIMETRY IN DIAGNOSTIC RADIOLOGY

The new substitutes are ideally suited for dosimetric studies in diagnostic radiology, especially those materials which are easily manipulated into typical body or organ phantoms. With the wider range of substitutes that are now available more realistic phantoms may be readily manufactured giving a degree of simulation which has not been possible in the past.

An application which is currently being investigated is the measurement of skin dose during mammography. A series of breast shaped phantoms (FIGURE 8.1), constructed of fat, fat/water (50:50, by weight) and muscle substitutes, have been used to measure the skin doses delivered by the Mammomat and Senographe X-ray units. Using typical machine settings, surface and exit doses were measured with thermoluminescent dosemeters. The sites of the dosemeters are illustrated in TABLE 8.2, which also depicts in (a) the combined results from the two machines when the '50:50' mixture, BR6, was used. The two sets of figures represent the doses received during Xeroradiography (50 kV, 50 mAs) and conventional radiography. TABLE 8.2(b) shows the maximum skin doses delivered by the Senographe machine when breast phantoms simulating the range of possible breast tissues, were employed. In this case, maximum doses increased from 3.4 to 4.2 rads as the phantom material was changed from a fat to a muscle substitute.

These experiments, which show that significant doses are

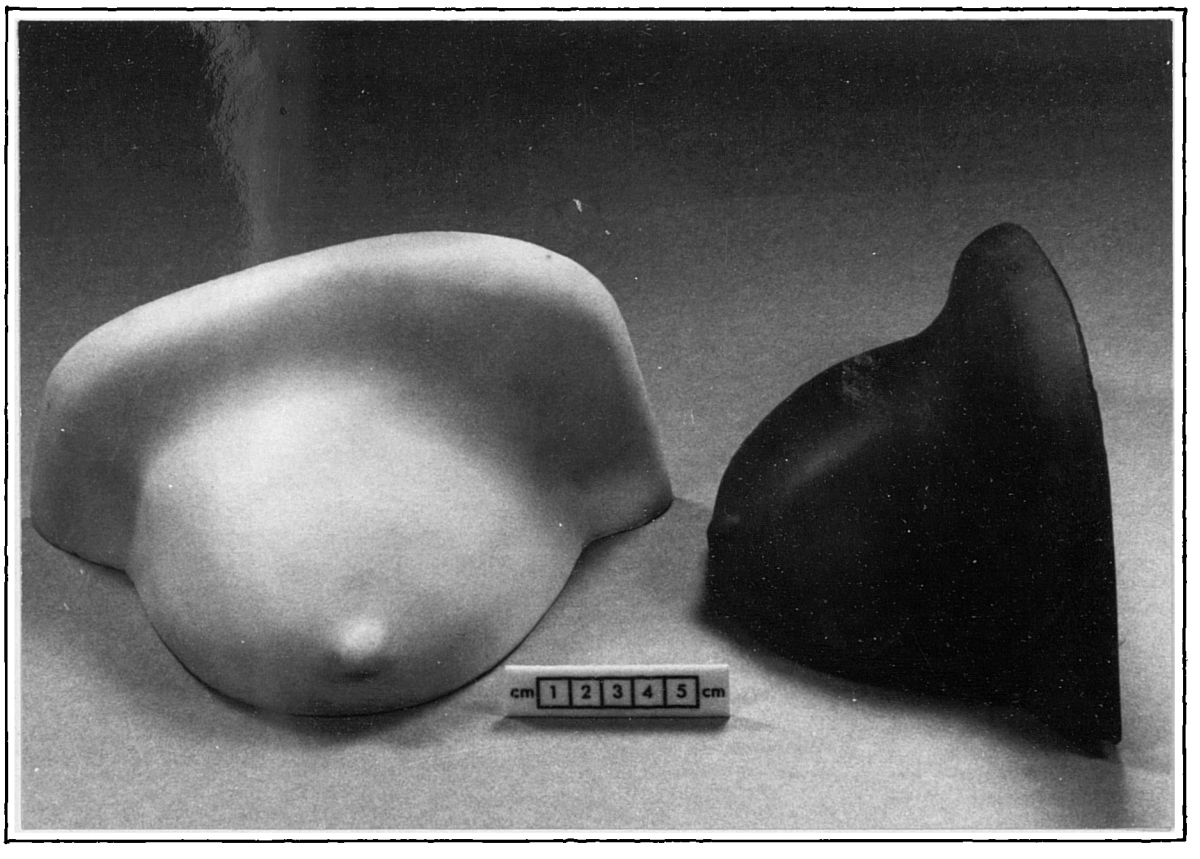

FIGURE 8.1 TWO BREAST PHANTOMS USED FOR DOSIMETRY IN MAMMOGRAPHY PROCEDURES

(a) SENOGRAPHE AND MAMMOMAT : 'BREAST' MATERIAL - BR6

MACHINE	SETTING	DOSES IN RADS					
		A	B	C	D	E	F
SENOGRAPHE	30kV., 45mAs	2.9	3.6	3.0	0.58	0.70	<0.02
MAMMOMAT	50kV, 50mAs	4.2	6.4	8.4	1.6	3.1	0.22
	28kV, 400mAs	8.8	12.0	17.0	2.6	3.6	0.09

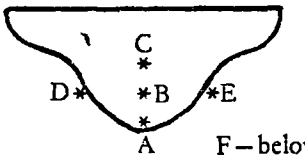

F – below phantom

(b) SENOGRAPHE ONLY

BREAST PHANTOM MATERIAL	MAX. DOSE (rads) (POSITION B)
'FAT'(FT5)	3.4
'BREAST'(BR6)	3.6
'MUSCLE'(MS2 & MS5)	4.2

TABLE 8.2 EXPERIMENTAL RESULTS OF MAMMOGRAPHY DOSE MEASUREMENTS

recorded during this important diagnostic procedure, are essential if long-term patient screening investigations are contemplated. An extension of these measurements is being planned so that a wider range of X-ray machines and techniques are considered.

8.3 TEST OBJECTS

Test objects are frequently required in diagnostic X-ray departments for checking the resolution of radiographs when parameters such as beam quality, film type or processing are varied. Many types of test objects have been used in the past varying from metal step wedges to strips of human or animal tissue embedded in wax. As the results are to be applied to the clinical situation it is obviously better to employ objects which closely resemble, in their photon absorption and scattering characteristics, the biological materials likely to be encountered.

Two different test objects have already been produced using the new materials, but many more could be designed once the different tissues to be resolved have been specified.

The first of the two new objects was a model of a hand requested for an investigation of the radiographic contrast obtained from different types of film. An epoxy resin based muscle substitute was cast around the skeleton of a hand and provided a simple, yet effective object for these tests.

More elaborate test objects have been designed for checking the resolution of mammography X-ray machines. FIGURE 8.2 shows the contents of the latest version, Mk IV, in a series which has undergone many modifications in their development. Step wedges of fat and muscle substitutes, 'fat' monofilaments, calcium phosphate cylinders, aluminium oxide spheres and powdered

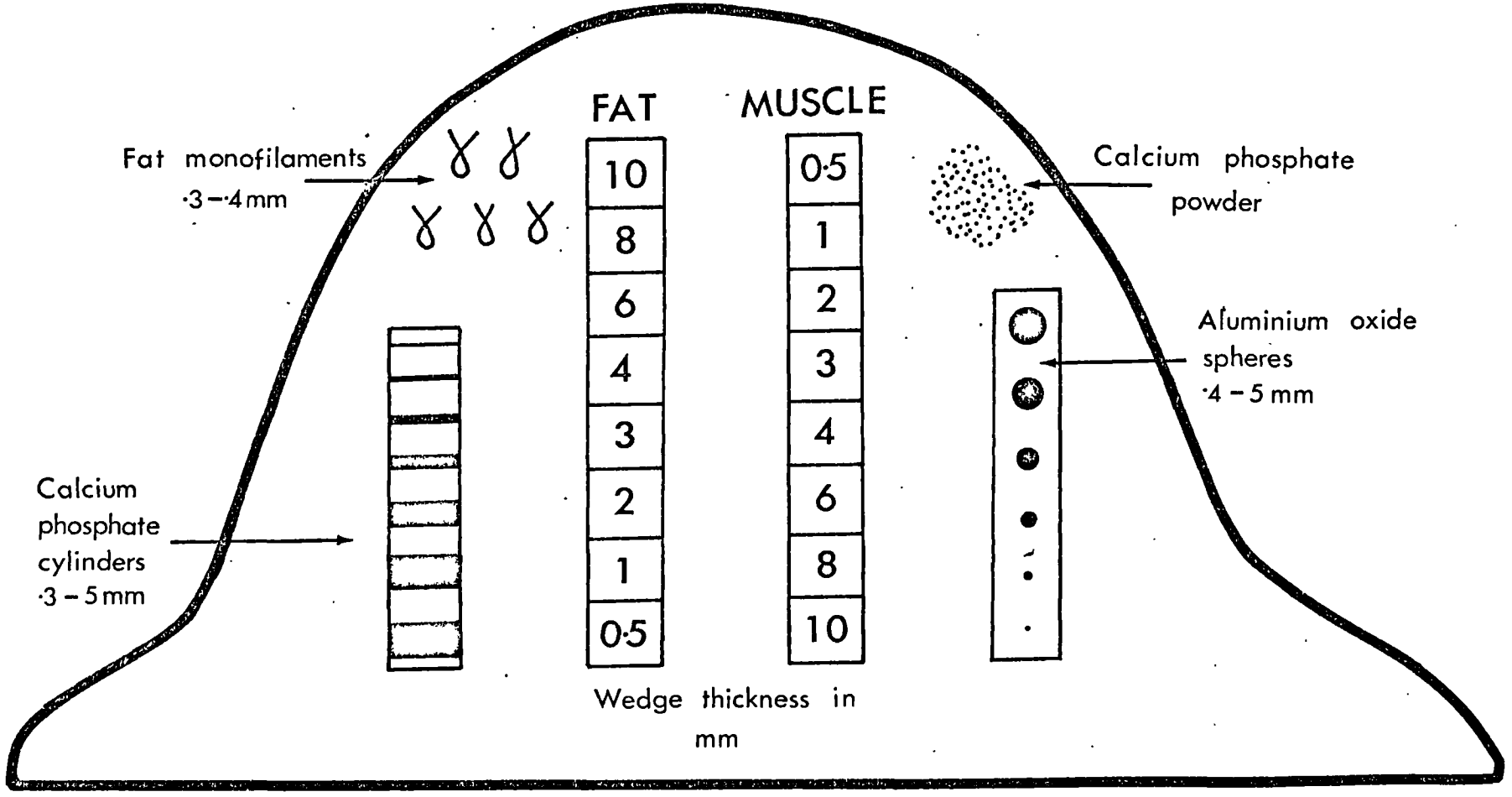

FIGURE 8.2 CONTENTS OF THE MK IV MAMMOGRAPHY TEST OBJECT

calcifications are all contained within a breast shaped phantom constructed of a 'breast tissue' substitute. These objects have already been used to check the resolution of the X-ray machines mentioned in the previous section.

Test objects are also used in other disciplines and are not confined to diagnostic radiology. An example is their use in gamma ray scanning procedures. A large bone step wedge has been constructed from a bone substitute, SB3, and is being used in the calibration of the nucleonic equipment designed for bone density studies.

The application of the substitutes to the manufacture of test objects is very important and should contribute to the improvement of radiographic techniques.

8.4 'AIR EQUIVALENT' IONIZATION CHAMBERS

A number of air substitutes were tabulated in Chapter 5 (TABLE 5.15) for use in the construction of the 'air equivalent' walls required in thimble ionization chambers. A variety of base materials were considered, in the hope that the poor selection of existing air substitutes could be enhanced.

In order that the substitute AR1 could be tested experimentally, the thimble of a 0.6 cc Farmer Ionization Chamber was replaced by a thimble constructed of this electrically conducting material (Volume Resistivity 10^4 ohm.cm). The mechanical properties of AR1 allowed the thimble to be readily machined to the necessary tolerances. Preliminary results of a comparison of this modified version to a conventional Farmer Chamber are promising, and have indicated a more uniform response at low photon energies for the new chamber.

Tests on AR1 and other suitable materials are in progress which should ultimately lead to improved dosimetric systems.

8.5 RADIONUCLIDE DOSIMETRY

The water, acrylic and epoxy resin based substitutes may readily be applied to the study of the dosimetry of organs containing radionuclides. If the shape and chemical composition of the organ is accurately known, an experimental shell replica may be constructed into which the substitute containing the radionuclide, may be poured. Dosemeters placed at defined points within the volume will permit the dose distribution to be plotted.

Water based substitutes are ideal for water soluble solid or liquid radionuclides as the procedure may be repeated. Acrylic or epoxy resin based substitutes may be used with radionuclides in powder form, when the active material is added when the substitute is in the liquid phase.

FIGURE 8.3 shows a liver phantom made up of a thin sealed acrylic shell containing five tubes machined to hold columns of TLD capsules. The phantom was designed for water based substitutes such as LV2 and the TLD powder TL3. FIGURE 8.4 shows a typical set of isodose curves resulting when technetium - 99m (22.2mCi) was added to the aqueous liver substitute (1500ml). The dosemeters were left in position for 3 days when the residual activity had decayed to below 0.2%.

Future experiments along these lines are planned for other radionuclides and organs, in particular thyroid and kidneys. In its present form dose distributions may only be investigated in the

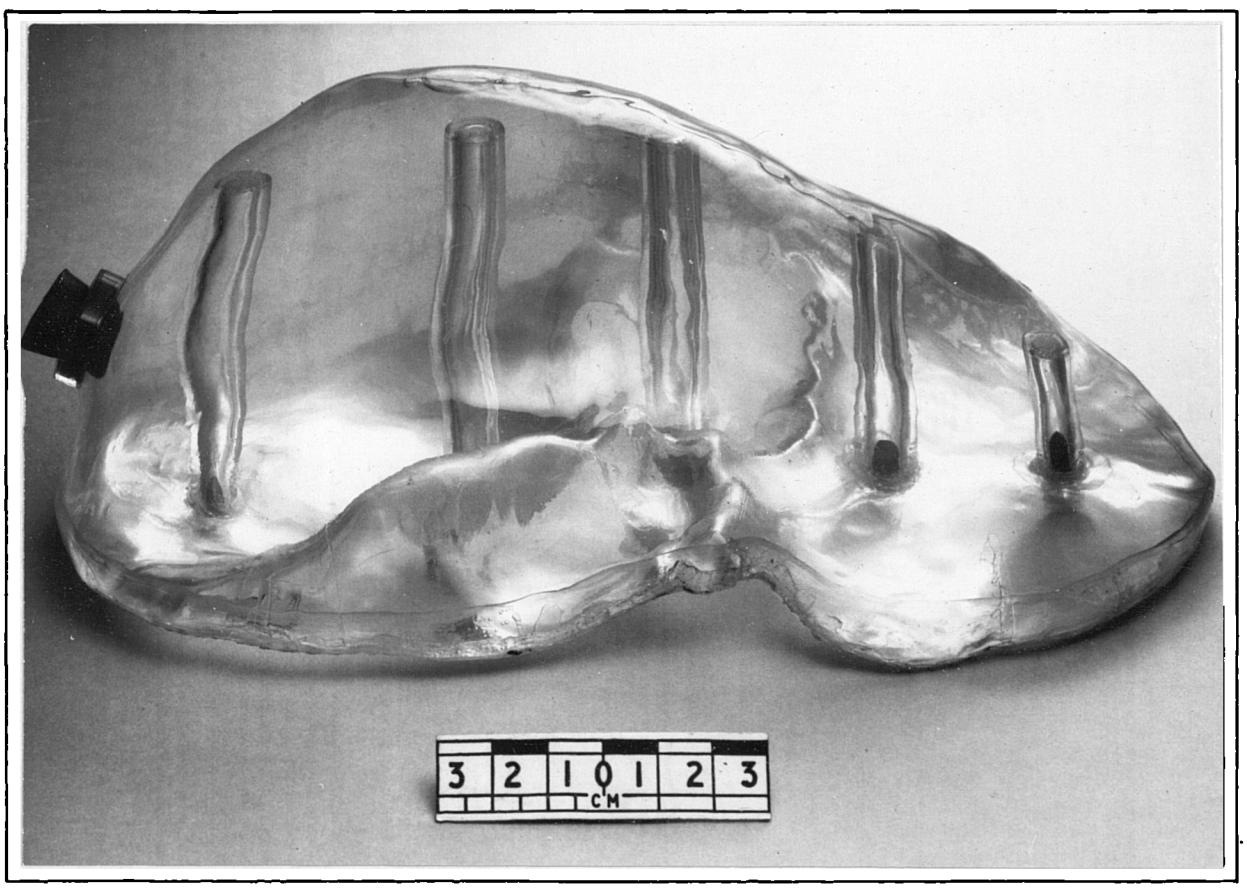

FIGURE 8.3 A LIVER PHANTOM FOR RADIONUCLIDE DOSIMETRY

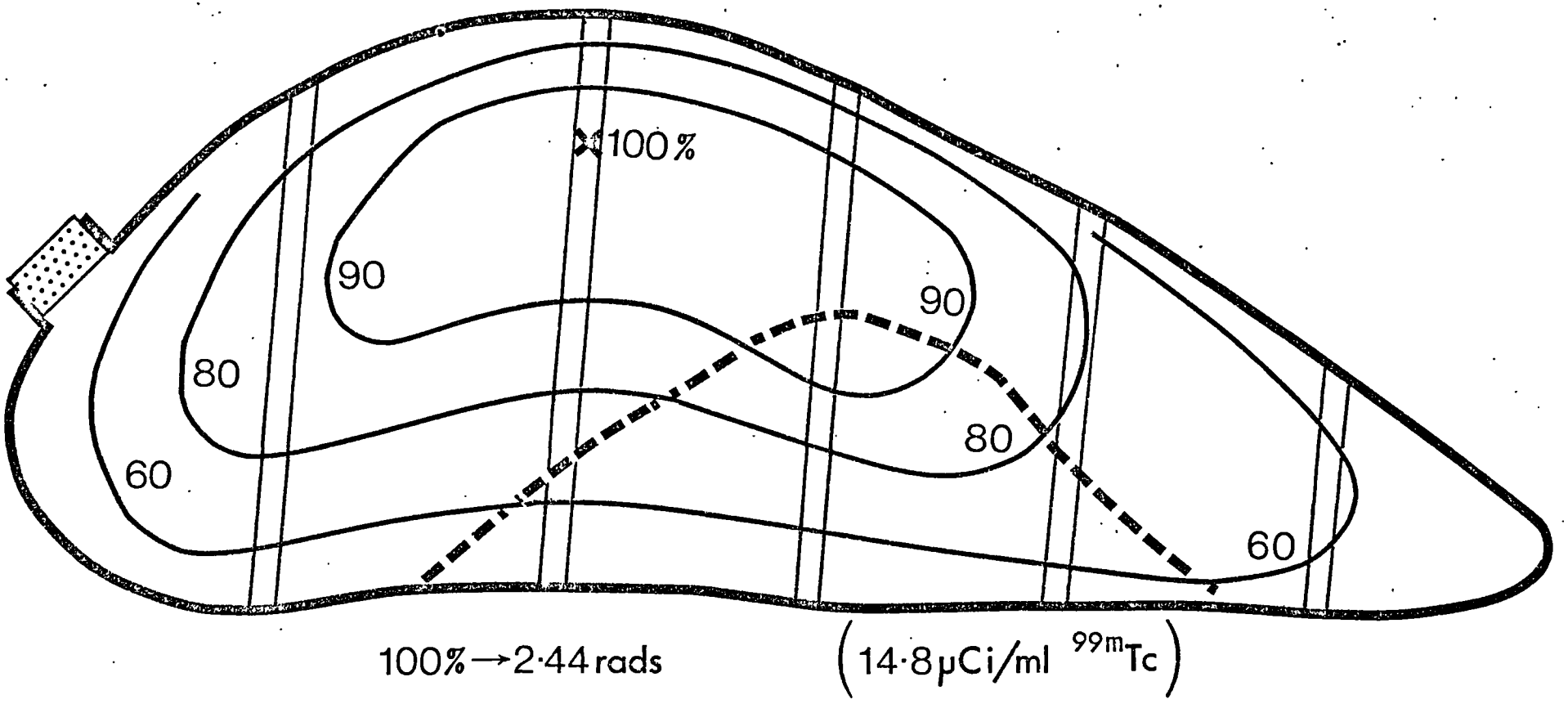

FIGURE 8.4 ISODOSE CURVES IN THE CENTRAL PLANE OF THE LIVER PHANTOM (LONG AXIS) FOR TECHNITIUM-99m

situation when the radionuclides are uniformly distributed. Non-uniform concentrations may be considered if the phantom is constructed in small solid blocks or as a compartmented shell, each block or compartment containing the requisite activity.

8.6 RADIONUCLIDE COUNTING STANDARDS

Many clinical radionuclide tests rely on counting standards as a means of calibrating nucleonic equipment. The new substitutes allow standards to be made for a wider range of tissues and organs than was feasible in the past. For example realistically shaped thyroid phantoms, either completely solid or shells containing liquids with a known activity of the relevant radioiodine, could be constructed and used for calibrating thyroid uptake counters.

At the request of the National Radiological Protection Board (BAILEY, 1974) a skull phantom has been manufactured in the bone substitute, SB3. During the manufacturing process, a known quantity of lead-210 will be added to the epoxy resin and filler when the mixture is in the liquid phase. After adequate mixing and evacuation the material will be poured into a rubber mould and left to harden. The resulting model will ultimately be used as a counting standard in lead-210 retention tests on miners.

8.7 BONE MODELS

The commercial body phantoms currently being sold all suffer from a serious dimensional defect, because small Asian skeletons are embedded in large European sized bodies. The 'inner bone' substitutes, simulating the mixture of trabecular bone and red marrow was devised as a possible solution to the problem. A complete full sized skeleton of 'inner bone' could be manufactured and then coated in a cortical bone substitute to produce a skeleton acceptable in macroscopic dosimetry. In the next section it will be seen that this scheme has been used successfully in a modified form.

Experimental studies evaluating the X-ray doses received in cavities within trabecular bone are in progress. The general procedure is to construct cavities of varying sizes in small blocks of bone and muscle substitutes. TLD powder is then added to the cavities and the absorbed doses assessed when the blocks are irradiated with X-rays. Similar tests are feasible using the radiation from radionuclides dispersed within the substitute blocks instead of external sources.

The possibility of using polyurethane based bone substitutes to produce foams which closely resemble trabecular bone is also being investigated.

8.8 REALISTIC BODY PHANTOMS

The new range of tissue substitutes make the manufacture of sophisticated body phantoms, once the exclusive domain of large commercial enterprises, within the scope of most hospital physics laboratories. The fact that any tissues of known chemical composition can now be simulated means that more realistic phantoms may be constructed.

FIGURE 8.5 shows a mid-thoracic body section (2 cm thick) that was manufactured from the new substitutes. The outlines of the principal tissues were drawn onto a slab of expanded polystyrene. Bone, lung and fat volumes were cut from the block and epoxy resin based substitutes poured into the cavities. In the case of the bone volumes, the edges of the cavities in the polystyrene were first coated, to a few millimetres thick, with a cortical bone substitute (SB1) and then filled with an inner bone material. When the resins had hardened the remaining polystyrene was removed with acetone and the other substitutes (muscle and fat) were poured into the relevant cavities. When these materials had hardened the whole section was 'faced' on a lathe to produce a slab with parallel, plane faces. In this fashion a complete body phantom, comprising of 2 cm thick sections could be built up in a reasonably short time.

This technique could be used for distributions of many more types of tissues, so long as each set of non-adjacent volumes are

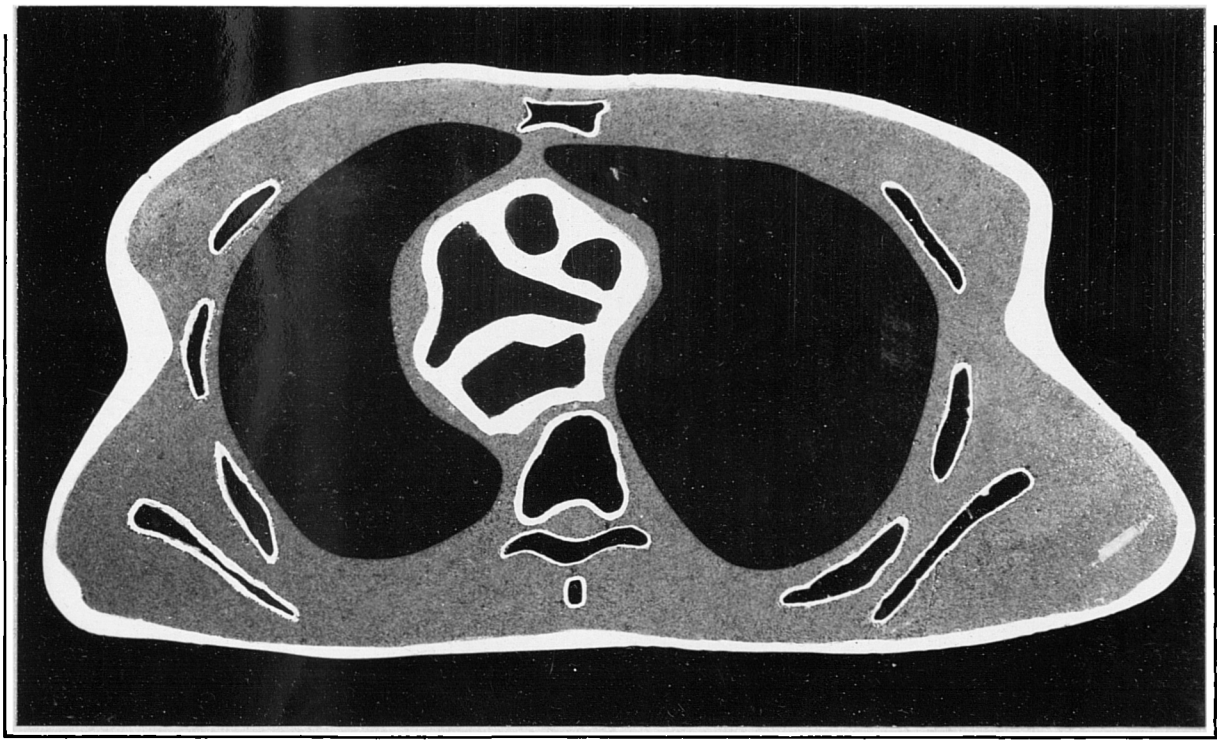

FIGURE 8.5 PHOTOGRAPH OF A MID-THORACIC BODY SECTION

completed and allowed to harden before the next is considered.

A more flexible variation on this theme might be the use of small blocks, perhaps interlocking, representing the important tissues. These blocks would be built into any array producing sections which could be tailored to individual patients.

Body phantoms made up in this segmented fashion, with either fixed or variable geometry, are particularly useful in dosimetry applied to radiotherapy or diagnostic radiology as dosemeters can easily be sandwiched between sections or within individual tissues and organs. They are also applicable in radiological protection studies when radiation scatter distributions similar to practical situations are frequently required.

From these discussions it can be seen that the number of applications of the new substitutes is due principally to their manufacturing flexibility and to the diversity of the tissues that can now be simulated. It is hoped that future applications will demand even more tissue substitutes to be formulated, so that the full potential of the new selection procedures may be realized.

CHAPTER 9

CONCLUSIONS AND SUGGESTIONS FOR FUTURE WORK

This study has shown that although the choice of substitutes is extensive, many of the existing products give poor simulation for both photon and electron interactions. This is particularly true at low photon energies when discrepancies exceeding 20% frequently exist between the attenuation and energy absorption coefficients for the substitute and the material being simulated.

Many published substitutes, claimed to be'tissue equivalent', have unknown, variable or poorly defined chemical compositions, so that comparisons are difficult. Pressdwood is a typical example which is still used as a 'muscle equivalent' material, although 30 years ago it was realized that its variable composition made it unacceptable for reliable measurements. The chemical composition of many commercial products are frequently shrouded in secrecy, so that only attenuation measurements or chemical analyses can establish their characteristics.

Lung and bone substitutes are possibly the least acceptable, as materials of the correct mass density, irrespective of composition, are selected and used in dosimetric studies applied directly to clinical situations.

Despite the fact that much effort has been directed to the improvement of accuracy in the measuring systems, comparatively

little effort has been applied to the improvement of the materials being used. It seems curious that dosemeters capable of recording doses to within 1 or 2% are employed in phantoms constructed of substitutes differing in attenuation characteristics from those of the true tissue by more than 20%. No solid muscle substitute, probably the most commonly used material, has been developed during the past 12 years, although in that time many new polymers and resins have been introduced.

The types of tissues considered also requires some comment. Existing substitutes have been limited, almost exclusively, to muscle, lung and bone tissues. Most tissues and organs appear to be composed basically of fat, protein, water and trace elements. The relative proportions of fat and water are very important and strongly govern the attenuation properties of the tissues. Typically. these proportions (by weight) can vary from 1.6% fat and 77.8% water found in the spleen, to 10.0% fat and 72.7% water in the heart (TIPTON, 1970). Surprisingly few fat substitutes have been developed, and polyethylene, giving 20% errors in attenuation and energy absorption coefficients at low energies, remains the most popular material. Consequently the available materials do not adequately cover the different types of tissues likely to require dosimetric investigations.

Attenuation and energy absorption coefficients, electron stopping and angular scattering powers, from 10 keV to 100 MeV, were calculated for all of the published substitutes with known composition.

The computation procedures, described in Chapter 1, appeared to be adequate. Recent work by KIM (1973) on the derivation of the density correction in stopping power calculations requires investigation. If this new procedure is acceptable, the accuracy of absolute stopping power data at high energies for compounds will be greatly improved.

Of the nearly 80 substitutes described in the literature, the only systems having low energy (10-300 keV) attenuation and energy absorption coefficients within 5% of the simulated material were as follows:

MUSCLE: LIQUID SYSTEMS (FRIGERIO and SAMPSON, 1969)
M3 (MARKUS, 1956)
POWDER SYSTEMS (SPIERS, 1943)
WATER

FAT: TRIOLEIN

AIR CONDUCTING PLASTIC (SHONKA et al., 1958)

The number of acceptable materials for electron interactions is similarly sparse. The systems having stopping and angular scattering powers within 5% of the simulated material, for the energies 10 keV-100 MeV, were as follows:

MUSCLE: LIQUID & GEL SYSTEMS (ROSSI & FAILLA, 1956) (and derivatives)
LIQUID SYSTEMS (FRIGERIO & SAMPSON, 1969)
WATER

FAT: POLYETHYLENE
POLYSTYRENE
TRIOLEIN

BONE: RESIN SYSTEM (POLL, 1972)

The choice of substitute for a particular investigation is frequently governed by finance, availability and the previous studies performed at the centre, rather than the need for perfect simulation. From the poor results indicated by the calculated data it is indeed fortunate that water has remained the most popular muscle substitute.

Most of the important formulated substitutes such as MIX D, TEMEX, RANDO and LINCOLNSHIRE BOLUS, were based on effective atomic numbers, usually only for photoelectric interactions. As large errors occurred at these low energies, this quantity, or its manipulation, was put in question. An evaluation of the techniques adopted by the authors showed that a combination of both these factors contributed to the discrepancies. It was found that better agreement resulted from the use of the quantity $\overline{Y}(x)$, or $n_o [\overline{Z}(x)]^x$ with the values of x for the photoelectric process higher than normally employed. The analysis of Z-dependence provided useful data for all of the photon and electron interactions, enabling these quantities to be applied more widely.

The two new selection procedures and their associated computer programs have both been extremely successful, yielding excellent formulations for every simulation problem considered. This

success was, in part, due to the large library of compounds scanned at each run. In the library, the inorganic compounds and the polymers have proved to be most useful, being readily available in the finely ground powders required for homogeneous samples. The extensive range of organic compounds, which because of their diversity was expected to provide many acceptable formulations, was only a limited success, due probably to the small variation in attenuation properties between compounds. The complete library of compounds should enable the elemental equivalence method to be evaluated in more detail.

Many hundreds of new two-component substitutes have been formulated and the 77 systems presented in Chapter 5 represent the best formulae, based upon radiation characteristics and manufacturing feasibility. A wide range of tissues was considered so that the flexibility of the selection procedures could be evaluated while at the same time providing a more comprehensive set of substitutes than was currently available.

The manufacture of these substitutes produced some interesting problems. Wax based materials were found to be extremely difficult to produce in homogeneous, air-free samples, and should not be used in dosimetric investigations. Polymer based materials, requiring specialized equipment beyond the scope of Hospital Physics Laboratories, were always difficult to manufacture, and only the large commercial organisations, such as I.C.I., had the

necessary expertise to provide acceptable samples. The need for accurate weighing of the components, adequate mixing and freedom from contamination was beyond the capabilities of many smaller firms. Epoxy resins overcame most of these problems, when the products could readily be manipulated with modest equipment. The manufacturing procedures that were developed for the resin systems proved to be reliable so long as the viscosity of the liquid resin, after the fillers had been added, permitted efficient de-gassing without filler separation. Considerable exotherms were experienced with large volumes of epoxy based substitutes having small filler concentrations.

The most effective quality testing procedures were Xeroradiography and specific gravity determinations, providing the relevant important information quickly and with reasonable accuracy.

High precision, low energy photon attenuation measurements confirmed the reliability of the new selection procedures and provided a means of testing the attenuation properties of materials with unknown composition. A contaminant of high atomic number was discovered in the epoxy resin systems and later confirmed by the manufacturers. Chemical analyses of this resin by two independent organisations did not indicate this contaminant. The attenuation measurements could be used to establish the properties of a large batch of resin so that subsequent formulations would be within the desired limits of accuracy. High atomic number contaminants were not present in the polymers investigated showing

that these materials are eminently suitable in powdered form as fillers.

The measurement of electron stopping and angular scattering powers for this range of materials would yield important data for clinical dosimetry. Due to relatively small variation in stopping powers between different materials, very accurate experimental procedures are necessary. The possibility of using conversion electrons from radionuclide sources, together with a solid state detector, is currently being evaluated.

The diversity of the new substitutes is indicated by the many applications given in the previous chapter. The use of the materials in radionuclide dosimetry, counting standards and in the formation of realistic body phantoms with fixed or variable geometry, appear particularly promising. Thermoluminescent materials could easily benefit from an extensive analysis using the ZEDIT programs.

A possible improvement to the whole concept of tissue substitutes could result from the formulation of three epoxy resin based substitutes simulating respectively fat, protein and water. These systems could then be added together in any desired proportions to simulate any specific organ or tissue. Trace elements could be added as required and mass density corrections made by the addition of microspheres or foaming agents. This procedure would greatly simplify the practical problems of formulating substitutes for each tissue. Reliable data on the composition of

tissues and organs are required if this scheme is to be successful.

It is hoped that this study will stimulate more interest in substitute materials and will result in improved clinical dosimetry. If the chemical compositions of the tissue or organ to be simulated and the base material are known precisely, then either of the new selection procedures should produce acceptable formulations, simulating to within 1-2% for all of the photon and electron interactions. This degree of simulation is obligatory if the full advantages of modern dosimetric measurements are to be utilized.

APPENDIX 1

LIST OF SYMBOLS AND PHYSICAL CONSTANTS

$A(M)$	Atomic weight (Molecular weight)
a_i	Polynomial coefficients
α_i	Fractional electron content of i^{th} element or compound
β	v/c
β_A, β_B	Fractions $[F(w, C)]$ - FIGURE 3.6
C	General term - 'coefficient' or 'power'
c	Velocity of Light
δ	Density correction
E	Energy
f	Fitting Ratio
I	Mean excitation energy (eV)
$\langle I \rangle$	Adjusted mean excitation energy (eV)
K	Energy Ratio
k	A constant
ℓ	Path Length
m	Slope
m_e	Rest mass of electron (0.511006 MeV)
$\bar{\Theta}^2/\rho\ell$	Mass angular scattering power
S/ρ	Mass stopping power
$(S/\rho)_{col}$	Collision mass stopping power
$(S/\rho)_{rad}$	Radiation mass stopping power
μ	'Narrow beam' linear attenuation coefficient
μ/ρ	Mass attenuation coefficient
μ_{en}/ρ	Mass energy absorption coefficient
N_A	Avogadro's number (6.02252×10^{26} $kmol^{-1}$)
$(N)_A, (N)_B$	Total number of electrons in compounds A & B
n_i	Number of electrons in i^{th} element
n_o	Electron density
$(n_o)_A, (n_o)_B$	Electron densities of compounds A & B
ω	Weight proportion

p_e	Momentum of electron
p, q	Molecular proportions
ϕ_A, ϕ_B	Fractions $[F(n_o, \alpha_i)]$ - FIGURE 3.10
π	Constant - 3.14159
ψ_A, ψ_B	Fractions - $F(\alpha_i, [\bar{Z}(x)]^X)$ - FIGURE 3.11
R	$\bar{Z}$-Power Ratio
r_e	Electron radius (2.81777×10^{-15} m)
ρ	Mass density
σ	Photon cross section
τ	Kinetic energy in units of $m_e c^2$
$\bar{\Theta}^2$	Mean square scattering angle (electrons)
v	Velocity
x	$\bar{Z}$-exponent
$\bar{Y}(x)$	Product of n_o and $[\bar{Z}(x)]^X$
Z	Atomic number
$\langle Z/A \rangle$	Mean ratio Z/A for compound
$\bar{Z}(x)$	Effective atomic number
$[\bar{Z}(x)]^X$	$\bar{Z}$-Power (using electron fractions)
$[\bar{Z}(x)]^X_w$	$\bar{Z}$-Power (using weight proportions)

APPENDIX 2

THE ELEMENTAL DATA USED IN THE STUDY

Z	ELEMENT		ATOMIC WT.	Z	ELEMENT		ATOMIC WT.
1	HYDROGEN	(H)	1.00797	37	RUBIDIUM	(RB)	85.47
2	HELIUM	(HE)	4.0026	38	STRONTIUM	(SR)	87.62
3	LITHIUM	(LI)	6.939	39	YTTRIUM	(Y)	88.905
4	BERYLLIUM	(BE)	9.0122	40	ZIRCONIUM	(ZR)	91.22
5	BORON	(B)	10.811	41	NIOBIUM	(NB)	92.906
6	CARBON	(C)	12.01115	42	MOLYBDENUM	(MO)	95.94
7	NITROGEN	(N)	14.0067	47	SILVER	(AG)	107.870
8	OXYGEN	(O)	15.9994	48	CADMIUM	(CD)	112.40
9	FLUORINE	(F)	18.9984	50	TIN	(SN)	118.69
10	NEON	(NE)	20.183	51	ANTIMONY	(SB)	121.75
11	SODIUM	(NA)	22.9898	52	TELLURIUM	(TE)	127.60
12	MAGNESIUM	(MG)	24.312	53	IODINE	(I)	126.9044
13	ALUMINIUM	(AL)	26.9815	55	CAESIUM	(CS)	132.905
14	SILICON	(SI)	28.086	56	BARIUM	(BA)	137.34
15	PHOSPHORUS	(P)	30.9738	57	LANTHANUM	(LA)	138.91
16	SULPHUR	(S)	32.064	58	CERIUM	(CE)	140.12
17	CHLORINE	(CL)	35.453	62	SAMARIUM	(SM)	150.35
18	ARGON	(AR)	39.948	63	EUROPIUM	(EU)	151.96
19	POTASSIUM	(K)	39.102	64	GADOLINIUM	(GD)	157.25
20	CALCIUM	(CA)	40.08	65	TERBIUM	(TB)	158.924
21	SCANDIUM	(SC)	44.956	67	HOLMIUM	(HO)	164.930
22	TITANIUM	(TI)	47.90	68	ERBIUM	(ER)	167.26
23	VANADIUM	(V)	50.942	69	THULIUM	(TM)	168.934
24	CHROMIUM	(CR)	51.996	70	YTTERBIUM	(YB)	173.04
25	MANGANESE	(MN)	54.9380	71	LUTETIUM	(LU)	174.97
26	IRON	(FE)	55.847	74	TUNGSTEN	(W)	183.85
27	COBALT	(CO)	58.9332	77	IRIDIUM	(IR)	192.2
28	NICKEL	(NI)	58.71	78	PLATINUM	(PT)	195.09
29	COPPER	(CU)	63.54	79	GOLD	(AU)	196.967
30	ZINC	(ZN)	65.37	80	MERCURY	(HG)	200.59
31	GALLIUM	(GA)	69.72	82	LEAD	(PB)	207.19
32	GERMANIUM	(GE)	72.59	83	BISMUTH	(BI)	208.980
33	ARSENIC	(AS)	74.9216	84	POLONIUM	(PO)	(210)
34	SELENIUM	(SE)	78.96	88	RADIUM	(RA)	(226)
35	BROMINE	(BR)	79.909	90	THORIUM	(TH)	232.038

AVOGADROS NUMBER : 6.02252×10^{26} KMOL^{-1}

APPENDIX 3

A TABULATION OF THE COMPOUND LIBRARY

	NAME	FORMULA
1	ALUMINIUM	AL
2	ALUMINIUM CARBIDE	AL_4C_3
3	ALUMINIUM FLUORIDE	ALF_3
4	ALUMINIUM NITRIDE	ALN
5	ALUMINIUM OXIDE	AL_2O_3
6	ALUMINIUM PHENOXIDE	$ALC_{18}H_{15}O_3$
7	ALUMINIUM ORTHOPHOSPHATE	$ALPO_4$
8	ALUMINIUM SILICATE (A)	AL_2SIO_5
9	ALUMINIUM SILICATE (B)	$AL_6Si_2O_{13}$
10	ALUMINIUM SULPHATE	$AL_2S_3O_{12}$
11	BORON	B
12	BORON NITRIDE	BN
13	BORON OXIDE	B_2O_3
14	BORON TRISULPHIDE	B_2S_3
15	CALCIUM ALUMINATE (A)	$CAAL_2O_4$
16	CALCIUM METABORATE	CAB_2O_4
17	CALCIUM TETRABORATE	CAB_4O_7
18	CALCIUM CARBIDE	CAC_2
19	CALCIUM CARBONATE (ARGONITE)	$CACO_3$
20	CALCIUM CARBONATE (CALCITE)	$CACO_3$
21	CALCIUM FLUORIDE	CAF_2
22	CALCIUM HYDRIDE	CAH_2
23	CALCIUM HYDROXIDE	CAO_2H_2
24	CALCIUM LACTATE	$CAC_6H_{20}O_{11}$
25	CALCIUM LAURATE	$CAC_{24}H_{46}O_5$
26	CALCIUM NITRIDE	CA_3N_2
27	CALCIUM OLEATE	$CAC_{36}H_{66}O_4$
28	CALCIUM OXIDE	CAO
29	CALCIUM PEROXIDE	CAO_2
30	CALCIUM ORTHOPHOSPHATE	$CA_3P_2O_8$
31	CALCIUM METASILICATE (A)	$CASIO_3$
32	CALCIUM METASILICATE (B)	$CASIO_3$
33	CALCIUM STEARATE	$CAC_{36}H_{70}O_4$
34	CALCIUM SULPHATE	$CASO_4$
35	CARBON	C
36	CARBON SULPHIDE	CS
37	CHROMIUM	CR
38	CHROMIUM CARBIDE	CR_3C_2
39	CHROMOUS FLUORIDE	CRF_2
40	CHROMIC FLUORIDE	CRF_3
41	CHROMIUM NITRIDE	CRN
42	CHROMIUM SESQUIOXIDE	CR_2O_3
43	CHROMIUM DIOXIDE	CRO_2
44	HYDRAZINE DIHYDROCHLORIDE	$N_2H_6CL_2$
45	HYDRAZINE SULPHATE	$N_2H_6SO_4$
46	HYDROXYLAMINE HYDROCHLORIDE	NH_4OCL
47	HYDROXYLAMINE SULPHATE	$N_2H_8O_6S$
48	LITHIUM AMIDE	$LINH_2$
49	LITHIUM METABORATE	$LIBO_2$
50	LITHIUM CARBONATE	LI_2CO_3
51	LITHIUM FLUORIDE	LIF
52	LITHIUM HYDRIDE	LIH
53	LITHIUM HYDROXIDE	LIOH
54	LITHIUM LAURATE	$LiC_{12}H_{23}O_2$
55	LITHIUM MYRISTATE	$LIC_{14}H_{27}O_2$
56	LITHIUM NITRATE	$LINO_3$
57	LITHIUM NITRIDE	LI_3N
58	LITHIUM OXIDE	LI_2O
59	LITHIUM PALMITATE	$LIC_{16}H_{31}O_2$
60	LITHIUM ORTHOPHOSPHATE	LI_3PO_4
61	LITHIUM ORTHOSILICATE	LI_4SIO_4
62	LITHIUM METASILICATE	LI_2SIO_3
63	LITHIUM SODIUM FLUOALUMINATE	$LI_3NA_3AL_2F_{12}$
64	LITHIUM STEARATE	$LIC_{18}H_{35}O_2$
65	LITHIUM SULPHATE	LI_2SO_4
66	MAGNESIUM	MG
67	MAGNESIUM ALUMINATE	$MGAL_2O_4$
68	MAGNESIUM CARBONATE	$MGCO_3$
69	MAGNESIUM CHLORIDE	$MGCL_2$
70	MAGNESIUM FLUORIDE	MGF_2
71	MAGNESIUM HYDROXIDE	MGO_2H_2
72	MAGNESIUM MYRISTATE	$MGC_{28}H_{54}O_4$
73	MAGNESIUM NITRIDE	MG_3N_2
74	MAGNESIUM OXIDE	MGO
75	MAGNESIUM PALMITATE	$MGC_{32}H_{62}O_4$
76	MAGNESIUM PYROPHOSPHATE	$MG_2P_2O_7$
77	MAGNESIUM METASILICATE	$MGSIO_3$
78	MAGNESIUM SILICIDE	MG_2SI
79	MAGNESIUM SULPHATE	$MGSO_4$
80	MANGANESE	MN
81	MANGANESE FLUORIDE	MNF_2
82	MANGANESE OXIDE (2)	MNO
83	MANGANESE OXIDE (2,3)	MN_3O_4
84	MANGANESE OXIDE (3)	MN_2O_3
85	MANGANESE DIOXIDE	MNO_2
86	MANGANESE PYROPHOSPHATE	$MN_2P_2O_7$
87	MANGANESE PHOSPHIDE	MNP
88	MANGANESE DIPHOSPHIDE	MN_3P_2
89	MANGANESE METASILICATE	$MNSIO_3$
90	MANGANESE SILICIDE (1)	MN_2SI
91	MANGANESE SILICIDE (2)	MNSI
92	MANGANESE SULPHATE	$MNSO_4$
93	PHOSPHORUS HEPTASULPHIDE	P_4S_7
94	POTASSIUM AZIDE	KN_3
95	POTASSIUM METABORATE	KBO_2
96	POTASSIUM CHLORATE	$KCLO_3$
97	POTASSIUM PERCHLORATE	$KCLO_4$
98	POTASSIUM CHLORIDE	KCL
99	POTASSIUM CHROMATE	K_2CRO_4
100	POTASSIUM CITRATE	$K_3C_6H_7O_8$
101	POTASSIUM FLUOBORATE	KBF_4
102	POTASSIUM FLUOSULPHONATE	$KFSO_3$
103	POTASSIUM MAGNESIUM SULPHATE	$K_2MG_2S_3O_{12}$
104	POTASSIUM TRIOXIDE	K_2O_3
105	POTASSIUM SUPEROXIDE	KO_2
106	POTASSIUM 1-PHENOL-2-SULPHONATE	$KC_6H_7O_5S$
107	POTASSIUM 1-PHENOL-4-SULPHONATE	$KC_6H_5O_4S$
108	POTASSIUM METASILICATE	K_2SIO_3
109	POTASSIUM DISILICATE	$K_2SI_2O_5$
110	POTASSIUM HYDROGEN DISILICATE	$KHSI_2O_5$

	NAME	FORMULA
111	POTASSIUM TETRASILICATE	$K_2Si_4H_2O_{10}$
112	POTASSIUM STEARATE	$KC_{36}H_{71}O_4$
113	POTASSIUM HYDROGEN SUCCINATE	$KC_4H_5O_4$
114	POTASSIUM SULPHATE	K_2SO_4
115	POTASSIUM PYROSULPHATE	$K_2S_2O_7$
116	POTASSIUM DISULPHIDE	K_2S_2
117	POTASSIUM TRISULPHIDE	K_2S_3
118	POTASSIUM HYDROGEN SULPHITE	$KHSO_3$
119	SCANDIUM	SC
120	SCANDIUM CHLORIDE	$SCCL_3$
121	SCANDIUM ACETYLACETONATE	$SCC_{15}H_{21}O_6$
122	SILICON	SI
123	SILICON CARBIDE	SIC
124	SILICON NITRIDE	Si_3N_4
125	SILICON DIOXIDE	SiO_2
126	SODIUM ACETATE	$NAC_2H_3O_2$
127	SODIUM FLUOALUMINATE	Na_3ALF_6
128	SODIUM ALUMINUM SILICATE	$NA_2AL_2Si_8O_{16}$
129	SODIUM AMIDE	$NANH_2$
130	SODIUM TETRABORATE	$NA_2B_4O_7$
131	SODIUM HYDROGEN CARBONATE	$NACHO_3$
132	SODIUM CHLORATE	$NACLO_3$
133	SODIUM CHLORIDE	NACL
134	SODIUM ENANTHATE	$NAC_7H_{13}O_2$
135	SODIUM FLUORIDE	NAF
136	SODIUM HYDRIDE	NAH
137	SODIUM NITRATE	$NANO_3$
138	SODIUM NITRIDE	Na_3N
139	SODIUM HYPONITRITE	$NA_2N_2O_2$
140	SODIUM OLEATE	$NAC_{18}H_{32}O_2$
141	SODIUM PEROXIDE	NA_2O_2
142	SODIUM PALMITATE	$NAC_{16}H_{31}O_2$
143	SODIUM HYPOPHOSPHATE	$NA_2H_2P_2O_6$
144	SODIUM PYROPHOSPHATE	$NA_4P_2O_7$
145	SODIUM METASILICATE	NA_2SiO_3
146	SODIUM DISILICATE	$NA_2Si_2O_5$
147	SODIUM SULPHATE	NA_2SO_4
148	SODIUM HYDROGEN SULPHATE	$NAHSO_4$
149	SODIUM ORTHOVANADATE	Na_3VO_4
150	SODIUM METAVANADATE	$NAVO_3$
151	TITANIUM	TI
152	TITANIUM CARBIDE	TIC
153	TITANIUM NITRIDE	TIN
154	TITANIUM MONOXIDE	TIO
155	TITANIUM SESQUIOXIDE	Ti_2O_3
156	TITANIUM DIOXIDE	TiO_2
157	VANADIUM	V
158	VANADIUM CARBIDE	VC
159	VANADIUM TRIFLUORIDE	VF_3
160	VANADIUM TETRAFLUORIDE	VF_4
161	VANADIUM NITRIDE	VN
162	VANADIUM SESQUIOXIDE	V_2O_3
163	VANADIUM DIOXIDE	VO_2
164	VANADIUM PENTOXIDE	V_2O_5
165	ALUMINIUM ACETYLACETONATE	$ALC_{15}H_{21}O_6$

	NAME	FORMULA
166	ALUMINIUM BUTOXIDE	$ALC_{12}H_{27}O_3$
167	ALUMINIUM DIETHYLMALONATE	$ALC_{21}H_{33}O_{12}$
168	ALUMINIUM ETHOXIDE	$ALC_6H_{15}O_3$
169	ALUMINIUM ISOPROPOXIDE	$ALC_9H_{21}O_3$
170	ALUMINIUM PALMITATE	$ALC_{16}H_{33}O_4$
171	ALUMINIUM PROPOXIDE	$ALC_9H_{21}O_3$
172	ALUMINIUM STEARATE	$ALC_{54}H_{105}O_6$
173	BORON CARBIDE	B_4C
174	BORON HYDRIDE	$B_{10}H_{14}$
175	BORON PHOSPHIDE	BP
176	BORON PENTASULPHIDE	B_2S_5
177	CALCIUM ALUMINATE (B)	$CA_3AL_2O_6$
178	CALCIUM ALUMINOSILICATE (A)	$CA_2AL_2SiO_5$
179	CALCIUM ALUMINOSILICATE (B)	$CAAL_2Si_2O_8$
180	CALCIUM BORIDE	CAB_6
181	CALCIUM PERCHLORATE	$CA_2CL_2O_8$
182	CALCIUM CHLORIDE FLUORIDE ORTHOPHOSPHATE	$CA_{10}CLFP_6O_{24}$
183	CALCIUM HYPOCHLORITE	$CACL_2O_2$
184	CALCIUM MAGNESIUM CARBONATE	$CAMGC_2O_6$
185	CALCIUM MAGNESIUM METASILICATE	$CAMGSi_2O_6$
186	CALCIUM METAPHOSPHATE	CAP_2O_6
187	CALCIUM PYROPHOSPHATE	$CA_2P_2O_7$
188	CALCIUM PHOSPHIDE	CA_3P_2
189	CALCIUM ORTHOSILICATE	CA_2SiO_4
190	CALCIUM SILICATE	CA_3SiO_5
191	CALCIUM METATITANATE	$CATiO_3$
192	CARBON HEXACHLORIDE	C_2CL_6
193	CHROMIUM MONOBORIDE	CRB
194	CHROMIUM CARBONYL	CRC_6O_6
195	CHROMIUM 2,4-PENTANDIONE	$CRC_{15}H_{21}O_6$
196	CHROMIUM MONOSULPHIDE	CRS
197	CHROMIUM SESQUISULPHIDE	CR_2S_3
198	HYDRAZINE FORMATE	$N_2H_6C_2O_4$
199	HYDRAZINE OXALATE	$N_4H_{10}C_2O_4$
200	HYDRAZINE HYPOPHOSPHATE	$N_2H_6P_2O_6$
201	HYDRAZINE TARTRATE	$N_2H_{10}C_4O_6$
202	HYDROXYLAMINE ORTHOPHOSPHATE	$N_3H_{12}PO_7$
203	LITHIUM META-ALUMINATE	$LIALO_2$
204	LITHIUM ALUMINIUM HYDRIDE	$LIALH_4$
205	LITHIUM TETRABORATE	$Li_2B_4O_7$
206	LITHIUM BOROHYDRATE	$LIBH_4$
207	LITHIUM PERCHLORATE	$LICLO_4$
208	LITHIUM CHLORIDE	LICL
209	LITHIUM MONOHYDRATE FORMATE	$LICH_3O_3$
210	LITHIUM METAPHOSPHATE	$LIPO_3$
211	LITHIUM HYDROGEN SULPHATE	$LIHSO_4$
212	LITHIUM MONOHYDRATE SULPHATE	$Li_2H_2SO_5$
213	LITHIUM MONOHYDRATE SULPHITE	$Li_2H_2SO_4$
214	MAGNESIUM ACETATE	$MGC_4H_6O_4$
215	MAGNESIUM AMIDE	MGN_2H_4
216	MAGNESIUM BORIDE	MGB_6
217	MAGNESIUM HYDRIDE	MGH_2
218	MAGNESIUM ORTHOPHOSPHATE	$MG_3P_2O_8$
219	MAGNESIUM ORTHOSILICATE	MG_2SiO_4
220	MAGNESIUM SULPHIDE	MGS

	NAME	FORMULA
221	MANGANESE TITANATE	$MnTiO_3$
222	PHOSPHORUS CHLORIDE NITRIDE	$P_4N_4Cl_8$
223	PHOSPHORUS SESQUISULPHIDE	P_4S_3
224	POTASSIUM ALUMINOSILICATE	$KAlSi_3O_8$
225	POTASSIUM ALUMINIUM METASILICATE	$KAlSi_2O_6$
226	POTASSIUM PENTABORATE	$K_2B_5H_9$
227	POTASSIUM ALUMINIUM ORTHOSILICATE	$KAlSiO_4$
228	POTASSIUM DIBORANE	$K_2B_2H_6$
229	POTASSIUM DIHYDROXYDIBORANE	$K_2B_2H_6O_2$
230	POTASSIUM BOROHYDRIDE	KBH_4
231	POTASSIUM CALCIUM SULPHATE	$K_2CaH_2S_2O_8$
232	POTASSIUM DICHROMATE	$K_2Cr_2O_7$
233	POTASSIUM PEROXYCHROMATE	K_3CrO_8
234	POTASSIUM CHROMIUM CHROMATE	$K_2CrCr_5H_2O_{14}$
235	POTASSIUM HEXAFLUOROPHOSPHATE	KPF_6
236	POTASSIUM MANGANATE	K_2MnO_4
237	POTASSIUM PERMANGANATE	$KMnO_4$
238	POTASSIUM MANGANESE SULPHATE	$K_2Mn_2S_3O_{12}$
239	POTASSIUM MYRISTATE	$KC_{28}H_{55}O_4$
240	POTASSIUM PALMITATE	$KC_{32}H_{63}O_4$
241	POTASSIUM PHENYLSULPHATE	$KC_6H_5SO_4$
242	POTASSIUM PICRATE	$KC_6H_2N_3O_7$
243	POTASSIUM SORBATE	$KC_6H_7O_2$
244	POTASSIUM HYDROGEN SUCCINATE	$KC_8H_{11}O_6$
245	POTASSIUM TETRASULPHIDE	K_2S_4
246	POTASSIUM PYROSULPHITE	$K_2S_2O_5$
247	POTASSIUM ETHYLXANTHATE	$KC_3H_5S_2O$
248	SILICON MONOXIDE	SiO
249	SILICON DISULPHIDE	SiS_2
250	SILICON MONOSULPHIDE	SiS
251	SODIUM META-ALUMINATE	$NaAlO_2$
252	SODIUM ALUMINIUM METASILICATE	$Na_2Al_2Si_4O_{12}$
253	SODIUM ALUMINIUM ORTHOSILICATE	$Na_3Al_2Si_2O_8$
254	SODIUM METABORATE	$NaBO_2$
255	SODIUM BOROHYDRIDE	$NaBH_4$
256	SODIUM CARBIDE	Na_2C_2
257	SODIUM FLUOROACETATE	$NaC_2H_2FO_2$
258	SODIUM FLUOROPHOSPHATE	Na_2FPO_3
259	SODIUM OXALATE	$Na_2C_2O_4$
260	SODIUM DIHYDROGEN PYROPHOSPHATE	$Na_2H_{14}P_2O_{13}$
261	SODIUM ORTHOSILICATE	Na_4SiO_4
262	SODIUM TRITITANATE	$Na_2Ti_3O_7$
263	SODIUM PYROVANADATE	$Na_4V_2O_7$
264	TITANIUM BORIDE	TiB_2
265	TITANIUM FLUORIDE	TiF_3
266	TITANIUM HYDRIDE	TiH_2
267	VANADIUM SULPHIDE	V_2S_3
268	CHROMIUM CHLORIDE	$CrCl_3$
269	ACENAPHTHENEQUINONE	$C_{12}H_6O_2$
270	ACETAMIDINE ACETATE	$C_4H_{10}N_2O_2$
271	P-ACETAMIDOBENZALDEHYDE	$C_9H_9NO_2$
272	P-ACETAMIDOBENZOIC ACID	$C_9H_9NO_3$
273	3-ACETAMIDOQUINOLINE	$C_{11}H_{10}N_2O$
274	2-ACETAMIDOTHIAZOLE	$C_5H_6N_2OS$
275	ACETONE SEMICARBAZONE	$C_4H_9N_3O$

	NAME	FORMULA
276	P-ACETOTOLUIDIDE	$C_9H_{11}NO$
277	P-ACETOXYCINNAMIC ACID	$C_{11}H_{10}O_4$
278	4-ACETOXY-3-METHOXYCINNAMIC ACID	$C_{12}H_{12}O_5$
279	11A-ACETOXYPREGN-4-ENE-3,20-DIONE	$C_{23}H_{32}O_4$
280	N-ACETYLANTHRANILIC ACID	$C_9H_9NO_3$
281	ACETYLENEDICARBOXAMIDE	$C_4H_4N_2O_2$
282	N-ACETYL-L-(-)-GLUTAMIC ACID	$C_7H_{11}NO_5$
283	N-ACETYL-L-(-)-GLUTAMINE	$C_7H_{12}N_2O_4$
284	ACETYLGLYCINE	$C_4H_7NO_3$
285	N-ACETYL-L-(-)-LEUCINE	$C_8H_{15}NO_3$
286	1-ACETYL-3-METHYLUREA	$C_4H_8N_2O_2$
287	(P-ACETYLPHENOXY)ACETIC ACID	$C_{10}H_{10}O_4$
288	N-ACETYL-L-(+)-PHENYLALANINE	$C_{11}H_{13}NO_3$
289	N-ACETYL-N-PHENYLGLYCINE	$C_{10}H_{11}NO_3$
290	N-ACETYLSULPHANILYL CHLORIDE	$C_8H_8ClNO_3S$
291	1-ACETYL-2-THIOHYDANTOIN	$C_5H_6N_2O_2S$
292	1-ACETYL-2-THIOUREA	$C_3H_6N_2OS$
293	N-ACETYL-DL-TRYPTOPHAN	$C_{13}H_{14}N_2O_3$
294	ACETYLUREA	$C_3H_6N_2O_2$
295	9(10H)-ACRIDONE	$C_{13}H_9NO$
296	ADENOSINE	$C_{10}H_{13}N_5O_4$
297	ADIPAMIDE	$C_6H_{12}N_2O_2$
298	ADIPIC ACID	$C_6H_{10}O_4$
299	ADIPIC ACID DIHYRAZIDE	$C_6H_{14}N_4O_2$
300	L-ALANINE	$C_3H_7NO_2$
301	ALIZARIN	$C_{14}H_8O_4$
302	ALLOXAN	$C_4H_4N_2O_5$
303	N-AMIDINOALANINE	$C_4H_9N_3O_2$
304	N-AMIDINOBENZAMIDE	$C_8H_9N_3O$
305	4-AMINOACETANILIDE	$C_8H_{10}N_2O$
306	2-AMINOANTHRAQUINONE	$C_{14}H_9NO_2$
307	2-AMINOBENZIMIDAZOLE	$C_7H_7N_3$
308	5-AMINO-2-BENZIMIDAZOLETHIOL	$C_7H_7N_3S$
309	P-AMINOBENZOIC ACID	$C_7H_7NO_2$
310	3-AMINO-2-BENZOYLACETANILIDE	$C_{15}H_{14}N_2O_2$
311	4-AMINOBUTYRIC ACID	$C_4H_9NO_2$
312	2-AMINO-3-CHLOROANTHRAQUINONE	$C_{14}H_8ClNO_2$
313	2-AMINO-5-CHLOROBENZIMIDAZOLE	$C_7H_6ClN_3$
314	2-AMINOETHANETHIOLSULPHURIC ACID	$C_2H_7NO_3S_2$
315	2-AMINOETHYL HYDROGEN SULPHATE	$C_2H_7NO_4S$
316	2-AMINO-5-ETHYL-1,3,4-THIADIAZOLE	$C_4H_7N_3S$
317	6-AMINOHEXANOIC ACID	$C_6H_{13}NO_2$
318	P-AMINOHIPPURIC ACID	$C_9H_{10}N_2O_3$
319	2-AMINO-2(HYDROXYMETHYL)-1,3-PROPANEDIOL	$C_4H_{11}NO_3$
320	6-AMINO-3-INDAZOLINONE DIHYDROCHLORIDE	$C_7H_9Cl_2N_3O$
321	3-AMINO-4-METHOXYBENZENESULPHONIC ACID	$C_7H_9NO_4S$
322	4-AMINO-2-METHYL-1-NAPHTHOL HYDROCHLORIDE	$C_{11}H_{12}ClNO$
323	4-AMINO-3-METHYLPHENOL	C_7H_9NO
324	1-AMINO-2-NAPHTHOL HYDROCHLORIDE	$C_{10}H_{10}ClNO$
325	2-AMINO-1,4-NAPHTHOQUINONE	$C_{10}H_7NO_2$
326	2-AMINONAPHTHO(1,2)THIAZOLE	$C_{11}H_8N_2S$
327	4-AMINO-3-NITROBENZOIC ACID	$C_7H_6N_2O_4$
328	1-AMINO-3-NITROGUANIDINE	$CH_5N_5O_2$
329	2-AMINO-5-NITROPHENOL	$C_6H_6N_2O_3$
330	2-AMINO-5-NITROTHIAZOLE	$C_3H_3N_3O_2S$

	NAME	FORMULA
331	5-AMINO-1-OCTYL-1H-TETRAZOLE	$C_9H_{19}N_5$
332	P-AMINOPHENOL	C_6H_7NO
333	P-AMINOPHENOL HYDROCHLORIDE	C_6H_8ClNO
334	P-AMINOPHENYLACETIC ACID	$C_8H_9NO_2$
335	P-AMINOPHENYLACETONITRILE HYDROCHLORIDE	$C_8H_9ClN_2$
336	2-(P-AMINOPHENYL)BENZOXASOLE	$C_{13}H_{10}N_2O$
337	2-AMINO-4-PHENYLPHENOL	$C_{12}H_{11}NO$
338	3-AMINOPHTHALIMIDE	$C_8H_8N_2O_2$
339	2-AMINO-4-QUINOLINOL	$C_9H_8N_2O$
340	5-AMINO-1H-TETRAZOLE	CH_5N_5O
341	5-AMINO-1,3,4-THIADIAZOLE-2-THIOL	$C_2H_3N_3S_2$
342	ANDROSTA-1,4-DIENE-3,11,17-TRIONE	$C_{19}H_{22}O_3$
343	ANDROST-4-ENE-3,11,17-TRIONE	$C_{19}H_{24}O_3$
344	ANILINE HYDROCHLORIDE	C_6H_8ClN
345	ANILINE TRICHLOROACETATE	$C_8H_8Cl_3NO_2$
346	3-ANILINO-1,4-DIPHENYL-5-PHENYLIMINO-1,2,4-TRIAZOLINE	$C_{26}H_{21}N_5$
347	2-ANILINO-1,4-NAPHTHOQUINONE	$C_{16}H_{11}NO_2$
348	P-ANISIC ACID	$C_8H_8O_3$
349	O-ANISIDINE HYDROCHLORIDE	$C_7H_{10}ClNO$
350	ANTHRACENE	$C_{14}H_{10}$
351	9,10-ANTHRACENEDICARBONITRILE	$C_{16}H_8N_2$
352	9,10-ANTHRACENEDICARBOXALDEHYDE	$C_{16}H_{10}O_2$
353	9-ANTHRACENEMETHANOL	$C_{15}H_{12}O$
354	ANTHRAQUINONE	$C_{14}H_8O_2$
355	ANTHRONE	$C_{14}H_{10}O$
356	9-ANTHRONITRILE	$C_{15}H_9N$
357	L-(+)-ARABINOSE	$C_5H_{10}O_5$
358	D-(-)-ARABOASCORBIC ACID	$C_6H_8O_6$
359	L-(+)-ARGININE	$C_6H_{14}N_4O_2$
360	4-4-AZOBIS(N,N-DIMETHYLANILINE)	$C_{16}H_{20}N_4$
361	1-1-AZOBISFORMAMIDE	$C_2H_4N_4O_2$
362	4,4-AZODIANILINE	$C_{12}H_{12}N_4$
363	2-2-AZODIPHENOL	$C_{12}H_{10}N_2O_2$
364	4-4-AZOXYDIBENZOYL CHLORIDE	$C_{14}H_8Cl_2N_2O_3$
365	BATHOPHENANTHROLINE	$C_{24}H_{16}N_2$
366	BBOT	$C_{26}H_{26}N_2O_2S$
367	BENZALDEHYDE P-NITROPHENYLHYDRAZONE	$C_{13}H_{11}N_3O_2$
368	BENZALDEHYDE PHENYLHYDRAZONE	$C_{13}H_{12}N_2$
369	BENZAMIDINE HYDROCHLORIDE	$C_7H_9ClN_2$
370	BENZANILIDE	$C_{13}H_{11}NO$
371	BENZ(A)ANTHRACENE	$C_{18}H_{12}$
372	BENZ(A)ANTHRACENE-7,12-DIONE	$C_{18}H_{10}O_2$
373	7H-BENZ(DE)ANTHRACENE-7-ONE	$C_{17}H_{10}O$
374	BENZENEPHOSPHONIC ACID	$C_6H_7O_3P$
375	BENZENESULPHONAMIDE	$C_6H_7NO_2S$
376	1,3,5-BENZENETRISULPHONYL CHLORIDE	$C_6H_3Cl_3O_6S_3$
377	BENZIL DIHYDRAZONE	$C_{14}H_{14}N_4$
378	BENZILIC ACID	$C_{14}H_{12}O_3$
379	BENZIMIDAZOLE	$C_7H_6N_2$
380	7,8-BENZOFLAVONE	$C_{18}H_{12}O_2$
381	BENZOIC ACID AMMONIUM SALT	$C_7H_9NO_2$
382	O-BENZOIC SULPHIMIDE	$C_7H_5NO_3S$
383	BENZOIN ANTI-OXIME	$C_{14}H_{13}NO_2$
384	BENZONITRILE	C_7H_5N
385	BENZO(A)PYRENE	$C_{20}H_{12}$

	NAME	FORMULA
386	2-BENZOTHIAZOLETHIOL	$C_7H_5NS_2$
387	2-BENZOXAZOLETHIOL	C_7H_5NOS
388	N-BENZOYL-DL-ALANINE	$C_{10}H_{11}NO_3$
389	G-BENZYL L-(+)-GLUTAMATE	$C_{12}H_{15}NO_4$
390	5-BENZYLIDENE-2-THIOHYDANTOIN	$C_{10}H_8N_2OS$
391	1-BENZYL-3-PHENYL-2-THIOUREA	$C_{14}H_{14}N_2S$
392	2-BENZYL-2-THIOPSEUDOUREA HYDROCHLORIDE	$C_8H_{11}ClN_2S$
393	BETAINE ETHYL ESTER CHLORIDE	$C_7H_{16}ClNO_2$
394	BETAINE HYDROCHLORIDE	$C_5H_{12}ClNO_2$
395	1,1-BI-2-NAPHTHOL	$C_{20}H_{14}O_2$
396	1,1-BINAPHTHYL	$C_{20}H_{14}$
397	BIOCHANIN A	$C_{16}H_{12}O_5$
398	P-P-BIPHENOL	$C_{12}H_{10}O_2$
399	4-BIPHENYLCARBOXYLIC ACID	$C_{13}H_{10}O_2$
400	4,4-BIPHENYLDICARBONITRILE	$C_{14}H_8N_2$
401	2,2-BIQUINOLINE	$C_{18}H_{12}N_2$
402	3,3-BIS(P-AMINOPHENYL)PHTHALIDE	$C_{20}H_{16}N_2O_2$
403	4,6-BIS(BUTYLAMINO)-S-TRIAZIN-2-OL	$C_9H_{19}N_5O$
404	BIS(2-CHLOROETHYL)AMINE HYDROCHLORIDE	$C_4H_{10}Cl_3N$
405	BIS(4-CHLORO-2-NITROPHENYL)-DISULPHIDE	$C_{12}H_6Cl_2N_2O_4S_2$
406	4,4-BIS(DIMETHYLAMINO)-BENZOPHENONE	$C_{17}H_{20}N_2O$
407	A,A-BIS(P-DIMETHYLAMINOPHENYL)-P-CRESOL	$C_{23}H_{26}N_2O$
408	4,4-BIS(DIMETHYLAMINO)-THIOBENZOPHENONE	$C_{17}H_{20}N_2S$
409	3,3-BIS(5,6-DIMETHYL-1,2,4-TRIAZINE)	$C_{10}H_{12}N_6$
410	BIS(2,4-DINITROPHENYL)METHANE	$C_{13}H_8N_4O_8$
411	4,6-BIS(ETHYLAMINO)-S-TRIAZIN-2-OL	$C_7H_{13}N_5O$
412	BIS(4-FLUORO-3-NITROPHENYL)SULPHONE	$C_{12}H_6F_2N_2O_6S$
413	(BIS(2-HYDROXYETHYL)AMINO)-P-BENZOQUINONE	$C_{10}H_{13}NO_4$
414	N,N-BIS(2-HYDROXYETHYL)GLYCINE	$C_6H_{13}NO_4$
415	BIS(MSB)	$C_{24}H_{22}$
416	1,5-BIS(P-NITROPHENYL)-CARBOHYDRAZIDE	$C_{13}H_{12}N_6O_5$
417	BIS(O-NITROPHENYL)DISULPHIDE	$C_{12}H_8N_2O_4S_2$
418	BIS(P-NITROPHENYL)METHANE	$C_{13}H_{10}N_2O_4$
419	BIS(P-NITROPHENYL)SULPHIDE	$C_6H_4NO_2S$
420	BIUREA	$C_2H_6N_4O_2$
421	BIURET	$C_2H_5N_3O_2$
422	D-2,3-BORNANEDIONE	$C_{10}H_{14}O_2$
423	2,3-BUTANEDIONE OXIME THIOSEMICARBAZONE	$C_5H_{10}N_4OS$
424	P-TERT.-BUTYLBENZOIC ACID	$C_{11}H_{14}O_2$
425	TERT.-BUTYLUREA	$C_5H_{12}N_2O$
426	CADION	$C_{18}H_{14}N_6O_2$
427	CAFFEINE	$C_8H_{10}N_4O_2$
428	D-CAMPHORIC ACID	$C_{10}H_{16}O_4$
429	D-CAMPHORIC ANHYDRIDE	$C_{10}H_{14}O_3$
430	DL-10-CAMPHORSULPHONIC ACID	$C_{10}H_{16}O_4S$
431	CARBAZOLE	$C_{12}H_9N$
432	N-CARBOBENZOXY-L-(-)-ARGININE	$C_{14}H_{20}N_4O_4$
433	N-CARBOBENZOXY-L-(+)-ASPARAGINE	$C_{12}H_{14}N_2O_5$
434	CARBOHYDRAZIDE	CH_6N_4O
435	CARBOMETHOXYMETHYLENETRIPHENYLPHOSPHORANE	$C_9H_9O_2P$
436	2-4-CARBONYLDIBENZOIC ACID	$C_{15}H_{10}O_5$
437	A-CARBOXY-O-ANISIC ACID	$C_9H_8O_5$
438	P-CARBOXYBENZENESULPHONYL AZIDE	$C_7H_5N_3O_4S$
439	S-CARBOXYMETHYL N,N-DIMETHYLDITHIOCARBAMATE	$C_5H_9NO_2S_2$
440	D-(+)-CELLOBIOSE	$C_{12}H_{22}O_{11}$

	NAME	FORMULA
441	D-(+)-CELLOBIOSE OCTAACETATE	$C_{28}H_{38}O_{19}$
442	CHLORANIL	$C_6Cl_4O_2$
443	CHLORACETALDEHYDE 2,4-DINITROPHENYLHYDRAZONE	$C_8H_7ClN_4O_4$
444	4-CHLORACETANILIDE	C_8H_8ClNO
445	4-CHLORACETYLACETANILIDE	$C_{10}H_{10}ClNO_2$
446	2-CHLORANTHRAQUINONE	$C_{14}H_7ClO_2$
447	P-CHLOROBENZOIC ACID	$C_7H_5ClO_2$
448	N-(4-CHLOROBENZYL)-N-(1-NAPHTHYLMETHYL)AMINE HYDROCHLORIDE	$C_{18}H_{17}Cl_2N$
449	2-(P-CHLOROBENZYL)-2-THIOPSEUDOUREA HYDROCHLORIDE	$C_8H_{10}Cl_2N_2S$
450	8-CHLOROCAFFEINE	$C_8H_9ClN_4O_2$
451	2-CHLORO-3,4-DIHYDROXYACETOPHENONE	$C_8H_7ClO_3$
452	2-CHLORO-N,N-DIMETHYLETHYLAMINE HYDROCHLORIDE	$C_4H_{11}Cl_2N$
453	2-CHLORO-N,N-DIMETHYLPROPYLAMINE HYDROCHLORIDE	$C_5H_{13}Cl_2N$
454	(2-CHLOROETHYL)TRIMETHYLAMMONIUM CHLORIDE	$C_5H_{13}Cl_2N$
455	4-(CHLOROMETHYL)-2,2-DIMETHYL-1,3-DIOXOLANE	$C_6H_{11}ClO_2$
456	3-(CHLOROMETHYL)HEPTANE	$C_8H_{17}Cl$
457	2-(CHLOROMETHYL)-5-HYDROXY-4H-PYRAN-4-ONE	$C_6H_5ClO_3$
458	4-CHLORO-3-NITROBENZOIC ACID	$C_7H_4ClNO_4$
459	5-CHLORO-3-NITRO-O-PHENYLENEDIAMINE	$C_6H_6ClN_3O_2$
460	P-CHLOROPHENOXYACETIC ACID	$C_8H_7ClO_3$
461	5-CHLOROSALICYLANILIDE	$C_{13}H_{10}ClNO_2$
462	5-CHLOROSALICYLIC ACID	$C_7H_5ClO_3$
463	2-CHLOROTRIETHYLAMINE HYDROCHLORIDE	$C_6H_{15}Cl_2N$
464	CHOLESTEROL	$C_{27}H_{46}O$
465	CHOLESTERYL BENZOATE	$C_{34}H_{50}O_2$
466	CHOLESTERYL CINNAMATE	$C_{36}H_{52}O_2$
467	CHOLESTERYL 3,5-DINITROBENZOATE	$C_{34}H_{48}N_2O_6$
468	CHOLESTERYL P-NITROBENZOATE	$C_{34}H_{49}NO_4$
469	CHOLIC ACID	$C_{24}H_{40}O_5$
470	CINCHONINE	$C_{19}H_{22}N_2O$
471	CINNAMAMIDE	C_9H_9NO
472	L-(+)-CITRULLINE	$C_6H_{13}N_3O_3$
473	COUMARILIC ACID	$C_9H_6O_3$
474	O-CRESOLPHTHALEIN	$C_{22}H_{18}O_4$
475	CURCUMIN	$C_{21}H_{20}O_6$
476	2-CYANOACETANILIDE	$C_9H_8N_2O$
477	P-CYANOBENZOIC ACID	$C_8H_5NO_2$
478	CYANOGUANIDINE	$C_2H_4N_4$
479	1,2-CYCLOHEXANEDICARBOXYLIC ACID	$C_8H_{12}O_4$
480	CYCLOHEXANESULPHAMIC ACID	$C_6H_{13}NO_3S$
481	1,2,3-CYCLOHEXANETRIONE TRIOXIME	$C_6H_9N_3O_3$
482	CIS-4-CYCLOHEXENE-1,2-DICARBOXYLIC ACID	$C_8H_{10}O_4$
483	1,2,4-CYCLOPENTANETETRACARBOXYLIC ACID	$C_9H_{10}O_8$
484	1,2,3,4-CYCLOPENTANETETRACARBOXYLIC-1,2:3,4-DIANHYDRIDE	$C_9H_6O_6$
485	DEHYDROABIETIC ACID	$C_{20}H_{28}O_2$
486	DEHYDROCHOLIC ACID	$C_{24}H_{34}O_5$
487	DIACETYLFLUORESCEIN	$C_{24}H_{16}O_7$
488	DIALLYLAMINE HYDROCHLORIDE	$C_6H_{12}ClN$
489	2,4-DIAMINO-6-PHENYL-S-TRIAZINE	$C_9H_9N_5$
490	2,6-DIAMINO-4-PYRIMIDINOL	$C_4H_6N_4O$
491	DIANTIPYRYLMETHANE	$C_{23}H_{24}N_4O_2$
492	DIANTIPYRYLPROPYLMETHANE	$C_{26}H_{30}N_4O_2$
493	DIBENZ(A,H)ANTHRACENE	$C_{22}H_{14}$
494	1,3-DIBENZYLUREA	$C_{15}H_{16}N_2O$
495	2,5-DI-TERT.-BUTYL-P-BENZOQUINONE	$C_{14}H_{20}O_2$
496	2,5-DI-TERT.-BUTYLHYDROQUINONE	$C_{14}H_{22}O_2$
497	2,6-DI-TERT.-BUTYL-4-NITROSOPHENOL	$C_{14}H_{21}NO_2$
498	DIBUTYL 4,4-SULPHONYLDIBENZOATE	$C_{22}H_{26}O_6S$
499	9,10-DICHLORANTHRACENE	$C_{14}H_8Cl_2$
500	4,4-DICHLOROAZOXYBENZENE	$C_{12}H_8Cl_2N_2O$
501	2,4-DICHLOROBENZOIC ACID	$C_7H_4Cl_2O_2$
502	2,5-DICHLORO-P-BENZOQUINONE	$C_6H_2Cl_2O_2$
503	1,4-DICHLOROBUTANE	$C_4H_8Cl_2$
504	2,3-DICHLORO-5,6-DICYANOBENZOQUINONE	$C_8Cl_2N_2O_2$
505	3,6-DICHLOROFLUORAN	$C_{20}H_{10}Cl_2O_3$
506	2,7-DICHLOROFLUORESCIN DIACETATE	$C_{24}H_{16}Cl_2O_7$
507	DICHLOROGLYOXIME	$C_2H_2Cl_2N_2O_2$
508	2,5-DICHLOROHYDROQUINONE	$C_6H_4Cl_2O_2$
509	2,3-DICHLORO-1,4-NAPHTHOQUINONE	$C_{10}H_4Cl_2O_2$
510	2,6-DICHLORO-4-NITROANILINE	$C_6H_4Cl_2N_2O_2$
511	2,3-DICHLOROQUINOXALINE	$C_8H_4Cl_2N_2$
512	3,5-DICHLOROSALICYLIC ACID	$C_7H_4Cl_2O_3$
513	DICHOLESTERYL ADIPATE	$C_{60}H_{98}O_4$
514	DICHOLESTERYL PHTHALATE	$C_{62}H_{94}O_4$
515	9-(DICYANOMETHYLENE)-2,4,7-TRINITROFLUORENE	$C_{16}H_5N_5O_6$
516	N-N-DICYCLOHEXYLDITHIOOXAMIDE	$C_{14}H_{24}N_2S_2$
517	N,N-DICYCLOHEXYLSULPHAMIDE	$C_{12}H_{24}N_2O_2S$
518	1,3-DICYCLOHEXYLUREA	$C_{13}H_{24}N_2O$
519	DIETHYLAMINE HYDROCHLORIDE	$C_4H_{12}ClN$
520	9-(P-DIETHYLAMINOBENZYLIDENE)-RHODANINE	$C_{14}H_{16}N_2OS_2$
521	4-(P-DIETHYLAMINOSTYRYL)QUINOLINE MONOHYDROCHLORIDE	$C_{21}H_{23}ClN_2$
522	1,2-DIFORMYLHYDRAZINE	$C_2H_4N_2O_2$
523	1,2-DIHYDRO-4-METHYL-3,6-PYRIDAZINEDIONE	$C_5H_6N_2O_2$
524	2-5-DIHYDROXYACETOPHENONE	$C_8H_8O_3$
525	1,3-DIHYDROXYANTHRAQUINONE	$C_{14}H_8O_4$
526	2,4-DIHYDROXYBENZOIC ACID	$C_7H_6O_4$
527	3,6-DIHYDROXYBENZONORBORNANE	$C_{11}H_{12}O_2$
528	4,4-DIHYDROXY-3,3-DIMETHYLBIPHENYL	$C_{14}H_{14}O_2$
529	4,4-DIHYDROXY-3,3-DINITROBENZOPHENONE	$C_{13}H_8N_2O_7$
530	11A,17B-DIHYDROXY-17-METHYLANDROST-4-EN-3-ONE	$C_{20}H_{30}O_3$
531	6,7-DIHYDROXY-4-METHYLCOUMARIN	$C_{10}H_8O_4$
532	2,4-DIHYDROXYPROPIOPHENONE OXIME	$C_9H_{11}NO_3$
533	DIMETHANESULPHONAMIDE	$C_2H_7NO_4S_2$
534	2,5-DIMETHOXY-4-NITROACETANILIDE	$C_{10}H_{12}N_2O_5$
535	2,5-DIMETHOXY-4-NITROANILINE	$C_8H_{10}N_2O_4$
536	P-DIMETHYLAMINOBENZOIC ACID	$C_9H_{11}NO_2$
537	DIMETHYL 5-AMINOISOPHTHALATE	$C_{10}H_{11}NO_4$
538	4-DIMETHYLAMINO-4-NITROSTILBENE	$C_{16}H_{16}N_2O_2$
539	2,5-DIMETHYLANILINE HYDROCHLORIDE	$C_8H_{12}ClN$
540	N,N-DIMETHYL-4,4-AZODIANILINE	$C_{14}H_{16}N_4$
541	3,5-DIMETHYLBENZOIC ACID	$C_9H_{10}O_2$
542	DIMETHYL 4,4-BIPHENYLDICARBOXYLATE	$C_{18}H_{14}O_4$
543	2,2-DIMETHYLCARBANILIDE	$C_{15}H_{16}N_2O$
544	5,5-DIMETHYL-1,3-CYCLOHEXANEDIONE	$C_8H_{12}O_2$
545	DIMETHYLGLYOXIME	$C_4H_8N_2O_2$
546	5,5-DIMETHYLHYDANTOIN	$C_5H_8N_2O_2$
547	DIMETHYL 4,5-IMIDAZOLEDICARBOXYLATE	$C_7H_6N_2O_4$
548	N,N-DIMETHYL-1,4-NAPHTHALENEDIAMINE DIHYDROCHLORIDE	$C_{12}H_{16}Cl_2N_2$
549	3,3-DIMETHYLNAPHTHIDINE	$C_{22}H_{20}N_2$
550	N,N-DIMETHYL-P-NITROANILINE	$C_8H_{10}N_2O_2$

	NAME	FORMULA
551	N,N-DIMETHYL-M-PHENYLENEDIAMINE DIHYDROCHLORIDE	$C_8H_{14}Cl_2N_2$
552	DIMETHYL PGPGP	$C_{26}H_{20}N_2O_2$
553	DIMETHYL TETRACHLOROTEREPHTHALATE	$C_{10}N_5Cl_4O_4$
554	4,4-DIMETHYLTHIOCARBANILIDE	$C_{15}H_{16}N_2S$
555	N,N-DI-2-NAPHTHYL-P-PHENYLENEDIAMINE	$C_{26}H_{20}N_2$
556	1,3-DI(2-NAPHTHYL)-1,3-PROPANEDIONE	$C_{23}H_{16}O_2$
557	1,3-DI-1-NAPHTHYLUREA	$C_{21}H_{16}N_2O$
558	2,4-DINITROANILINE	$C_6H_5N_3O_4$
559	P-DINITROBENZENE	$C_6H_4N_2O_4$
560	4,6-DINITROBENZOFURAZAN-1-OXIDE	$C_6H_2N_4O_6$
561	2,5-DINITROBENZOIC ACID	$C_7H_4N_2O_8$
562	3,5-DINITROBENZOIC ACID	$C_7H_4N_2O_6$
563	4,4-DINITROBIBENZYL	$C_{14}H_{12}N_2O_4$
564	4,4-DINITROBIPHENYL	$C_{12}H_8N_2O_4$
565	2,4-DINITRODIPHENYLAMINE	$C_{12}H_9N_3O_4$
566	3,5-DINITRO-2-HYDROXYPYRIDINE	$C_5H_3N_3O_5$
567	1,8-DINITRONAPHTHALENE	$C_{10}H_6N_2O_4$
568	2,4-DINITRO-1-NAPTHOL-7-SULPHONIC ACID	$C_{10}H_{10}N_2O_{10}S$
569	2,4-DINITROPHENYLACETIC ACID	$C_8H_6N_2O_6$
570	2,4-DINITROPHENYLHYDRAZINE	$C_6H_6N_4O_4$
571	3,5-DINITROSALICYLIC ACID	$C_7H_4N_2O_7$
572	2,4-DINITROSO-1,3-NAPHTHALENEDIOL	$C_{10}H_6N_2O_4$
573	1,4-DINITROSOPIPERAZINE	$C_4H_8N_4O_2$
574	2,5-DI-TERT.-PENTYLHYDROQUINONE	$C_{16}H_{26}O_2$
575	DIPHENIC ACID	$C_{14}H_{10}O_4$
576	N,N-DIPHENYLBENZIDINE	$C_{24}H_{20}N_2$
577	2,5-DIPHENYL-P-BENZOQUINONE	$C_{18}H_{12}O_2$
578	1,4-DIPHENYL-1,3-BUTADIENE	$C_{16}H_{14}$
579	S-DIPHENYLCARBAZONE	$C_{25}H_{20}N_6O_2$
580	1,5-DIPHENYLCARBOHYDRAZIDE	$C_{13}H_{14}N_4O$
581	DIPHENYLFUMARONITRILE	$C_{16}H_{10}N_2$
582	DIPHENYLGLYOXIME	$C_{14}H_{12}N_2O_2$
583	1,3-DIPHENYLGUANIDINE	$C_{13}H_{13}N_3$
584	1,6-DIPHENYL-1,3,5-HEXATRIENE	$C_{18}H_{16}$
585	5,5-DIPHENYLHYDANTOIN	$C_{15}H_{12}N_2O_2$
586	N,N-DIPHENYL-P-PHENYLENEDIAMINE	$C_{18}H_{16}N_2$
587	1,1-DIPHENYL-2-PICRYLHYDRAZINE	$C_{18}H_{13}N_5O_6$
588	1,4-DIPHENYLSEMICARBAZIDE	$C_{13}H_{13}N_3O$
589	5,5-DIPHENYL-2-THIOHYDANTOIN	$C_{15}H_{12}N_2OS$
590	1,4-DIPHENYL-3-THIOSEMICARBAZIDE	$C_{13}H_{13}N_3S$
591	1,1-DIPHENYL-2-THIOUREA	$C_{13}H_{12}N_2S$
592	1,1-DIPHENYLUREA	$C_{13}H_{12}N_2O$
593	DIPHTHALIMIDO OXALATE	$C_{16}H_8N_2O_8$
594	DIPICOLINIC ACID	$C_7H_5NO_4$
595	DIPROPYLAMINE HYDROCHLORIDE	$C_6H_{16}ClN$
596	5,5-DITHIOBIS(2-NITROBENZOIC ACID)	$C_{14}H_8N_2O_8S_2$
597	2,5-DITHIOBIUREA	$C_2H_6N_4S_2$
598	2,2-DITHIODIBENZOIC ACID	$C_{14}H_{10}O_4S_2$
599	1,1-DITHIODIFORMAMIDINE DIHYDROCHLORIDE	$C_2H_8Cl_2N_4S_2$
600	1,3-DI-O-TOLYLGUANIDINE	$C_{15}H_{17}N_3$
601	2,6-DIVANILLYLIDENECYCLOHEXANONE	$C_{22}H_{22}O_5$
602	DPB	$C_{16}H_{14}$
603	DPH	$C_{18}H_{16}$
604	ERGOSTEROL	$C_{28}H_{44}O$
605	2,2-(ETHANEDIYLIDENEDINITRILO)-DIPHENYL	$C_{14}H_{12}N_2O_2$

	NAME	FORMULA
606	(ETHANEDIYLIDENETETRATHIO)-TETRAACETIC ACID	$C_{10}H_{14}O_8S_4$
607	P-ETHOXYBENZOIC ACID	$C_9H_{10}O_3$
608	P-ETHOXYPHENYL P-HYDROXYBENZOATE	$C_{15}H_{14}O_4$
609	ETHYL ALLOPHANATE	$C_4H_8N_2O_3$
610	ETHYL M-AMINOBENZOATE METHANESULPHONATE	$C_{10}H_{15}NO_5S$
611	ETHYL BIS(2,4-DINITROPHENYL) ACETATE	$C_{16}H_{12}N_4O_{10}$
612	N,N-ETHYLENEBISBENZAMIDE	$C_{16}H_{16}N_2O_2$
613	(ETHYLENEBIS(OXYETHYLENENITRILO))-TETRAACETIC ACID	$C_{14}H_{24}N_2O_{10}$
614	ETHYLENEDIAMINE MONO-(+)-TARTRATE	$C_8H_{14}N_2O_6$
615	6,6-(ETHYLENEDIIMINO)DIQUINOLINE	$C_{20}H_{18}N_4$
616	1,1-ETHYLENEDIUREA	$C_4H_{10}N_4O_2$
617	1-ETHYL-1-(1-NAPHTHYL)-2-THIOUREA	$C_{13}H_{14}N_2S$
618	ETHYLSULPHURIC ACID POTASSIUM SALT	$C_2H_5KO_4S$
619	N-2-FLUORENYLACETAMIDE	$C_{15}H_{13}NO$
620	FLUORESCEIN	$C_{20}H_{12}O_5$
621	1-FLUORANTHRAQUINONE	$C_{14}H_7FO_2$
622	P-FLUOROBENZOIC ACID	$C_7H_5FO_2$
623	FORMAMIDINE ACETATE	$C_3H_8N_2O_2$
624	P-FORMYLPHENOXYACETIC ACID	$C_9H_8O_4$
625	1-FORMYL-3-THIOSEMICARBAZIDE	$C_2H_5N_3OS$
626	FURIL	$C_{10}H_6O_4$
627	FURIL DIOXIME	$C_{10}H_8N_2O_4$
628	D-(+)-GALACTOSE	$C_6H_{12}O_6$
629	GIRARD REAGENT D	$C_4H_{12}ClN_3O$
630	GIRARD REAGENT P	$C_7H_{10}ClN_3O$
631	GLUCOSE PHENYLOSAZONE	$C_{18}H_{22}N_4O_4$
632	D-(+)-GLUCURONOLACTONE	$C_6H_8O_6$
633	L-(+)-GLUTAMIC ACID	$C_5H_9NO_4$
634	L-(+)-GLUTAMIC ACID HYDROCHLORIDE	$C_5H_{10}ClNO_4$
635	L-(+)-GLUTAMINE	$C_5H_{10}N_2O_3$
636	GLUTARIMIDE	$C_5H_7NO_2$
637	GLYCINE	$C_2H_5NO_2$
638	GLYOXIME	$C_2H_4N_2O_2$
639	GUANIDINE NITRATE	$CH_6N_4O_3$
640	HELIANTHRONE	$C_{28}H_{14}O_2$
641	HEXACHLOROBENZENE	C_6Cl_6
642	HEXACHLOROETHANE	C_2Cl_6
643	((HEXAHYDRO-2,4,6-TRIOXO-5-PYRIMIDINYL)IMINO)DIACETIC ACID	$C_8H_9N_3O_7$
644	HEXAMETHYLBENZENE	$C_{12}H_{18}$
645	N,N-HEXAMETHYLENEDIPHTHALIMIDE	$C_{22}H_{20}N_2O_4$
646	HEXAMETHYL MELLITATE	$C_{18}H_{18}O_{12}$
647	2,2,4,4,6,6-HEXANITRODIPHENYLAMINE	$C_{12}H_5N_7O_{12}$
648	HEXYL NICOTINATE	$C_{12}H_{17}NO_2$
649	HIPPURIC ACID	$C_9H_9NO_3$
650	DL-HISTIDINE HYDROCHLORIDE	$C_6H_{14}ClN_3O_4$
651	HYDANTOIN	$C_3H_4N_2O_2$
652	P-HYDRAZINOACRIDINE	$C_{13}H_{11}N_3$
653	P-HYDRAZINOBENZENESULPHONIC ACID	$C_6H_8N_2O_3S$
654	P-HYDRAZINOBENZOIC ACID	$C_7H_8N_2O_2$
655	P-HYDRAZINOBENZOIC ACID HYDROCHLORIDE	$C_7H_9ClN_2O_2$
656	2-HYDRAZINOBENZOTHIAZOLE	$C_7H_7N_3S$
657	HYDROQUINONE	$C_6H_6O_2$
658	2-HYDROXYACETANILIDE	$C_8H_9NO_2$
659	P-HYDROXYBENZOIC ACID	$C_7H_6O_3$
660	4-(4-HYDROXYBENZYLIDENE)-1-PHENETHYL-2,3-DIOXOPYRROLIDINE	$C_{19}H_{17}NO_3$

	NAME	FORMULA
661	N-(2-HYDROXY-1,1-BIS(HYDROXYMETHYL)ETHYL)TAURINE	$C_6H_{15}NO_6S$
662	5-(4-HYDROXYBUTYL)HYDANTOIN	$C_7H_{12}N_2O_3$
663	P-HYDROXYCINNAMIC ACID	$C_9H_8O_3$
664	4-HYDROXYCOUMARIN	$C_9H_6O_3$
665	3-HYDROXY-2,4-DIMETHYL-2-NAPHTHANILIDE	$C_{19}H_{17}NO_2$
666	3-HYDROXYFLAVONE	$C_{15}H_{10}O_3$
667	5-HYDROXYISOPHTHALIC ACID	$C_8H_6O_5$
668	HYDROXYLAMINE HYDROCHLORIDE	H_4ClNO
669	5-HYDROXY-DL-LYSINE MONOHYDROCHLORIDE	$C_6H_{15}ClN_2O_3$
670	2-HYDROXY-5-METHOXYBENZHYDRAZIDE	$C_8H_{10}N_2O_3$
671	4-HYDROXY-3-METHOXYBENZOIC ACID	$C_8H_8O_4$
672	4-(4-HYDROXY-3-METHOXYBENZYLIDENE)PHENETHYL DIOXOPYRROLIDINE	$C_{20}H_{19}NO_4$
673	4-HYDROXY-3-METHOXYCINNAMIC ACID	$C_{10}H_{10}O_4$
674	2-HYDROXY-5-METHOXYISOPHTHALIC ACID	$C_9H_8O_6$
675	4-HYDROXY-N-METHYLACETANILIDE	$C_9H_{11}NO_2$
676	17B-HYDROXY-17-METHYLANDROSTA-4,9(11)-DIEN-3-ONE	$C_{20}H_{28}O_2$
677	2-HYDROXY-3-METHYLBENZOIC ACID	$C_8H_8O_3$
678	3-HYDROXY-2-METHYLCINCHONINIC ACID	$C_{11}H_9NO_3$
679	2-HYDROXYMETHYL-2-METHYL-1,3-PROPANEDIOL	$C_5H_{12}O_3$
680	N-HYDROXYNAPHTHALIMIDE	$C_{12}H_7NO_3$
681	1-HYDROXY-2-NAPHTHAMIDE	$C_{11}H_9NO_2$
682	3-HYDROXY-2-NAPHTHOIC ACID	$C_{11}H_8O_3$
683	2-HYDROXY-1,4-NAPHTHOQUINONE	$C_{10}H_6O_3$
684	3-HYDROXY-2-NAPHTHYDRAZIDE	$C_{11}H_{10}N_2O_2$
685	(P-HYDROXYPHENOXY)ACETIC ACID	$C_8H_8O_4$
686	P-(P-HYDROXYPHENYLAZO)-BENZOIC ACID	$C_{13}H_{10}N_2O_3$
687	N-(P-HYDROXYPHENYL)GLYCINE	$C_8H_9NO_3$
688	N-HYDROXYPHTHALIMIDE	$C_8H_5NO_3$
689	L-(-)-HYDROXYPROLINE	$C_5H_9NO_3$
690	4-HYDROXYPROPIOPHENONE	$C_9H_{10}O_2$
691	4,5-IMIDAZOLEDICARBOXYLIC ACID	$C_5H_4N_2O_4$
692	2-IMIDAZOLIDINETHIONE	$C_3H_6N_2S$
693	3-IMINOPHTHALIMIDINE	$C_8H_6N_2O$
694	INDAN	C_9H_{10}
695	3-INDAZOLINONE	$C_7H_6N_2O$
696	3-INDOLEACETIC ACID	$C_{10}H_9NO_2$
697	INDOLE-3-CARBOXALDEHYDE	C_9H_7NO
698	INDOLE-2,3-DIONE	$C_8H_5NO_2$
699	INDOLE-2,3-DIONE 3-OXIME	$C_8H_6N_2O_2$
700	INDOLE-2,3-DIONE 3-THIOSEMICARBAZONE	$C_9H_8N_4OS$
701	INOSINE	$C_{10}H_{12}N_4O_5$
702	INOSITOL	$C_6H_{12}O_6$
703	ISATOIC ANHYDRIDE	$C_8H_5NO_3$
704	ISETHIONIC ACID SODIUM SALT	$C_2H_5NaO_4S$
705	L-(+)-ISOLEUCINE	$C_6H_{13}NO_2$
706	ISONICOTINAMIDE	$C_6H_6N_2O$
707	ISONICOTINIC ACID	$C_6H_5NO_2$
708	ISONICOTINIC ACID HYDRAZIDE	$C_6H_7N_3O$
709	ISONICOTINONITRILE-1-OXIDE	$C_6H_4N_2O$
710	ISONIPECOTAMIDE	$C_6H_{12}N_2O$
711	ISONIPECOTIC ACID	$C_6H_{11}NO_2$
712	ISOPHTHALIC ACID	$C_8H_6O_4$
713	ISOPHTHALIC DIHYDRAZIDE	$C_8H_{10}N_4O_2$
714	ISOPHTHALONITRILE	$C_8H_4N_2$
715	ITACONIC ACID	$C_5H_6O_4$
716	B-D-LACTOSE	$C_{12}H_{22}O_{11}$
717	LOPHINE	$C_{21}H_{16}N_2$
718	DL-LYSINE MONOHYDROCHLORIDE	$C_6H_{15}ClN_2O_2$
719	MALONAMIDE	$C_3H_6N_2O_2$
720	MALONANILIDE	$C_{15}H_{14}N_2O_2$
721	D-MANNITOL	$C_6H_{14}O_6$
722	MELAMINE	$C_3H_6N_6$
723	2-MERCAPTOACETANILIDE CARBAMATE	$C_9H_{10}N_2O_2S$
724	O-MERCAPTOBENZOIC ACID	$C_7H_6O_2S$
725	2-MERCAPTO-6-NITROBENZOTHIAZOLE	$C_7H_4N_2O_2S_2$
726	MERCAPTOSUCCINIC ACID	$C_4H_6O_4S$
727	MESACONIC ACID	$C_5H_8O_4$
728	L-(-)-METHIONINE	$C_5H_{11}NO_2S$
729	P-((P-METHOXYBENZYLIDENE)AMINO)-PHENOL	$C_{14}H_{13}NO_2$
730	N-P-METHOXYBENZYLIDENE-P-PHENYLAZOANILINE	$C_{20}H_{17}N_3O$
731	8-METHOXYCAFFEINE	$C_9H_{12}N_4O_3$
732	P-METHOXYCINNAMIC ACID	$C_{10}H_{10}O_3$
733	4-METHOXY-3-NITROBENZOIC ACID	$C_8H_7NO_5$
734	5-METHOXY-2-NITROSOPHENOL	$C_7H_7NO_3$
735	METHYLAMINE HYDROCHLORIDE	CH_6ClN
736	1-METHYLAMINOANTHRAQUINONE	$C_{15}H_{11}NO_2$
737	P-(METHYLAMINO)BENZOIC ACID	$C_8H_9NO_2$
738	N-METHYLANTHRANILIC ACID	$C_8H_9NO_2$
739	2-METHYLANTHRAQUINONE	$C_{15}H_{10}O_2$
740	2-METHYLBENZIMIDAZOLE	$C_8H_8N_2$
741	2-METHYLCARBANILIDE	$C_{14}H_{14}N_2O$
742	3-METHYLCHOLANTHRENE	$C_{21}H_{16}$
743	4-METHYL-4-CYCLOHEXENE-1,2-DICARBOXYLIC ACID	$C_9H_{12}O_4$
744	4,4METHYLENEBIS(2,6-DI-TERT.-BUTYLPHENOL)	$C_{29}H_{44}O_2$
745	4,4-METHYLENEDIANILINE DIHYDROCHLORIDE	$C_{13}H_{18}Cl_2N_2$
746	3,4-METHYLENEDIOXYCINNAMIC ACID	$C_{10}H_8O_4$
747	5,5-METHYLENEDISALICYLIC ACID	$C_{15}H_{12}O_6$
748	METHYL GALLATE	$C_8H_8O_5$
749	METHYL A-D-GLUCOSIDE	$C_7H_{14}O_6$
750	METHYLGUANIDINE SULPHATE	$C_4H_{16}N_8O_4S$
751	4,4,4-METHYLIDYNETRIS-(N,N-DIMETHYLANILINE)	$C_{25}H_{31}N_3$
752	N,N,N-METHYLIDYNETRISFORMAMIDE	$C_4H_7N_3O_3$
753	5-METHYLISATIN	$C_9H_7NO_2$
754	3-METHYL-2-(METHYLTHIO)BENZOTHIAZOLIUM P-TOLUENESULPHONATE	$C_{16}H_{17}NO_3S_3$
755	N-(2-METHYL-1-NAPHTHYL)ACETAMIDE	$C_{13}H_{13}NO$
756	N-METHYL-P-NITROANILINE	$C_7H_8N_2O_2$
757	2-METHYL-6-NITROBENZOTHIAZOLE	$C_8H_6N_2O_2S$
758	A-METHYL-P-NITROCINNAMIC ACID	$C_{10}H_9NO_4$
759	N-METHYL-O-PHENYLENEDIAMINE DIHYDROCHLORIDE	$C_7H_{12}Cl_2N_2$
760	METHYLPHENYLGLYOXIME	$C_9H_{10}N_2O_2$
761	3-METHYL-2-PYRAZOLIN-5-ONE	$C_4H_6N_2O$
762	N-METHYLSULPHANILIC ACID	$C_7H_9NO_3S$
763	2-(METHYLTHIO)BENZIMIDAZOLE	$C_8H_8N_2S$
764	2-METHYL-2-THIOPSEUDOUREA SULPHATE	$C_4H_{14}N_4O_4S_3$
765	6-METHYL-2-THIOURACIL	$C_5H_6N_2OS$
766	4-METHYLUMBELLIFERONE	$C_{10}H_8O_3$
767	4-METHYLUMBELLIFERONE PHOSPHATE	$C_{10}H_9O_6P$
768	MUCIC ACID	$C_6H_{10}O_8$
769	1-NAPHTHALENEACETAMIDE	$C_{12}H_{11}NO$
770	2,7-NAPHTHALENEDIOL	$C_{10}H_8O_2$

	NAME	FORMULA
771	NAPHTHALIC ANHYDRIDE	$C_{12}H_6O_3$
772	NAPHTHALIMIDE	$C_{12}H_7NO_2$
773	1-NAPHTHOHYDROXAMIC ACID	$C_{11}H_9NO_2$
774	2-NAPHTHOIC ACID	$C_{11}H_8O_2$
775	N-1-NAPHTHYLACETAMIDE	$C_{12}H_{11}NO$
776	(2-NAPHTHYLOXY)ACETIC ACID	$C_{12}H_{10}O_3$
777	1-(1-NAPHTHYL)-2-THIOUREA	$C_{11}H_{10}N_2S$
778	NEOCUPROINE	$C_{14}H_{12}N_2$
779	NICOTINIC ACID	$C_6H_5NO_2$
780	NICOTINIC ACID HYDROCHLORIDE	$C_6H_6ClNO_2$
781	NITRILOTRIACETIC ACID	$C_6H_9NO_6$
782	3,3,3-NITRILOTRISPROPIONAMIDE	$C_9H_{18}N_4O_3$
783	4-NITROACETANILIDE	$C_8H_8N_2O_3$
784	P-NITROANILINE	$C_6H_6N_2O_2$
785	4-NITROANTHRANILIC ACID	$C_7H_6N_2O_4$
786	5-NITROBARBITURIC ACID	$C_4H_3N_3O_5$
787	P-NITROBENZAMIDE	$C_7H_6N_2O_3$
788	P-NITROBENZENESULPHONAMIDE	$C_6H_6N_2O_4S$
789	P-NITROBENZHYDRAZIDE	$C_7H_7N_3O_3$
790	5-NITROBENZIMIDAZOLE	$C_7H_5N_3O_2$
791	5-NITRO-2-BENZIMIDAZOLETHIOL	$C_7H_5N_3O_2S$
792	P-NITROBENZOIC ACID	$C_7H_5NO_4$
793	P-NITROCINNAMIC ACID	$C_9H_7NO_4$
794	3-NITRODIBENZOFURAN	$C_{12}H_7NO_3$
795	2-NITROFLUORENE	$C_{13}H_9NO_2$
796	NITROGUANIDINE	$CH_4N_4O_2$
797	5-NITRO-1H-INDAZOLE	$C_7H_5N_3O_2$
798	NITRON	$C_{20}H_{16}N_4$
799	3-NITRO-9-NITROSOCARBAZOLE	$C_{12}H_7N_3O_3$
800	P-NITROPHENOXYACETIC ACID	$C_8H_7NO_5$
801	P-NITROPHENYLACETIC ACID	$C_8H_7NO_4$
802	4-(P-NITROPHENYLAZO)-1-NAPHTHOL	$C_{16}H_{11}N_3O_3$
803	4-(P-NITROPHENYLAZO)ORCINOL	$C_{13}H_{11}N_3O_4$
804	4-(P-NITROPHENYLAZO)RESORCINOL	$C_{12}H_9N_3O_4$
805	2-(P-NITROPHENYL)BENZOXAZOLE	$C_{13}H_8N_2O_3$
806	4-NITRO-O-PHENYLENEDIAMINE	$C_6H_7N_3O_2$
807	N-(P-NITROPHENYL)GLYCINE	$C_8H_8N_2O_4$
808	P-NITROPHENYLHYDRAZINE	$C_6H_7N_3O_2$
809	4-(P-NITROPHENYL)-MORPHOLINE	$C_{10}H_{12}N_2O_3$
810	3-NITROPHTHALIC ACID	$C_8H_5NO_6$
811	3-NITROPHTHALIC ANHYDRIDE	$C_8H_3NO_5$
812	3-NITROPHTHALIMIDE	$C_8H_4N_2O_4$
813	5-NITROSALICYLALDOXIME	$C_7H_6N_2O_4$
814	5-NITROSALICYLIC ACID	$C_7H_5NO_5$
815	5-NITROSO-8-QUINOLINOL	$C_9H_6N_2O_2$
816	6-NITROSOTHYMOL	$C_{10}H_{13}NO_2$
817	NITROTEREPHTHALIC ACID	$C_8H_5NO_6$
818	5-NORBORNENE-2,3-DICARBOXYLIC ANHYDRIDE	$C_9H_8O_3$
819	NOREPHEDRINE HYDROCHLORIDE	$C_9H_{14}ClNO$
820	OCTADECYLAMINE HYDROCHLORIDE	$C_{18}H_{40}ClN$
821	OCTAPHENYLCYCLOTETRASILOXANE	$C_{48}H_{40}O_4Si_4$
822	L-(+)-ORNITHINE MONOHYDROCHLORIDE	$C_5H_{13}ClN_2O_2$
823	OROTIC ACID	$C_5H_4N_2O_4$
824	OXALIC ACID	$C_2H_2O_4$
825	OXALOHYDROXAMIC ACID	$C_2H_4N_2O_4$

	NAME	FORMULA
826	OXALYL DIHYDRAZIDE	$C_2H_6N_4O_2$
827	OXANILIDE	$C_{14}H_{12}N_2O_2$
828	4,4-OXYDIANILINE	$C_{12}H_{12}N_2O$
829	4,4-OXYDIBENZONITRILE	$C_{14}H_8N_2O$
830	4,4-OXYDIBENZOPHENONE	$C_{26}H_{18}O_3$
831	4,4-OXYDIPHENOL	$C_{12}H_{10}O_3$
832	PARABANIC ACID	$C_3H_2N_2O_3$
833	PENTACHLOROPHENOL	C_6HCl_5O
834	PENTAERYTHRITOL	$C_5H_{12}O_4$
835	1,2,3-PHENENYL TRIACETATE	$C_{12}H_{12}O_6$
836	P-PHENETYLUREA	$C_9H_{12}N_2O_2$
837	PHENOLPHTHALEIN	$C_{20}H_{14}O_4$
838	PHENOLPHTHALEIN DIPHOSPHATE	$C_{20}H_{16}O_{10}P_2$
839	PHENOLPHTHALIN	$C_{20}H_{16}O_4$
840	PHENOTHIAZINE	$C_{12}H_9NS$
841	2-PHENYLACETOPHENONE AZINE	$C_{28}H_{24}N_2$
842	L-(-)-PHENYLALANINE	$C_9H_{11}NO_2$
843	N-PHENYLANTHRANILIC ACID	$C_{13}H_{11}NO_2$
844	P-PHENYLAZOBENZOIC ACID	$C_{13}H_{10}N_2O_2$
845	P-PHENYLAZOPHENOL	$C_{12}H_{10}N_2O$
846	N-(P-PHENYLAZOPHENYL)MALEIMIDE	$C_{16}H_{11}N_3O_2$
847	4-PHENYLAZORESORCINOL	$C_{12}H_{10}N_2O_2$
848	N,N-P-PHENYLENEBISACETAMIDE	$C_{10}H_{12}N_2O_2$
849	(P-PHENYLENEDIOXY)DIACETIC ACID	$C_{10}H_{10}O_6$
850	DL-2-PHENYLGLYCINE	$C_8H_9NO_2$
851	PHENYLHYDRAZINE HYDROCHLORIDE	$C_6H_9ClN_2$
852	5-PHENYL-2,4-PENTADIENOIC ACID	$C_{11}H_{10}O_2$
853	P-PHENYLPHENOL	$C_{12}H_{10}O$
854	N-PHENYLPHTHALIMIDE	$C_{14}H_9NO_2$
855	3-PHENYL-2-PYRAZOLIN-5-ONE	$C_9H_8N_2O$
856	3-PHENYLRHODANINE	$C_9H_7NOS_2$
857	1-PHENYLSEMICARBAZIDE	$C_7H_9N_3O$
858	4-PHENYLSEMICARBAZIDE HYDROCHLORIDE	$C_7H_{10}ClN_3O$
859	PHENYLSUCCINIC ACID	$C_{10}H_{10}O_4$
860	1-PHENYL-3-THIOSEMICARBAZIDE	$C_7H_9N_3S$
861	1-PHENYL-2-THIOUREA	$C_7H_8N_2S$
862	PHLOROGLUCINOL	$C_6H_{10}O_3$
863	PHTHALAMIDE	$C_8H_8N_2O_2$
864	PHTHALIC ACID	$C_8H_6O_4$
865	PHTHALIMIDE	$C_8H_5NO_2$
866	4-PICOLINE-1-OXIDE	C_6H_7NO
867	PICOLINIC ACID HYDROCHLORIDE	$C_6H_6ClNO_2$
868	PICRAMIC ACID	$C_6H_5N_3O_5$
869	PICRAMIDE	$C_6H_4N_4O_6$
870	PIPERONYLIC ACID	$C_9H_8O_4$
871	POPOP	$C_{24}H_{16}N_2O_2$
872	PREGN-4-ENE-3,11,20-TRIONE	$C_{21}H_{28}O_3$
873	L-(-)-PROLINE	$C_5H_9NO_2$
874	1,2,3-PROPANETRICARBOXYLIC ACID	$C_6H_8O_6$
875	P-ISO-PROPYLCINNAMIC ACID	$C_{12}H_{14}O_2$
876	4-4-ISO-PROPYLIDENEDIPHENOL	$C_{15}H_{16}O_2$
877	PROPYL RED	$C_{19}H_{23}N_3O_2$
878	ISO-PROPYLUREA	$C_4H_{10}N_2O$
879	PURPURIN	$C_{14}H_8O_5$
880	PYRENE	$C_{16}H_{10}$

	NAME	FORMULA
881	1-PYRENEBUTYRIC ACID	$C_{20}H_{18}O_2$
882	PYRIDINE SULPHUR TRIOXIDE	$C_5H_5NO_3S$
883	PYRIDOXINE HYDROCHLORIDE	$C_8H_{13}CLNO_3$
884	2-PYRIMIDINOL	$C_4H_4N_2O$
885	PYROMELLITIC DIANHYDRIDE	$C_{10}H_2O_6$
886	PYRUVOYL CHLORIDE (P-NITROPHENYL)-HYDRAZONE	$C_9H_8CLN_3O_3$
887	P-QUATERPHENYL	$C_{24}H_{18}$
888	QUINALDIC ACID	$C_{10}H_7NO_2$
889	QUINHYDRONE	$C_{12}H_{10}O_4$
890	QUINIZARIN	$C_{14}H_8O_4$
891	6-QUINOLINECARBOXYLIC ACID	$C_{10}H_7NO_2$
892	2-QUINOLINETHIOL	C_9H_7NS
893	2-QUINOLINOL	C_9H_7NO
894	N-8-QUINOLYL-P-TOLUENESULPHONAMIDE	$C_{16}H_{14}N_2O_2S$
895	2-3-QUINOXALINEDITHIOL	$C_8H_6N_2S_2$
896	2-QUINOXALINOL	$C_8H_6N_2O$
897	B-RESORCYLALDOXIME	$C_7H_7NO_3$
898	RHODANINE	$C_3H_3NOS_2$
899	RIBOFLAVIN	$C_{17}H_{20}N_4O_6$
900	SALICIN	$C_{13}H_{18}O_7$
901	SALICYLALAZINE	$C_{14}H_{12}N_2O_2$
902	SALICYLIC ACID	$C_7H_6O_3$
903	N-SALICYLIDENEANTHRANILIC ACID	$C_{14}H_{11}NO_3$
904	L-(-)-SERINE	$C_3H_7NO_3$
905	STIGMASTEROL	$C_{29}H_{48}O$
906	SUCCINAMIDE	$C_4H_8N_2O_2$
907	SUCCINIC ACID	$C_4H_6O_4$
908	SULPHANILAMIDE	$C_6H_8N_2O_2S$
909	SULPHANILANILIDE	$C_{12}H_{12}N_2O_2S$
910	4,4-SULPHONYLBIS(2-AMINOPHENOL)	$C_{12}H_{12}N_2O_4S$
911	4,4-SULPHONYLDIPHENOL	$C_{12}H_{10}O_4S$
912	SYRINGIC ACID	$C_9H_{10}O_5$
913	(+)-TARTARIC ACID	$C_4H_6O_6$
914	TEREPHTHALONITRILE	$C_8H_4N_2$
915	P-TERPHENYL	$C_{18}H_{14}$
916	TETRABUTYLAMMONIUM PERCHLORATE	$C_{16}H_{36}CLNO_4$
917	2,2,6,6-TETRACHLORO-P-P-BIPHENOL	$C_{12}H_6CL_4O_2$
918	TETRACHLOROHYDROQUINONE	$C_6H_2CL_4O_2$
919	TETRACHLOROPHTHALIC ANHYDRIDE	$C_8CL_4O_3$
920	3,4,5,6-TETRACHLOROPHTHALIMIDE	$C_8HCL_4NO_2$
921	3,3,4,5-TETRACHLOROSALICYLANILIDE	$C_{13}H_7CL_4NO_2$
922	TETRACHLOROTETRAHYDRONAPHTHALENE	$C_{10}H_8CL_4$
923	TETRACYANOETHYLENE	C_6N_4
924	7,7,8,8-TETRACYANOQUINODIMETHAN	$C_{12}H_4N_4$
925	B-(5,6,7,8-TETRAHYDRO-2-NAPHTHOYL)BENZOIC ACID	$C_{18}H_{16}O_3$
926	2,2,4,4-TETRAHYDROXYBENZOPHENONE	$C_{13}H_{10}O_5$
927	TETRAMETHYLAMMONIUM(1,1,2,3,3-PENTACYANOPROPENIDE)	$C_{12}H_{12}N_6$
928	TETRAMETHYLAMMONIUM THIOACETATE	$C_6H_{15}NOS$
929	N,N,N,N-TETRAMETHYLBENZIDINE	$C_{16}H_{20}N_2$
930	1,2,4,5-TETRAMETHYL-3,6-DINITROBENZENE	$C_{10}H_{12}N_2O_4$
931	2,2,6,6-TETRAMETHYL-4-PIPERIDONE OXIME	$C_9H_{18}N_2O$
932	2,2,5,5-TETRAMETHYL-1-PYRROLIDINYLOXY-3-CARBOXAMIDE	$C_9H_{17}N_2O_2$
933	2,2,5,5-TETRAMETHYL-3-PYRROLINE-3-CARBOXAMIDE	$C_9H_{16}N_2O$
934	2,2,5,5-TETRAMETHYL-3-PYRROLIN-1-YLOXY-3-CARBOXAMIDE	$C_9H_{15}N_2O_2$
935	N,N,N,N-TETRAPHENYLBENZIDINE	$C_{36}H_{28}N_2$
936	1,1,4,4-TETRAPHENYL-1,3-BUTADIENE	$C_{28}H_{22}$
937	TETRAPHENYLETHYLENE	$C_{26}H_{20}$
938	N,N,N,N-TETRAPHENYL-P-PHENYLENEDIAMINE	$C_{30}H_{24}N_2$
939	2,3,4,5-TETRAPHENYLPYRROLE	$C_{28}H_{21}N$
940	THEOBROMINE	$C_7H_8N_4O_2$
941	THIANTHRENE	$C_{12}H_8S_2$
942	4-THIAZOLIDINECARBOXYLIC ACID	$C_4H_7NO_2S$
943	2-THIOBARBITURIC ACID	$C_4H_4N_2O_2S$
944	THIOCARBANILIDE	$C_{13}H_{12}N_2S$
945	THIOCARBOHYDRAZIDE	CH_6N_4S
946	5,5-THIODISALICYLIC ACID	$C_{14}H_{10}O_6S$
947	2-THIOHYDANTOIN	$C_3H_4N_2OS$
948	2-THIOUROTIC ACID	$C_5H_4N_2O_3S$
949	THIOSEMICARBAZIDE	CH_5N_3S
950	1-THIOURACIL	$C_4H_4N_2OS$
951	THIOUREA	CH_4N_2S
952	3,6-THIOXANTHENEDIAMINE-10,10-DIOXIDE	$C_{13}H_{12}N_2O_2S$
953	L-(-)-THREONINE	$C_4H_9NO_3$
954	THYMOLPHTHALEIN	$C_{28}H_{30}O_4$
955	P-TOLUAMIDE	C_8H_9NO
956	P-TOLUIC ACID	$C_8H_8O_2$
957	P-TOLUIDINE HYDROCHLORIDE	$C_7H_{10}CLN$
958	6-P-TOLUIDINO-2-NAPHTHALENESULPHONIC ACID	$C_{17}H_{15}NO_3S$
959	P-TOLYL SULPHONE	$C_{14}H_{14}O_2S$
960	TPB	$C_{28}H_{22}$
961	TRIAMINOGUANIDINE HYDROCHLORIDE	CH_8CLN_5
962	2,4,6-TRIAMINOPYRIMIDINE	$C_4H_7N_5$
963	2,4,5-TRICHLOROPHENOXYACETIC ACID	$C_8H_5CL_3O_3$
964	TRIETHANOLAMINE HYDROCHLORIDE	$C_6H_{16}CLNO_3$
965	TRIETHYLAMINE HYDROCHLORIDE	$C_6H_{16}CLN$
966	TRIETHYLENEDIAMINE	$C_6H_{12}N_2$
967	TRIETHYL 2,4,6-TRIAZINETRIACETATE	$C_{15}H_{21}N_3O_6$
968	4,4,4-TRIFLUORO-1-(3-PYRIDYL)-1,3-BUTANEDIONE	$C_9H_6F_3NO_2$
969	2,3,4-TRIHYDROXYACETOPHENONE	$C_8H_8O_4$
970	2,4,5-TRIHYDROXYBUTYROPHENONE	$C_{10}H_{12}O_4$
971	4,5,7-TRIHYDROXYISOFLAVONE	$C_{15}H_{10}O_5$
972	2,4,6-TRIHYDROXY-2-(P-METHOXYPHENYL)ACETOPHENONE	$C_{15}H_{14}O_5$
973	TRIMELLITIC ACID	$C_9H_6O_6$
974	TRIMELLITIC ANHYDRIDE	$C_9H_4O_5$
975	TRIMESIC ACID	$C_9H_6O_6$
976	TRIMETHYLPHENYLAMMONIUM BENZENESULPHONATE	$C_{15}H_{19}NO_3S$
977	2,4,6-TRIMETHYLPYRYLIUM TETRAFLUOROBORATE	$C_8H_{11}BF_4O$
978	2,4,6-TRINITROBENZOIC ACID	$C_7H_3N_3O_8$
979	2,4,7-TRINITRO-9-FLUORENONE	$C_{13}H_5N_3O_7$
980	2,4,6-TRINITRORESORCINOL	$C_6H_3N_3O_8$
981	TRIPHENYLMETHANOL	$C_{19}H_{16}O$
982	TRIPHENYLPHOSPHINE OXIDE	$C_{18}H_{15}OP$
983	TRIPTYCENE	$C_{20}H_{14}$
984	TRIPTYCENE-8-CARBOXYLIC ACID	$C_{21}H_{14}O_2$
985	TRIPTYCENE-8-METHANOL	$C_{21}H_{16}O$
986	2,3,5-TRIPHENYL-2H-TETRAZOLIUM CHLORIDE	$C_{19}H_{15}CLN_4$
987	2,4,6-TRIPHENYL-S-TRIAZINE	$C_{21}H_{15}N_3$
988	S-TRITHIANE	$C_3H_6S_3$
989	2,4,6-TRI-P-TOLYLPYRYLIUM TETRAFLUOROBORATE	$C_{28}H_{25}BF_4O_2$
990	TRITYLIUM TETRAFLUOROBORATE	$C_{19}H_{15}BF_4$

	NAME	FORMULA	NAME	FORMULA
991	DL-TRYPTOPHAN	$C_{11}H_{12}N_2O_2$		
992	DL-TYROSINE	$C_9H_{11}NO_3$		
993	URACIL	$C_4H_4N_2O_2$		
994	UROCANIC ACID	$C_6H_6N_2O_2$		
995	VANADIUM OXBIS-(1-PHENYL-1,3-BUTANEDIONATE)	$C_{20}H_{18}VO_5$		
996	VANILLIN AZINE	$C_{16}H_{16}N_2O_4$		
997	VERATRIC ACID	$C_9H_{10}O_4$		
998	XANTHEN-9-ONE	$C_{13}H_8O_2$		
999	ACETIC ACID	$C_2H_4O_2$		
1000	ACETONE	C_3H_6O		
1001	ANILINE	C_6H_7N		
1002	BENZENE	C_6H_6		
1003	BENZYL ALCOHOL	C_7H_8O		
1004	CARBON TETRACHLORIDE	CCL_4		
1005	CHLOROFORM	$CHCL_3$		
1006	DIOXAN	$C_4H_8O_2$		
1007	ETHANOL	C_2H_6O		
1008	ETHER	$C_4H_{10}O$		
1009	ETHOXYETHANOL	$C_4H_{10}O_2$		
1010	HYDROCHLORIC ACID	CCL		
1011	METHANOL	CH_4O		
1012	NITRIC ACID	HNO_3		
1013	PHENOL	C_6H_6O		
1014	SULPHURIC ACID	H_2SO_4		
1015	TOLUENE	C_7H_8		
1016	XYLENE	C_8H_{10}		
1017	ACRYLICS	$C_5H_8O_2$		
1018	CELLULOSIC PLASTICS	$C_{20}H_{28}O_{14}$		
1019	FLUORINATED POLYMERS - P.T.F.E	C_2F_4		
1020	FLUORINATED POLYMERS - P.T.F.C.E.	C_2F_3CL		
1021	MELAMINE FORMALDEHYDES	$C_6H_6N_6O_3$		
1022	NYLONS - TYPE 6	$C_6H_{11}NO$		
1023	NYLONS - TYPE 6/6	$C_{12}H_{22}N_2O_2$		
1024	NYLONS - TYPE 6/10	$C_{16}H_{30}N_2O_2$		
1025	NYLONS - TYPE 11	$C_{11}H_{21}NO$		
1026	NYLONS - TYPE 12	$C_{12}H_{23}NO$		
1027	PHENOL FORMALDEHYDES	$C_{43}H_{36}O_7$		
1028	POLYACETALS	CH_2O		
1029	POLYCARBONATES	$C_{16}H_{14}O_3$		
1030	POLYESTERS - MELINEX	$C_{10}H_8O_4$		
1031	POLYIMIDES	$C_{44}H_{20}N_4O_{10}$		
1032	POLYOLEFINS - POLYETHYLENE	C_2H_4		
1033	POLYOLEFINS - POLYPROPYLENE	C_3H_6		
1034	POLYOLEFINS - TPX	C_8H_{12}		
1035	POLYSTYRENES	C_8H_8		
1036	POLYURETHANES - CAST ELASTOMER	$C_{37}H_{57}N_3O_8CL$		
1037	POLYURETHANES - RIGID CAST URETHANE	$C_{13}H_{20}NO_4$		
1038	POLYURETHANES - FLEXIBLE FOAM	$C_{52}H_{87}N_4O_{18}$		
1039	POLYURETHANES - RIGID FOAM	$C_{52}H_{55}N_5O_{11}CL$		
1040	UREA FORMALDEHYDES	$C_3H_4N_2O$		
1041	VINYL POLYMERS	C_2H_3CL		
1042	VINYLIDENE CHLORIDE POLYMERS	$C_2H_2CL_2$		

APPENDIX 4

COMPUTER PROGRAMS

(1) TAPE WRITING ROUTINES:

The programs write the indicated data onto magnetic tape. The contents of the magnetic tapes stored at ULCC are given in the last column.

PROGRAM	DATA WRITTEN ON TAPE	CONTENTS OF ROUTINE TAPES
DATAPE	Coherent, incoherent, photoelectric and pair production cross sections (attenuation) for elements over 33 energy points from 10 keV-100 MeV	Cross sections for 70 elements
ENTAPE	Incoherent, photoelectric and pair production cross sections (energy absorption) as for DATAPE	Cross sections for 70 elements
ELTAPE	Collision and Radiation electron stopping powers for elements over the same energy range as DATAPE	Powers for 25 elements
ATTAPE	(1) Mass Attenuation coefficients for compounds	Coefficients for ~1040 compounds
	(2) Mass Attenuation coefficients for biological tissues (ICRP Reference Man)	Coefficients for 80 tissues
ZETAPE	(1) 30 effective atomic numbers (exponents 0.8-4.0), electron densities and $\overline{Z}$-Powers for compounds	Data for ~1040 compounds
	(2) As ZETAPE(1) but for biological tissues (ICRP Reference Man)	Data for 80 tissues
COTAPE	The contents of DATAPE, ENTAPE and ELTAPE	Cross sections for 70 elements and powers for 25 elements

Routines are also available for checking the accuracy of the data stored on the magnetic tapes. Error codes are given if the INTEGER and ALPHA NUMERIC data are not exactly reproduced and if the REAL (floating-point) data differs by more than 1 part per million

(2) COMPOUND CALCULATIONS

The programs compute and tabulate various properties of materials and tissues.

PROGRAM	DATA CALCULATED AND TABULATED
ATDATA	Mass attenuation coefficients
ENDATA	Mass energy absorption coefficients
ELDATA	Electron stopping powers (from elemental data)
STOPWR	Electron stopping powers (from first principles)
ASDATA	Electron mass angular scattering powers
ZEDATA	Effective atomic numbers, electron densities, $\overline{Y}$-values and $\overline{Z}$-powers
TABLEA	All above data for compounds
TABLEB	All above data for biological tissues
TABLEC	All above data for ZEDITA/ZEDITB formulae
CODATA	Energy ranges for which attenuation, absorption and stopping power data are within specified limits

(3) LINEAR REGRESSION CALCULATIONS

The programs calculate logarithmic linear regression data for equations of the form: $\ln(y) = \ln(k) + m \ln(x)$

PROGRAM	y-input	x-input
DATFIT	Attenuation cross sections	Atomic number or photon energy
ENFITT	Energy Absorption cross section	Atomic number or photon energy
ELFITT	Elemental electron stopping powers	Atomic number or photon energy
MASFIT	Elemental electron mass angular scattering powers	Atomic number or photon energy
ATFITT	Mass attenuation coefficients	$\overline{Y}$-Values
ARATIO	Mass attenuation coefficient ratios	$\overline{Z}$-Ratios

(4) CALCOMP AND MICROFILM PLOTTING

PROGRAM	DATA PLOTTED/TABULATED
ATPLOT	Mass attenuation coefficients versus photon energy plotted
ELPLOT	Element names, atomic numbers and atomic weights tabulated
COPLOT	Compound names, formulae and specific gravities tabulated

(5) EQUIVALENT MATERIAL CALCULATIONS

PROGRAM	FUNCTION
ZEDITA	Produces a tabulation of formulations that simulate a specified material (from $\overline{Y}$-data)
ZEDITB	As ZEDITA, but from attenuation and energy absorption coefficients and stopping power data
NEDITA	Produces a tabulation of formulations suitable for neutron studies

APPENDIX 5

PUBLISHED AND PROFERRED PAPERS

BY

D. R. WHITE

(1) HALL., F.M., and WHITE, D.R., 1964. A 'wedged counter' for thyroid measurements. Br. J. Radiol., 37, 794-795.

(2) WHITE, D.R., 1966. The efficiencies and costs of scintillation mixes for tritiated aqueous samples. Liquid Scintillation Counting Symposium, National Physical Laboratory, October, 1966.

(3) WHITE, D.R., and MALLION, W.E., 1967. A punched-card interlock for a superficial therapy set. Br. J. Radiol., 40, 69-70.

(4) WHITE, D.R., and MALLION, W.E., 1967. Digital control panel for a cobalt-60 radiotherapy unit. Physics Exhibition Handbook, 51, 123-124.

(5) WHITE, D.R., MALLION, W.E., and HALL, F.M., 1967. A low-cost three-channel renogram apparatus. Med. and Biol. Engng., 5, 397-400.

(6) WHITE, D.R., 1967. The evaluation of liquid scintillation mixtures of aqueous samples. Beckman Summer School, (London) 1967.

(7) WHITE, D.R., 1968. An assessment of the efficiencies and costs of liquid scintillation mixes for aqueous tritium samples. Int. J. Appl. Radiat. Isotopes, 19, 49-61.

(8) WHITE, D.R., 1968. Toluene blended mixes for aqueous tritium samples. Bio-Med. Engng., 3, 76-79.

(9) MALLION, W.E., and WHITE, D.R., 1968. Immobilisation of the head in radiotherapy. Br. J. Radiol., 41, 236.

(10) WHITE, D.R., 1968. Counting with liquids. Radiography, 34, 99-105.

(11) WHITE, D.R., MALLION, W.E., and O'CONNOR, A.D., 1968. The design of a digital control panel for a cobalt-60 radiotherapy unit. Med. & Biol. Engng, 6, 341-344.

(12) WHITE, D.R., and GWYTHER, M.M., 1968. Some storage investigations on toluene blended and dioxan liquid scintillation mixes. Bio-Med Engng., 3, 208-214.

(13) WHITE, D.R., and MALLION, W.E., 1969. Modern electronics and the radiographer - Part (I). The new components. Radiography, 35, 3-11.

(14) WHITE, D.R., and MALLION, W.E., 1969. Modern electronics and the radiographer - Part (II). The applications. Radiography, 35, 27-33.

(15) WHITE, D.R., and OFFERMAN, J.L., 1969. Liquid scintillation counting in clinical and biological research. Bio-Med. Engng., 4, 362-368.

(16) JONES, A., GREATOREX, C.A., and WHITE, D.R., 1971. Dosimetric aspects of 'mantle' techniques of radiotherapy of Hodgkin's disease. Second Congress of the European Association of Radiology, (Amsterdam) June, 1971.

REFERENCES

AEBERSOLD, P.C., and CHAFFEE, M.A., 1939. Practical considerations in the comparison of depth doses achieved by 1,000 and 200 kilovolt X-ray apparatus. Radiology, 33, 759-767.

AKAGI, H., and LEHMAN, R.L., 1963. Neutron dosimetry in and around human phantoms by use of nuclear track emulsion. Health Phys., 9, 207-220.

ALDERSON, S.W., 1966. Radiotherapy phantom. U.K. Patent Specification, No.1,025, 962.

ALDERSON, S.W., LANZL, L.H., ROLLINS, M., and SPIRA, J., 1962. An instrumented phantom system for analog computation of treatment plans. Am. J. Roentg., 87, 185-195.

ALMOND, P.R., WRIGHT, A.E., and BOONE, M.L.M., 1967. High energy electron dose perturbations in regions of tissue heterogeneity. Part (II). Physical models of tissue heterogeneities. Radiology, 88, 1146-1153.

ALY, S.M., and WILSON, C.W., 1949. Observations on the ionization produced by high-voltage radiation in moulded ionization chambers with walls of various effective atomic numbers. Br. J. Radiol., 22, 243-254.

ANDERSON, R.E., D'ANGIO, G.J., and KHAN, F.M., 1969. Dosimetry of irregularly shaped radiation therapy fields. Part (II). Isodose contours obtained utilizing a simulated human thorax. Radiology, 92, 1097-1100.

ASPDEN, P., 1973. Private communication.

BAILEY, R.J., 1974. Private communication.

BAUMEISTER, L., 1923. Roentgen-ray measurements. Acta Radiologica, 2, 418-429.

BEHNKEN , H., and JAEGER, R., 1928. The standardization of X-ray dosage. Radiology, 10, 275-279.

BELOT, J., and DAUVILLIER, S., 1939. Arrangements for the use of the 600 kV tube of the Institute for Cancer of the Faculté de Médicine de Paris. Bull. et mém. Soc. de Radiol. Méd. de France, 27, 62-67. (Abstract in Radiology, 35, 756, 1940).

BERGER, M.J., and SELTZER, S.S., 1964. Tables of energy losses and ranges of electrons and positrons. National Research Council Report 1133, National Academy of Science.

BERNSTEDT, R., 1940. A determination of the dose constant, R/ImC-hour. Acta Radiologica, 21, 500-509.

BICHSEL, H., 1968. Charged-particle interactions. Contribution in Radiation Dosimetry, Volume 1, Ed by F.H. Attix and W.C. Roesch, Second Edition, 157-228. (Academic Press, New York).

BORDIER, H., 1907. Determination of the quantity of Roentgen Rays absorbed by different tissues. Archives d'Él Médicale, 15, 929-935. (Abstract in J. Roentgen Soc., 4, 80, 1908).

BRAESTRUP, C.B., and BLATZ, I.H., 1940. Physical factors of low voltage 'contact' roentgen therapy. Radiology, 35, 198-205.

BRAGG, W.H., and PEIRCE, S.E., 1914. The absorption coefficients of X-rays. Phil, Mag., 28, 626-630.

BRUNSKILL, R.T., 1973. Private communication.

BRYDSON, J.A., 1970, in 'Plastics Materials'. Second Edition. (ILIFFE Books, London).

BRYDSON, J.A., 1971)
) Private communications
BRYDSON, J.A., 1973)

CASS, M., 1971. Private communication.

CHRISTÉN, F.T., 1913, in 'Messung und Dosierung der Roentgenstrahlen' (Lucas, Gräfe and Sillen, Hamburg). (Abstract in Archives of the Roentgen Ray, 18, 280, 1913.

CLARKSON, J.R., 1973. Private communication.

COHEN, M., 1955. The unit of X-ray dose and its realization. (II) The patient and the roentgen. Br. J. Radiol, 28, 669-677.

DESLATTES, R.D., 1969. Estimates of X-ray attenuation coefficients for the elements and their compounds. Acta Cryst., A25, 89-93.

DESSAUER, F., and VIERHELLER, F., 1921. Die tiefenwirkung der Rontgenstrahlen. Strahlentherapie, 12, 655-690.

EASTMAN KODAK. Catalogue 46 'Organic Chemicals', 1971.

EDLING, L., 1944. Experiences with rotation therapy. Acta Radiologica, 15, 427-443.

FACEY, R.A., 1968. Dose and photon-energy measurements for bone marrow in a human phantom by thermoluminescence. Health Phys., 14, 557-568.

FAILLA, G., 1920. The absorption of radium radiations by tissues. Am. J. Roentg., 8, 215-232.

FAILLA, G., 1925. An objective method for the administration of X-rays. Acta Radiologica, 4, 85-128.

FAILLA, G., 1937. The measurement of tissue dose in terms of the same unit for all ionizing radiations. Radiology, 29, 202-215.

FAIRCHILD, R.G., 1965. Development and dosimetry of an 'epithermal' neutron beam for possible use in neutron capture therapy. (I) 'Epithermal' neutron beam development. Phys. Med. Biol., 10, 491-504.

FIELD, S.B., and PARNELL, C.J., 1965. The use of threshold detectors to determine changes in a fast neutron energy spectrum with depth in a phantom. Br. J. Radiol., 38, 618-621.

FOWLER, J.F., 1956. Absorbed dose near bone: A conductivity method of measurement. Br. J. Radiol., 30, 361-366.

FRANCIS, G.E., 1973. Private communication.

FRICKE, H., and GLASSER, O., 1925. A theoretical and experimental study of the small ionization chamber. (Studies on the physical foundations of Roentgen-ray therapy (II)). Am. J. Roentg., 13, 453-461.

FRIEDRICH, W., and GLASSER, O., 1922. The distribution of the radiation dose in intracorporeal radium and mesothorium therapy. Appendix in 'The Principles of Physics and Biology of Radiation Therapy' by B. Kroenig and W. Friedrich (Heinemann), 241-154.

FRIGERIO, N.A., 1962. Neutron penetration during neutron capture therapy. Phys. Med. Biol. 6, 541-549.

FRIGERIO, N.A., and SAMPSON, M.J., 1969. Tissue equivalent phantoms for standard man and muscle. Argonne National Laboratory Report, ANL-7635.

GLASSER, O., 1932. The physical foundation of grenz-ray therapy. Radiology, 18, 713-726.

GLASSER, O., PORTMANN, U.V., and SEITZ, V.B., 1928. The demonstration of the standardization of the roentgen ray dosage. Radiology, 10, 284-291.

GLOCKER, R., and KAUPP, E., 1927. Über eine in bezug auf die R-Einheit von der Qualität der Strahlung unabhängige Fingerhutkammer und über die messung der Streuzusatzdosis im Wasserphantom (II). Strahlentherapie, 24, 517-523.

GOODMAN, L.J., 1969. A modified tissue equivalent liquid. Health Phys., 16, 763.

GOODWIN, P.N., 1960. Calorimetric measurements of bone/tissue absorption ratios. Radiology, 75, 112-115.

GRIMMETT, L.G., 1939. Contributions to radium therapy. Am. J. Roentg., 41, 432-436.

GUILLEMINOT, H., 1909. Quantity of roentgen rays absorbed and transmitted by successive layers of tissue. Archives of the Roentgen Ray, 13, 252.

HANDBOOK OF PHYSICS AND CHEMISTRY, 1971-1972. Fifty-Second Edition. (Chemical Rubber Co.).

HARRIS, J.H., TUDDENHAM, W.J., STANTON, L., GLAUSER, F., and PENDERGRASS, E.P., 1956. The development of a chest phantom for use in radiologic dosimetry. Radiology, 67, 805-814,

HAYBITTLE, J.L., 1960. A 10 curie strontium-90 beta-ray therapy unit. Br. J. Radiol., 33, 52-54.

HENRIKSEN, T., and BAARLI, J., 1957. The effective atomic number. Radiat. Res., 6, 415-423.

HILDITCH, T.P., 1956 in 'The Chemical constitution of Natural Fats', Third Edition (WILEY).

HINE, G.J., 1952. Secondary electron emission and effective atomic numbers. Nucleonics, 10, 9-15.

HOED, D. den, and STOEL, G., 1929. Intensity measurements of radium rays. Acta Radiologica, 10, 442-461.

HOLFELDER, H.G.D., 1933. Private communication to PETTIT and LANDAUER, 1933.

HUBBELL, J.H., 1969. Photon cross sections, attenuation coefficients, and energy absorption coefficients from 10 keV to 100 GeV. National Bureau of Standards, NSRDS-NBS 29.

ICRP, 1959. Recommendations of the International Commission on Radiological Protection. Publication 2, Report of Committee II on permissible dose for internal radiation. (Pergamon Press, London, 1960).

ICRU, 1972. ICRU Report 21. Radiation dosimetry:electrons with initial energies between 1 and 50 MeV.

JACOBS, M.L., and PAPE, L., 1961. Dosimetry for a total-body irradiation chamber. Radiology, 77, 788-791.

JAYACHANDRAN, C.A., 1968. Radiation induced thermoluminescence in lithium fluoride and lithium borate. Ph.D. Thesis, University of London.

JENSEN, A., 1945. Dosis measurements in roentgen irradiation of the female pelvis. Acta Radiologica, 26, 99-116.

JONES, D.E.A., 1969. Private communication.

JONES, D.E.A., and RAINE, H.C., 1949. (Letter). Br. J. Radiol., 22, 549-550.

JÜNGLING, O., 1920. Untersuchungen zur chirurgischen Roentgentiefen-therapie. Strahlentherapie, 10, 576-584.

KIENBÖCK, R., 1906. On the quantimetric method. Archives of the Roentgen Ray, 11, 17-20.

KIM, Y.S., 1973. Density effect in dE/dx of fast charged particles traversing various biological materials. Radiat. Res., 56, 21-27.

KOREN, K., and MAUDAL, S., 1957. Gonad doses received during medical application of roentgen radiation. Acta Radiologica, 48, 273-279.

KORNELSEN, R.O., 1954. Tumour dose in the chest cavity. Br. J. Radiol., 27, 289-293.

LAUGHLIN, J.S., LUNDY, A., PHILLIPS, R., CHU, F., and SATTAR, A., 1965. Electron beam treatment planning in inhomogeneous tissue. Radiology, 85, 524-531.

LAUGHLIN, J.S., OVADIA, J., BEATTIE, J.W., HENDERSON, W.J., HARVEY, R.A. and HAAS, L.L., 1953. Some physical aspects of electron beam therapy. Radiology, 60, 165-184

LEDDY, E.T., and WITTING, V., 1930. The effect of varying volumes of air on the distribution of roentgen energy in a non-homogeneous medium. Radiology, 15, 579-584.

LINCOLN, T.A., and GUPTON, E.D., 1958. Radiation doses in diagnostic X-ray procedures. Radiology, 71, 208-215.

LINDSAY, D.D., and STERN, B.E., 1953. A new tissue-like material for use as bolus. Radiology, 60, 355-362.

LOCHMAN, D.J., 1955. Dosage in tangential radiation therapy of the postoperative breast portal. Am. J. Roentg. 73, 803-812.

McGINLEY, P.H. 1973. Lung-equivalent material for fast neutron dose distribution studies. Int. J. Appl. Radiat. Isotopes, 24, 477-478.

MARKUS, B., 1956. Über den Begriff der Gewebeäquivalenz und einige 'wasserähnliche' Phantomsubstanzen fur Quanten von 10 keV bis 100 MeV sourie schnelle Elektronen. Strahlentherapie, 101, 111-131.

MARKUS, B., 1960. Ionisationsdosimetrie und Dosisverteilungen schneller Elektronen in Knochengewebe. Strahlentherapie, 113, 379-393.

MARKUS, B., 1961. Energy determination of fast electrons from depth dose curves. Strahlentherapie, 116, 280-286.

MARTIN, R.J., 1971)
MARTIN, R.J., 1973) Private communications.
MARTIN, R.J., 1974)

MAY, E.A., 1934. Depth doses of roentgen radiation, striking at angles other than 90 degrees, measured in a water phantom. Radiology, 22, 559-568.

MAYNEORD, W.V., 1929(a). Experimental and theoretical studies in X-ray intensity measurements. (II) Distribution of X-rays within an irradiated medium. Br. J. Radiol., 2, 267-296.

MAYNEORD, W.V., 1929(b). The true absorption of the energy of electromagnetic radiations in light substances. Br. J. Radiol., 2, 373-389.

MAYNEORD, W.V., 1933. Notes on three problems of gamma ray therapy. Br. J. Radiol., 6, 598-614.

MAYNEORD, W.V., 1937. The significance of the roentgen. Acta of the International Union against Cancer, 2, 271-282.

MAYNEORD, W.V., and ROBERTS, J.E., 1937. An attempt at precision measurements of gamma rays. Br. J. Radiol., 10, 365-388.

MILLEDGE, H., 1973. Private communication.

MURTY, R.C., 1965. Effective atomic numbers of heterogeneous materials. Nature, 207, 398-399.

NAHON, J.R., and HAWKES, J.B., 1954. Energy distribution in the thorax during multiple field and rotational therapy. Am. J. Roentg., 72, 819-826.

National Bureau of Standards, 1963. Radiobiological Dosimetry. ICRU Report 10e. Handbook 88.

National Bureau of Standards, 1964. Physical aspects of irradiation. ICRU Report 10b. Handbook 85.

NIKL, I., 1965. A demountable phantom of variable geometry for intra-pelvic dosimetry in pregnancy - Preliminary report. Br. J. Radiol., 38, 472-477.

NORDBERG , U., 1972. Correction of isodose diagrams for ^{60}Co and 35 MeV electrons at penetration of lung tissue. Acta Radiologica, 11, 113-128.

OOSTERKAMP, W.J., and PROPER, J., 1959. (Letter). The water equivalence of 'MIX D' phantom material for soft X-rays. Br. J. Radiol, 32, 560.

OSBORN, S.B., TAVENER, D.R., and FARMER, F.T., 1945. Dosage distribution in the treatment of ringworm by X-rays. Br. J. Radiol., 18, 145-147.

OSHINO, M., 1973. Response of NTA personnel neutron monitoring film worn on human phantom. Health Phys., 24, 71-80.

OTLET, R.L., and GEORGE, J.D., 1960. The accurate comparison of exposure dose rate (output) from gamma emitting radioisotopes using capacitor ionization chambers. IAEA Symposium on Selected Topics in Radiation Dosimetry, Vienna. Harwell Document HL 60/2883.

OTT, P., 1937. Zur Röntgenstrahlenbehandlung oberflächlich gelagerter Tumoren. Strahlentherapie, 59, 189-223.

PAGES, L., BERTEL, E., JOFFRE, H., and SKLAVENITIS, L., 1970. Pertes d'energie, parcours et rendement de freinage pour les electrons de 10 keV à 100 MeV dans les elements simples et quelques composes chimiques. Report CEA-R-3942 (Centre d'Études Nucléaires de Saclay).

PETTIT, R.T., and LANDAUER, R.S., 1933. A rice phantom for depth dose measurements. Radiology, 21, 484-487.

PHILLIPS, M., 1973. Private communication.

POLL, V., 1972. Bone marrow dose from radioisotopes incorporated within replicated trabecular bone. Ph.D. Thesis, University of Leeds.

QUIMBY, E.H., 1928. The intensity of radiation in the vicinity of filtered radon implants. Radiology, 10, 365-376.

QUIMBY, E.H., and ARNESON, A.N., 1937. A comparison of paraffin and water phantoms for roentgen ray depth dose measurements. Am. J. Roentg., 37, 93-97.

QUIMBY, E.H., COPELAND, M.M., and WOODS, R.C., 1934. The distribution of roentgen rays within the human body. Am. J. Roentg., 32, 534-551.

QUIMBY, E.H., MARINELLI, L.D., and FARROW, J.H., 1938. A study of back-scatter. Am. J. Roentg., 39, 799-815.

RICHTMYER, F.K., and WARBURTON, F.W., 1923. The absorption of X-rays by iron, cobalt, nickel and copper. Phys. Rev., 22, 539-545.

RODERICK, J.F., 1959. Plastic roentgen ray phantoms. Am. J. Roentg., 81, 331-335.

ROGERS, R.T., 1970. A phantom material to represent lungs. Br. J. Radiol., 43, 441-444.

ROSSI, H.H., and FAILLA, G., 1956. Tissue-equivalent ionization chambers. Nucleonics, 14, 32-37.

RUSS, S., 1912(a). Secondary X-rays from animal tissues. Royal Society of Medicine Report. Cited in Archives of the Roentgen Ray, 17, 433-437, 1913.

RUSS, S., 1912(b). The clinical significance of X-ray and radium measurements. J. Roentgen Soc., 8, 35-40.

SALMOND, W.A., 1914. Experiments in X-ray filtration. Archives of the Roentgen Ray, 19, 127-132.

SCHMITZ, H., and HUTH, E., 1922. The determination of equal intensity curves (isodoses) of short radium capsules. Appendix in 'The Principles of Physics and Biology of Radiation Therapy' by B. Kroenig and W. Friedrich (Heinemann), 255-263.

SHONKA, F.R., ROSE, J.E., and FAILLA, G., 1958. Conducting plastic equivalent to tissue, air and polystyrene. Progress in Nuclear Energy, Series 12, 1, 184-187. (Geneva Conference Paper).

SIEVERT, R.M., 1937. Dosage units and the ionization method. Acta Radiologica, 18, 742-752.

SPIERS, F.W., 1943. Materials for depth dose measurements. Br. J. Radiol., 16, 90-97.

SPIERS, F.W., 1946. Effective atomic number and energy absorption in tissues. Br. J. Radiol, 19, 52-63.

SPIERS, F.W., 1949. The influence of energy absorption and electron range on dosage in irradiated bone. Br. J. Radiol., 22, 521-533.

SPIERS, F.W., 1971)
) Private communications.
SPIERS, F.W., 1972)

SPIERS, F.W., and CHESTERS, M.S., 1962. Theoretical and experimental dosimetry based on bone structure. 'Some Aspects of Internal Irradiation' (Pergamon Press), 423-434.

SPLETTSTOSSER, H.R., and SEEMANN, H.E., 1955. A phantom for physical studies in chest radiography. Radiology, 64, 114.

SPOKAS, J.J., 1973. Private communication.

STACEY, A.J., 1971. Private communication.

STACEY, A.J., 1972. The absorption and scattering of radiation in heterogeneous media. M.Phil Thesis, University of London.

STACEY, A.J., 1973. Private communication.

STACEY, A.J., BEVAN, A.R., and DICKENS, C.W., 1961. A new phantom material employing depolymerised natural rubber. Br. J. Radiol., 34, 510-515.

STENSTRÖM, W., 1926. Physics and Radiology. Acta Radiologica, 7, 547-558.

STONE, M., 1973. Private communication.

STORM, E., and ISRAEL, H.I., 1970. Photon cross sections from 1 keV to 100 MeV for elements Z = 1 to Z = 100. Nuclear Data Tables, A7, 565-681.

SZILARD, B., 1914. On the absolute measurement of the biological action of the X-rays and gamma rays. Archives of the Roentgen Ray, 19, 3-20.

TIPTON, I.H., 1970. Gross and elemental content of Reference Man. Preprint of ICRP document on Reference Man, Chapter 2, 1-72.

TIPTON, I.H., 1973. Private communication.

TROUT, E.D., and KELLEY, J.P., 1972. Scattered radiation from a tissue-equivalent phantom for X-rays from 50-300 kVp. Radiology, 104, 161-169.

TRÜBESTEIN, H., 1937. The absorption and scattering of monochromatic roentgen rays in water, triolein, blood, skeletal muscle and subcutaneous tissue of man. Strahlentherapie, 60, 330-354.

VAKHLAKOVA, T.V., and SKOROPAD, Y.D., 1972. Utilization of carbon tetrachloride-ethyl alcohol solution in absorbed dose measurements. Medskaya Radiol., 17, 67-70.

WALTER, B., 1926. Über die besten Formeln zur Berechnung der Absorption der Röntgenstrahlen in einem beliebigen Stoff. Fortschr. Geb. RöntgStrahl., 35, 929-947.

WEATHERWAX, J.L., and ROBB, C., 1930. Determination of the radiation values in lung tissue with variable qualities of radiation. Radiology, 14, 401-409.

WEATHERWAX, J.L., and WIDMANN, B.P., 1929. Physical factors in radiation therapy and their clinical application. Radiology, 12, 297-308.

WEBER, J., and BERGE, D.J. van den, 1969. The effective atomic number and the calculation of the composition of phantom materials. Br. J. Radiol., 42, 378-383.

WEST, E.S., TODD, W.R., MASON, H.S., and BRUGGEN, J.T. van., 1966 in 'Textbook of Biochemistry', Fourth Edition (Macmillan).

WESTMAN, A., 1924. A simplified dosimetric method in gynaecological deep roentgentherapy. Acta Radiologica, 3, 68-75.

WHEATLEY, B.M., and LISTER, W.C., 1957. The construction of the phantom. M.R.C. Report 'Leukaemia and aplastic anaemia in patients irradiated for ankylosing spondylitis, No.295, 99-100.

WHITE, A., HANDLER, P., and SMITH, E.L., 1968 in 'Principles of Biochemistry', Fourth Edition (McGraw Hill).

WILLIAMS, F.H., 1908. Method for measuring the relative density of different parts of the lungs by means of the X-rays. (Boston Medical and Surgical Journal). Abstract in Archives of the Roentgen Ray, 13, 206, 1909.

WILLIAMS, M., 1936. Radiation from an oil-immersed therapy tube. Radiology, 26, 749-755.

WILSON, C.W., and MYERS, G., 1936. Some direct measurements of the distribution of gamma radiation in human tissues by radium teletherapy. Br. J. Radiol., 9, 379-389.

WOODWARD, H.Q., 1962. The elementary composition of human cortical bone. Health Phys., 8, 513-517.

WRIGHT, S.J., 1973. Private communication.